STUDIES IN COLLOID AND POLYMER SCIENCE

Derek Y.C. Chan

A thesis submitted for the

degree of

Doctor of Philosophy

at the Australian National University

Canberra

December 1974

PREFACE

This dissertation is an account of work carried out between February 1972 and November 1974 at the Department of Applied Mathematics, Research School of Physical Sciences, the Australian National University, for the degree of Doctor of Philosophy.

Initially, studies commenced under the supervision of Dr. P. Richmond on the dispersion interaction between optically active molecules and on dynamical image interactions. A large portion of this work entails the re-derivation of known results using much simpler classical methods (Part III). However, the result on the three-body interaction between optically active molecules is new.

In Part I, the work on the interaction between identical double layers (Chapter 1) was carried out in collaboration with Dr. J.W. Perram, Mr. L.R. White and with Dr. T.W. Healy of the Department of Physical Chemistry, University of Melbourne. The study on the interaction between dissimilar double layers (Chapter 2) was a joint effort with Mr. L.R. White.

In Part II, the investigation on phase transitions in polymer solutions (Chapter 1) was carried out in collaboration with Professor B.W. Ninham, while that on polymer adsorption (Chapter 2) was with Professor B.W. Ninham, Dr. D.J. Mitchell and Mr. L.R. White.

None of the work reported here has been submitted to any other institution of learning for any degree.

D Chan

(D. CHAN)

PUBLICATIONS

1. The Interaction of Optically Active Molecules
   Chem. Phys. Lett. 16, 287 (1972)
   [with P. Richmond].

2. The Three-Body Interaction Between Optically Active Molecules
   Mol. Phys. 25, 1475 (1973)
   [with P. Richmond].

3. Classical Theory of Dynamical Image Interactions
   Surface Sci. 39, 437 (1973)
   [with P. Richmond].

4. Phase Transitions in Polymer Solutions and the Prediction of θ Temperatures
   J. Chem. Soc., Faraday II 70, 586 (1974).
   [with B.W. Ninham].

5. The Electrostatic Interaction Between Surfaces Bearing Amphoteric Groups Across a 1:1 Electrolyte
   J. Theor. Biol. 47 (1974) (in press)
   [with L.R. White].

6. The Configuration of a Non-Interacting Polymer Near a 'Sticky' Wall
   J. Chem. Soc., Faraday II (to appear)
   [with D.J. Mitchell, B.W. Ninham and L.R. White].

7. The Regulation of Surface Potential at Amphoteric Surfaces During Approach
   J. Chem. Soc., Faraday II (to appear)
   [with T.W. Healy, J.W. Perram and L.R. White].

8. Phase Transitions in Adsorbed Polymer Systems
   Disc. Farad. Soc.: Physical Adsorption in Condensed Phases (1974)
   [with D.J. Mitchell and L.R. White].

ACKNOWLEDGEMENTS

It has been my good fortune to be able to work under the supervision of Barry Ninham and Peter Richmond who introduced me to a myriad of fascinating problems. They have been excellent teachers and good friends, always ready to provide much needed advice on academic as well as personal problems. I am also grateful to them for their critical comments on the draft of this thesis.

The many hours of, sometimes vigorous, discussion with Lee White and John Mitchell, who were always ready to challenge and correct my misconceptions and faulty logic, provided much stimulus to study and research. The fruitful collaboration with them corrected much of the inadequacies of my own thinking process (and led Lee to a greater appreciation for the finer points of Chinese culinary art).

I owe what little knowledge I have about practical problems in colloid and surface chemistry to Tom Healy. I also thank him for his hospitality on the occasions I was in Melbourne to work with him.

I also appreciate the association with John Perram, Peter McIntyre, Allan Snyder, Colin Pask, John Love, Chris Barnes and other present and past members of the Department, and their willingness to assist with difficult points.

Thanks are also due to Kay Cross, Bente Donehue, Terry King and Pauline Wallace who cheerfully gave assistance in the necessary but unpleasant paper work.

I am fortunate to have Norma Chin to type this thesis. She did an excellent job in transcribing from an almost illegible draft and managed to correct the mistakes as well.

Thanks are due to the Australian Government and the Australian National University for financial support in the form of a post-graduate scholarship.

And to my wife, Florence, the most for her support and encouragement.

ABSTRACT

The subject matter of this thesis falls into three parts.

In Part I, the electrostatic interaction between plane parallel double layers is investigated under the Gouy-Chapman approximation. Each surface is considered to develop a surface charge by the association of ionizable surface groups. The interaction process is assumed to be at electrochemical equilibrium. An adsorption isotherm for potential determining ions can then be derived relating the surface charge and the surface potential in a self-consistent manner. This is used in place of the usual constant charge or constant potential boundary condition. In Chapter 1 the interaction between identical amphoteric surfaces are studied in detail. The relation between this new boundary condition and the constant charge or potential approximation is discussed. Numerical calculations based on model systems for hydrous oxides are given. In Chapter 2 the interaction between dissimilar amphoteric surfaces are considered. A new method, similar to the method of isodynamic curves, is developed to study this problem. This method can provide a qualitative description of the salient features of the surface charge, the surface potential and the pressure between the surfaces, as a function of separation without first having to obtain an exact solution of the problem.

In Part II, Chapter 1, a physical theory of phase transitions in polymer solutions is given in terms of long range dispersion interactions between the solvent and the polymer. The theory is based on a mean field approximation and the parameters used are given in terms of measurable dielectric and spectroscopic properties of the polymer and solvent. This provides a physical explanation of the θ temperature and also a criterion for the selection of θ solvents. In Chapter 2, the statistical mechanics of an adsorbed polymer is considered. The polymer is modelled as a string of non-interacting beads confined to a half-space by an impenetrable flat surface. Each bead interacts only with the surface via a one-body potential. Conformational properties of the

adsorbed polymer, such as the number of beads adsorbed, the spread of adsorbed beads on the surface, the density of beads away from the surface and the centre-of-mass of the polymer are derived. The behaviour of these quantities are found to undergo an adsorption/desorption phase transition at some critical value of the adsorption energy parameter. Assuming that the substrate-polymer interaction is due primarily to dispersion forces, it is possible to determine whether or not a given polymer/solvent/substrate system will exist in the adsorbed state. It is also found that temperature induced and mixed solvent induced phase transitions are theoretically possible.

In Chapter 1 of Part III the two- and three-body dispersion interaction energy between optically active molecules are studied using a semi-classical method. In Chapter 2, classical electrodynamics is again used to consider modifications to the static image potential between a moving charge and a half space due to surface plasmon excitations. It is demonstrated that in both examples, semi-classical methods are easy to use and also give the same results derived using more elaborate quantum mechanical analysis.

CONTENTS

PART II

THE CONFORMATION OF MACROMOLECULES

PART III

VAN DER WAALS AND DYNAMICAL INTERACTIONS

CHAPTER 1. TWO- AND THREE-BODY INTERACTIONS BETWEEN OPTICALLY ACTIVE MOLECULES — A SEMI-CLASSICAL APPROACH

CHAPTER 2. CLASSICAL THEORY OF DYNAMICAL IMAGE INTERACTIONS

PART I

ELECTROSTATIC DOUBLE LAYER INTERACTIONS AT ELECTROCHEMICAL EQUILIBRIUM

CHAPTER 1

DOUBLE LAYER INTERACTIONS UNDER SURFACE IONIZATION EQUILIBRIUM – IDENTICAL SURFACES

1. INTRODUCTION

A central problem in colloid science is the determination of the particle-particle interaction potential.[1,2,33-36] Deryaguin and Landau[1] and Verwey and Overbeek[2] (DLVO) were the first to consider this problem in detail. They considered "clean" particles with no adsorbed macromolecules and assumed the potential may be written as the sum of electrodynamic (van der Waals or dispersion) and electrostatic interactions.

In the DLVO formalism, it is assumed that the electrostatic contribution can be evaluated separately from the electrodynamic contribution. In solving the electrostatic problem, it has been usual to assume, as boundary conditions, that constant charge or constant potential is maintained on either or both surfaces throughout the interaction. Typically, the surfaces acquire a net charge by one or more of the following processes:[3,4]

(i) the presence of ionizable surface groups, such as -COOH, $-NH_3$ or amphoteric groups (e.g. oxides), which by the dissociation or association of potential determining ions (PDI) give the particles a net charge;

(ii) the unequal dissolution of oppositely charged ions which make up the particle (e.g. AgI crystals in water); and

(iii) the selective adsorption of particular ion-types from the surrounding medium.

For certain surfaces, where the charge is due, for example, to strong acid sites, the constant charge assumption may indeed be correct.

However, there are as yet no criteria for selecting the extent to which such an assumption is valid, nor are there criteria for determining *a priori* whether a constant charge or constant potential interaction is more appropriate for many other important colloidal systems. While Frens and Overbeek[5,6] did show that a perturbation of the bulk electrolyte composition resulted in a relatively slow restitution of the equilibrium potential of an Ag/AgI electrode, there is yet no direct measurement of the ability or otherwise of particles to adjust ion populations at the surface and in the interparticle fluid during collision.

A very extensive literature exists on the calculation of interactions between charged flat plates[1,2,7-17,55-58] and spheres[10-12,18-22] under constant surface charge or potential. Cases involving closed systems,[23,24] zero surface charge,[25] "periodic" surface charges,[26,27] and other geometries such as cross cylinders[28] and arrays[24,29,30] have also been studied. An alternative to the constant charge or potential approach has also been developed where the surface potential is related to surface concentration of PDI by the Nernst equation,[24] or a Langmuir type adsorption isotherm.[31]

In this chapter we shall extend a recent approach due to Ninham and Parsegian[32] (hereafter referred to as NP) in which the electrostatic potential of each of the interacting surfaces is regulated during approach by those equilibria at the surface that are responsible for the development of the surface charge. In other words, the magnitude of the surface charge which determines the potential distribution in the diffuse layer is itself given as a self-consistent functional of the surface potential. This concept of a self-consistent relationship between the surface charge and potential has in fact been exploited to interpret adsorption data[37] and mobility and titration experiments on polystyrene lattices[38] and hydrous oxides.[39-42]

We shall consider the situation where the approach of the interacting surfaces is sufficiently slow so that electrochemical equilibrium is maintained at all times during collision. This is *not* an assumption of "constant potential". Indeed it will be shown that conditions can be such that *both* charge and potential may change significantly during the interaction. Alternatively, if conditions are favourable for regulation then changes in charge *or* potential will be minimal during interaction.

We extend the NP model, which includes only basic surface groups,[32] to a general amphoteric surface[43] involving surface equilibria that are controlled by the chemical potential of PDI in bulk solution. We consider the simplest configuration of the two such plane surfaces interacting across a 1:1 electrolyte which contains PDI. The diffuse layer is assumed to be governed by the Poisson-Boltzmann (PB) equation. (The problem of interacting charged cylinders bearing basic surface groups has been considered by Brenner and McQuarrie[44] using the linearized Poisson-Boltzmann equation.) No attempt is made to model the inner Stern region (see section 3).

It is not necessary to specify the nature of the PDI. However, for the purposes of comparing theoretical results with experiments, it is convenient to assume that H^+ and OH^- are PDI as this is the case for hydrous oxide colloids, e.g. Fe_2O_3, Al_2O_3, TiO_2, SiO_2 and organic colloids with amine, carboxylate, sulphonate, etc. surface groups.

These restrictions simplify the mathematics and also allow us to elucidate in a clear manner the physics underlying the influence of adsorption (of PDI) on particle-particle interaction.[45,46]

2. FORMULATION

We consider initially a planar surface bearing ionizable amphoteric groups in contact with a solution of 1:1 electrolyte. The bulk concentration of PDI or the bulk pH (since H^+ and OH^- are assumed to be PDI) may be controlled. The reactions at the surface, written as dissociation reactions, are

$$AH^+ \rightleftharpoons A + H^+ \tag{2.1}$$

$$BH \rightleftharpoons B^- + H^+ \, . \tag{2.2}$$

The relative concentrations of positive (AH^+), neutral (A, BH), and negative (B^-) surface sites are related to the hydrogen ion concentration at the surface $[H^+]_s$ in the form

$$[A]\cdot[H^+]_s = [AH^+]\cdot K_+ \tag{2.3}$$

$$[B^-]\cdot[H^+]_s = [BH]\cdot K_- \, , \tag{2.4}$$

where K_+ and K_- are the effective surface dissociation constants for the above processes.

The arguments involved in obtaining equations (2.3) and (2.4) are as follows. Assuming that random mixing statistics apply, the total (random) number of configurations available to n_+ charged and n_0 uncharged species (AH^+ and A say) is[4,39]

$$\frac{N_A!}{n_+!\; n_0!} \, .$$

N_A is the total number of A-type sites per unit area. The electrochemical potential of a species i can then be written as

$$\tilde{\mu}_i = \mu_i^0 + kT \ln c_i + kT \ln \gamma_i \, , \tag{2.5}$$

where the last term represents the concentration (c_i) dependent part of the free energy of interaction of species i with its environment. The

electrochemical potential μ_i^0 corresponding to some standard state, is concentration independent. Contributions to the activity coefficients γ_i can be divided into two parts: an electrostatic interaction with charged species on the surface and in the electrolyte, and a dispersion interaction with neighbouring molecules. Hence for each species in the reaction

$$AH^+ \rightleftharpoons A + H^+ \tag{2.1}$$

we write

$$\tilde{\mu}_{AH^+} = \mu^0_{AH^+} + kT\, ln\, [AH^+] + kT\, ln\, \gamma_+ + e\psi_s \tag{2.6}$$

$$\tilde{\mu}_A = \mu^0_A + kT\, ln\, [A] + kT\, ln\, \gamma_0 \tag{2.7}$$

$$\tilde{\mu}_{H^+} = \mu^0_{H^+} + kT\, ln\, [H^+]_s + kT\, ln\, \gamma_{H^+_s} + e\psi_s\ . \tag{2.8}$$

The electrical part of $\tilde{\mu}$ should involve the micro-potential at the site, but here only the mean surface potential ψ_s will be used. This is tantamount to neglecting discreteness-of-charge effects.[9] Equilibrium requires

$$\tilde{\mu}_{AH^+} = \tilde{\mu}_A + \tilde{\mu}_{H^+}\ , \tag{2.9}$$

whence from equations (2.6) - (2.8) we have[47]

$$\frac{[A]\cdot[H^+]_s}{[AH^+]} = \frac{\gamma_0}{\gamma_+\ \gamma_{H^+_s}} K^0_+\ , \tag{2.10}$$

where the bulk dissociation constant K^0_+ is defined by

$$K^0_+ = \exp[(\mu^0_{AH^+} - \mu^0_A - \mu^0_{H^+})/kT]\ . \tag{2.11}$$

In general the ratio of activity coefficients in (2.10) is not independent of $[A]$, $[AH^+]$ and $[H^+]_s$. To calculate the functional dependence of this ratio upon the relevant concentrations would require a statistical theory of surface activity coefficients for high

concentrations, and such a theory is not available. However to proceed further without such a theory, all that is required is that the ratio of activity coefficients remain sufficiently constant as the surfaces approach each other so that the ratio of concentrations in (2.10) can be given by an effective surface dissociation constant. The activity coefficients γ_+ and γ_0 measure the dispersion interaction of AH^+ and A with their environment. Since AH^+ and A are similar molecular units, their polarizabilities and hence dispersion interaction energies with neighbouring molecules are expected to be similar, i.e. $\gamma_+ \simeq \gamma_0$. The surface activity coefficient of PDI is a function of the ionic concentration at the surface, which in turn is determined by the surface potential. As we shall show later, ψ_s the surface potential remains fairly constant in an equilibrium approach so the surface ionic concentration does not change dramatically throughout the interaction. Further, since activity coefficients are moderately insensitive functions of concentration,[59] the surface activity coefficient of the PDI at infinite separation should be a good approximation to the surface activity coefficient during approach.

These arguments imply that the ratio of concentration in (2.10) is to a large degree constant throughout the approach of the surfaces and hence justify, to a first approximation, the use of an equilibrium dissociation constant given by

$$K_+ = \frac{\gamma_+}{\gamma_0 \; \gamma_{H^+_s}} K_+^0 \; . \qquad (2.12)$$

A similar argument should also apply regarding the use of the other effective dissociation constant K_-. We should note here that the surface dissociation constants K_+, K_- are accessible from measurements on stable colloid systems.[38,48] Returning now to equations (2.1) and (2.2), let

us consider the surface charge density that arises from the dissociation reactions.

For N_A and N_B surface sites per unit area for each species, the net surface charge density is

$$\sigma = e N_A \theta_+ - e N_B \theta_- . \tag{2.13}$$

Here

$$\theta_+ = \frac{[AH^+]}{[AH^+] + [A]} = \frac{[AH^+]}{N_A} \tag{2.14}$$

and

$$\theta_- = \frac{[B^-]}{[BH] + [B^-]} = \frac{[B^-]}{N_B} \tag{2.15}$$

are the fractions of positively and negatively charged sites, and e is the protonic charge. If the local density of ions in the electrolyte is related to the electrostatic potential ψ at that point by the Boltzmann distribution, then for a surface potential ψ_s we have

$$[H^+]_s = H \exp(- e\psi_s/kT) , \tag{2.16}$$

where H is the concentration of hydrogen ions in the reservoir. Using equations (2.3) and (2.4) we can rewrite the surface charge density as

$$\sigma = \frac{e N_A}{1 + (K_+/H) \exp(e\psi_s/kT)} - \frac{e N_B}{1 + (H/K_-) \exp(- e\psi_s/kT)} . \tag{2.17}$$

This can be considered as an adsorption isotherm of the PDI (H^+) which, for a given bulk pH, relates the surface charge density to the surface potential.

For a bulk concentration c (moles/litre) of positive or negative species (PDI + inert supporting electrolyte) the net volume charge density ρ (cm^{-3}) at the point where the potential is ψ is (N = Avogadro's number)

$$\rho = 10^{-3} Nec[\exp(- e\psi/kT) - \exp(e\psi/kT)] . \tag{2.18}$$

The potential is in turn related to the charge density by Poisson's equation

$$\nabla^2\psi = -\frac{4\pi}{\varepsilon}\rho \ , \tag{2.19}$$

where ε is the dielectric constant of the solvent.

We shall examine the behaviour of the surface charge, surface potential and the free energy of interaction of two identical amphoteric flat surfaces as a function of their separation. We set up a system of Cartesian axes with the origin midway between the surfaces which are situated at $z = \pm L$. From the symmetry of the problem, we can confine our attention to the region $0 \leqslant z \leqslant L$. Combining equations (2.18) and (2.19) (in one dimension) we get

$$\frac{d^2\psi}{dz^2} = \frac{4\pi\ Nec}{10^3\varepsilon}\left[\exp(e\psi/kT) - \exp(-e\psi/kT)\right] . \tag{2.20}$$

which must be solved together with the boundary conditions

$$\left.\frac{d\psi}{dz}\right|_{z=L} = \frac{4\pi\sigma}{\varepsilon} \tag{2.21}$$

$$\left.\frac{d\psi}{dz}\right|_{z=0} = 0 \ . \tag{2.22}$$

In terms of the reduced variables

$$y = e\psi/kT \tag{2.23}$$

$$x = \kappa z \tag{2.24}$$

and

$$\kappa^2 = \frac{8\pi\ Ne^2 c}{10^3\varepsilon\ kT} \ , \tag{2.25}$$

where κ is the inverse Debye screening length, equation (2.20) becomes

$$\frac{d^2y}{dx^2} = \sinh y \ . \tag{2.26}$$

A first integration together with equation (2.22) gives

$$\left(\frac{dy}{dx}\right)^2 = 2(\cosh y - \cosh y_0) \ , \tag{2.27}$$

where $y_0 = e\psi(0)/kT$ is the reduced mid-plane potential. The remainig boundary condition (2.21) gives

$$\left(\frac{4\pi e}{\varepsilon\kappa\ kT}\right)^2 \sigma^2 = 2(\cosh y_L - \cosh y_0) , \qquad (2.28)$$

where $y_L = e\psi(L)/kT = e\psi_s/kT$ is the reduced surface potential.

The second integral of (2.27) can now be taken. The mathematics involved is straightforward. The details are given in a number of papers.[49] A substitution

$$\phi = \exp(-e|\psi|/2kT) = \exp(-|y|/2) \qquad (2.29)$$

enables us to write the solution in the form

$$\phi(z) = \phi_0\ \mathrm{cd}\left(\frac{\kappa z}{2\phi_0}; \phi_0^2\right) , \qquad (2.30)$$

where cd(x;k) is a Jacobi elliptic function of argument x and modulus k.[50,51] In particular, using

$$\phi_0 = \phi(0) = \exp(-e|\psi(0)|/2kT) = \exp(-|y_0|/2) \qquad (2.31)$$

and

$$\phi_L = \phi(L) = \exp(-e|\psi(L)|/2kT) = \exp(-|y_L|/2) \qquad (2.32)$$

$$= \phi_0\ \mathrm{cd}\left(\frac{\kappa L}{2\phi_0}; \phi_0^2\right) = \exp(-e|\psi_s|/2kT) \qquad (2.33)$$

equation (2.28) becomes

$$\left(\frac{4\pi e}{\varepsilon\kappa\ kT}\right)^2 \sigma^2 = (\phi_L^2 + \phi_L^{-2}) - (\phi_0^2 + \phi_0^{-2}) . \qquad (2.34)$$

Equations (2.17), (2.33) and (2.34) constitute a single transcendental equation to be solved for ϕ_0. Thus given the bulk concentrations of PDI (or equivalently, the value of the surface potential at infinite separation) and supporting inert electrolyte, the surface potential ψ_s and the surface charge density σ may be found self-consistently as a function of the separation (2L).

Using the small argument asymptotic forms of the Jacobi elliptic functions[51]

$$cd(x;k) \simeq 1 + O(x^2) + \ldots \tag{2.35}$$

it follows immediately from equations (2.17) and (2.34) that as $L \to 0$ (for fixed κ), $\sigma \to 0$, and the surface potential is given by a Nernst equation:[6]

$$\psi(0) \to \psi_s \to 2.303 \frac{kT}{e} (pH_0 - pH) \ . \tag{2.36}$$

Here the constant H_0 is given by

$$H_0 = \left(\frac{N_B}{N_A}\right)^{1/2} (K_+K_-)^{1/2}[(1+\gamma^2)^{1/2} + \gamma] \ , \tag{2.37}$$

where

$$\gamma = \tfrac{1}{2}\left(1 - \frac{N_A}{N_B}\right)\left(\frac{K_- N_B}{K_+ N_A}\right)^{1/2} \ . \tag{2.38}$$

In the *absence* of specific adsorption (apart from PDI) pH_0 *will* be the bulk pH corresponding to the point-of-zero charge (pzc).

In view of result (2.36), the repulsive pressure between the surfaces[2,13]

$$P = \frac{2Nckt}{10^3} [\cosh(e\psi(0)/kT) - 1] \tag{2.39}$$

remains finite for all separations.

The above analysis, where the acidic and basic groups are distinct chemical species, is applicable to bio-colloids ($BH = -COOH$, $AH^+ = -NH_3^+$). However, there are a large number of hydrous oxide colloids where the same surface group can dissociate to give both positive and negative sites (e.g. TiO_2, Fe_2O_3, Al_2O_2 and SiO_2). In general, these dissociation processes have the form

$$\left.\begin{aligned} AH_2^+ &\rightleftharpoons AH + H^+ \qquad (K_+) \\ AH &\rightleftharpoons A^- + H^+ \qquad (K_-) \end{aligned}\right\} \ . \tag{2.40}$$

Now the above analysis still holds except that equation (2.17) for the surface charge density should be replaced by (N_s amphoteric surface

groups/cm^2)

$$\sigma = eN_s \frac{(H/K_+) \exp(-e\psi_s/kT) - (K_-/H) \exp(e\psi_s/kT)}{1 + (H/K_+) \exp(-e\psi_s/kT) + (K_-/H) \exp(e\psi_s/kT)} . \quad (2.41)$$

And as before as $L \to 0$

$$\psi(0) \to \psi_s \to 2.303 \frac{kT}{e} (pH_0 - pH) , \quad (2.36)$$

where

$$pH_0 = \tfrac{1}{2}(pK_- + pK_+) . \quad (2.42)$$

3. RESULTS AND DISCUSSIONS

In order to examine the effect of regulation on the surface charge and potential, it is necessary to select values for the dissociation constants K_+ and K_-. An example of particular practical importance involves aqueous suspensions of hydrous oxides where H^+ are PDI.[52] It is appropriate to consider two typical classes of surfaces for which $\Delta pK \equiv pK_- - pK_+$ is small, $\Delta pK = 3$ say and, for which ΔpK is large $\Delta pK = 6$. Since it is important, for the purposes of comparison, to keep κ constant while varying pH over a wide range, we have selected the following two cases:

$$\text{(A)} \quad pH_0 = 7 , \quad pK_+ = 5.5 , \quad pK_- = 8.5 , \quad \Delta pK = 3$$

$$\text{(B)} \quad pH_0 = 7 , \quad pK_+ = 4 , \quad pK_- = 10 , \quad \Delta pK = 6 .$$

We also took the density of surface sites N_s to be[52]

$$N_s = 5 \times 10^{14} \text{ cm}^{-2} .$$

Using the above data we calculated the surface potential, surface charge and the free energy of interaction as a function of the particle separation.

The variation of the surface potential ψ_s with separation for 10^{-3} M electrolyte ($1/\kappa = 96$ Å) for cases (A) and (B) is shown in

Figures 3.1 and 3.2 respectively. The variation of the surface charge density σ with separation is shown in Figure 3.3 for several values of the surface potential at infinite separation. The effect of different ionic strengths on the variation of ψ_s with separation is shown in Figures 3.4 and 3.5 for concentrations of 10^{-2} and 10^{-4} M at $\Delta pK = 6,3$.

In Figure 3.6 we compare the interaction under constant charge with that under the present regulation mechanism. The dashed lines represent the variation in surface potential for interaction at constant charge corresponding to the same surface potential at infinite separations. The ionic strength is 10^{-3} M, $\Delta pK = 3$, $pH_0 = 6$. In Figure 3.7 we compare the electrostatic free energy of interaction (per unit area) obtained from integrating numerically the repulsive pressure given by equation (2.39). The result of the present theory (V^{Reg}) is contrasted with those obtained using the constant charge (V^{σ}) and constant potential (V^{ψ}) approach. We now proceed to comment on the results and discuss their implications in detail.

3a. The Mechanism of Regulation

The present model of two interacting double layers differs from earlier models in that the association/dissociation of surface groups provides a mechanism whereby electrochemical potentials are kept constant during interaction. Equilibrium is maintained throughout the interaction by the self-consistent relationship between the surface charge and the surface potential (equation (2.17) or (2.41)). Thus this surface regulation model is not interaction at constant potential but interaction while maintaining equilibrium.

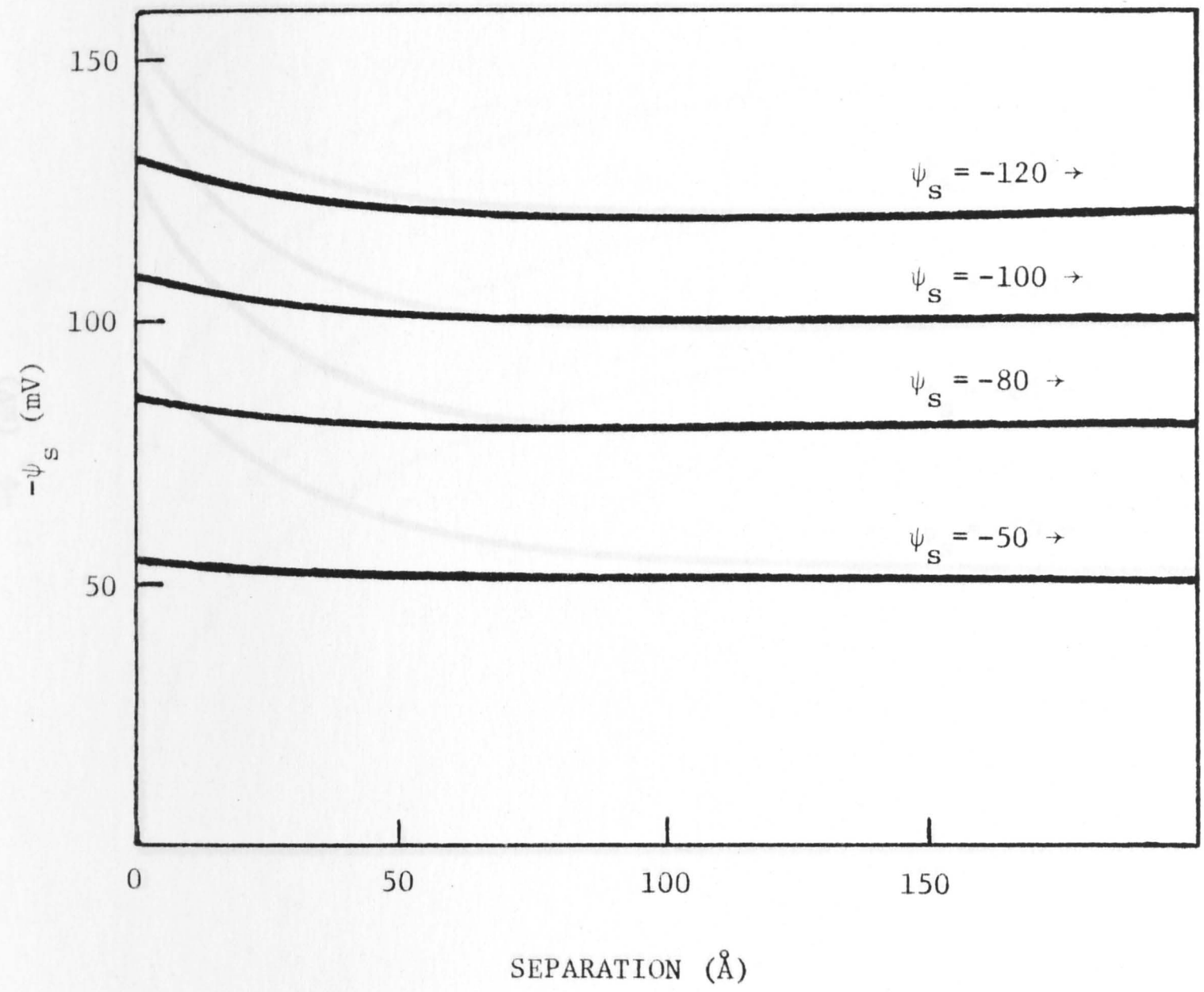

Figure 3.1: Variation of the surface potential ψ_s with distance of separation of two surfaces having points of zero charge at pH 7 for $\Delta pK = 3$ and 10^{-3} M ionic strength. The potentials shown at the right on each curve are the potentials at infinite separation.

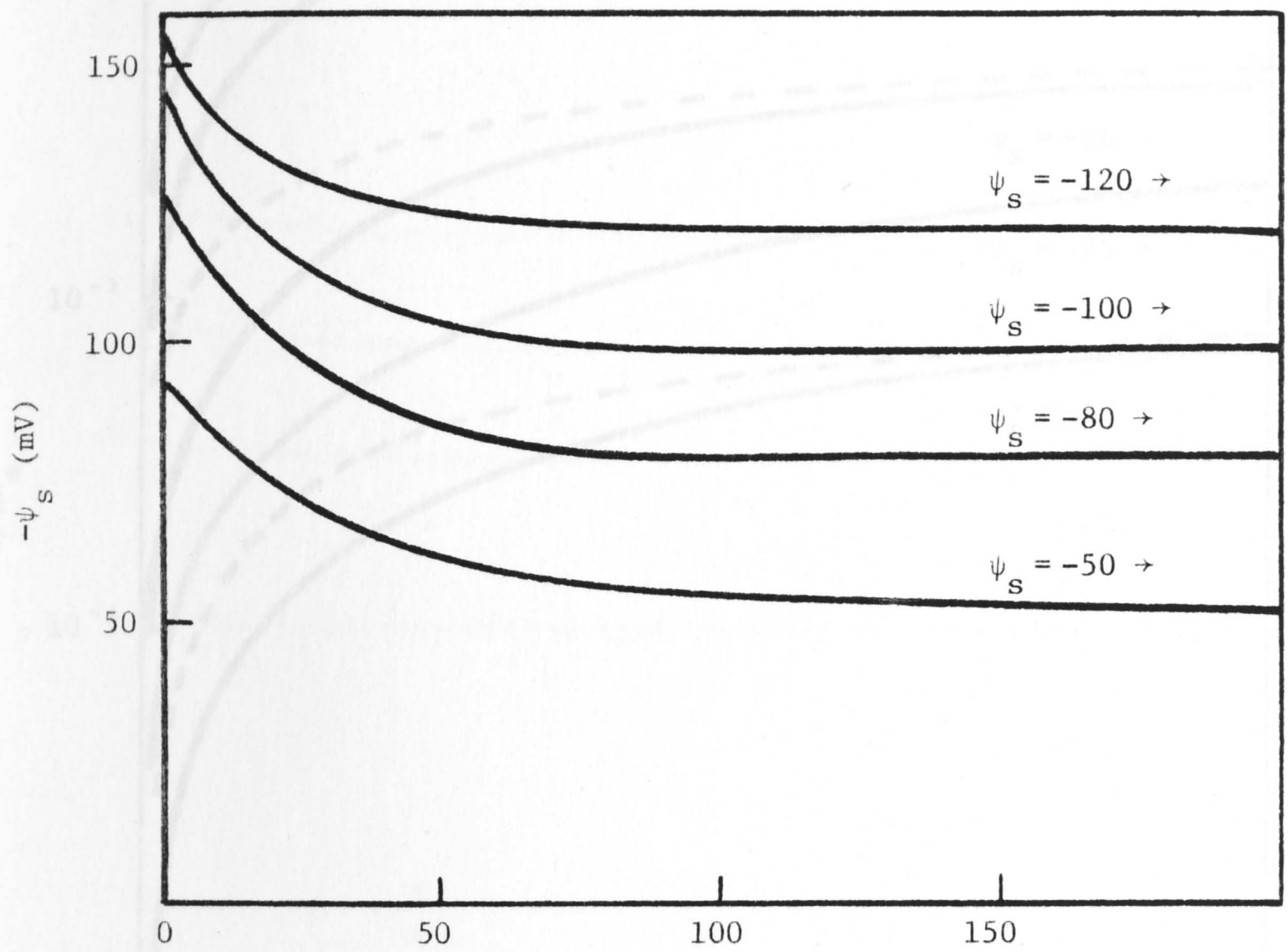

Figure 3.2: Variation of the surface potential ψ_s with distance of separation of two surfaces having points of zero charge at pH 7 for $\Delta pK = 6$ and 10^{-3} M ionic strength. The potentials shown at the right on each curve are the potentials at infinite separation.

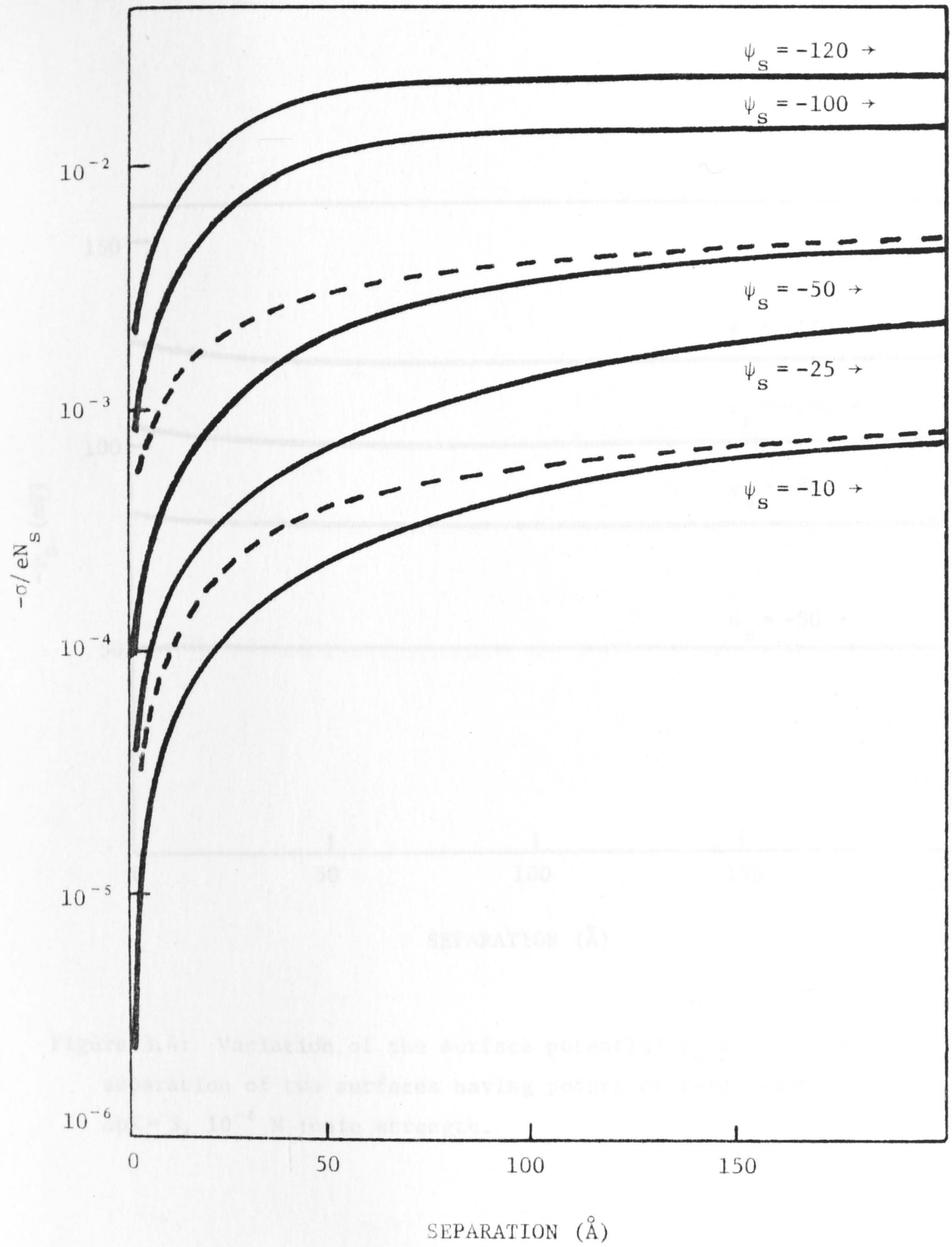

Figure 3.3: Variation of the surface charge σ with distance of separation of two surfaces having points of zero charge at pH 7 for ΔpK = 3 (solid lines) and ΔpK = 6 (dashed lines). The potentials shown at the right on each curve are the potentials (mV) at infinite separation. The ionic strength is 10^{-3} M in all cases.

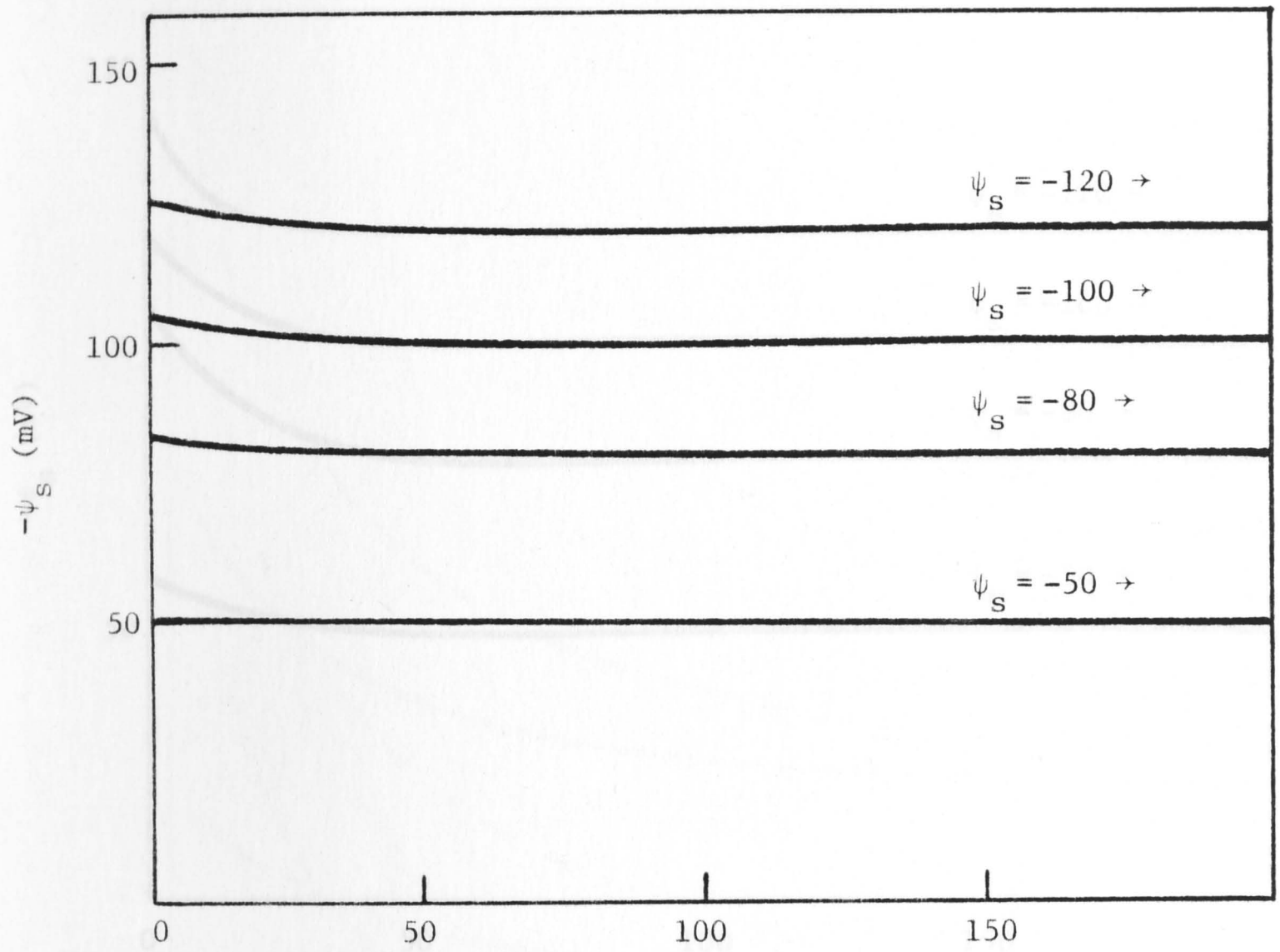

Figure 3.4: Variation of the surface potential ψ_s with distance of separation of two surfaces having points of zero charge of 7 and for $\Delta pK = 3$, 10^{-4} M ionic strength.

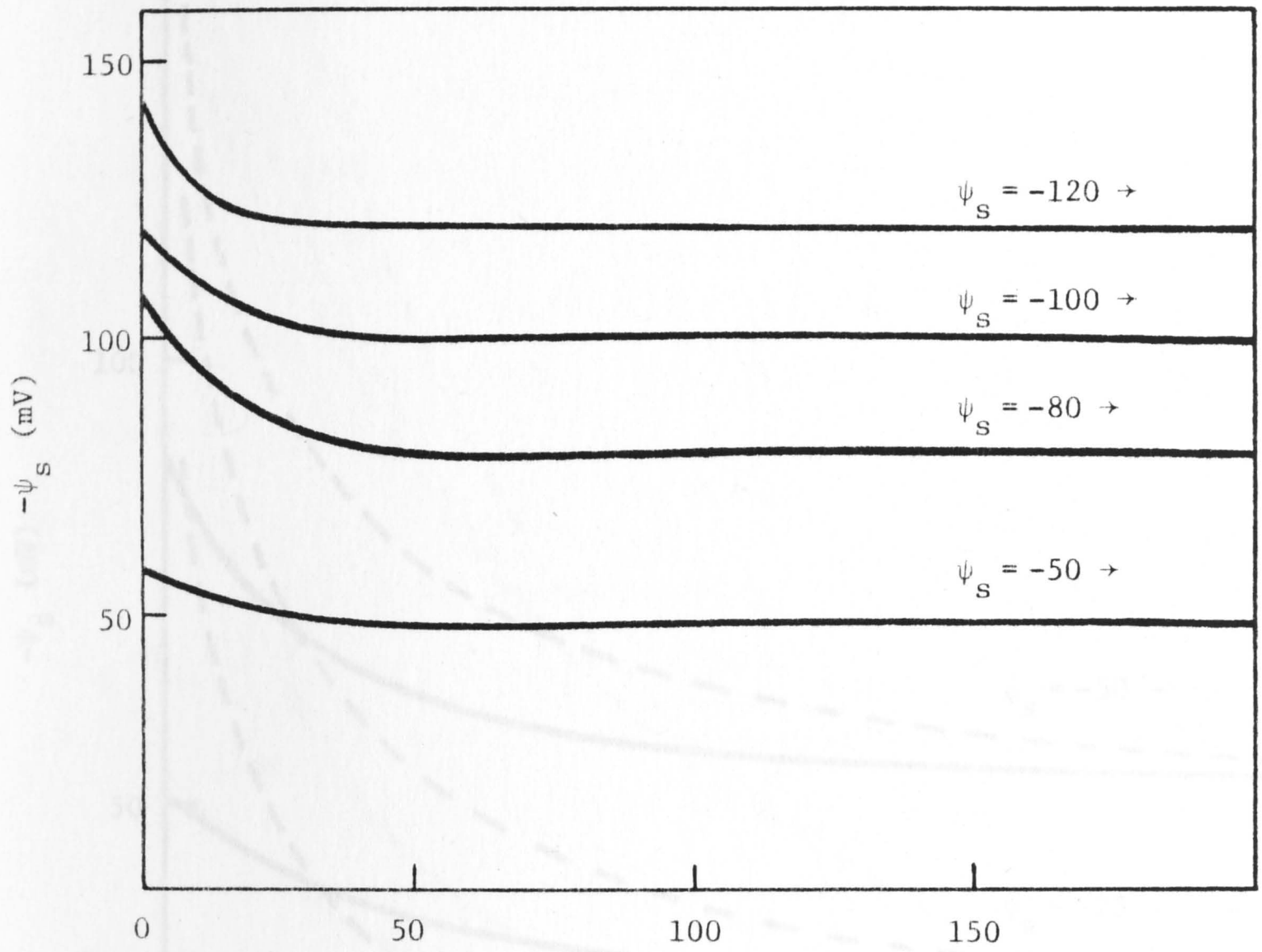

Figure 3.5: Variation of the surface potential ψ_s with distance of separation of two surfaces having points of zero charge of 7 and for $\Delta pK = 6$, 10^{-2} M ionic strength.

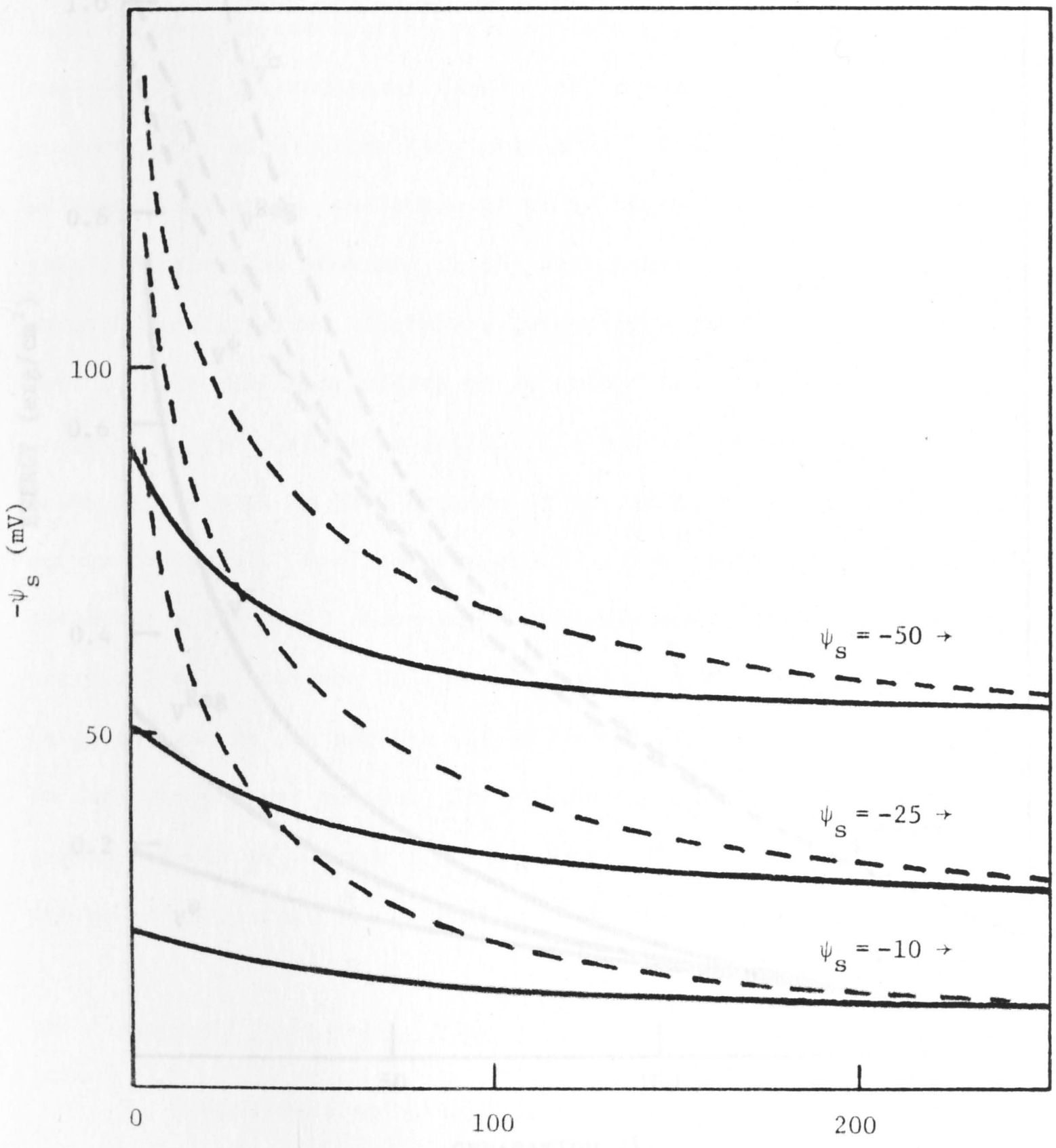

Figure 3.6: Comparison of the change in surface potential ψ_s during interaction under constant charge conditions (dashed lines) and under regulated interaction (solid lines). The ΔpK, ionic strength and point of zero charge are 6, 10^{-3} M and pH 6 respectively.

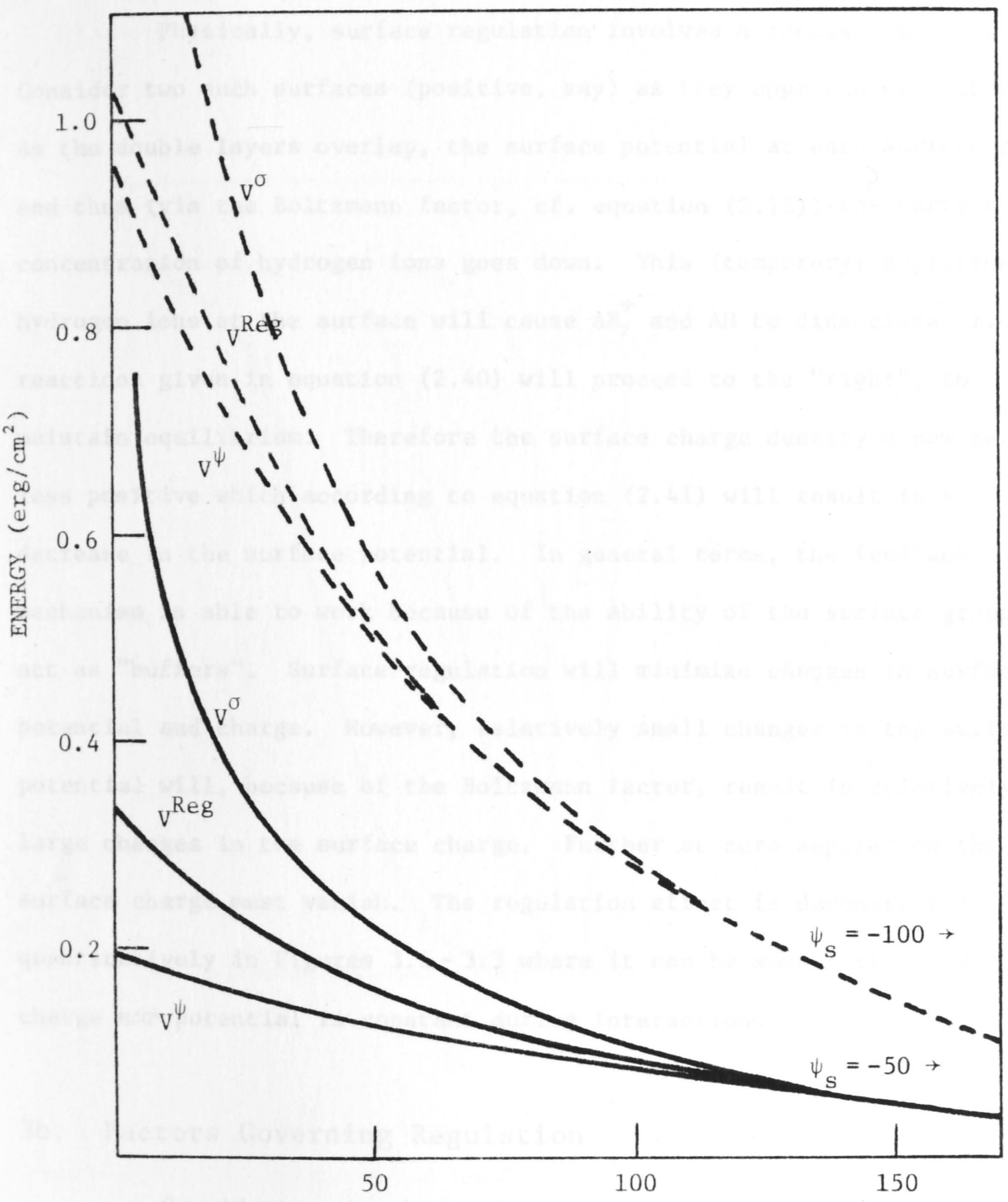

Figure 3.7: Comparison of the electrostatic free energy (per unit area) of interaction as a function of separation for interaction under constant charge (V^{σ}), constant potential (V^{ψ}) and under regulation (V^{Reg}) imposed by $\Delta pK = 3$ (dashed lines) and $\Delta pK = 6$ (solid lines) at pzc 7. In all cases, the ionic strength is 10^{-3} M. The potentials shown at the right of each set of curves are the potentials at infinite separation.

Physically, surface regulation involves a feedback mechanism. Consider two such surfaces (positive, say) as they approach each other. As the double layers overlap, the surface potential at each surface rises and thus (via the Boltzmann factor, cf. equation (2.15)) the surface concentration of hydrogen ions goes down. This (temporary) depletion of hydrogen ions at the surface will cause AH_2^+ and AH to dissociate, i.e. reactions given in equation (2.40) will proceed to the "right", to maintain equilibrium. Therefore the surface charge density σ now becomes less positive which according to equation (2.41) will result in a decrease in the surface potential. In general terms, the feedback mechanism is able to work because of the ability of the surface groups to act as "buffers". Surface regulation will minimize changes in surface potential and charge. However, relatively small changes in the surface potential will, because of the Boltzmann factor, result in relatively large changes in the surface charge. Further at zero separation the surface charge must vanish. The regulation effect is demonstrated quantitatively in Figures 3.1 - 3.3 where it can be seen that *neither* charge *nor* potential is constant during interaction.

3b. Factors Governing Regulation

Considering the change in potential with separation (Figures 3.1 and 3.2), it can be seen that the ability of the surface to regulate depends strongly on ΔpK: as ΔpK increases the ability to regulate decreases. The result can best be understood by considering Figure 3.8 where the magnitude of the (reduced) net surface charge is plotted against the surface pH which is given by (cf. equations (2.16) and (2.41))

$$pH_s = pH + \frac{e}{2.303\ kT}\ \psi_s \ . \qquad (3.1)$$

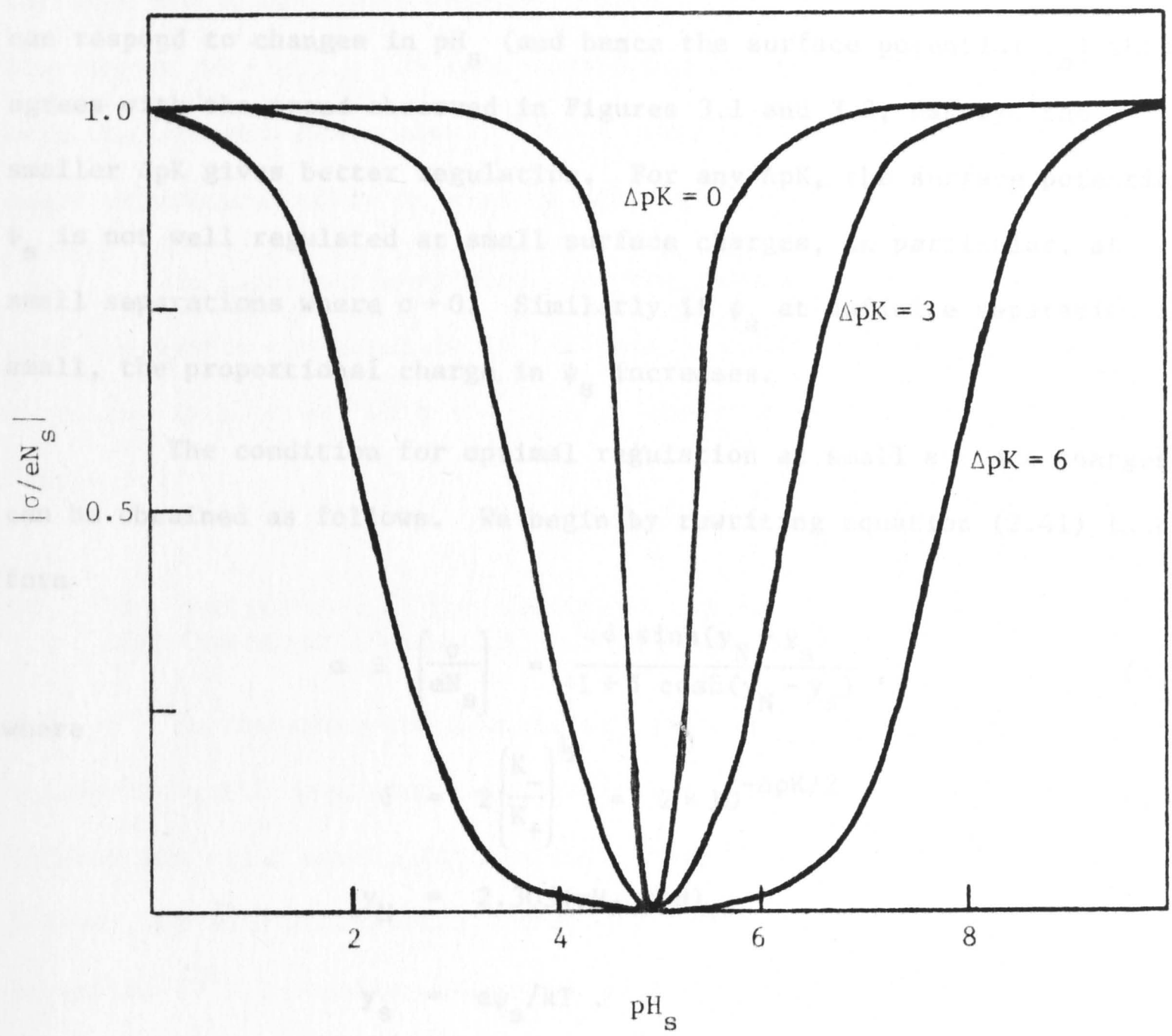

Figure 3.8: Variation of the magnitude of the reduced surface charge $|\sigma/eN_s|$ with surface pH (as defined by equation (3.1)) for ΔpK of 6, 3 and 0. The point of zero charge is taken as pH 7.

Three cases are shown $\Delta pK = 6,3,0$. The region where the surface charge σ is an insensitive function of pH_s (i.e. where $pH_s \approx pH_0$) increases as ΔpK increases. As the ability to regulate depends on the degree to which σ can respond to changes in pH_s (and hence the surface potential ψ_s) this agrees with the trend observed in Figures 3.1 and 3.2, namely, the smaller ΔpK gives better regulation. For any ΔpK, the surface potential ψ_s is not well regulated at small surface charges, in particular, at small separations where $\sigma \to 0$. Similarly if ψ_s at infinite separation is small, the proportional charge in ψ_s increases.

The condition for optimal regulation at small surface charges can be obtained as follows. We begin by rewriting equation (2.41) in the form

$$\alpha \equiv \left(\frac{\sigma}{eN_s}\right) = \frac{\delta \sinh(y_N - y_s)}{1 + \delta \cosh(y_N - y_s)} , \tag{3.2}$$

where

$$\delta = 2\left(\frac{K_-}{K_+}\right)^{\frac{1}{2}} = 2 \times 10^{-\Delta pK/2} \tag{3.3}$$

$$y_N = 2.303(pH_0 - pH) \tag{3.4}$$

$$y_s = e\psi_s/kT . \tag{3.5}$$

At low surface charges ($|\alpha| << 1$) we must have $y_s \approx y_N$ (cf. equation (2.36)). Clearly the condition for optimal regulation in this regime is when the surface charge is most sensitive to variations in the surface potential y_s. That is, when $|d\alpha/dy_s|$ evaluated at $y_s = y_N$ is a maximum. From equation (3.2) we obtain

$$\left|\frac{d\alpha}{dy_s}\right|_{y_s=y_N} = \left|\frac{\delta}{1+\delta}\right| < 1 . \tag{3.6}$$

It is clear then that optimal regulation is when $\delta \to \infty$, that is, when $\Delta pK \to -\infty$. In this limit the surface charge has the simple form

$$\sigma = eN_s \tanh(y_N - y_s) \quad . \tag{3.7}$$

At large values of $|\psi_s|$ where $pH_s >> pK_-$ or $pH_s << pK_+$ the surfaces are almost fully charged ($|\sigma/eN_s| \lesssim 1$) and σ is an insensitive function of pH_s or ψ_s. In this regime regulation will also be poor. Here the system behaves almost like a constant charge approach until at small separations where regulation will occur to reduce σ to zero.

An important consequence of the regulated interaction is that, when the system can regulate, ψ_s is kept remarkably constant during approach, in contrast with the case at constant surface charge, Figure 3.6.

3c. The Validity of the Constant Charge and Constant Potential Approximation

In comparing the (repulsive) electrostatic free energy of interaction, the regulated case should give the lowest energy of interaction since equilibrium is maintained at all distances of approach. However, we note in Figure 3.7 that the interaction under constant potential (V^{ψ}) is smaller than that under regulation (V^{Reg}). Clearly this is a physical impossibility. Further we note that a bigger ΔpK gives a larger deviation of V^{ψ} from V^{Reg}. The reason for this apparent error is that the constant potential assumption is invalid for the amphoteric systems considered here. There are, however, circumstances under which the constant potential assumption holds approximately. We now consider this case.

The constant potential case is in fact perfect regulation as was stressed by Verwey and Overbeek.[2] From equations (2.16) and (2.40) it follows that

$$\psi_s = 2.303 \frac{kT}{e} (pH_0 - pH) - \frac{kT}{2e} ln\left(\frac{[AH_2^+]}{[A^-]}\right) . \qquad (3.8)$$

This equation, in a slightly different form, has been discussed in detail by Levine and Smith.[39] The ln term represents a correction to the Nernst equation

$$\psi_s = 2.303 \frac{kT}{e} (pH_0 - pH) \qquad (3.3)$$

or equivalently to the constant potential approximation. Provided $[AH_2^+]/[A^-]$ is close enough to unity (at the pzc $\sigma = 0$, $[AH_2^+]/[A^-] = 1$, and the Nernst equation holds, see equation (2.36)) for the ln term to be negligible, the Nernst equation or the constant potential approach is valid. In the language of Levine and Smith, the correction to the Nernst equation is small provided the fraction of *neutral* sites at the pzc is small.

On the other hand, the constant charge approximation is a good description of the interaction process when collision times are sufficiently short such that the surfaces do not have time to make adjustments. The interaction will no longer be at equilibrium. Therefore the energy of interaction V^{σ} is higher than that at equilibrium V^{Reg} (Figure 3.7).

3d. Summary

The regulated approach of identical double layer interaction has two important limits. For systems where the Nernst equation is sensibly obeyed at infinite separation the interaction is to a good approximation at constant potential. If the surface potential ψ_s is in the regime of surface charge and potential such that σ is insensitive to changes in ψ_s, the interaction is effectively at constant charge until ψ_s enters the sensitive regimes, usually at smaller separations. Also if

the rate of attainment of equilibrium is smaller than the rate of approach of the two surfaces, the system cannot adjust during the "time of collision" and the constant charge interaction is appropriate.

If particles cross a coagulation barrier that is due to a constant charge interaction, the surface of particles in aggregate will then have time to equilibrate their surface potential and aging under regulation will occur. If the potential energy barrier under constant charge conditions is of the order of or greater than the average kinetic energy of the particles, then the velocity of approach may become slow enough that a change during collision from constant charge to regulated interaction is possible. The potential energy barrier under regulated interaction is lower than that under constant charge approach and instabilities that would not otherwise be predicted under constant charge approach may be observed.

In the above analysis we have not accounted properly for the inner region of the surface layer although there are a number of models that can adequately characterize the surface (ζ potential and titratable charge).[39,42,52-55] These models invoke the concept of site binding of inert ions or the existence of a surface gel layer. These in themselves provide further regulation of surface charge and potential. Here we have been interested mainly in studying the consequences and implications of surface regulation and it is not necessary at this stage to model the surface region with a more sophisticated theory. We anticipate that inclusion of these additional features would not drastically alter the main conclusions.

REFERENCES

(1) B.V. Derjaguin and L.D. Landau, *Acta Physicochim.* USSR 14, 633 (1941).

(2) E.J.W. Verwey and J.Th.G. Overbeek, *Theory of the Stability of Lyophobic Colloids*, Elsevier, Amsterdam (1948).

(3) D.J. Shaw, *Introduction to Colloid and Surface Chemistry*, Butterworth (1970).

(4) A.L. Smith, in *Dispersions of Powders in Liquids* (G.D. Parfitt, ed.), Applied Science, London (1973).

(5) G. Frens, D.J.C. Engel and J.Th.G. Overbeek, *Trans. Farad. Soc.* 63, 148 (1967).

(6) G. Frens and J.Th.G. Overbeek, *J. Coll. Interface Sci.* 38, 376 (1972).

(7) S. Levine and A. Suddaby, *Proc. Phys. Soc.* 64A, 287 (1951); *Proc. Phys. Soc.* 65A, 405 (1952).

(8) S. Levine and G.M. Bell, *J. Coll. Interface Sci.* 17, 838 (1962).

(9) S. Levine and G.M. Bell, *J. Phys. Chem.* 67, 1408 (1963).

(10) J.E. Jones and S. Levine, *J. Coll. Interface Sci.* 30, 241 (1969).

(11) E.P. Honig and P.M. Mul, *J. Coll. Interface Sci.* 36, 258 (1971).

(12) G.M. Bell and G.C. Peterson, *J. Coll. Interface Sci.* 41, 542 (1972).

(13) V.A. Parsegian and D. Gingell, *Biophys. J.* 12, 1192 (1972).

(14) J. Gregory, *J. Chem. Soc., Faraday II* 69, 1723 (1973).

(15) G. Kar, S. Chander and T.S. Mika, *J. Coll. Interface Sci.* 44, 347 (1973).

(16) S. Usui, *J. Coll. Interface Sci.* 44, 107 (1973).

(17) H. Ohshima, *Colloid and Polymer Sci.* 252, 158 (1974); *Colloid and Polymer Sci.* 252, 257 (1974).

(18) N.E. Hoskin and S. Levine, *Phil. Trans. Roy. Soc. London* A248, 449 (1956).

(19) R. Hogg, T.W. Healy and D.W. Fuerstenau, *Trans. Farad. Soc.* 62, 1638 (1966).

(20) K.J. Ives and J. Gregory, *Proc. Soc. Water Treat Exam* 15, 288 (1966).

(21) G.M. Bell, S. Levine and L.N. McCartney, *J. Coll. Interface Sci.* 33, 335 (1970).

(22) G.R. Wiese and T.W. Healy, *Trans. Farad. Soc.* 66, 490 (1970).

(23) G.M. Bell and S. Levine, *Trans. Farad. Soc.* 53, 143 (1957); *Trans. Farad. Soc.* 54, 785 (1958); *Trans. Farad. Soc.* 54, 975 (1958).

(24) C.S. Chen and S. Levine, *J. Chem. Soc., Faraday II* 68, 1497 (1972).

(25) G.M. Bell and S. Levine, *J. Chem. Phys.* 49, 4584 (1968).

(26) P. Richmond, *J. Chem. Soc., Faraday II* 70, 1066 (1974).

(27) P. Richmond, *J. Chem. Soc., Faraday II* (to appear).

(28) S.L. Brenner and V.A. Parsegian, *Biophys. J.* 14, 327 (1974).

(29) G.F. Elliot, *J. Theor. Biol.* 21, 71 (1968).

(30) V.A. Parsegian, *Trans. Farad. Soc.* 62, 848 (1966).

(31) A. Bierman, *J. Coll. Sci.* 10, 231 (1955).

(32) B.W. Ninham and V.A. Parsegian, *J. Theor. Biol.* 31, 405 (1971).

(33) R.J. Pugh and J.A. Kitchener, *J. Coll. Interface Sci.* 35, 656 (1971).

(34) G.D. Parfitt, J.A. Wood and R.T. Ball, *J. Chem. Soc., Faraday I* 69, 1908 (1973).

(35) G.D. Parfitt, *Croatica Chemica Acta* 42, 215 (1970).

(36) J.B. Melville, E. Willis and A.L. Smith, *J. Chem. Soc., Faraday I* 68, 450 (1972); see also, for example, references (10), (19) and (22).

(37) J.W. Bowden, M.D.A. Bollard, A.M. Poser and J.P. Quirk, *Nature (Physical Science)* 245, 81 (1973).

(38) R.H. Ottewill and J.N. Shaw, *Kolloid Z.* 218, 34 (1967).

(39) S. Levine and A.L. Smith, *Disc. Farad. Soc.* 52, 290 (1971).

(40) R.J. Hunter and H.J.L. Wright, *J. Coll. Interface Sci.* 37, 565 (1971).

(41) H.J.L. Wright and R.J. Hunter, *Aust. J. Chem.* 26, 1183 (1973); *Aust. J. Chem.* 26, 1191 (1973).

(42) D.E. Yates, S. Levine and T.W. Healy, *J. Chem. Soc., Faraday II* (to appear).

(43) E.A. Moelwyn-Hughes, *Physical Chemistry*, Pergamon Press, 2nd ed. (1969); see also reference (39).

(44) S.L. Brenner and D.A. McQuarrie, *J. Coll. Interface Sci.* 44, 298 (1973); *J. Theor. Biol.* 39, 343 (1973); *Biophys. J.* 13, 301 (1973).

(45) D.G. Hall, *J. Chem. Soc., Faraday II* 68, 2169 (1972).

(46) S.G. Ash, D.H. Everett and C. Radke, *J. Chem. Soc., Faraday II* 69, 1256 (1973).

(47) R. Simon and L. Bass, *J. Chem. Soc., Faraday II* 68, 1872 (1972).

(48) H.P. Boehm, *Disc. Farad. Soc. (Surface Chemistry of Oxides)* 52, 264 (1971) and the discussion that follows. In particular, the comments by P.W. Schindler and H. Gamsjuger, *ibid.*, 52, 286 (1971).

(49) See, for example, references (2), (7) and (32).

(50) E.T. Whittaker and G.N. Watson, *A Course of Modern Analysis*, Cambridge U.P. (1969).

(51) M. Abramowitz and I.A. Stegun, *Handbook of Mathematical Functions*, Dover, N.Y. (1965).

(52) J.W. Perram, R.J. Hunter and H.J.L. Wright, *Aust. J. Chem.* 27, 461 (1974).

(53) J.W. Perram, R.J. Hunter and H.J.L. Wright, *Chem. Phys. Lett.* 23, 265 (1973).

(54) J.W. Perram, *J. Chem. Soc., Faraday II* 69, 993 (1973).

(55) Frumkin and Gorodetzkaja, *Acta Physicochim.* 9, 327 (1938).

(56) I. Langmuir, *J. Chem. Phys.* 6, 893 (1938).

(57) Bergmann, Low-Beer and Zucher, *J. Physik Chem. A* 781, 301 (1938).

(58) B.V. Derjaguin, *Acta Physicochim.* 10, 333 (1939); *Trans. Farad. Soc.* 36, 203 (1940).

(59) G.W. Castellan, *Physical Chemistry*, Addison-Wesley, Reading, Mass. (1972).

CHAPTER 2

DOUBLE LAYER INTERACTIONS UNDER SURFACE IONIZATION EQUILIBRIUM – DISSIMILAR SURFACES

1. INTRODUCTION

In a variety of situations that involve particles of colloidal dimensions, for instance, in fibrous bed filtration of emulsions,[1,2] mineral flotation and separation, flocculation of mixed sols, and cell adhesion,[3] it is necessary to understand the interaction between dissimilarly charged particles.

In the previous chapter, we have considered in detail the electrical double layer interaction between two identically charged planar surfaces. We studied the interaction at equilibrium, in particular, where the surface charge and surface potential are related self-consistently by surface ionization processes. In essence, this approach includes the contribution of the surface chemical potential in the thermodynamic argument that connects the surface potential and the bulk concentration of potential determining ions (PDI).[10,17,27,28] The constant potential and constant charge boundary conditions emerge as special limits. Here we extend this theory to include interacting dissimilar amphoteric surfaces.

The problem of interacting dissimilar double layers has been considered by a number of authors.[4-15,26] In all instances, the constant charge or constant potential boundary condition was employed. It has been recognized for some time that these boundary conditions lead to an infinitely large surface potential or surface charge, as the case may be, at small inter-particle separations. This difficulty can be avoided by invoking some minimum cut-off in the separation[16] or, perhaps more satisfactorily, by a proper consideration of the chemical potential

of adsorbed ionic species at the surface.[17,18-19] It is interesting to note, in particular, the work of Bierman[17] who derived a Langmuir-type isotherm describing the adsorption of cations. This theory gave the surface potential as a function of the surface concentration of adsorbed species, i.e. the surface charge. Although the mechanism of adsorption was not specified, he was able to conclude that for interacting planar double layers, the surface potentials become equal when the separation approaches zero while the surface charges become equal in magnitude but opposite in sign. In the special case where the two surfaces have the same isoelectric point, the surface potentials at zero separation are equal and are given by the Nernst equation (cf. results of the previous chapter). Both surface charges reduce to zero in this limit.

Using the notions developed in the preceding chapter, we consider the double layer interaction between two dissimilar amphoteric surfaces. As before, we adopt the idea that each surface develops a surface charge via dissociation equilibrium of the amphoteric surface groups.[20-23,27,28] The reactions may be written as:

$$AH_2^+ \rightleftharpoons AH + H^+ \tag{1.1}$$

$$AH \rightleftharpoons A^- + H^+ . \tag{1.2}$$

Although the discussion is independent of the type of PDI, we shall assume they are (univalent) hydrogen ions as, for example, in hydrous metallic oxides.[24] We assume that, for each reaction, the ratios of the concentration of surface species are given by some surface dissociation constants:

$$\frac{[AH][H^+]_s}{[AH_2^+]} = K^+ \tag{1.3}$$

$$\frac{[A^-][H^+]_s}{[AH]} = K_- . \tag{1.4}$$

The dissociation constants K_+, K_- are assumed to be only functions of temperature and pressure. The validity of equations (1.3) and (1.4) has been discussed in the previous chapter.

For N_s surface groups per unit area, the net surface charge density is (e = protonic charge)

$$\sigma = eN_s \frac{[AH_2^+] - [A^-]}{[AH] + [AH_2^+] + [A^-]} \equiv eN_s\alpha \ . \qquad (1.5)$$

The fraction α, defined by equation (1.5), can assume any value between plus and minus one.

In the Gouy-Chapman approximation, which we shall adopt, the concentration of ionic species at any point is related to the bulk value by the Boltzmann factor $\exp(-e\psi/kT)$. The electrostatic potential ψ is measured with respect to the value at the reservoir (taken to be zero). In particular, the surface concentration of PDI is

$$[H^+]_s = H \exp(-e\psi_s/kT) \ , \qquad (1.6)$$

where H is the bulk concentration of PDI and ψ_s is the surface potential. Combining equations (1.3), (1.4) and (1.6) the surface charge can be written as

$$\sigma = eN_s \frac{(H/K_+) \exp(-e\psi_s/kT) - (K_-/H) \exp(e\psi_s/kT)}{1 + (H/K_+) \exp(-e\psi_s/kT) + (K_-/H) \exp(e\psi_s/kT)} \ . \qquad (1.7)$$

This is identical to equation (2.41) in the previous chapter. Given the dissociation constants, K_+ and K_- which characterizes the surface, and the bulk concentration of PDI, equation (1.7) represents a canonical relationship between the values of the surface charge and the surface potential. It is used in place of the constant charge or potential boundary condition for solving the Poisson-Boltzmann (PB) equation that governs the distribution of the diffuse layer. If during the interaction

the surface potential changes from ψ_s to ψ_s' the surface charge will change from σ to σ', where (ψ_s,σ) and (ψ_s',σ') must satisfy equation (1.7). Thus equation (1.7) is an "equation of state" of the surface. It specifies all possible values of the "co-ordinate" (ψ_s,σ).

It is instructive to rewrite equation (1.7) in the form

$$\sigma = eN_s \frac{\delta \sinh[e(\psi_N - \psi_s)/kT]}{1+\delta \cosh[e(\psi_N - \psi_s)/kT]} \equiv eN_s\alpha , \qquad (1.8)$$

where

$$\delta = 2\times 10^{-\Delta pK/2} = 2\left(\frac{K_-}{K_+}\right)^{\frac{1}{2}} \qquad (1.9)$$

and

$$\Delta pK = pK_- - pK_+ . \qquad (1.10)$$

We shall call the potential

$$\psi_N = \frac{kT}{e} 2.303\ (pH_0 - pH) \qquad (1.11)$$

the Nernst potential since it is related to the point-of-zero-charge (pzc)

$$pH_0 = \tfrac{1}{2}(pK_+ + pK_-) \qquad (1.12)$$

by the Nernst equation (1.11). We note from equation (1.8) that $\sigma \gtrless 0$ if $\psi_s \lessgtr \psi_N$ and $\sigma = 0$ when $\psi_s = \psi_N$. When the surface potential is far away from the Nernst value, the surface charge attains the saturation values $\pm eN_s$. In view of equations (1.10) to (1.12), the surface equation of state can be completely specified by the pzc (pH_0) and ΔpK together with the bulk pH or equivalently the Nernst potential.

In the next section, we shall formulate the problem of the double layer interaction between two planar amphoteric surfaces. (For particles of other geometries, we can use the Deryaguin approximation at close separations[25,26,10] and the overlap approximation when the surfaces are far apart.[9]) From the first integral of the PB equation

and the boundary condition, we can predict the behaviour of the repulsive pressure, surface potential and charge as a function of the separation. Our analysis is analogous to the method of isodynamic curves due to Deryaguin.[4] The interaction between surfaces having like signs at infinity (but different magnitudes in the charge and potential) is discussed in Section 3; that between unlike surfaces, in Section 4.

2. FORMULATION

Consider the general Poisson-Boltzmann (PB) equation that governs the electrostatic potential ψ in an electrolyte:

$$\nabla^2\psi = -\frac{4\pi e}{\varepsilon}\sum_i n_i \nu_i \exp(-e\nu_i\psi/kT) \ . \qquad (2.1)$$

In equation (2.1) n_i is the bulk number density of ion types having valence ν_i and ε is the dielectric constant of the solvent. For the one-dimensional problem of two charged flat surfaces at $z = 0$ (hereafter referred to as Surface 1) and at $z = L$ (Surface 2) interacting across the electrolyte, equation (2.1) can be written as

$$\frac{d^2\psi}{dz^2} = -\frac{4\pi e}{\varepsilon}\sum_i n_i \nu_i \exp(-e\nu_i\psi/kT) \ . \qquad (2.2)$$

This has to be solved with the usual boundary conditions

$$\left.\frac{d\psi}{dz}\right|_{z=0} = -\frac{4\pi}{\varepsilon}\sigma_1(\psi_1) \qquad (2.3)$$

$$\left.\frac{d\psi}{dz}\right|_{z=L} = \frac{4\pi}{\varepsilon}\sigma_2(\psi_2) \ . \qquad (2.4)$$

According to equation (1.7) the surface charges σ_1, σ_2 are functions of the surface potentials ψ_1, ψ_2 when we have dissociation equilibrium at the surface. The exact forms of the functions are determined by the dissocation constants of each surface and the bulk concentration of PDI.

A first integral of (2.2) yields

$$\left(\frac{d\psi}{dz}\right)^2 = \frac{8\pi kT}{\varepsilon} \sum_i n_i [\exp(-e\nu_i\psi/kT) + C] \quad . \tag{2.5}$$

Applying the boundary conditions, we get two equations for the surface potentials ψ_1, ψ_2 and the constant of integration C:

$$\sigma_1(\psi_2) = \frac{\varepsilon}{4\pi} \left\{\frac{8\pi kT}{\varepsilon} \sum_i n_i [\exp(-e\nu_i\psi_1/kT) + C]\right\}^{\frac{1}{2}} \tag{2.6}$$

$$\sigma_2(\psi_2) = \frac{\varepsilon}{4\pi} \left\{\frac{8\pi kT}{\varepsilon} \sum_i n_i [\exp(-e\nu_i\psi_2/kT) + C]\right\}^{\frac{1}{2}} \quad . \tag{2.7}$$

We observe that if electrical neutrality were to be preserved in the limit of small separations we must either have $\sigma_1 = -\sigma_2$ or $\sigma_1 = 0 = \sigma_2$ as $L \to 0$.[17] In either case, both surface potentials must become the same in this limit (see equations (2.6) and (2.7)). Further if both $\sigma_1, \sigma_2 \to 0$ as $L \to 0$ both surface potentials must approach their own Nernst values (equation (1.8)), and this is only possible when both surfaces have the same pzc (pH_0) but different ΔpKs (to remain as dissimilar surfaces at infinity).

The repulsive pressure between the plates ($P > 0$ implies repulsion) can be written in the physically perspicuous form

$$P = kT \sum_i n_i [\exp(-e\nu_i\psi/kT) - 1] - \frac{\varepsilon}{8\pi} \left(\frac{d\psi}{dz}\right)^2 \quad . \tag{2.8}$$

We can now use equation (2.5), giving

$$P = -2nkT(C + 1) \quad , \tag{2.9}$$

where

$$n = \tfrac{1}{2} \sum_i n_i \quad . \tag{2.10}$$

It is well known[31] that the second integration of the PB equation requires a knowledge of whether

$$\text{(i)} \quad C < -1 \quad \text{(i.e. } P > 0 \text{ repulsive)} \tag{2.11}$$

(ii) $|C| < 1$ (i.e. $P < 0$ attractive) (2.12)

or (iii) $C > 1$ (i.e. $P > 0$ attractive) (2.13)

because the integration procedure is different for each case. Therefore, a third relation between ψ_1, ψ_2 and C can be obtained. This, together with equation (2.8) and (2.9) would enable us to obtain a complete solution of the problem.

Before proceding further, we shall make one simplifying assumption by considering only the case of a 1:1 electrolyte. The PB equation (2.2) now takes on the simpler form

$$\frac{d^2\psi}{dz^2} = \frac{8\pi ne}{\varepsilon} \sinh(e\psi/kT) \ . \qquad (2.14)$$

A moment's reflection will reveal that only the three types of solution illustrated in Table 2.1 are allowed. These results will be useful in later discussions.

Table 2.1: Examples showing the three types of solutions allowed by the Poisson-Boltzmann equation together with some general relations between σ and ψ.

I. *Like charges and like potentials*

If $|\sigma_1| \gtrless |\sigma_2|$ then $|\psi_1| \gtrless |\psi_2|$

and vice versa.

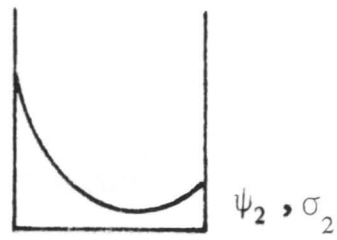

II. *Unlike charges and like potentials*

If $|\sigma_1| \gtrless |\sigma_2|$ then $|\psi_1| \gtrless |\psi_2|$

and vice versa.

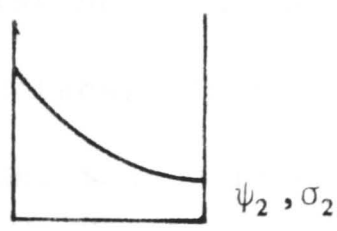

III. *Unlike charges and unlike potentials*

At $\psi = 0$, $\frac{d^2\psi}{dx^2} = 0$.

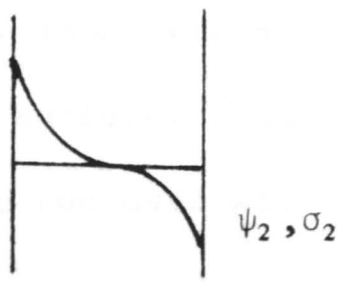

For notational convenience, we introduce the reduced potential

$$y = e\psi/kT \,, \tag{2.15}$$

the Debye screening parameter

$$\kappa = \left(\frac{8\pi ne^2}{\varepsilon kT}\right)^{\frac{1}{2}} \,, \tag{2.16}$$

and the dimensionless constant

$$\gamma_i = \frac{\kappa N_{si}}{4n} \,, \quad i = 1,2 \,. \tag{2.17}$$

The subscripts 1,2 will refer, as before, to surface 1 and 2. Equations (2.6) and (2.7) can now be written in the form

$$\eta_1(y_1) \equiv -\tfrac{1}{2}(C+1) = \tfrac{1}{2}(\cosh y_1 - 1) - \gamma_1^2\alpha_1^2(y_1^2)$$

$$= \sinh^2(y_1/2) - \gamma_1^2\alpha_1^2(y_1) \tag{2.18}$$

$$\eta_2(y_2) \equiv -\tfrac{1}{2}(C+1) = \sinh^2(y_2/2) - \gamma_2^2\alpha_2^2(y_2) \tag{2.19}$$

where (cf. equations (1.5) and (1.8))

$$\alpha_i(y_i) = \frac{\delta_i \sinh(y_{N_i} - y_i)}{1 + \delta_i \cosh(y_{N_i} - y_i)} \,, \quad i = 1,2 \,. \tag{2.20}$$

Since the pressure must be the same on both surfaces, the relation

$$\eta_1(y_1) = \eta_2(y_2) \tag{2.21}$$

must hold for the functions η_1, η_2 defined by the above equations.

The key to solving the problem of interacting dissimilar amphoteric surfaces lies in understanding the interplay between the curve $\sinh^2(y/2)$ and the charge curves, $\gamma^2\alpha^2(y)$, of each surface. Therefore, it is important that we systematically characterize the manner in which these curves intersect each other. To begin with, let us plot $\sinh^2(y/2)$ and $\gamma^2\alpha^2(y)$ as a function of the *surface* potential y. (Subscripts 1 and 2 will be suppressed when we are considering a general surface. The *surface* potential y under consideration should not be confused with the

potential at some general position $y = y(z)$.) This is shown schematically in Figure 2.1. We have shown, without loss of generality, values of the concentration of PDI such that the Nernst potential, y_N, is positive. For ease of later discussions, it is useful to adopt the following nomenclature. Since $\eta(y)$ is the (vertical) difference between the two curves, we can delineate regions where $\eta > 0$, $0 > \eta > -1$, $\eta < -1$ corresponding to cases (i), (ii) and (iii) in equations (2.11) to (2.13). We label the points of intersection between the two curves (where $\eta = 0$) as a, b, c and d with the corresponding potentials y_a, y_b, y_c and y_d. The point a is defined as the intersection where y_a falls between the origin and the Nernst potential y_N. Points b and c are the intersections where y_b and y_c have the same sign as y_N. Under some circumstances there may be no intersections b and c or the points b and c may coincide. The point of intersection on the opposite side of the origin to y_N is labelled d.

For a single surface in equilibrium with a bulk solution containing a given concentration of PDI, there is no net force exerted on the surface. Therefore the pressure P is identically zero, that is, $\eta = -\frac{1}{2}(C+1) = 0$. Of the four points where $\eta = 0$, only point a, where the surface charge and the surface potential have the same sign, satisfies the PB equation. Thus we obtain the general result that the surface potential of an isolated amphoteric surface always lies between zero and the Nernst potential. The only occasion when y_a equals zero is when the Nernst potential is zero. That is, the concentration of PDI is at the point-of-zero-charge, $pH = pH_0$ and $\sigma = 0$.

To study the electrostatic interaction between two dissimilar amphoteric surfaces, we need to examine the functions $\eta_1(y_1)$ and $\eta_2(y_2)$

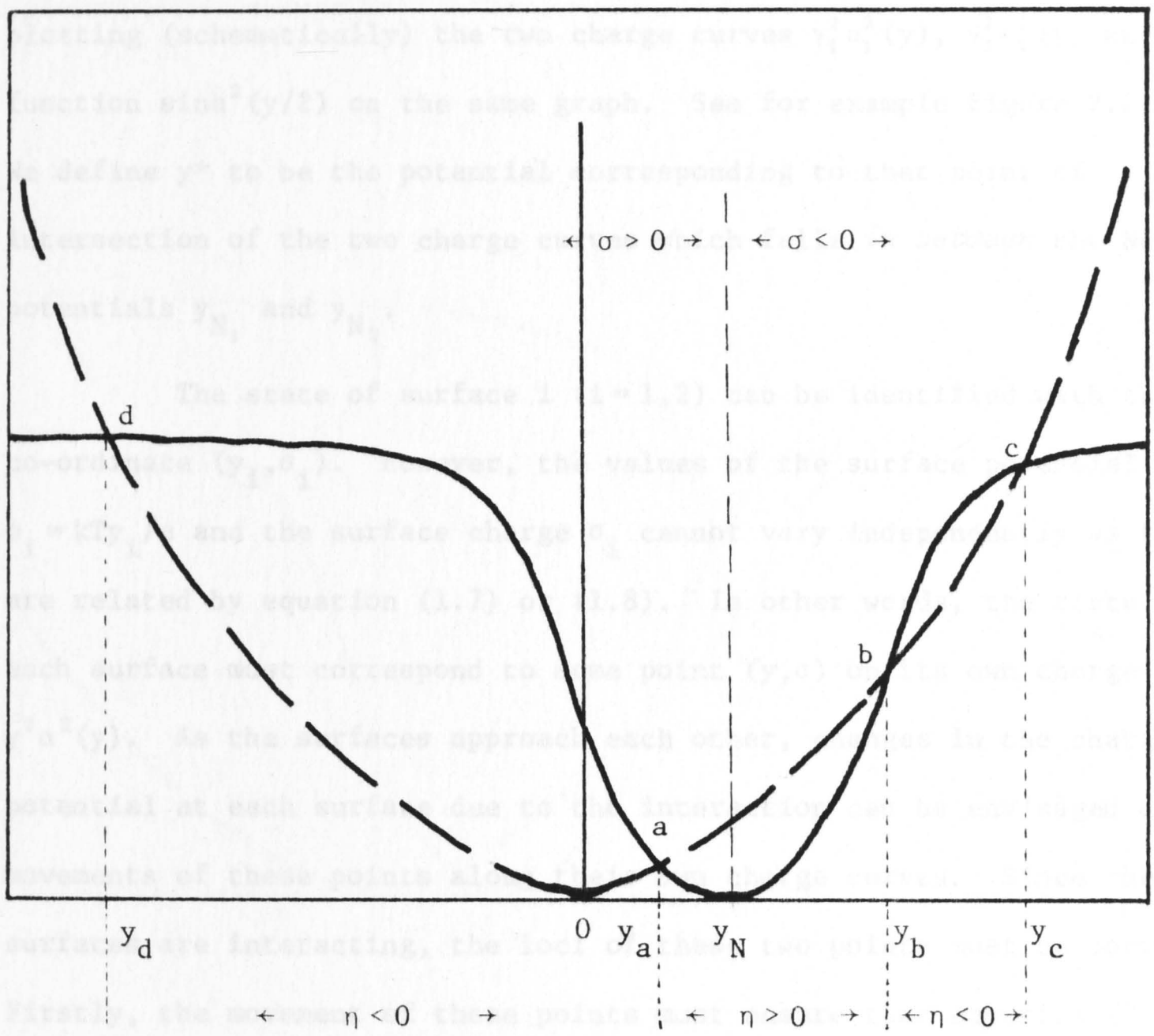

Figure 2.1: A plot of the functions $\sinh^2(y/2)$ (– – –) and $\gamma^2\alpha^2(y)$ (——) showing the points of intersection between these curves, and the regions where the function $\eta(y)$ and the surface charge σ is positive or negative.

given in equations (2.18) and (2.19). This is best accomplished by plotting (schematically) the two charge curves $\gamma_1^2\alpha_1^2(y)$, $\gamma_2^2\alpha_2^2(y)$ and the function $\sinh^2(y/2)$ on the same graph. See for example Figure 2.2 a,b. We define y* to be the potential corresponding to that point of intersection of the two charge curves which falls *in between* the Nernst potentials y_{N_1} and y_{N_2}.

The state of surface i (i = 1,2) can be identified with the co-ordinate (y_i,σ_i). However, the values of the surface potential $\psi_i = kTy_i/e$ and the surface charge σ_i cannot vary independently as they are related by equation (1.7) or (1.8). In other words, the state of each surface must correspond to some point (y,σ) on its own charge curve $\gamma^2\alpha^2(y)$. As the surfaces approach each other, changes in the charge and potential at each surface due to the interaction can be envisaged as movements of these points along their own charge curves. Since the surfaces are interacting, the loci of these two points must be correlated. Firstly, the movement of these points must ensure that equation (2.21) (cf. equations (2.18) and (2.19)) is satisfied. Secondly, the values of y_1 and y_2 must satisfy the PB equation. That is, the relationship between the charge and potential at each surface and between surfaces must fall within one of the three types listed in Table 2.1. Thus it is possible to obtain a description of the behaviour of the repulsive pressure, surface potential and charges as a function of separation by considering the charge curves $\gamma_1^2\alpha_1^2(y)$, $\gamma_2^2\alpha_2^2(y)$ and the function $\sinh^2(y/2)$. Most of the results we are about to describe can be deduced from the fact that $\sinh^2(y/2)$ increases monotonically as $|y|$ increases and that the charge curves $\gamma^2\alpha^2(y)$ have an absolute minimum at $y = y_N$.

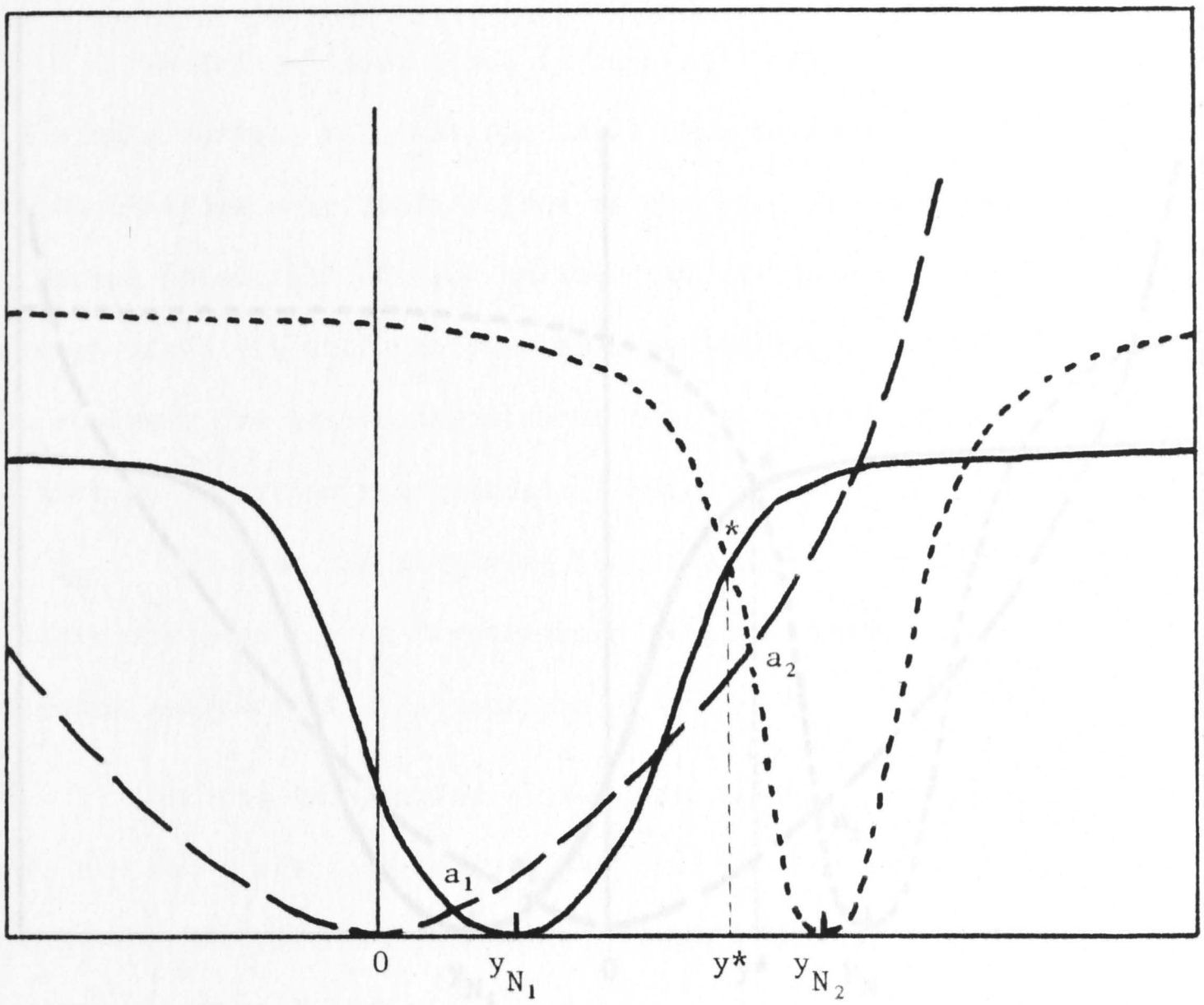

Figure 2.2a: Showing a typical arrangement of the charge curves of surface 1 (——) and surface 2 (----) for surfaces having *like* (positive) signs at infinite separation. Note that $y_{N_1} < y^* < y_{N_2}$. Surface 1 is defined as the surface that has the *lower* Nernst potential ($y_{N_1} < y_{N_2}$). The function $\sinh^2(y/2)$ is given in dashed lines (– – –).

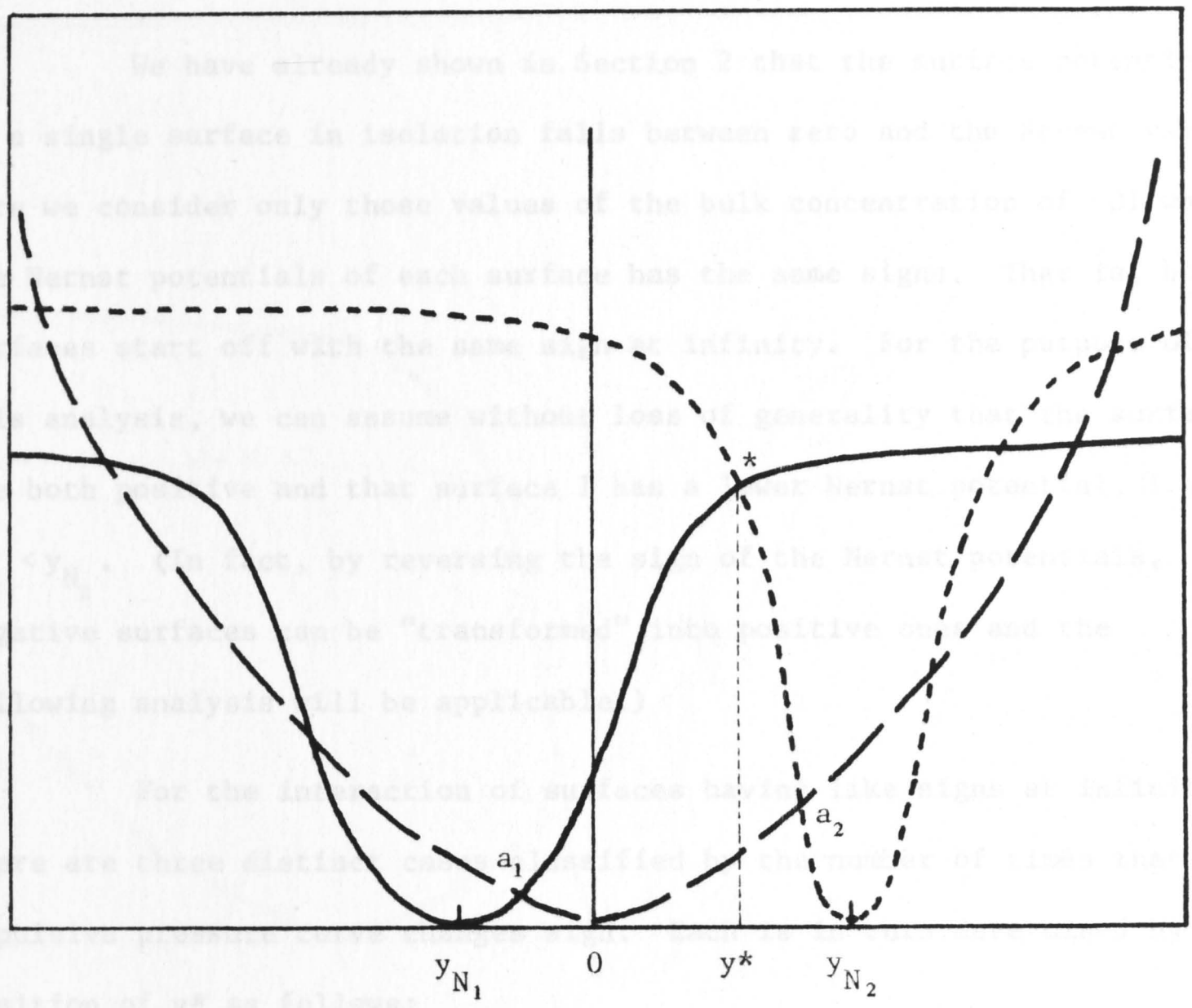

Figure 2.2b: Showing a typical arrangement of the charge curves for surface 1 (——) and surface 2 (----) for surfaces having *unlike* signs at infinite separation. Note that $y_{N_1} < y^* < y_{N_2}$. Surface 1 is defined as the surface that is *negative* at infinite separation ($y_{N_2} < 0$). The function $\sinh^2(y/2)$ is given in dashed lines (– – –).

3. THE INTERACTION BETWEEN LIKE SURFACES

We have already shown in Section 2 that the surface potential of a single surface in isolation falls between zero and the Nernst value. Here we consider only those values of the bulk concentration of PDI where the Nernst potentials of each surface has the same signs. That is, both surfaces start off with the same sign at infinity. For the purpose of this analysis, we can assume without loss of generality that the surfaces are both positive and that surface 1 has a lower Nernst potential, i.e. $y_{N_1} < y_{N_2}$. (In fact, by reversing the sign of the Nernst potentials, negative surfaces can be "transformed" into positive ones and the following analysis will be applicable.)

For the interaction of surfaces having like signs at infinity, there are three distinct cases classified by the number of times that the repulsive pressure curve changes sign. Each is in turn determined by the position of y* as follows:

$$\text{Case 1:} \quad y^* \leq y_{b_1}$$

$$\text{Case 2:} \quad y_{b_1} \leq y^* \leq y_{c_1}$$

$$\text{Case 3:} \quad y_{c_1} \leq y^* \, .$$

We shall consider each of these separately.

3a. Case 1

The appropriate charge curves for this case are given in Figure 3.1 a,b. The characteristic feature of these sets of curves is that y* (the potential corresponding to the intersection of the two charge curves that falls in between the Nernst potentials) is less than y_{b_1}. This case also includes the situation where surface 1 (defined to

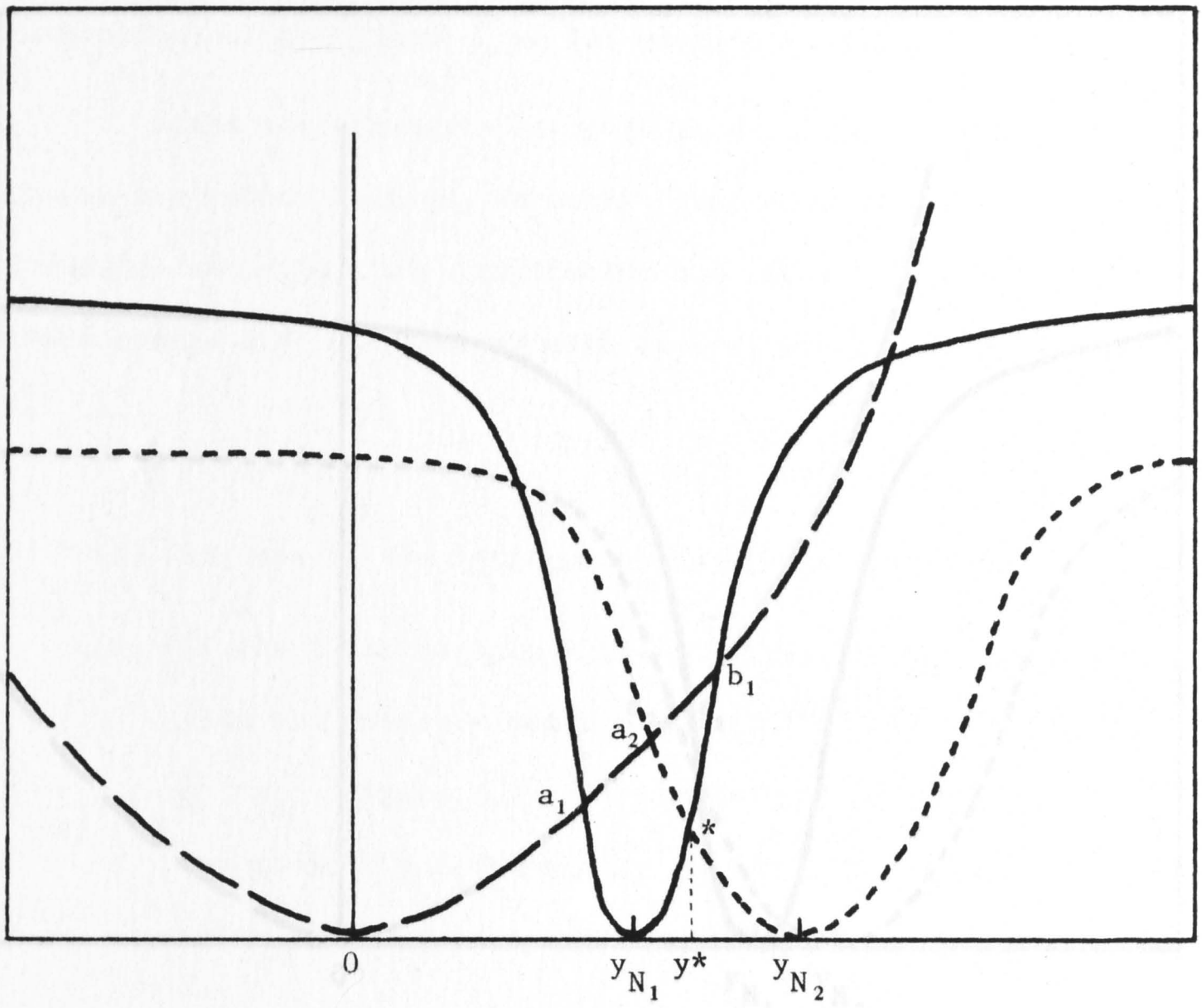

Figure 3.1a: Showing the relative positions between the charge curves curves for Case 1 ($y_{a_1} < y^* < y_{b_1}$) for the situation where Surface 2 has the higher surface potential at infinite separation ($y_{a_2} > y_{a_1}$).

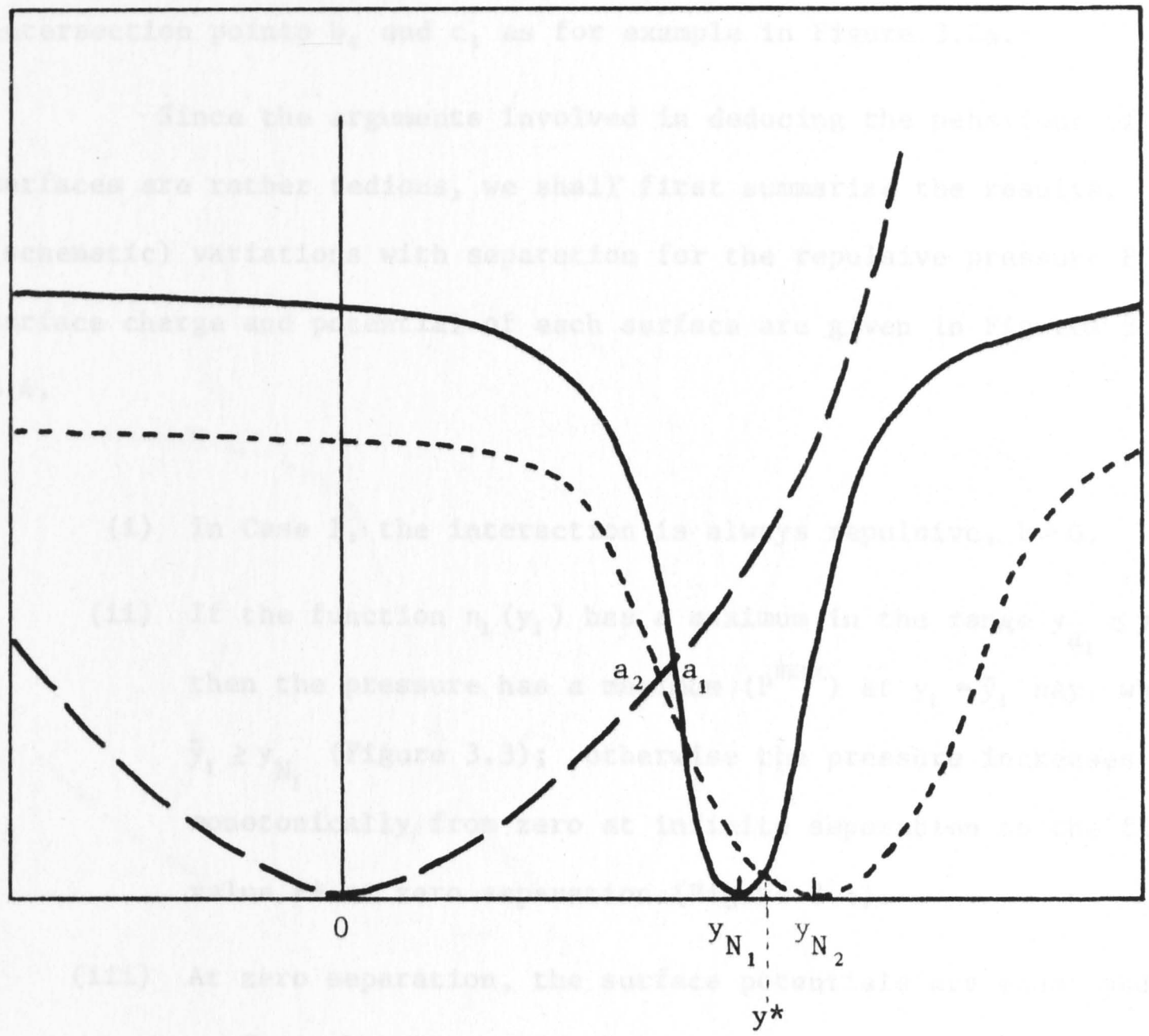

Figure 3.1b: Showing the relative positions of the charge curves for Case 1 for the situation where Surface 1 has the higher surface potential at infinite separation ($y_{a_1} > y_{a_2}$).

be the one with the lower Nernst potential) does not have the intersection points b_1 and c_1 as for example in Figure 3.2a.

Since the arguments involved in deducing the behaviour of the surfaces are rather tedious, we shall first summarize the results. The (schematic) variations with separation for the repulsive pressure P, surface charge and potential of each surface are given in Figures 3.3 and 3.4.

(i) In Case 1, the interaction is always repulsive, $P > 0$.

(ii) If the function $\eta_1(y_1)$ has a maximum in the range $y_{a_1} \leq y_1 \leq y^*$, then the pressure has a maximum (P^{max}) at $y_1 = \bar{y}_1$ say, where $\bar{y}_1 \geq y_{N_1}$ (Figure 3.3); otherwise the pressure increases monotonically from zero at infinite separation to the final value P* at zero separation (Figure 3.4).

(iii) At zero separation, the surface potentials are equal and the surface charges are equal in magnitude but opposite in sign[17] (cf. discussion in Section 1).

The results summarized in Figures 3.3 and 3.4 can be deduced from Figure 3.1 a,b if we bear in mind the discussion in Section 2 regarding the charge curves. We shall briefly summarize the main points:

(A) The surface charge and potential of each surface is related to each other by equations (1.7) or (1.8). A state of the surface, i.e. (y,σ), can be represented by a point on the charge curve $\gamma^2\alpha^2(y)$.

(B) Changes in the surface charge and potential due to interaction are described by the movement of this point along the charge curve.

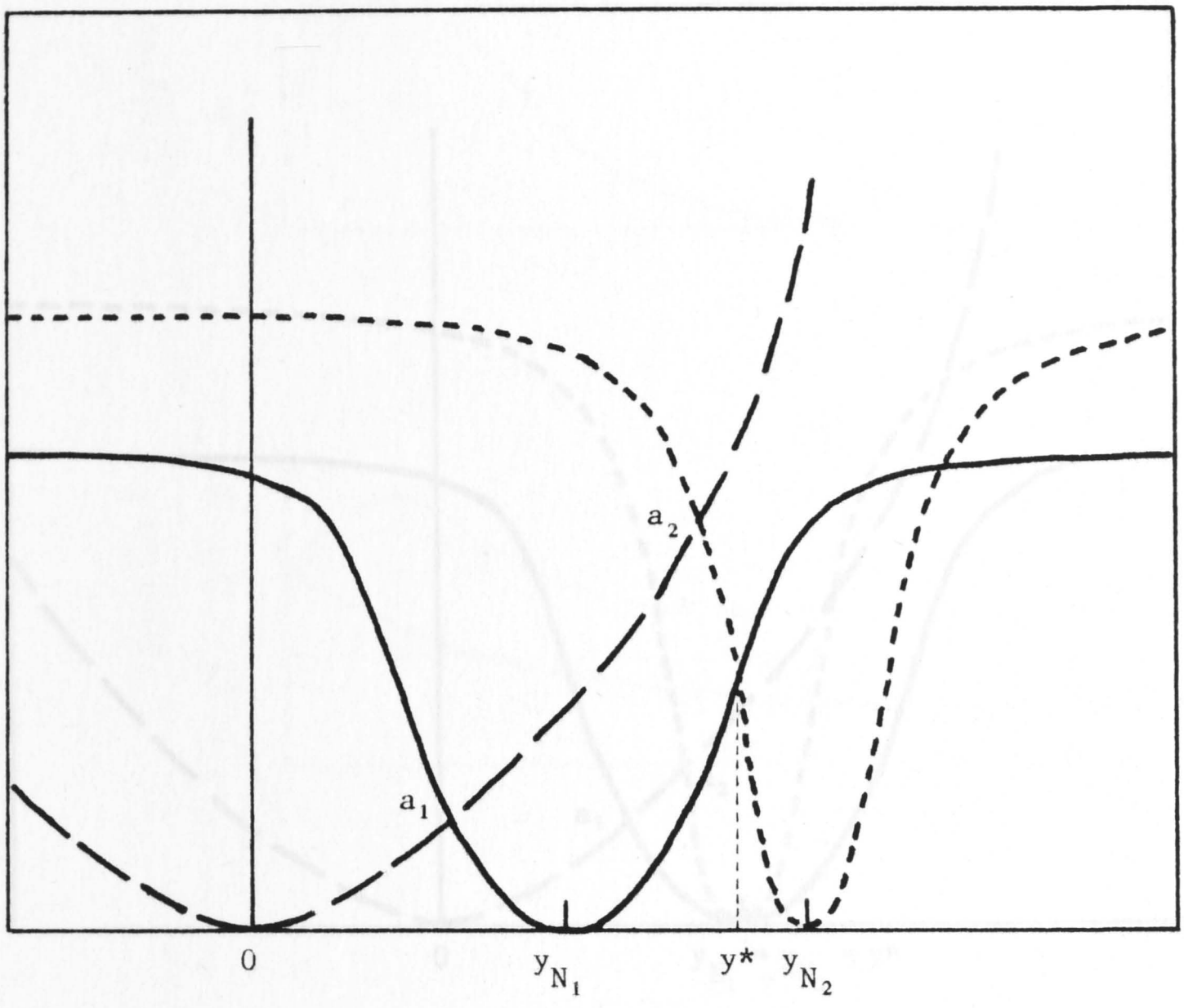

Figure 3.2a: An example of the charge curves for Case 1 for the situation where the intersection point b_1 does not exist.

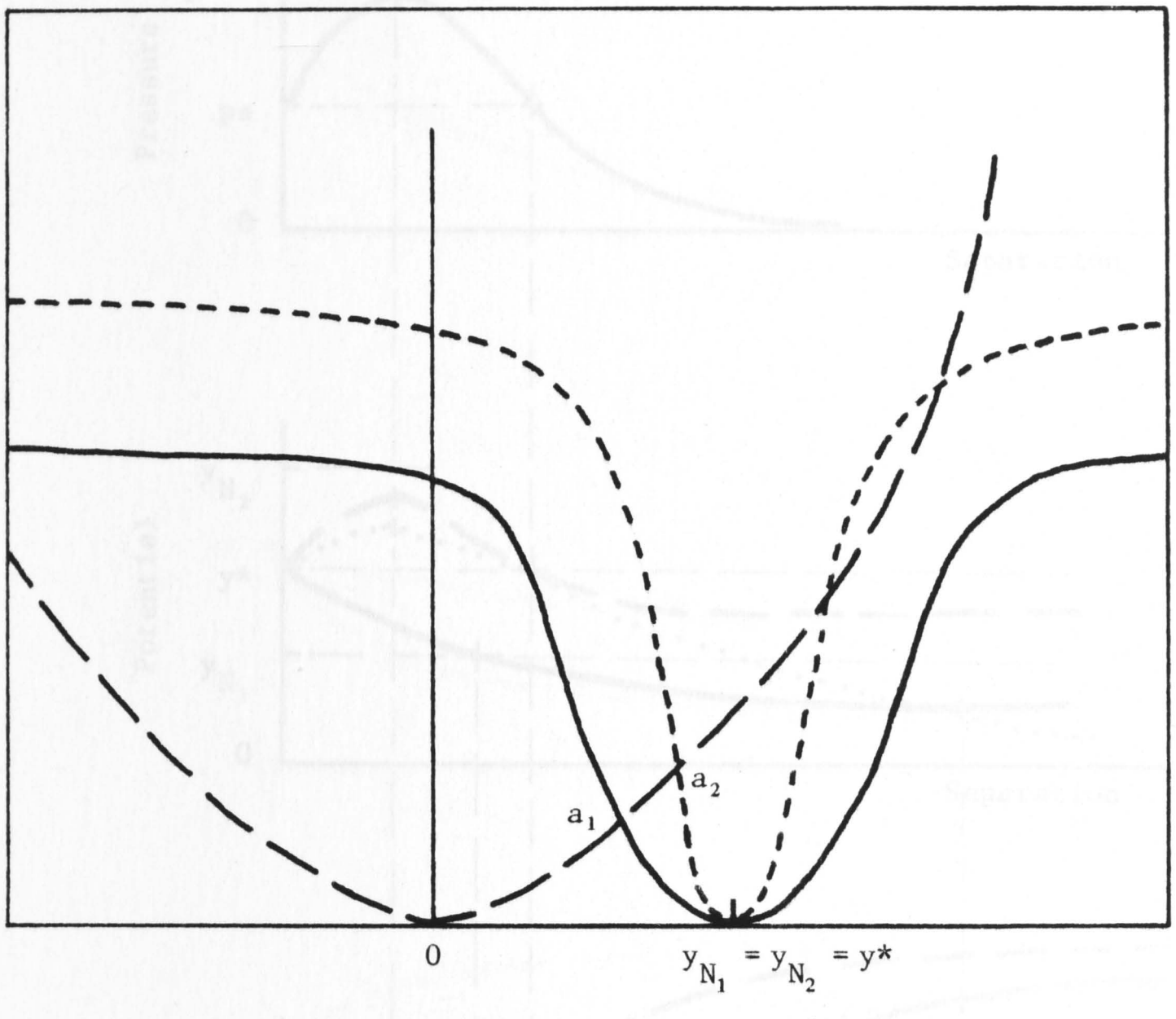

Figure 3.2b: An example of the charge curves for Case 1 for the situation where the two surfaces have the same Nernst potential ($y_{N_1} = y_{N_2}$).

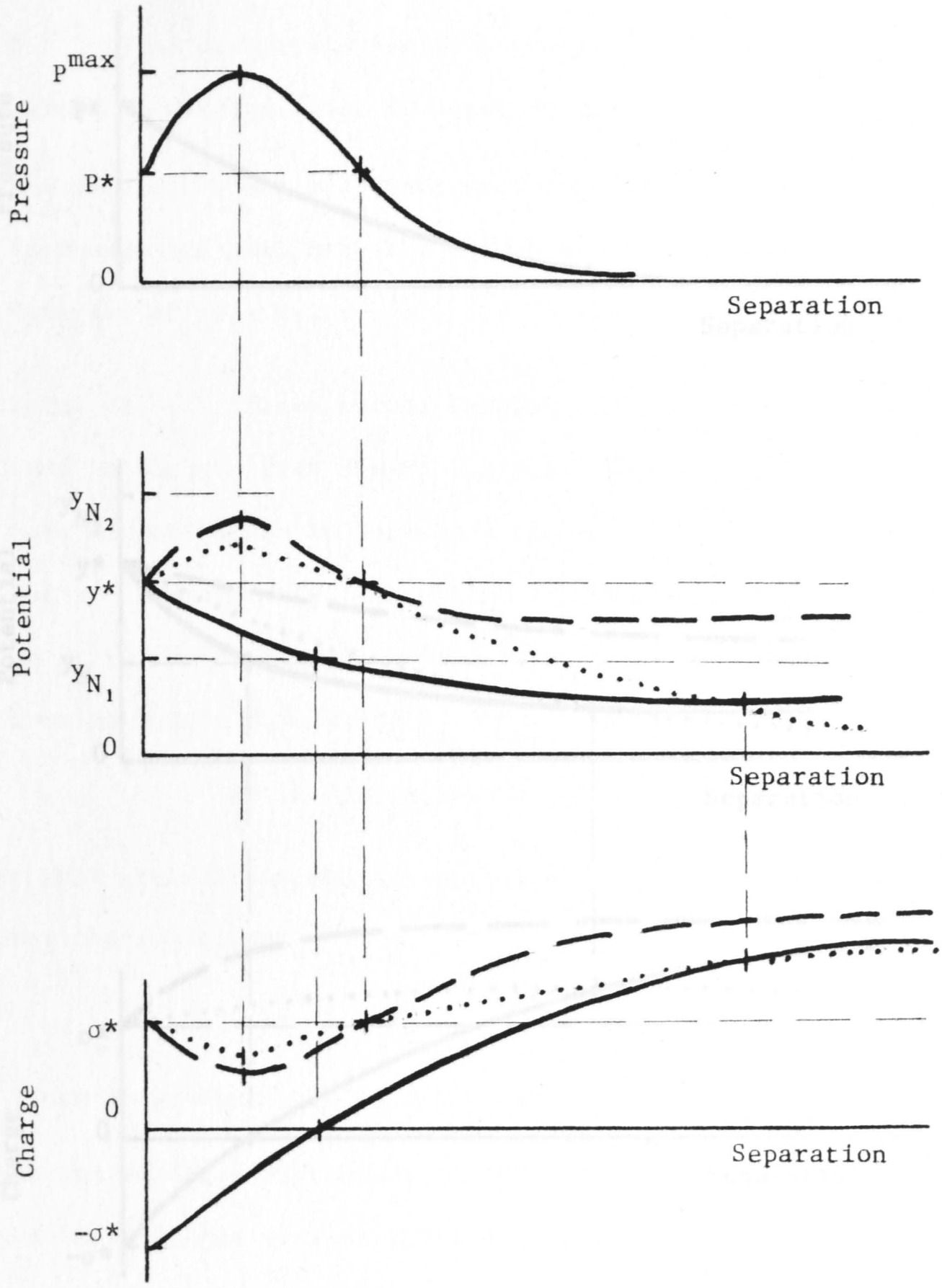

Figure 3.3: Case 1. Showing the main features and schematic variations of the pressure, surface potentials and surface charges as a function of the separation between the surfaces for the case where $\eta_1(y_1)$ has a maximum between y_{a_1} and y* (see text). The potential and charge of Surface 1 are given in solid lines (——). Those of Surface 2 are given in dashed lines (– – –) when $y_{a_2} > y_{a_1}$, and in dotted lines (····) when $y_{a_2} < y_{a_1}$.

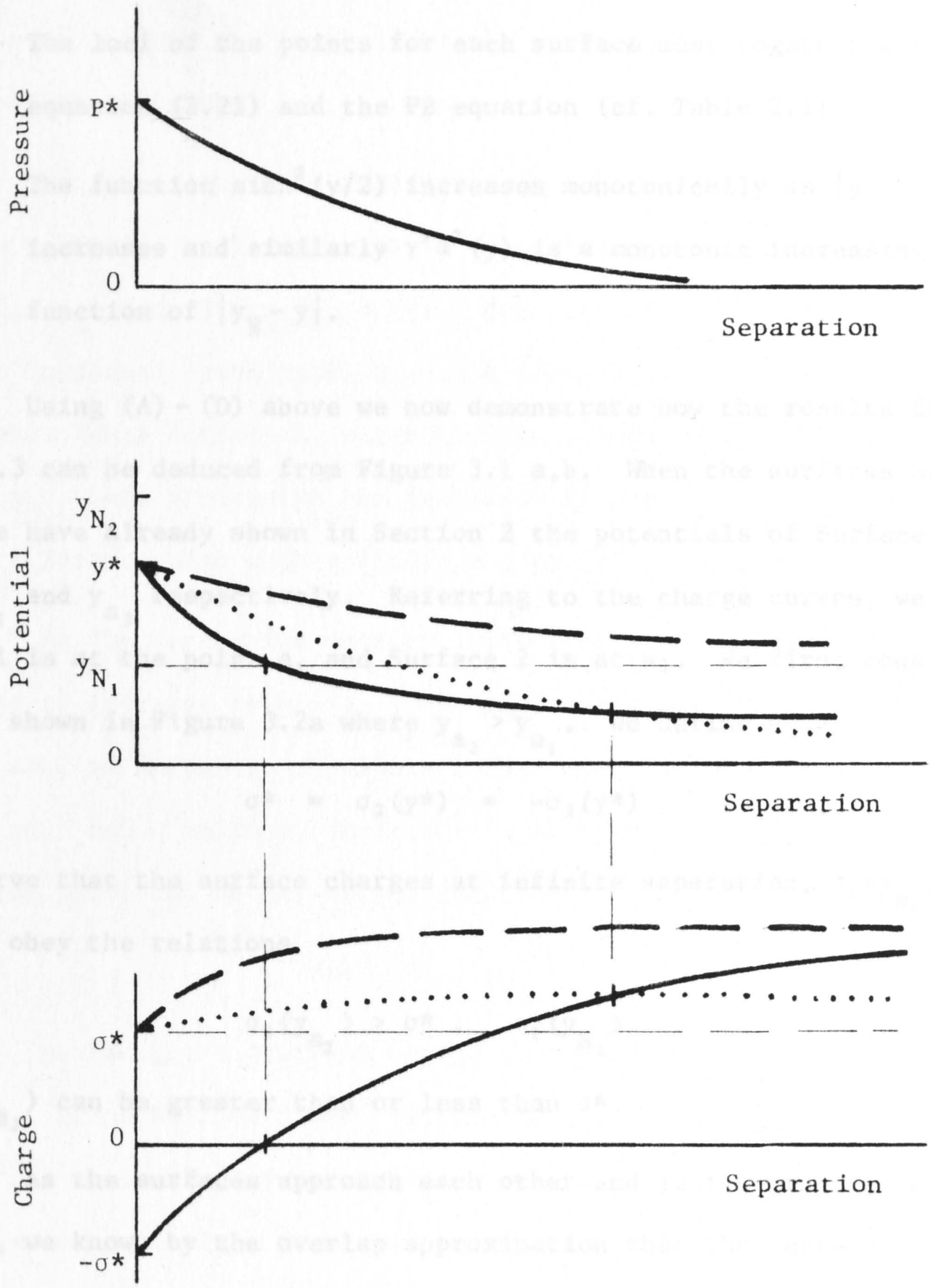

Figure 3.4: Case 1. Showing the main features and schematic variations of the pressure, surface potentials and charges as a function of the separation between the surfaces for the case where $\eta_1(y_1)$ does not have a maximum between y_{a_1} and y* (see text). The potentials and charge of Surface 1 are given in solid lines (——). Those of Surface 2 are given in dashed lines (– – –) when $y_{a_2} > y_{a_1}$, and in dotted lines (····) when $y_{a_2} < y_{a_1}$.

(C) The loci of the points for each surface must together satisfy equation (2.21) and the PB equation (cf. Table 2.1).

(D) The function $\sinh^2(y/2)$ increases monotonically as $|y|$ increases and similarly $\gamma^2\alpha^2(y)$ is a monotonic increasing function of $|y_N - y|$.

Using (A) - (D) above we now demonstrate how the results from Figure 3.3 can be deduced from Figure 3.1 a,b. When the surfaces are far apart, we have already shown in Section 2 the potentials of Surface 1 and 2 are y_{a_1} and y_{a_2} respectively. Referring to the charge curves, we say Surface 1 is at the point a_1 and Surface 2 is at a_2. We first consider the case shown in Figure 3.2a where $y_{a_2} > y_{a_1}$. We define

$$\sigma^* = \sigma_2(y^*) = -\sigma_1(y^*) \tag{3.1}$$

and observe that the surface charges at infinite separation, $\sigma_1(y_{a_1})$, $\sigma_2(y_{a_2})$, obey the relations

$$\sigma_2(y_{a_2}) > \sigma^* , \quad \sigma_1(y_{a_1}) \tag{3.2}$$

but $\sigma_1(y_{a_1})$ can be greater than or less than σ^*.

As the surfaces approach each other and just beginning to interact, we know, by the overlap approximation that the surface potentials must increase and the interaction is repulsive. That is $P > 0$, $\eta_1(y_1) = \eta_2(y_2) > 0$ (cf. equations (2.9), (2.18 - (2.21)). Therefore both surfaces would move along its own charge curve towards their respective Nernst potentials. While the surface potentials increase, the surface charges decrease. This minimizes the interaction energy. As the surfaces approach the rate of change of the charge and potential of each surface with separation (i.e. the velocities along the charge curves)

must of necessity be difficult since the equality $\eta_1(y_1) = \eta_2(y_2)$ must be maintained at all times.

We assume that the function $\eta_1(y_1)$ has a maxima between y_{a_1} and y* ($y_{a_1} \leq y_1 \leq y^*$); at $\bar{y}_1$ say. It is clear from point (D) above that $\bar{y}_1$ is between y_{N_1} and y* ($y_{N_1} \leq \bar{y}_1 \leq y^*$). Now, as the separation between the surfaces decreases, both surfaces would move closer to their Nernst potentials. When Surface 1, which has the lower Nernst potential, reaches y_{N_1} where its charge has decreased to zero, Surface 2 is still below its Nernst value with a finite and positive surface charge.

As the separation further decreases, the potential of Surface 1 continues to increase beyond y_{N_1}, but with a surface charge of opposite sign to that at infinity (cf. Figure 2.1). When Surface 1 reaches $\bar{y}_1$ where $\eta_1(y_1)$ has a maximum, Surface 2 is at $\bar{y}_2$ where $\eta_1(\bar{y}_1) = \eta_2(\bar{y}_2)$. Again from point (D) we can deduce that

$$y^* \leq \bar{y}_2 < y_{N_2} .$$

As Surface 1 proceeds beyond $\bar{y}_1$ towards y*, $\eta_1(y_1)$ can only decrease. Hence Surface 2 must retrace its path along the charge curve from $\bar{y}_2$ and approach y* from above. Therefore Surface 2, which has the higher Nernst potential, never reaches y_{N_2} and so its surface charge always retain the same sign as that at infinite separation.

Now both surfaces must reach y* at the same time because $\eta_1(y^*) = \eta_2(y^*)$. Here we have $\gamma_1^2\alpha_1^2(y^*) = \gamma_2^2\alpha_2^2(y^*)$ and the potentials are equal but the charges are equal and opposite. The surfaces cannot proceed beyond y* as this would violate the PB equation (cf. Type II, Table 2.1). Clearly, the boundary conditions $y_1 = y_2$, $\sigma_1 = -\sigma_2$ can only be attained when the separation between the surfaces is zero.

The above results are summarized in Figure 3.3. The variations with separation of the charge and potential of Surface 1 are given in solid lines, and those of Surface 2 in dashed lines.

It will be shown that:

(iv) for interactions between surfaces having like signs at infinity, the surface with the *lower* Nernst potential would *always* reach its Nernst potential and reverses the sign of its surface charge while the other surface never changes sign.

Obviously, this excludes the degenerate case where both surfaces have the same Nernst potential. In this instance, neither surface charge changes sign.

Now it is possible for Surface 2, which by definition has the higher Nernst potential, to have a lower surface potential than Surface 1 when they are far apart (see Figure 3.1b). It is clear from the figure that the surface charges at infinity obey the inequalities

$$\sigma_1(y_{a_1}) > \sigma_2(y_{a_2}) > \sigma^*.$$

If $\eta_1(y_1)$ has a maximum in $y_{a_1} \leq y_1 \leq y^*$, the results for Surface 2 are given in dotted lines in Figure 3.3. These can be derived using the arguments given above. The only noticeable difference between this case ($y_{a_2} < y_{a_1}$) and the previous case ($y_{a_2} > y_{a_1}$) are the cross-over points between the charge and potential curves. These must occur when both σ_1 and σ_2 are greater than σ^*. The behaviour of the repulsive pressure and the properties of Surface 1 remain essentially the same for both cases.

If $\eta_1(y_1)$ does not have a maxima in the range $y_{a_1} \leq y_1 \leq y^*$, the interaction is still repulsive but there are no turning points in the pressure, potential and charge curve (Figure 3.4). The arguments needed

to deduce these results follow along the line of those given above. The results pertaining to Surface 1 are given in solid curves.

If $y_{a_2} > y_{a_1}$ ($y_{N_2} > y_{N_1}$) the charges at infinite separation satisfy

$$\sigma_2(y_{a_2}) > \sigma^* , \quad \sigma_1(y_{a_1})$$

but $\sigma_1(y_{a_1})$ can be greater or less than σ^*. The charge and potential for Surface 2 for this case are given in dashed lines.

If $y_{a_2} < y_{a_1}$ ($y_{N_2} > y_{N_1}$) the results for Surface 2 are given in dotted lines. Here $\sigma_1(y_{a_1}) > \sigma_2(y_{a_2}) > \sigma^*$ and the cross-over points in the potential and charge must occur when the charges of Surfaces 1 and 2 greater than σ^*.

When the Nernst potentials are very far apart (Figure 3.2a), the pressure may exhibit a local minimum after the maximum. However the pressure still remains positive for all separation (see Figure 3.5). The charges and potentials will have corresponding maxima and minima.

In the degenerate case where the surfaces have the same Nernst potential (i.e. the same pzc, see Figure 3.2b), e.g. identical surfaces, then $y^* = y_{N_1} = y_{N_2}$ and neither surface changes sign. The surface potentials start off at y_{a_1} and y_{a_2}, and increase monotonically towards their Nernst values. The surface charges decrease monotonically to zero. At zero separation, both potentials are equal and surface charges are reduced to zero.

This completes the discussion on the various possible types of behaviour under Case 1.

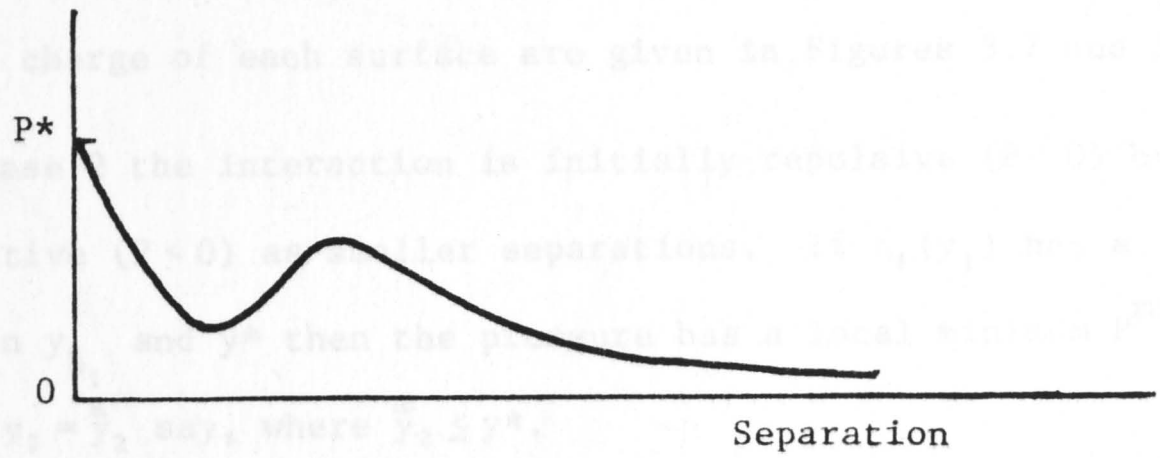

Figure 3.5: Case 1. Showing the possibility of two turning points in the pressure curve when the Nernst potentials are far apart in the situation depicted in Figure 3.2a (see text).

3b. Case 2

The appropriate charge curves for this case are shown in Figure 3.6. The characteristic feature of this set of curves is that

$$y_{b_1} < y^* < y_{c_1} .$$

The variations with separation of the repulsive pressure P, surface potential and charge of each surface are given in Figures 3.7 and 3.8.

In Case 2 the interaction is initially repulsive ($P > 0$) but becomes attractive ($P < 0$) as smaller separations. If $\eta_1(y_1)$ has a minimum between y_{b_1} and y^* then the pressure has a local minimum $P^{min} < 0$ at $y_1 = \bar{\bar{y}}_1$ and $y_2 = \bar{\bar{y}}_2$ say, where $\bar{\bar{y}}_2 \leq y^*$.

Let us now deduce the results in Figures 3.7 and 3.8 from the charge curves in Figure 3.6. As with Case 1, Surfaces 1 and 2 start at a_1 and a_2 respectively, and move along their charge curves towards their Nernst potentials as the surfaces approach. Clearly $\eta_1(y_1)$ has a maximum at some $\bar{y}_1$ where $y_{N_1} \leq \bar{y}_1 \leq y_{b_1}$. This maximum corresponds to the maximum in the repulsive pressure. Thus as the potential of Surface 1 increases from y_{a_1} to y_{N_1} and then onto $\bar{y}_1$, its surface charge decreases to zero at $y_1 = y_{N_1}$ and changes sign between y_{N_1} and $\bar{y}_1$. Meanwhile the potential of Surface 2 increases steadily from y_{a_2} to $\bar{y}_2$ where $\eta_2(\bar{y}_2) = \eta_1(\bar{y}_1)$ while the charge decreases from $\sigma_2(y_{a_2})$ to $\sigma_2(\bar{y}_2)$. Since $\bar{y}_2 < y_{N_2}$, the sign of the charge on Surface 2 does not change.

As Surface 1 now moves from $\bar{y}_1$ to y_{b_1}, $\eta_1(y_1)$ can only decrease; therefore Surface 2 must return along its charge curve towards y_{a_2} increasing the charge and decreasing the potential. When Surface 1 reaches the point b_1, Surface 2 reaches a_2 where $\eta_1(y_{b_1}) = 0 = \eta_2(y_{a_2})$ and the pressure is zero at this point.

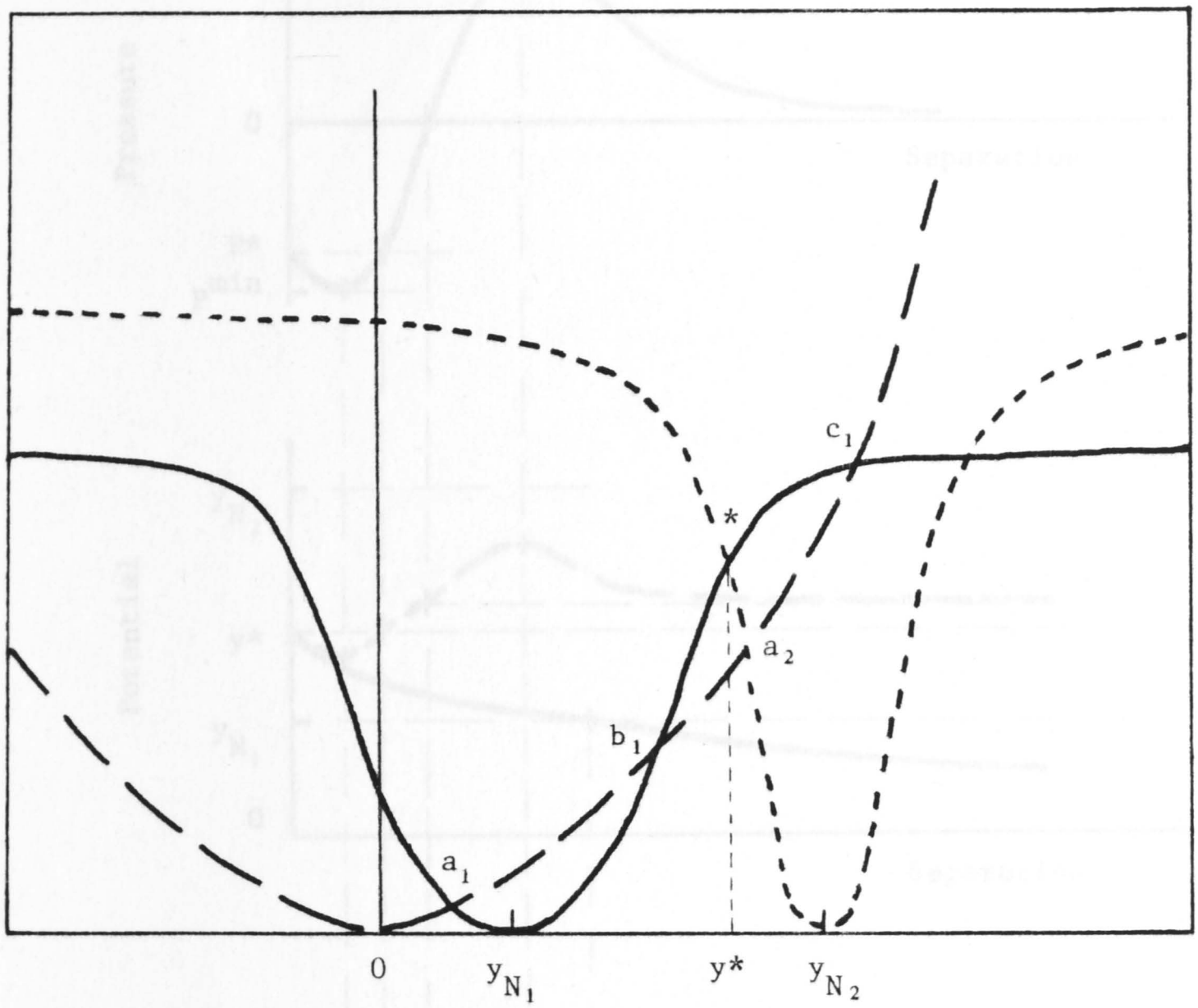

Figure 3.6: Showing the relative positions of the charge curves for Case 2 ($y_{b_1} < y^* < y_{c_1}$).

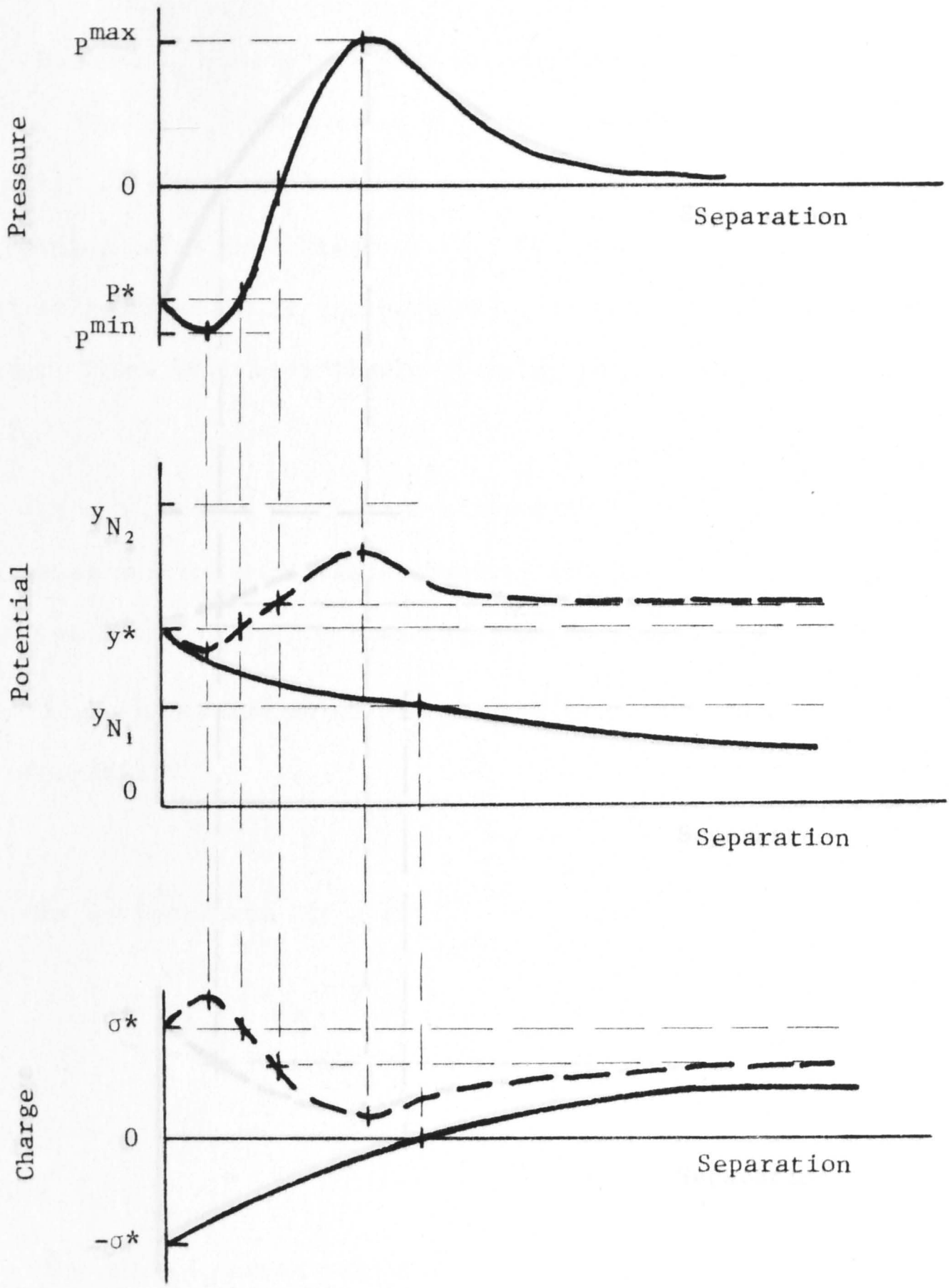

Figure 3.7: Case 2. Showing the main features and schematic variations of the pressure, surface potentials and charges as a function of the separation between the surfaces for the case where the pressure has a local minimum. The potential and charge of Surface 1 are given in solid lines (——); those of Surface 2 are given in dashed lines (– – –).

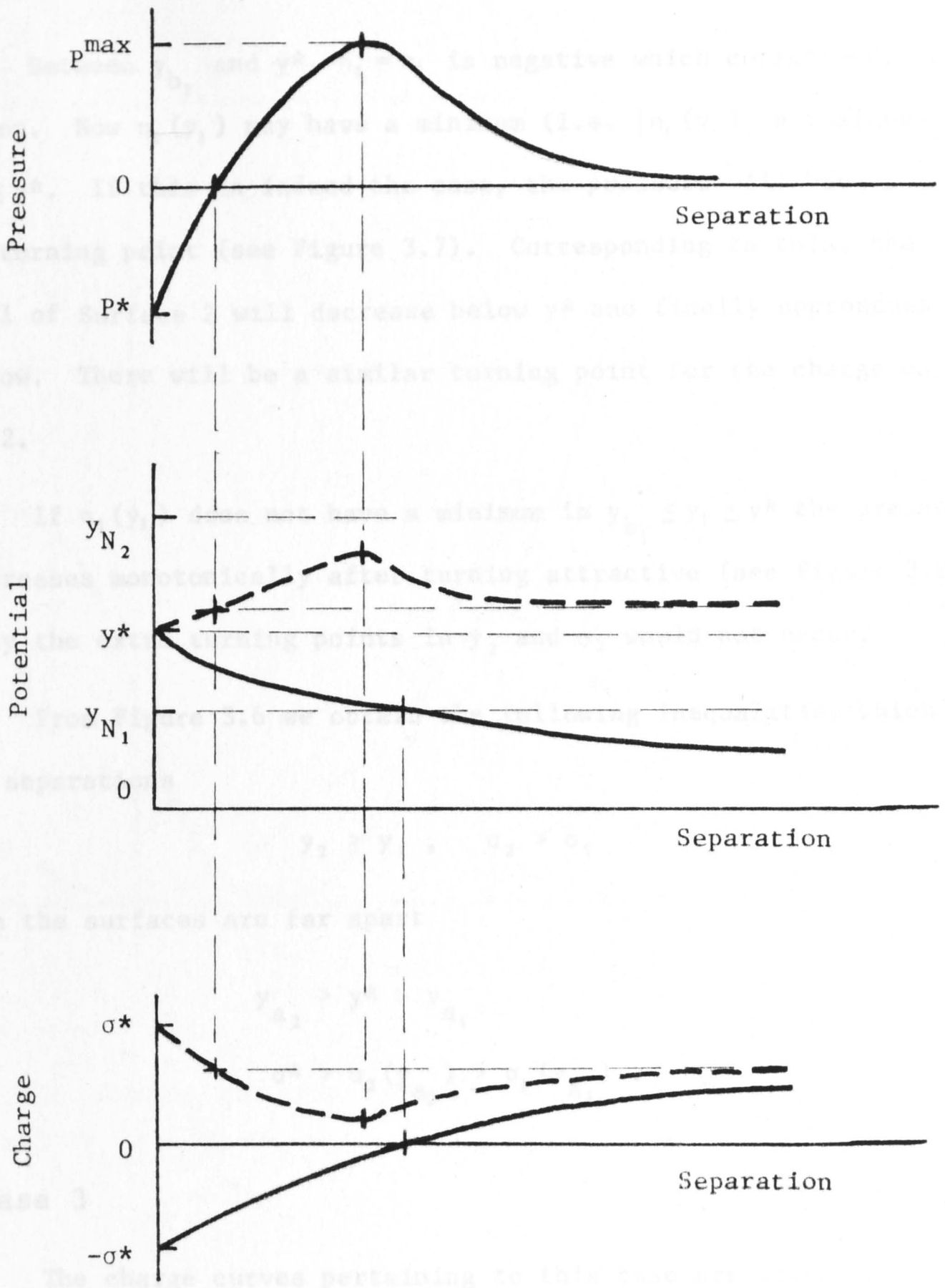

Figure 3.8: Case 2. Showing the main features and schematic variations of the pressure, surface potentials and charges as a function of the separation between the surfaces for the situation where the pressure does not have a local minimum. The potential and charge of Surface 1 are given in solid lines (——); those of Surface 2 are in dashed lines (– – –).

Between y_{b_1} and y*, $\eta_1 = \eta_2$ is negative which corresponds to attraction. Now $\eta_1(y_1)$ may have a minimum (i.e. $|\eta_1(y_1)|$ a maximum) for $y_{b_1} \leq y_1 \leq y^*$. If this is indeed the case, the pressure will have a minimum turning point (see Figure 3.7). Corresponding to this, the potential of Surface 2 will decrease below y* and finally approaches y* from below. There will be a similar turning point for the charge on Surface 2.

If $\eta_1(y_1)$ does not have a minimum in $y_{b_1} \leq y_1 \leq y^*$ the pressure just decreases monotonically after turning attractive (see Figure 3.8). Similarly the extra turning points in y_2 and σ_2 would not occur.

From Figure 3.6 we obtain the following inequalities which hold for all separations

$$y_2 > y_1 , \quad \sigma_2 > \sigma_1$$

and when the surfaces are far apart

$$y_{a_2} > y^* > y_{a_1}$$

$$\sigma^* > \sigma_2(y_{a_2}) > \sigma_1(y_{a_1}) .$$

3c. Case 3

The charge curves pertaining to this case are given in Figure 3.9. They are characterized by the inequality $y^* > y_{c_1}$. The variations with separation of the repulsive pressure, surface potential and charge of each surface are given in Figure 3.10. These results can be derived from the charge curves in Figure 3.9 by a similar consideration to that given in the previous two cases.

In Case 3 the interaction is initially repulsive ($P > 0$), then it turns attractive ($P < 0$) and finally becomes repulsive again as the separation decreases from infinity to zero.

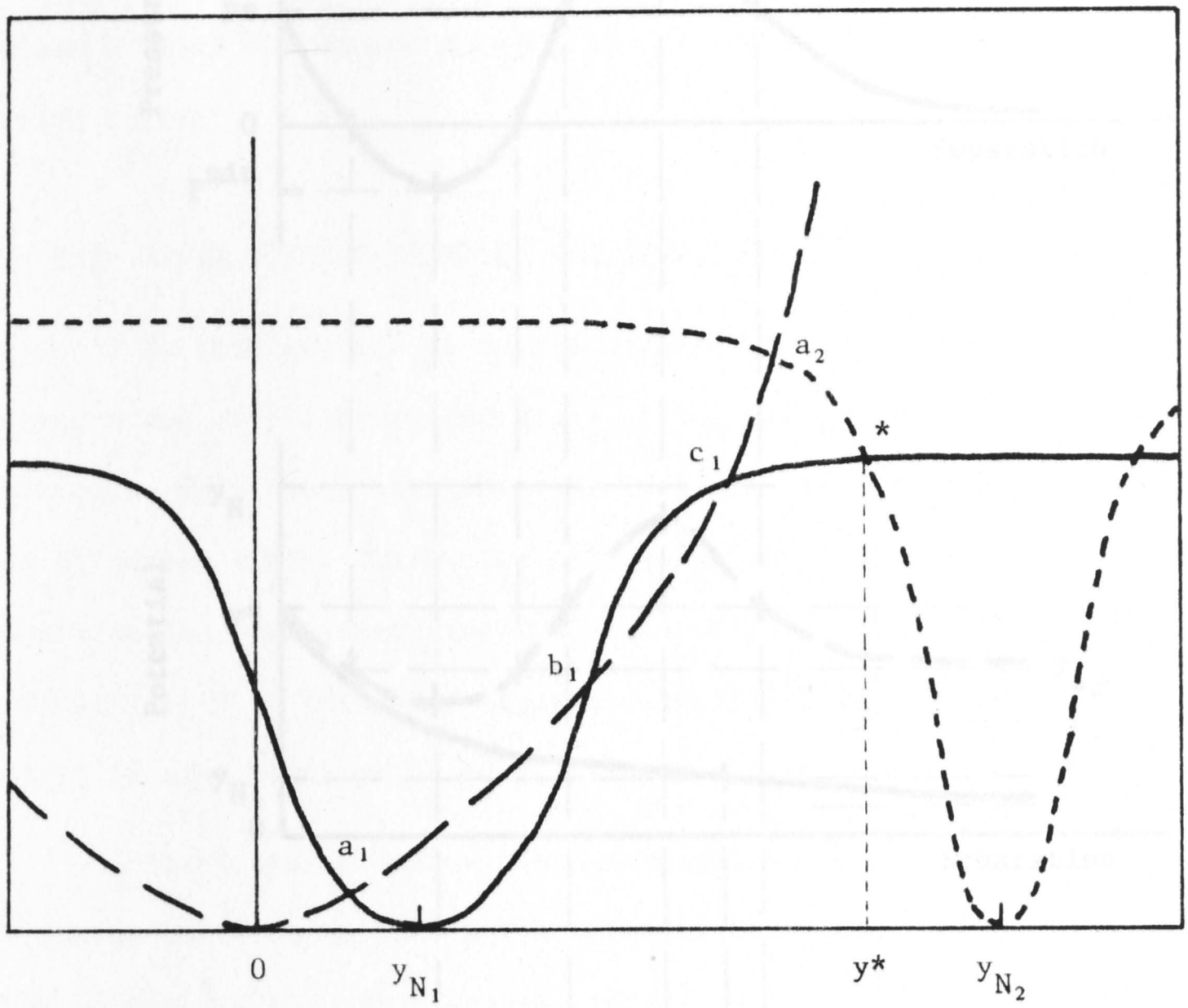

Figure 3.9: Showing the relative positions of the charge curves for Case 3 ($y_{c_1} < y_{a_2}$).

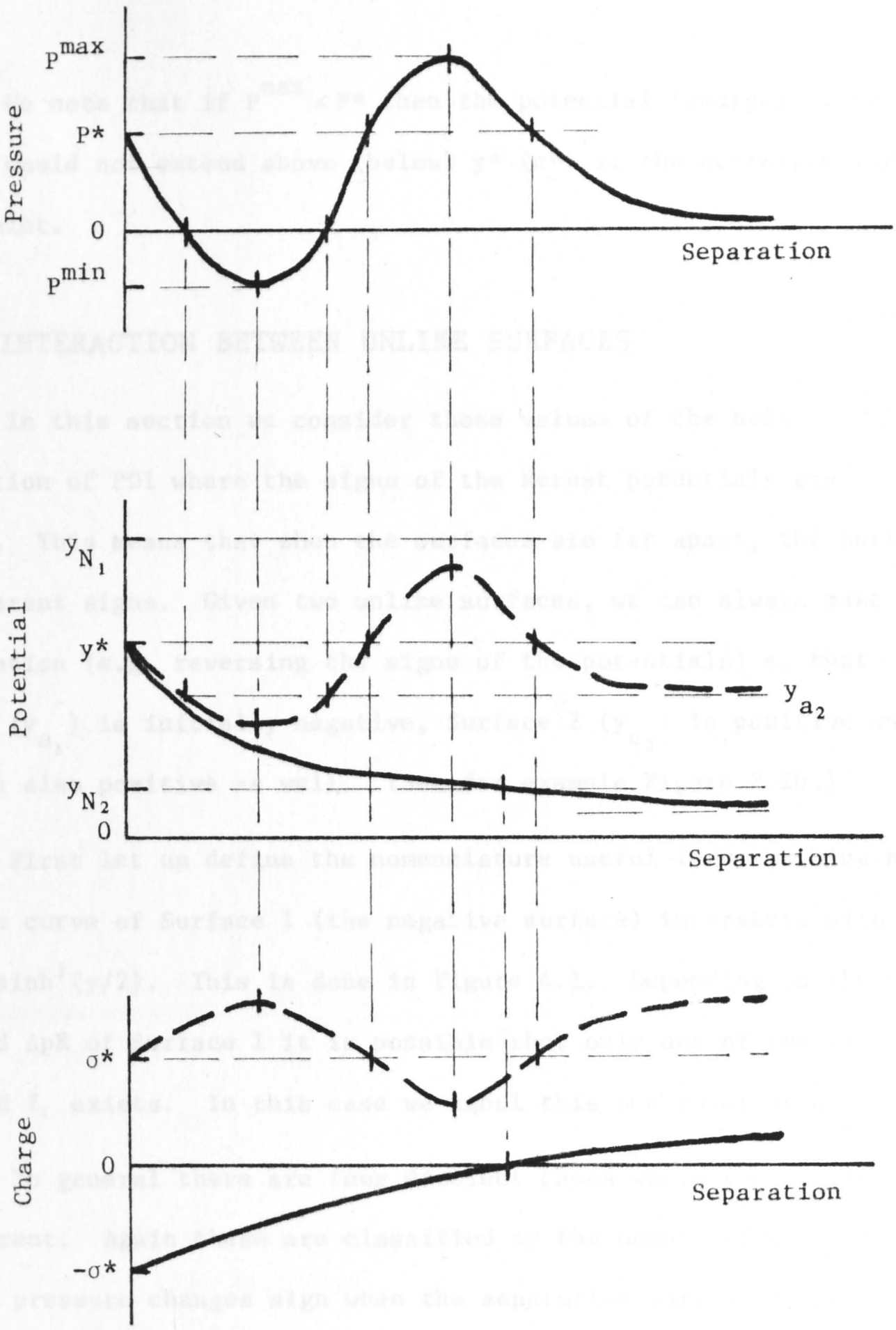

Figure 3.10: Case 3. Showing the pressure, surface potentials and charges as a function of separation between the surfaces. The potentials and charge of Surface 1 are given in solid lines (——); those of Surface 2 are in dashed lines (– – –).

We note that if $P^{max} < P^*$ then the potential (charge) curve of Surface 2 would not extend above (below) y^* (σ^*) at the corresponding turning point.

4. THE INTERACTION BETWEEN UNLIKE SURFACES

In this section we consider those values of the bulk concentration of PDI where the signs of the Nernst potentials are different. This means that when the surfaces are far apart, the surfaces have different signs. Given two unlike surfaces, we can always make a transformation (e.g. reversing the signs of the potentials) so that Surface 1 (y_{a_1}) is initially negative, Surface 2 (y_{a_2}) is positive *and* that y^* is also positive as well. (See for example Figure 2.2b.)

First let us define the nomenclature useful in describing how the charge curve of Surface 1 (the negative surface) intersects with the curve of $\sinh^2(y/2)$. This is done in Figure 4.1. Depending on the value of y_{N_1} and ΔpK of Surface 1 it is possible that only one of the points d_1, e_1 and f_1 exists. In this case we label this one point as d_1.

In general there are four distinct cases where the interactions are different. Again these are classified by the number of times the repulsive pressure changes sign when the separation varies from zero to infinity. These cases are determined by the position of y^* and hence by the relative position and shape of the charge curve of Surface 2 (the positive surface). Each case is defined as follows:

Case 1. $\quad 0 \leq y^* \leq y_{d_1}$

Case 2. $\quad y_{d_1} \leq y^* \leq y_{e_1}$

Case 3. $\quad y_{e_1} \leq y^* \leq y_{f_1}$

Case 4. $\quad y_{f_1} \leq y^*$.

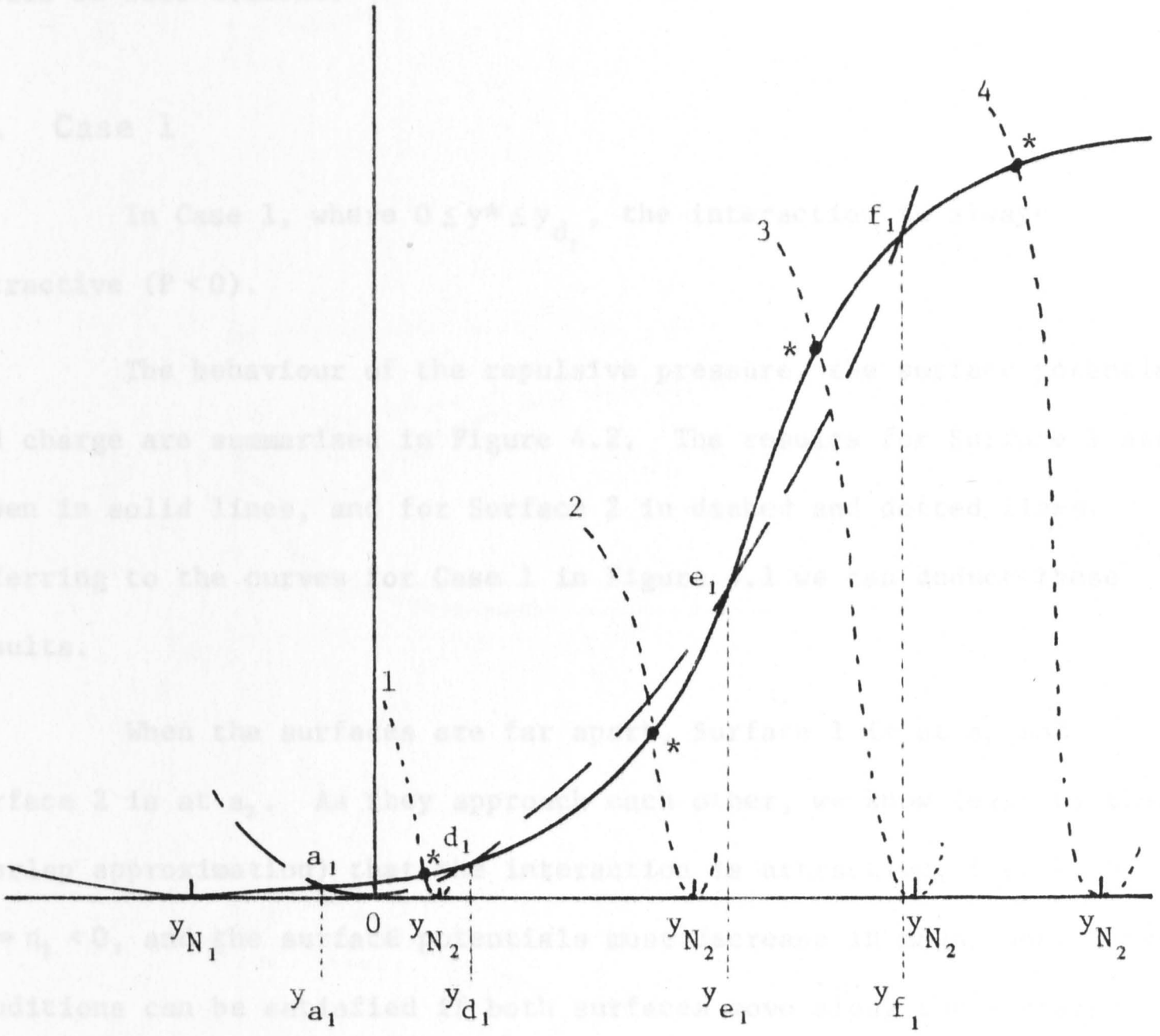

Figure 4.1: Showing the relative positions between the function $\sinh^2(y/2)$ (----), the charge curve of Surface 1 (——) and of Surface 2 (----) for:

(1) Case 1 $(y_{a_1} < y^* < y_{d_1})$

(2) Case 2 $(y_{d_1} < y^* < y_{e_1})$

(3) Case 3 $(y_{e_1} < y^* < y_{f_1})$

(4) Case 4 $(y_{e_1} < y^*)$

when the surfaces have unlike signs at infinite separation.

We shall only outline how the given results can be deduced from the charge curve for Cases 1 and 2. The results of the other cases should be self evident.

4a. Case 1

In Case 1, where $0 \leq y^* \leq y_{d_1}$, the interaction is always attractive ($P < 0$).

The behaviour of the repulsive pressure, the surface potential and charge are summarized in Figure 4.2. The results for Surface 1 are given in solid lines, and for Surface 2 in dashed and dotted lines. Referring to the curves for Case 1 in Figure 4.1 we can deduce these results.

When the surfaces are far apart, Surface 1 is at a_1 and Surface 2 is at a_2. As they approach each other, we know (e.g. by the overlap approximation) that the interaction is attractive, i.e. $P < 0$, $\eta_1 = \eta_2 < 0$, and the surface potentials must decrease in magnitude. These conditions can be satisfied if both surfaces move along their charge curves towards $y = 0$. This way the interaction energy is minimized (i.e. maximize attraction) by making the positive surface (2) more positive and the negative surface (1) more negative.

We observe that if $\eta_1(y_1)$ has a minimum ($|\eta_1(y_1)|$ a maximum) for some $\bar{y}_1$ $(0 \leq \bar{y}_1 \leq y^*)$ then there would be a minimum in the pressure and corresponding turning points in the potential and charge of Surface 2 — see dashed lines in Figure 4.2. Otherwise, all quantities are monotonic in the separation (dotted lines).

We note that since $\bar{y}_2$, where $\eta_1(\bar{y}_1) = \eta_2(\bar{y}_2)$, is always positive, the potential of Surface 2 never changes sign. (This is in

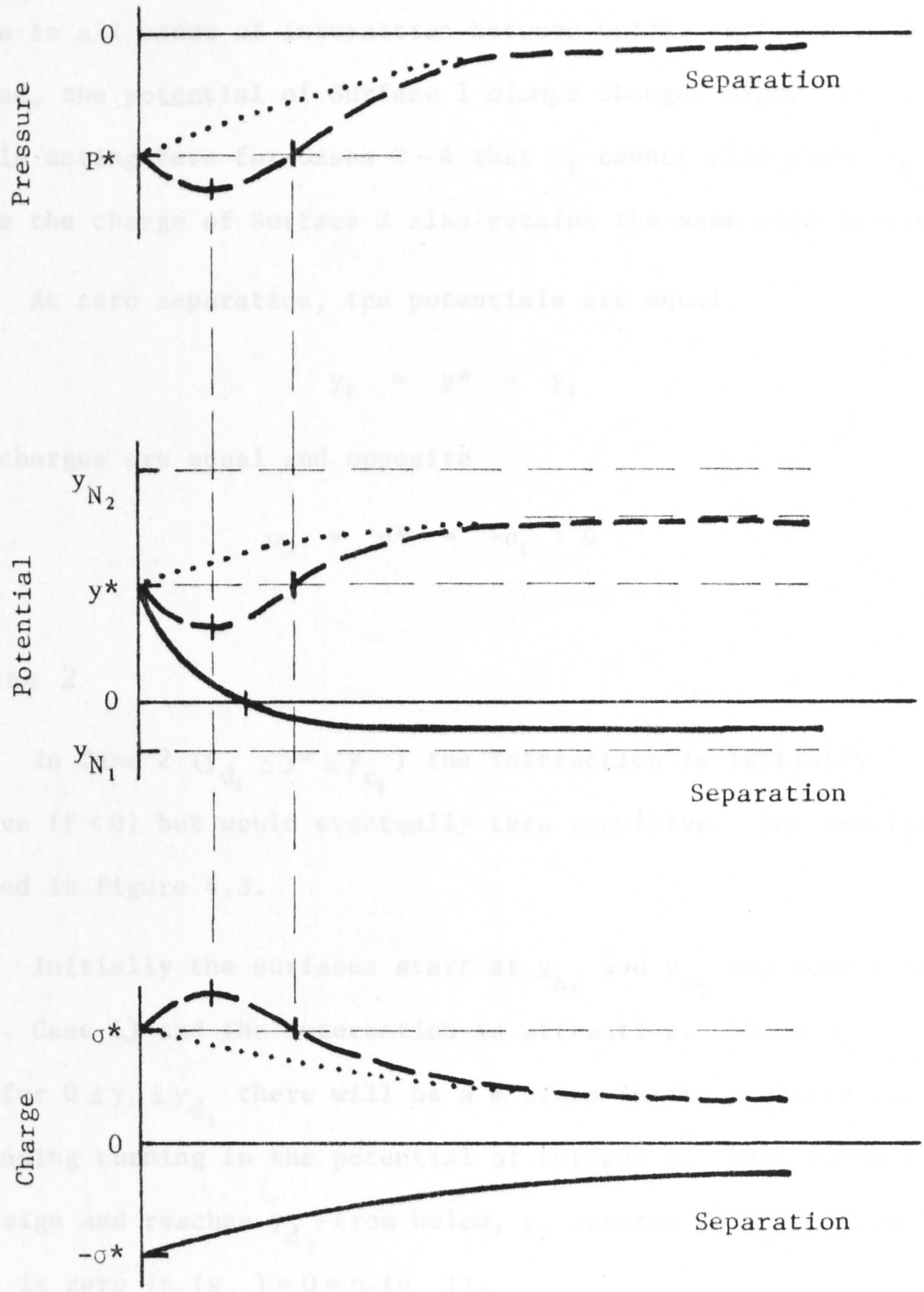

Figure 4.2: Case 1. Variations of the pressure, surface potentials and surface charges with the distance of separation between the surfaces. The potential and charge of Surface 1 are shown in solid lines (——). Those of Surface 2 are given in dashed lines (– – –) if the pressure has a minimum; otherwise they are given instead by the portions in dotted lines (····).

fact true in all cases of interaction between unlike surfaces.) On the other hand, the potential of Surface 1 *always* changes sign. It is worthwhile noting here for Cases 2 - 4 that y_2 cannot rise above y_{N_2}; therefore the charge of Surface 2 also retains the same sign (positive).

At zero separation, the potentials are equal

$$y_1 = y^* = y_2$$

and the charges are equal and opposite

$$\sigma_2 = \sigma^* = -\sigma_1 > 0 .$$

4b. Case 2

In Case 2 ($y_{d_1} \leq y^* \leq y_{e_1}$) the interaction is initially attractive ($P < 0$) but would eventually turn repulsive. The results are summarized in Figure 4.3.

Initially the surfaces start at y_{a_1} and y_{a_2} and move towards $y = 0$ (cf. Case 1) and the interaction is attractive. Since $\eta_1(y_1)$ has a minimum for $0 \leq y_1 \leq y_{d_1}$ there will be a minimum in the pressure and a corresponding turning in the potential of Surface 2. When Surface 1 changes sign and reaches y_{d_1} from below, y_2 returns to y_{a_2}. Here the pressure is zero ($\eta_1(y_{d_1}) = 0 = \eta_2(y_{a_2})$).

When Surface 1 now moves from y_{d_1} to y^* the interaction becomes repulsive. If $\eta_1(y_1)$ has a maximum between y_{d_1} and y^* the potential of Surface 2 will increase past y^* and then return to approach y^* from above. There will also be a similar maximum in the pressure curve (see dashed curves). If $\eta_1(y_1)$ does not have this maximum there would not be a final turning point for y_2 and P (see dotted curves).

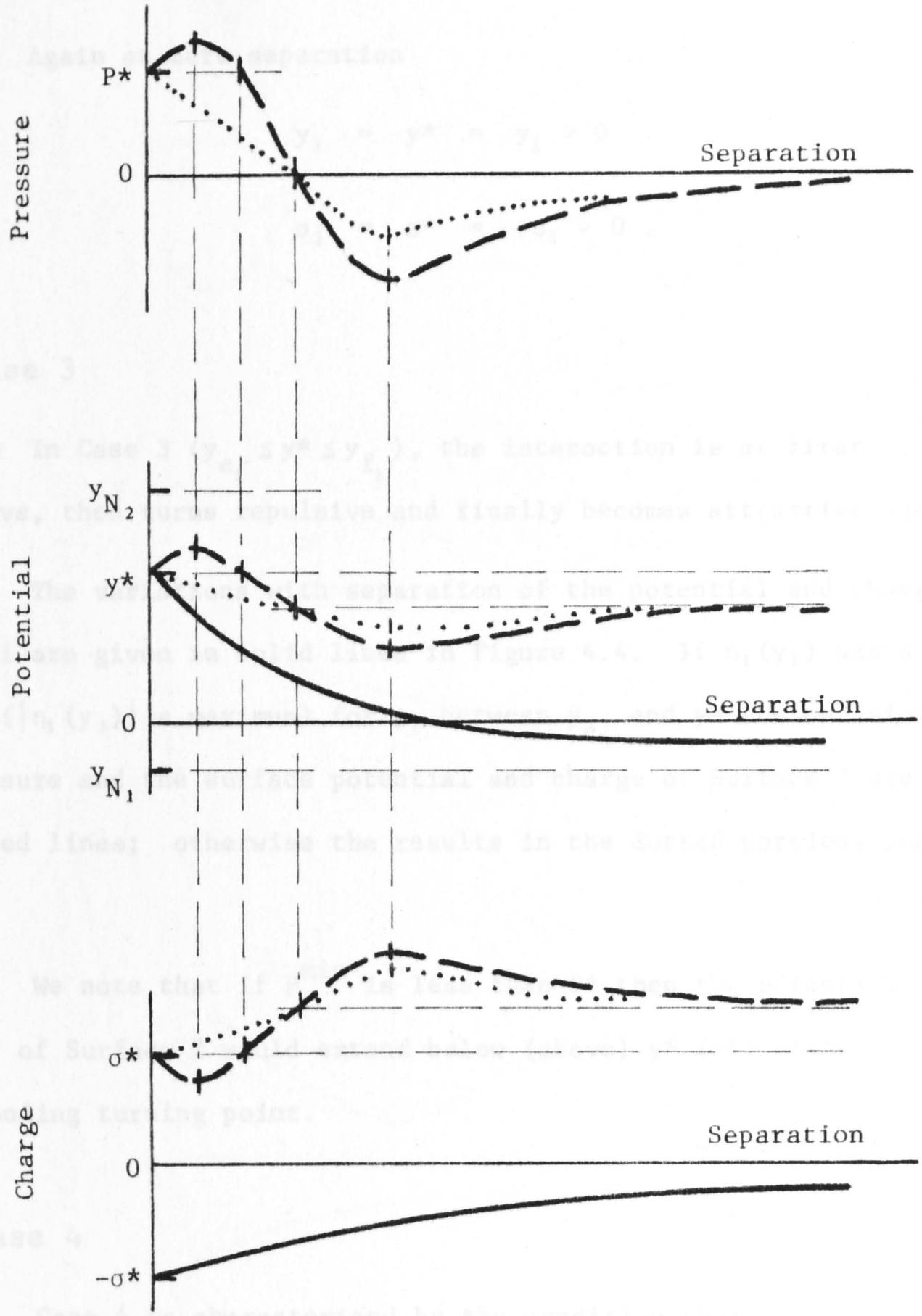

Figure 4.3: Case 2. Variations of the pressure, surface potentials and charges with the distance of separation between the surfaces. The potential and charge of Surface 1 are shown in solid lines (——). Those of Surface 2 are given in dashed lines (– – –) if the pressure has a local maximum; otherwise they are given instead by the portions in dotted lines (····).

Again at zero separation

$$y_1 = y^* = y_2 > 0$$

and

$$\sigma_2 = \sigma^* = -\sigma_1 > 0 .$$

4c. Case 3

In Case 3 ($y_{e_1} \leq y^* \leq y_{f_1}$), the interaction is at first attractive, then turns repulsive and finally becomes attractive again.

The variations with separation of the potential and charge of Surface 1 are given in solid lines in Figure 4.4. If $\eta_1(y_1)$ has a minimum ($|\eta_1(y_1)|$ a maximum) for y_1 between y_{e_1} and y^* the behaviour of the pressure and the surface potential and charge of Surface 2 are given the dashed lines; otherwise the results in the dotted portions would hold.

We note that if P^{min} is less than P^* then the potential (charge) of Surface 2 would extend below (above) y^* (σ^*) at the corresponding turning point.

4d. Case 4

Case 4 is characterized by the condition that $y_{f_1} \leq y^*$.

The behaviour of the pressure, surface charges and potentials are illustrated in Figure 4.5 – solid lines for Surface 1, dashed lines for Surface 2. In the degenerate case where points e_1 and f_1 do not exist, the portions of the curves indicated by dotted lines should hold for the various quantities.

If $P^{max} > P^*$ the corresponding turning points for y_2 and σ_2 will extend beyond y^* and σ^*.

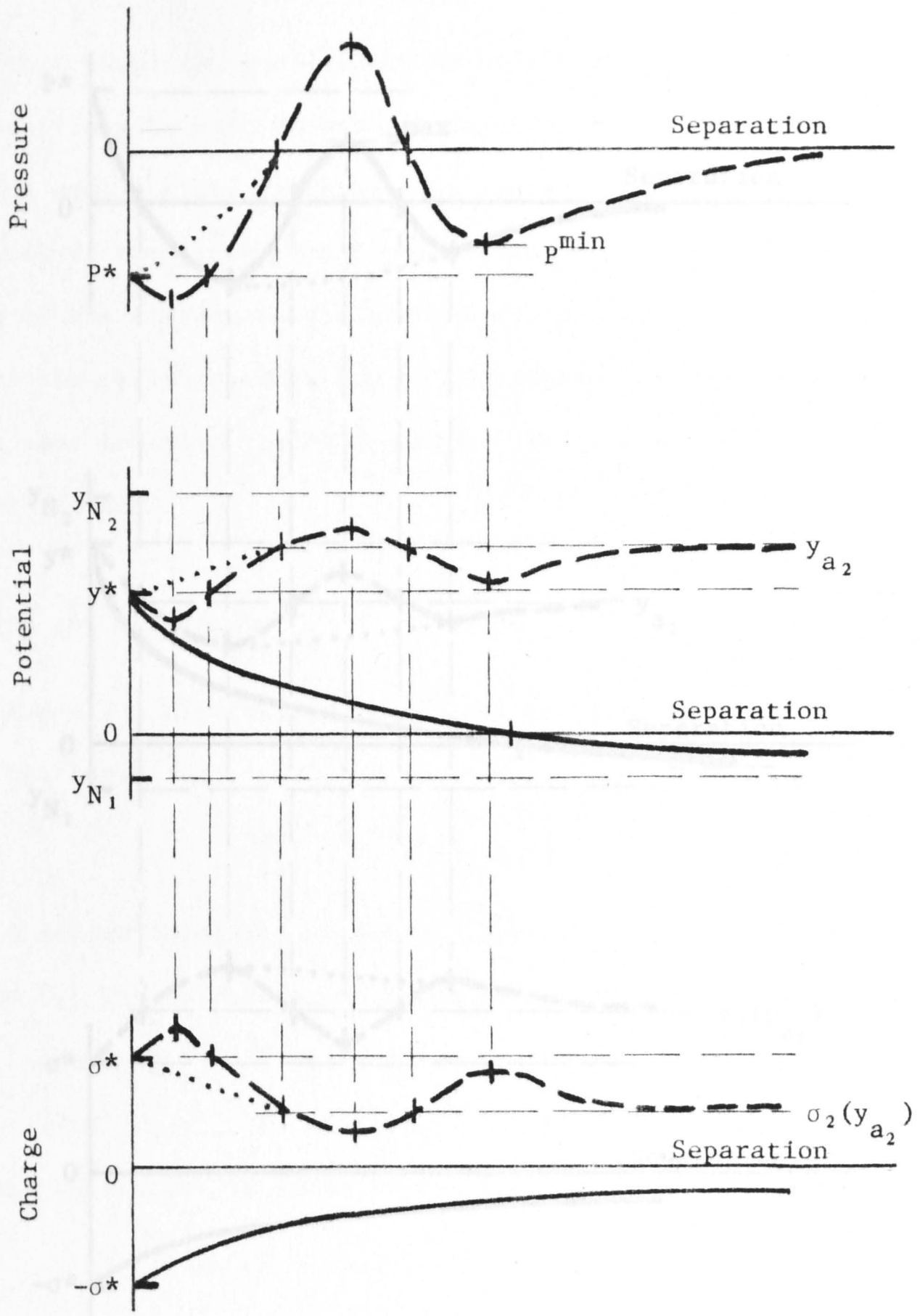

Figure 4.4: Case 3. Variations of the pressure, surface potentials and charges with the distance of separation between the surfaces. The potential and charge of Surface 1 are shown in solid lines (——). Those of Surface 2 are given in dashed lines (– – –) if the pressure has two local minima. If there is only one local minimum, the portions in dotted lines (····) would apply.

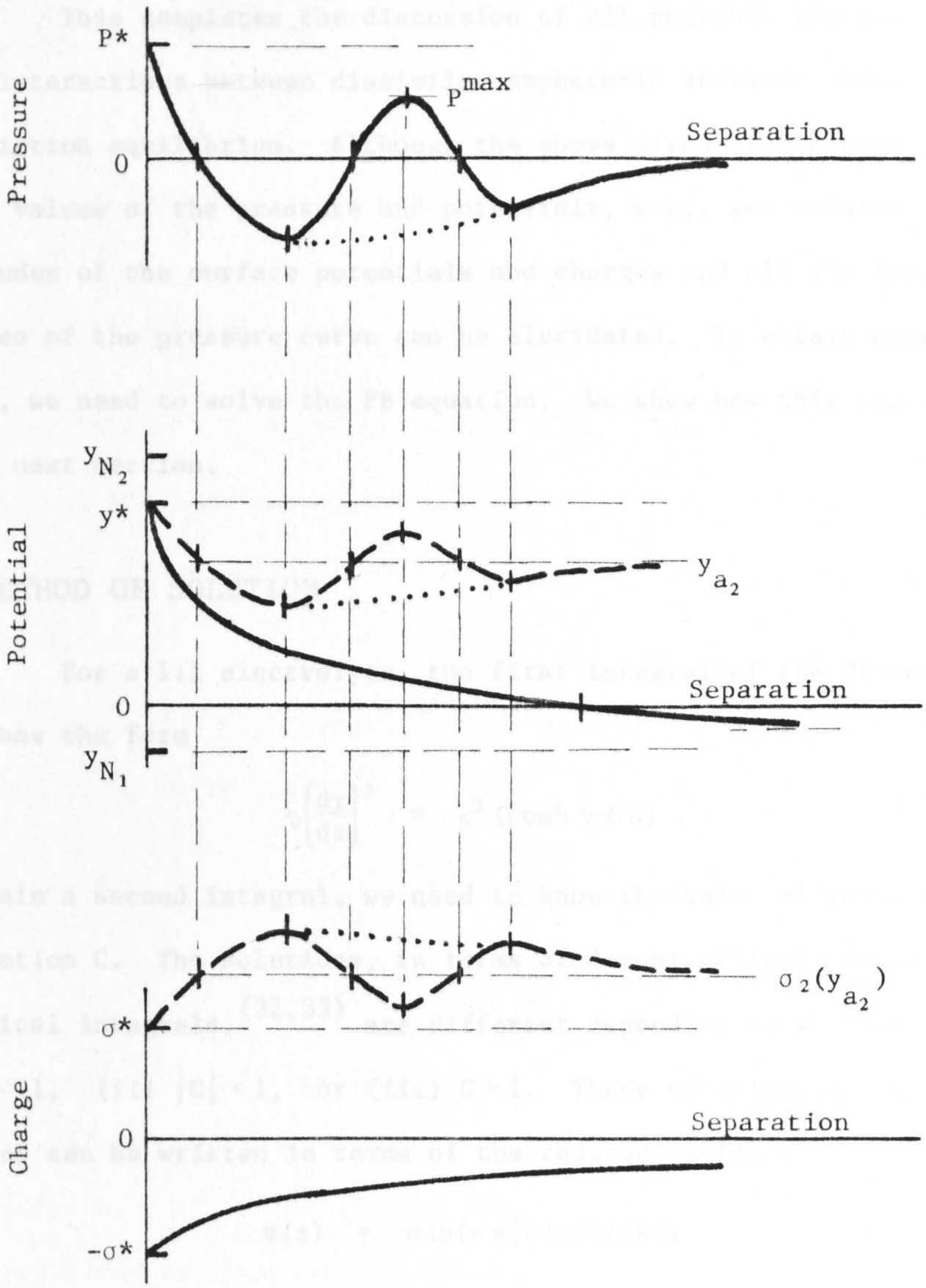

Figure 4.5: Case 4. Variations of the pressure, surface potentials and charges with the distance of separation between the surfaces. The potential and charge of Surface 1 are shown in solid lines (——). Those of Surface 2 are in dashed lines (– – –). If the intersection points d_1 and e_1 do not exist, this is equivalent to the Case 2 dotted lines (····) (cf. Figure 4.3).

This completes the discussion of all possible types of double layer interactions between dissimilar amphoteric surfaces under dissociation equilibrium. Although the above discussion cannot give the actual values of the pressure and potentials, etc., yet relative magnitudes of the surface potentials and charges and all the interesting features of the pressure curve can be elucidated. To obtain numerical values, we need to solve the PB equation. We show how this can be done in the next section.

5. METHOD OF SOLUTION

For a 1:1 electrolyte, the first integral of the PB equation (2.5) has the form

$$\tfrac{1}{2}\left(\frac{dy}{dz}\right)^2 = \kappa^2 (\cosh y + C) \quad . \tag{5.1}$$

To obtain a second integral, we need to know the value of the constant of integration C. The solutions, in terms of Jacobi elliptic functions or elliptical integrals,[32,33] are different depending on whether (i) $C < -1$, (ii) $|C| < 1$, or (iii) $C > 1$. These solutions are well known and they can be written in terms of the reduced variable

$$\phi(z) = \exp(-e|\psi(z)|/2kT) \quad . \tag{5.2}$$

(i) $C < -1$ Repulsive

$$\phi(z) = \phi_0 \, \mathrm{cd}\left[\frac{\kappa (z - z_0)}{2\phi_0} ; \phi_0^2\right] \quad , \tag{5.3}$$

where $\phi_0 = \phi(z_0)$ and at $z = z_0$

$$\left.\frac{d\psi}{dz}\right|_{z=z_0} = 0 \quad . \tag{5.4}$$

Here z_0 can be inside or outside the range $z = 0$ to L.

(ii) $|C| < 1$ Attractive

$$\frac{1-\phi^2(z)}{1+\phi^2(z)} = \left(\frac{1+C}{2}\right)^{\frac{1}{2}} \mathrm{sd}\left\{\kappa|z-z_0| \; ; \left(\frac{1-C}{2}\right)^{\frac{1}{2}}\right\} , \tag{5.5}$$

where at $z = z_0$, the potential $\psi(z_0) = 0$, that is $\phi_0 = \phi(z_0) = 1$.

(iii) $C > 1$ Attractive

$$\phi(z) = \phi_0 \; \mathrm{sc}\left[\tfrac{1}{2}K(\sqrt{1-\phi_0^4}) - \frac{\kappa|z-z_0|}{\phi_0} \; ; (1-\phi_0^4)^{\frac{1}{2}}\right] . \tag{5.6}$$

Here K(k) is the complete elliptic integral of the first kind of modulus k. The constant C is given by

$$C = \tfrac{1}{2}(\phi_0^2 + \phi_0^{-2}) \tag{5.7}$$

and at $z = z_0$, $\psi(z_0) = 0$. Equation (5.7) is suitable for $0 < z_0 < L$. For z_0 outside 0 to L, it is convenient to write the solution in the form

$$\phi(z) = \phi_0 \; \mathrm{sc}\left\{\mathrm{sc}^{-1}\left(\frac{\phi_1}{\phi_2}\right) - \frac{\kappa z}{2\phi_0} \; ; \sqrt{1-\phi_0^4}\right\} , \quad z > z_0 \tag{5.8}$$

$$= \phi_0 \; \mathrm{sc}\left\{\mathrm{sc}^{-1}\left(\frac{\phi_1}{\phi_2}\right) + \frac{\kappa z}{2\phi_0} \; ; \sqrt{1-\phi_0^4}\right\} , \quad z < z_0 , \tag{5.9}$$

where $\phi_1 = \phi \; (z = 0)$. In equations (5.3), (5.5), (5.6), (5.8) and (5.9) cd(x;k), sd(x;k) and sc(x;k) are Jacobi elliptic functions of argument x and modulus k, sc^{-1} is the inverse function of sc with the same modulus. These solutions match up at the transition points $c = \pm 1$, as expected.

From equations (2.18) - (2.20) we can solve for values of the surface potentials at C = -1,1, i.e. at $\eta_1 = \eta_2 = 0,-1$. Putting the appropriate values of the reduced potentials ϕ_1 and ϕ_2 at C = -1 ($\eta_1 = \eta_2 = 0$) into equation (5.3) we can eliminate z_0 to give

$$(\kappa L)_{C=-1} = 2 \tanh^{-1}\left(\frac{|\phi_1 - \phi_2|}{1-\phi_1\phi_2}\right) . \tag{5.10}$$

The length $(L)_{C=-1}$ is the value of the separation where the transition from $C < -1$ to $|C| < 1$ takes place.

Similarly from equations (2.18) - (2.20) we can obtain the potential of Surfaces 1 and 2 at $C = 1$ is $\eta_1 = -1 = \eta_2$. Using these values in equation (5.5) and setting $C = 1$, we can eliminate z_0 to get

$$F_2 = \pm[(1 - F_1^2)^{\frac{1}{2}} \sin(\kappa L) \mp F_1 \cos(\kappa L)] \quad \text{for} \quad L \leq z_0 , \tag{5.11}$$

where

$$F_i = \frac{1 - \phi_i^2}{1 + \phi_i^2} , \quad i = 1,2 . \tag{5.12}$$

This gives us the separation where the transition from $|C| < 1$ to $C > 1$ occurs.

Hence given the dissociation constants for each surface, the bulk concentration of PDI and the ionic strength, we know which of the types of solutions (i), (ii) or (iii) to use for a given value of the separation L. This then gives us a complete solution of the problem. The qualitative descriptions given in the previous sections will enable us to keep track of the signs and relative magnitudes of the potentials and charges. Further it also helps in determining the position of z_0, that is, whether $z_0 < 0$, $0 < z_0 < L$ or $z_0 > L$, and choose the appropriate solutions for the cases $|C| < 1$ and $C > 1$.

The numerical solutions of the various cases listed are presently under investigation.

6. DISCUSSION

In a practical situation, the dissociation constants of the surfaces are fixed, only the concentration of PDI can be varied (provided the particles do not dissolve at extreme concentrations of PDI!). In terms of the charge curves, this means that the relative positions of the two Nernst potentials are fixed. Any variations in the concentration of PDI merely shift both charge curves relative to $\sinh^2(y/2)$ by the same

amount. From the definition of the Nernst potential (assuming H^+ are the PDI)

$$y_N = 2.303\ (pH_0 - pH) = 2.303\ \Delta pH\ , \qquad (6.1)$$

we see that y_N is proportional to the change in pH. Therefore, for like (positive, say) surfaces the effect of decreasing pH can be described by the curves in Figure 6.1 a,b.

In Figure 6.1a, y_{N_1} and y_{N_2} are close together. As pH increases we pass from Case 1 (pH_1) to Case 2 (pH_2). However when y_{N_1} and y_{N_2} are sufficiently far apart, Figure 6.1b, we pass from Case 1 (pH_1) to Case 3 (pH_3) to Case 2 (pH_2) as pH increases. Clearly we can only consider pH values smaller than the pzc of Surface 1 (the surface with the lower pzc) otherwise we would not have like positive surfaces! Thus on a plot of pH versus separation, we can construct regions where the interaction is attractive or repulsive. In Figure 6.2 a,b we have constructed such diagrams corresponding to the situations in Figure 6.1 a,b. The lines delineating the attractive and repulsive regions can be obtained from equation (5.10) for various pH values. Notice that when we are at the pzc of Surface 1, the interaction is always attractive.

We have developed a method whereby we can analyse the main features of the force curve due to double layer interaction between two dissimilar amphoteric surfaces under dissociation equilibrium. The resultant free energy of interaction must of necessity be the lowest possible since equilibrium is assumed to be maintained throughout the approach of the particles. Depending on the characteristics of each surface, it is possible to obtain force barriers and minima in the repulsive pressure from just the electrostatics alone. When combined with the contributions from van der Waals interactions (which in itself may be repulsive and/or attractive) to form the total force curve needed

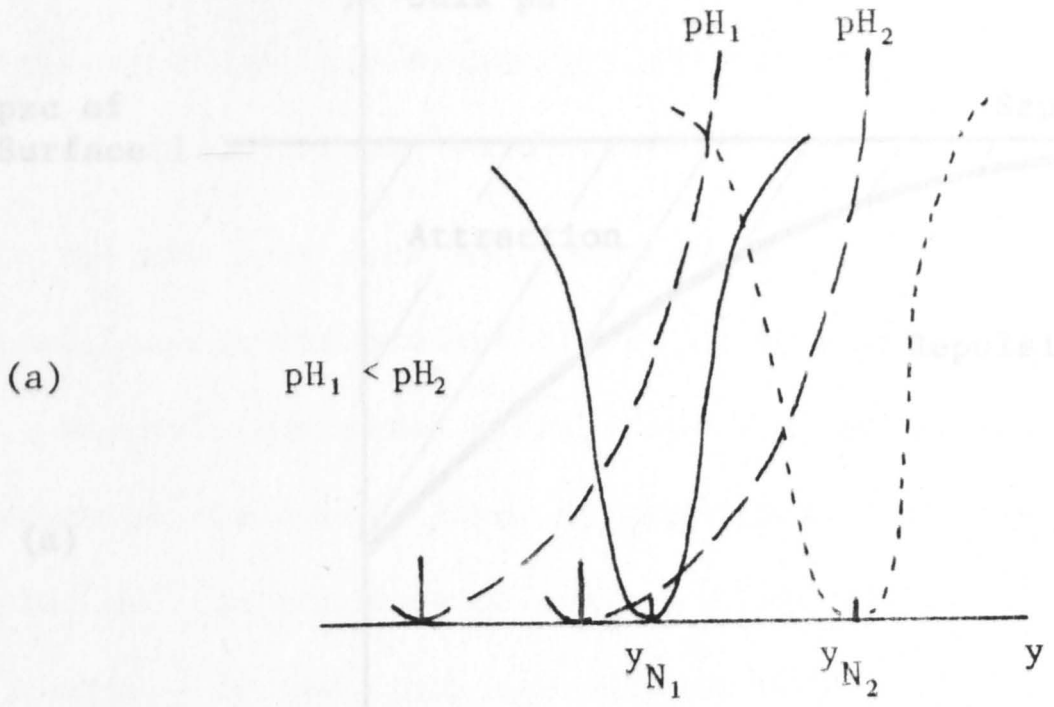

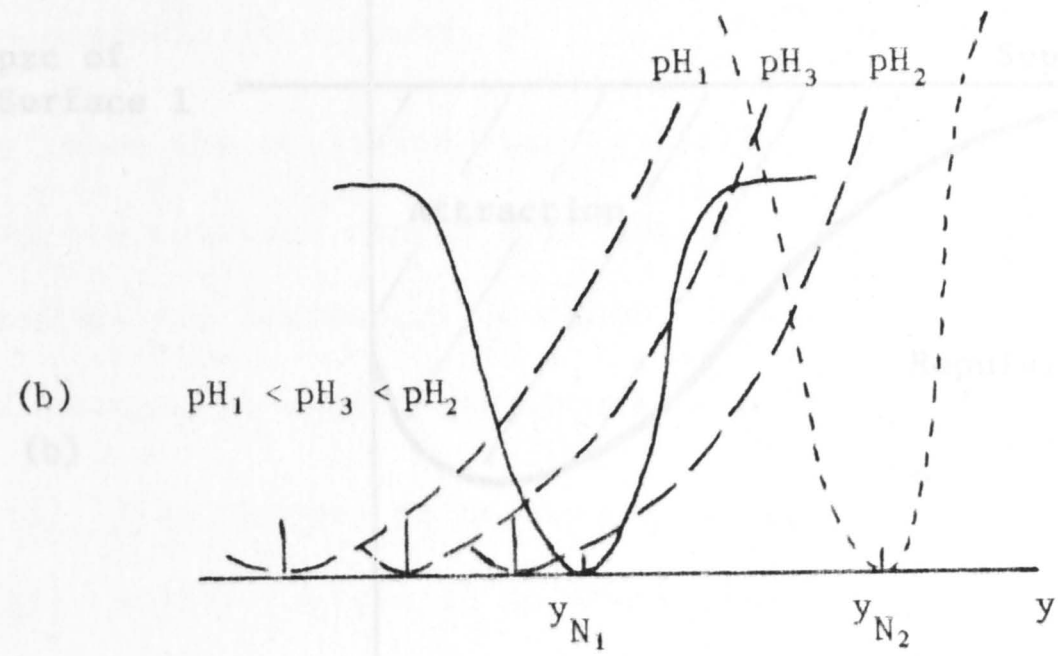

Figure 6.1 a,b: Showing the relative positions of the charge curves and the function $\sinh^2(y/2)$ as the bulk concentration of PDI (bulk pH) is varied.

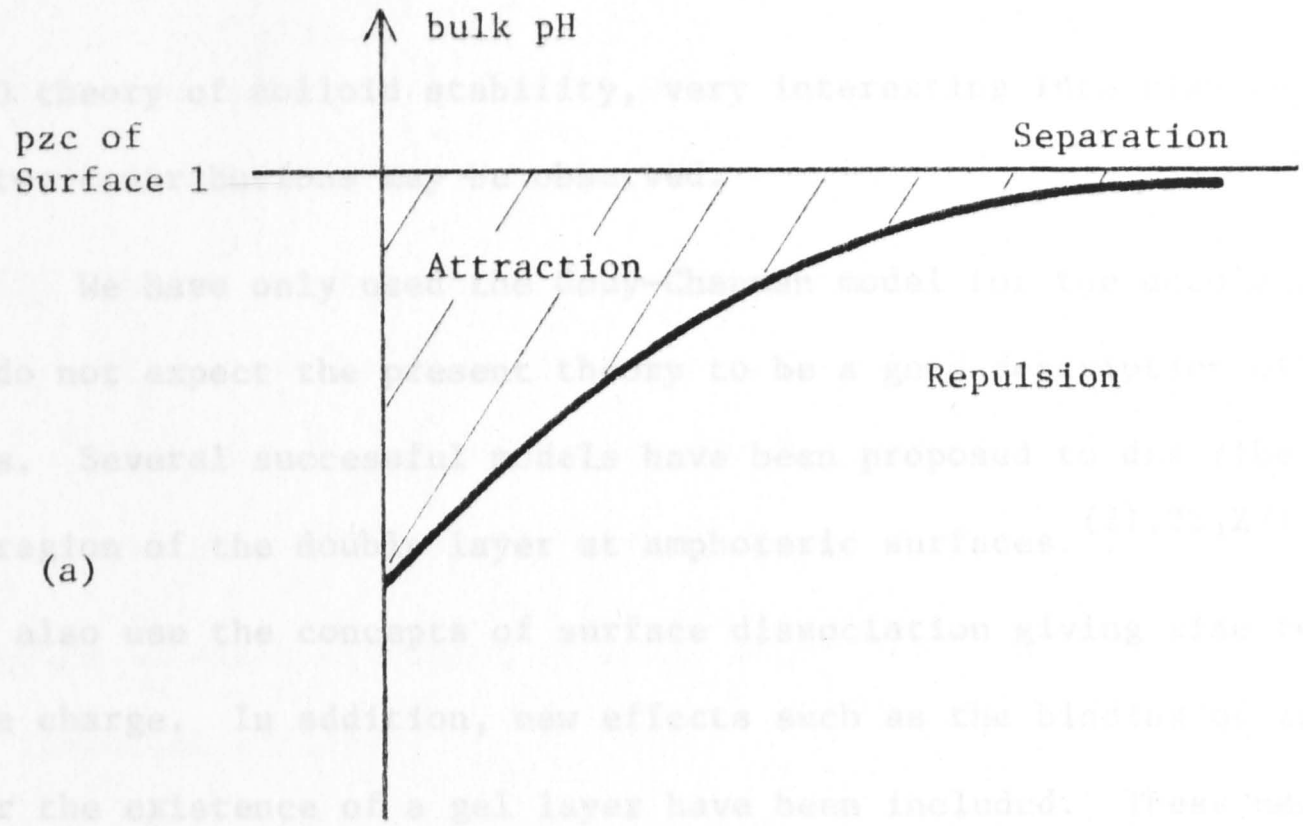

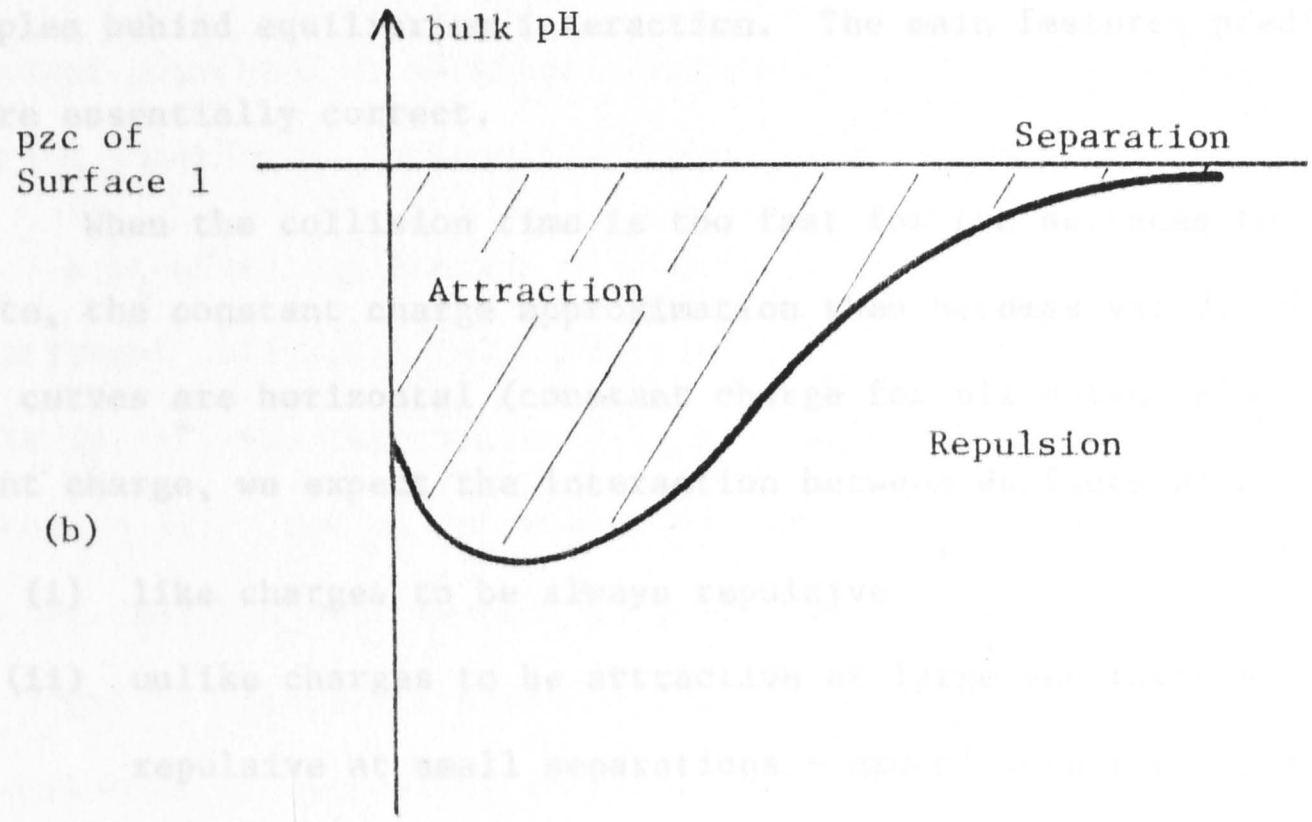

Figure 6.2 a,b: Showing the schematic variation of the regions of repulsion and attraction for given values of bulk pH (PDI) and separation (see text).

in DVLO theory of colloid stability, very interesting interplay between these two contributions may be observed.

We have only used the Gouy-Chapman model for the double layer so we do not expect the present theory to be a good description of real systems. Several successful models have been proposed to describe the inner region of the double layer at amphoteric surfaces.[21,22,27] These models also use the concepts of surface dissociation giving rise to the surface charge. In addition, new effects such as the binding of inert ions or the existence of a gel layer have been included. These new features are in themselves charge and potential regulating. Thus by using the Gouy-Chapman model, we have embraced all the basic physical principles behind equilibrium interaction. The main features predicted here are essentially correct.

When the collision time is too fast for the surfaces to regulate, the constant charge approximation then becomes valid. Here the charge curves are horizontal (constant charge for all potentials). At constant charge, we expect the interaction between surfaces with

(i) like charges to be always repulsive

(ii) unlike charges to be attractive at large separations and repulsive at small separations – *except* when the surfaces have equal and opposite charges where the interaction is then always attractive.

The pressure will always diverge at small separations except for the "*equal and opposite situation*" where it remains finite.

When the regulation of potential is perfect, i.e. constant pontential, the charge curve is essentially an infinitely narrow "V" centred at the Nernst potential. There are no saturation plateaux when

the potential is far from the Nernst value. Under constant potential interaction, surfaces (at infinity) with

(i) unlike potentials will always attract

(ii) like (but not identical) potentials will repel at large separations and attract at small separations. Identical surfaces however will always repel.

The pressure is again divergent at small separations except for that between identical surfaces.

Of the various cases given for interaction between like and unlike surfaces under regulation, Case 3 for like surfaces and Cases 3 and 4 for unlike surfaces (Figures 3.10, 4.4, 4.5) cannot be predicted by the constant potential or constant charge approximation. If the equilibrium interaction is possible these cases may be observable.

A possible application of theory is to consider a mixture of three different sols 1,2,3 (all positive) that is stable at some given pH. That is, all the interaction 1-2, 1-3, 2-3 are all purely repulsive (see Figure 6.3a). Now by increasing the pH we can make the 1-3 interaction unstable with respect to heterocoagulation (see Figure 6.3b), while 1-2 and 2-3 are still stable. Thus by adjusting the bulk pH we have a mechanism of separating the sols 1 and 3 from 2.

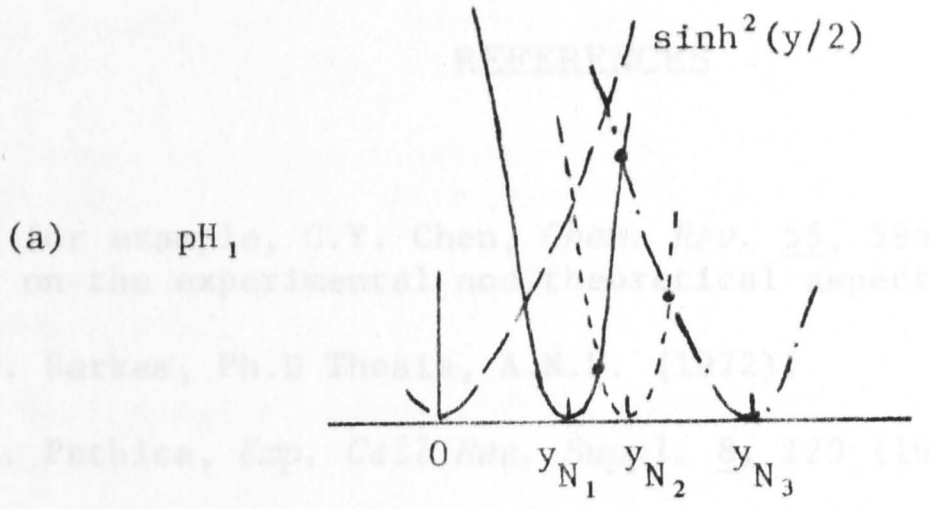

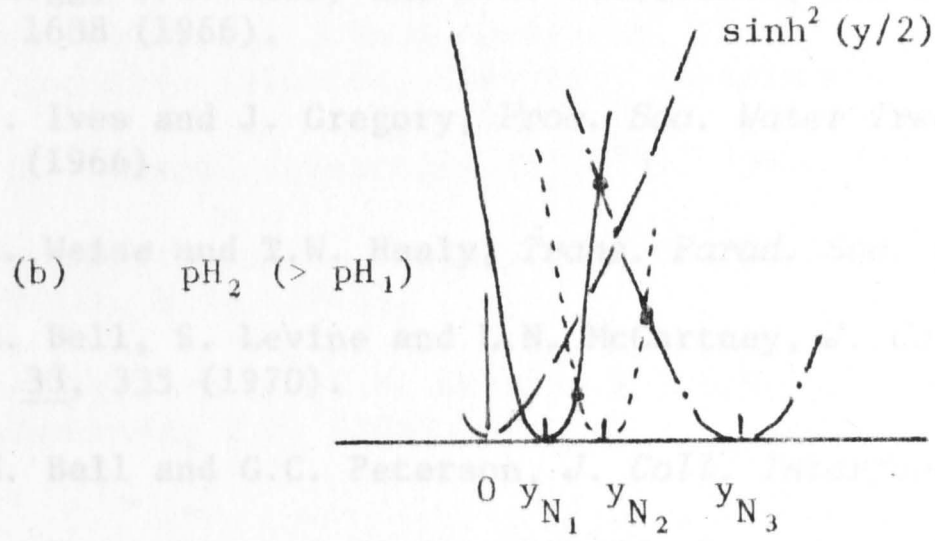

Figure 6.3: An illustration of how "selective coagulation" can be brought about by changing the bulk pH (PDI) (see text).

REFERENCES

(1) See for example, C.Y. Chen, *Chem. Rev.* 55, 595 (1955) for a review on the experimental and theoretical aspects if fibrous beds.

(2) K.W. Sarkes, Ph.D Thesis, A.N.U. (1972).

(3) B.A. Pethica, *Exp. Cell Res. Suppl.* 8, 123 (1961).

(4) B.V. Deryaguin, *Discuss. Farad. Soc.* 18, 85 (1954).

(5) O.F. Devereux and P.L. deBruyn, *Interaction of Plane Parallel Double Layers*, M.I.T. Press, Cambridge (1963).

(6) R. Hogg, T.W. Healy and D.W. Fuerstenau, *Trans. Farad. Soc.* 62, 1638 (1966).

(7) K.J. Ives and J. Gregory, *Proc. Soc. Water Treat. Exam.* 15, 93 (1966).

(8) G.R. Weise and T.W. Healy, *Trans. Farad. Soc.* 66, 470 (1970).

(9) G.M. Bell, S. Levine and L.N. McCartney, *J. Coll. Interface Sci.* 33, 335 (1970).

(10) G.M. Bell and G.C. Peterson, *J. Coll. Interface Sci.* 41, 542 (1972).

(11) V.A. Parsegian and D. Gingell, *Biophys. J.* 12, 1192 (1972).

(12) U. Usui, *Recent Prog. Surface Memb. Sci.* 5, 223 (1972).

(13) U. Usui, *J. Coll. Interface Sci.* 44, 107 (1973).

(14) G. Kar, S. Chander and T.S. Mika, *J. Coll. Interface Sci.* 44, 347 (1973).

(15) H. Ohshima, *Colloid and Polymer Sci.* 252, 257 (1974).

(16) G. Frens and J.Th.G. Overbeek, *J. Coll. Interface Sci.* 38, 376 (1972).

(17) A. Bierman, *J. Coll. Sci.* 10, 231 (1955).

(18) S. Levine and G.M. Bell, *J. Coll. Sci.* 17, 838 (1962).

(19) S. Levine and G.M. Bell, *J. Phys. Chem.* 67, 1408 (1963).

(20) R.H. Ottewill and J.N. Shaw, *Kolloid Z.* 218, 34 (1967).

(21) J.W. Perram, R.J. Hunter and H.J.L. Wright, *Aust. J. Chem.* 27, 461 (1974).

(22) D.E. Yates, S. Levine and T.W. Healy, *J. Chem. Soc., Faraday Trans.* (to appear).

(23) H.J.L. Wright and R.J. Hunter, *Aust. J. Chem.* 26, 1183 (1973); *Aust. J. Chem.* 26, 1191 (1973).

(24) Y.G. Bérubé and P.L. deBruyn, *J. Coll. Interface Sci.* 27, 305 (1968); *J. Coll. Interface Sci.* 28, 92 (1968).

(25) B.V. Deryaguin, *Kolloid Z.* 69, 155 (1934); *Trans. Farad. Soc.* 36, 203 (1940).

(26) N.E. Hoskin and S. Levine, *Phil. Trans. Roy. Soc. London* A248, 449 (1956).

(27) S. Levine and A.L. Smith, *Disc. Farad. Soc.* 52, 290 (1971).

(28) B.W. Ninham and V.A. Parsegian, *J. Theor. Biol.* 31, 405 (1971).

(29) I. Langmuir, *J. Chem. Phys.* 6, 893 (1938).

(30) E.J.W. Verwey and J.Th.G. Overbeek, *Theory of the Stability of Lyophobic Colloids*, Elsevier, Amsterdam (1948).

(31) See for example references (4), (5), (10), (12), (15).

(32) M. Abramowitz and I. Stegun, *Handbook of Mathematical Functions*, Dover, N.Y. (1965).

(33) E.T. Whittaker and G.N. Watson, *A Course of Modern Analysis*, Cambridge U.P. (1969).

PART II

THE CONFORMATION OF MACROMOLECULES

CHAPTER 1

PHASE TRANSITIONS IN POLYMER SOLUTIONS AND THE PREDICTION OF θ TEMPERATURES

1. INTRODUCTION

Interest in the study of polymer conformation arises from the diverse practical situations where polymers are involved: in industry (paint, adhesion, lubrication), in technology (soil improvement, effluent treatment) and in biology (conformation and adsorption of macromolecules and polyelectrolytes) — just to name a few examples. In this chapter, we shall consider some aspects of a polymer in dilute solution; and in the next, some of the salient features of an adsorbed polymer.

One of the central problems in the theory of dilute polymer solutions is the effect of intra-molecular forces on the shapes and sizes of the polymer chains.[1] It has been shown that polymer chains in *dilute* solution would tend to avoid configurations in which the domains of different chains overlap extensively.[2] Therefore, a reasonable model of dilute polymer solutions can be obtained by neglecting *inter*-molecular interactions and considering only the effect of *intra*-molecular and polymer-solvent interactions on the configurations of a single isolated chain.

Following Flory,[3] we classify intra-molecular interactions into short-range and long-range effects. By short-range effects, we include restrictions on bond angles, rotational hindrances, and interferences due to finite size or "hard-core" volume exclusion effects of individual segments or monomer units. These factors are properties of the polymer molecule alone and they exist under all conditions, independent of the environment of the polymer. The single isolated polymer molecule in solution is also subjected to osmotic action of the

surrounding solvent. That is, long-range solvent-polymer and polymer-polymer interactions also determine the conformation of the polymer. These interactions are of electrostatic (e.g. polyelectrolytes in ionic solution) or electrodynamic (e.g. van der Waals or dispersion forces) in origin; therefore, long-range effects are dependent upon the environment of the polymer. In particular they are functions of temperature, and of the electrostatic and dielectric properties of the materials involved.

The presence of long-range interactions expands or contracts the polymer about those configurations determined only by short-range effects. An elastic reaction (not unlike that induced on deforming rubber) consequently develops and balances the osmotic forces to maintain equilibrium. Since polymer-solvent and polymer-polymer interactions are temperature-dependent it is possible that, in certain solvent/polymer systems, there is some temperature θ at which the long-range interactions exactly cancel all short-range excluded volume effects and the polymer behaves like a random flight chain. The residual bond angle restrictions and rotational hindrances can be handled by replacing these effects by an "equivalent" random flight chain with a new effective step size.[4]

Of the various conformational properties of an isolated polymer that can be extracted from experiments such as light scattering and intrinsic viscosity measurements, the mean square radius, $\langle r^2 \rangle$, has received a considerable amount of attention. Mathematically the problem of an interacting polymer has been formulated as a self-avoiding random walk, a problem of considerable complexity. Especially as a result of Edwards' paper[5] some real progress has been made towards the solution of the self-avoiding walk problem. It seems generally agreed by theorists[6] and confirmed by experiments[7] and computer simulations[8-17] that the original prediction of Flory[18-21] namely,

for a positive excluded volume effect $\langle r^2 \rangle \sim N^{6/5}$, where N is the number of monomer units in the polymer, is correct. This is in contrast with the volumeless random flight result $\langle r^2 \rangle \sim N$ which occurs at the θ point. And depending whether or not polymer-solvent interactions are favoured over polymer-polymer interactions, the net result will be a positive or negative excluded volume (self-avoidance) effect.

In this chapter we study the contribution of dispersion forces to the long-range interactions in dilute polymer solutions. Using the simplified version of Edwards' analysis[5] as given by de Gennes[22] together with the notion of the dispersion self-energy of a molecule developed by Mahanty and Ninham,[23] we demonstrate how the polymer segment density $p(\underset{\sim}{r})$ can be determined self-consistently and how the transition from $\langle r^2 \rangle \sim N^{6/5}$ to $\langle r^2 \rangle \sim N$ takes place. The theory is then applied to real polymer/solvent systems to demonstrate how dielectric and spectroscopic properties can be used to provide a criterion for θ solvents, and data from handbooks are used to test the conclusions of the theory.

2. de GENNES' FORMULATION

Consider an "ideal" volumeless polymer. The equilibrium configuration of a polymer is determined by distortions due to long-range polymer-polymer and polymer-solvent interactions and by elastic reactions as a result of entropy losses. In de Gennes' formulation[22] the entropic part of the free energy is related, in a mean field approximation, to an external potential which expands or contracts the polymer.

The polymer is pictured as a collection of beads located at positions $\underset{\sim}{r}_1, \underset{\sim}{r}_2, \ldots, \underset{\sim}{r}_N$, held at a fixed distance $a = |\underset{\sim}{r}_{n+1} - \underset{\sim}{r}_n|$ apart. In the presence of an external force field, the mean orientation of the (n,n+1) link is $\langle \underset{\sim}{r}_{n+1} - \underset{\sim}{r}_n \rangle \equiv \underset{\sim}{u}_n$. For small orientational distortion of the link $|\underset{\sim}{u}_n| << a$, when $\underset{\sim}{u}_n = 0$ corresponding to complete orientational disorder, the associated decrease in entropy is[22] (k = Boltzmann constant)

$$\Delta S_n = - \frac{3k}{2a^2} u_n^2 \quad . \tag{2.1}$$

For if $\tilde{p}(\theta)$ denotes the probability of finding the mean orientation $\underset{\sim}{u}$ at angle θ, the most general form for $\tilde{p}$ leading to a small polarization $\underset{\sim}{u}$ $(u << a)$ is[22]

$$\tilde{p}(\theta) = \tfrac{1}{2}\left(1 + 3\left(\frac{u}{a}\right)\cos\theta + \left(\frac{u}{a}\right)^2 f(\theta) + \ldots\right) \tag{2.2}$$

with $f(\theta)$ arbitrary except the normalization of $\tilde{p}$

$$\int_0^{\pi} \tilde{p}(\theta) \sin\theta \, d\theta = 1 \tag{2.3}$$

requires that

$$\int_0^{\pi} f(\theta) \sin\theta \, d\theta = 0 \, . \tag{2.4}$$

The entropy of the link is[24]

$$S = - k \int_0^{\pi} \tilde{p}(\theta) \, \ell n \, \tilde{p}(\theta) \sin\theta \, d\theta \tag{2.5}$$

which to leading order in u is the result given in equation (2.1).

With this decrease in entropy, the corresponding change in free energy is

$$\Delta G_n = - T \Delta S_n = \frac{3kT}{2a^2} u_n^2 \quad . \tag{2.6}$$

The total change in the free energy

$$G = \frac{3kT}{2a^2} \sum_n (\underset{\sim}{r}_{n+1} - \underset{\sim}{r}_n)^2 \tag{2.7}$$

can be obtained by summing over all links. Differentation of the free energy with respect to $\underset{\sim}{r}_n$ yields the force acting on the n^{th} bead. In the continuum limit this force is

$$\underset{\sim}{F}(\underset{\sim}{r}) = - \frac{\partial G}{\partial \underset{\sim}{r}_n} \rightarrow \frac{3kT}{a^2} \left(\frac{\partial^2 r}{\partial n^2} \right) . \tag{2.8}$$

This expression may be integrated to give

$$\phi(r) - \frac{3kT}{2a^2} \left(\frac{\partial \underset{\sim}{r}}{\partial n} \right)^2 = \text{constant} \tag{2.9}$$

if the force can be derived from a potential:

$$\underset{\sim}{F} = - \nabla \phi .$$

In dealing with the excluded problem, de Gennes[22] shows that $\phi(\underset{\sim}{r})$ is proportional to $p(\underset{\sim}{r})$ the average segment or bead density at $\underset{\sim}{r}$. Further, if one assumes radial symmetry, the number of segments in the range r to r+dr is

$$dn = 4\pi r^2 \, p(r) \, dr . \tag{2.10}$$

The average bead density p(r) is defined such that N, the total number of beads, is given by

$$N = \int_0^{\langle r^2 \rangle^{\frac{1}{2}}} 4\pi r^2 \, p(r) \, dr . \tag{2.11}$$

Hence by setting

$$\phi(r) = kT \, v \, p(r) , \tag{2.12}$$

where v is the "excluded volume parameter", p(r) may be determined self-consistently. If the excluded volume parameter is a constant, substitution of equation (2.12) and (2.10) into (2.9) (with constant = 0) gives $p(r) \sim r^{-4/3}$ which from (2.11) yields $\langle r^2 \rangle \sim N^{6/5}$ and no θ point exists.

3. DISPERSION SELF-ENERGY AND POLYMER CONFORMATION

To examine the role of dispersion interactions in determining polymer conformations in real polymer-solvent systems we require an expression for $\phi(r)$ as the equivalent one-body potential of a polymer segment. This potential must be temperature- and density-dependent and should be expressed in terms of the dielectric properties of the polymer solution. In principle, knowledge of the dielectric properties of the solvent and polymer should provide implicitly a good description of the polymer-polymer, polymer-solvent and solvent-solvent interactions which are ultimately responsible for the chain configuration.

We confine our attention to non-aqueous solvents, where dispersion forces are the dominant interaction mechanism. Then with each polymer segment, we identify the one-body potential with its dispersion self-energy.[23]

The dispersion self-energy of a molecule in vacuum can be defined as the change in energy due to coupling with the electromagnetic field. When in the presence of a material medium, this field is modified by the surrounding molecules, and the self-energy of the molecule will include all interactions with itself and with the molecules of the medium. In the regime where linear response theory is valid, this self-energy is[23]

$$G = \frac{4\pi}{b^3 \pi^{3/2}} kT \sum_{n=0}^{\infty}{}' \frac{\alpha(i\xi_n)}{\varepsilon(i\xi_n)} , \qquad (3.1)$$

where α and ε are respectively the frequency dependent (isotropic) polarizability of the molecule and the homogeneous, isotropic dielectric susceptibility of the medium. The constant b is a measure of the size of the molecule. The summation is over imaginary frequencies, $i\xi_n = i2\pi nkT/\hbar$ with k the Boltzmann constant, T the absolute temperature, $2\pi\hbar$ Planck's

constant and the prime over the summation sign indicates half weight for the $n = 0$ term.

A detailed discussion of the concept of self-energy and the derivation of equation (3.1) is given in reference (23).

If the polarizability α_p of each bead, of radius b, is assumed to be isotropic, the self-energy per bead is

$$G_p = \frac{4\pi}{b^3 \pi^{3/2}} kT \sum_{n=0}^{\infty}{}' \frac{\alpha_p(i\xi_n)}{\varepsilon_m(i\xi_n)} , \qquad (3.2)$$

where ε_m is the dielectric susceptibility of the *solution*. G_p provides a measure of the interaction between the polymer segment and the solvent as well as the interaction between the polymer segment and all other such segments.

To be precise, one should take into account the spatial distribution of polymer segments, that is spatial variations in ε_m when evaluating the self-energy. This can be accomplished as follows. The dispersion self-energy of a molecule given by equation (3.2) is derived from a Green function $G(\underset{\sim}{r},\underset{\sim}{r}';\omega)$ which for a homogeneous medium satisfies the equation

$$\varepsilon_m \nabla^2 G = \delta(\underset{\sim}{r} - \underset{\sim}{r}') . \qquad (3.3)$$

If the dielectric susceptibility of the medium ε_m is a function of spatial co-ordinates (e.g. due to a spatial distribution of polymer segments) the equation for G should be

$$\varepsilon_m \nabla^2 G + \nabla\varepsilon_m \cdot \nabla G = \delta(\underset{\sim}{r} - \underset{\sim}{r}') . \qquad (3.4)$$

Provided the polymer solution is dilute (typically the density of beads within the polymer domain is $\sim 1\%$)[25] we may write[26]

$\varepsilon_m = \varepsilon_s + p(\partial\varepsilon_m/\partial p)_{p=0}$, $[\varepsilon_s >> p(\partial\varepsilon_m/\partial p)]$ where ε_s is the dielectric susceptibility of the pure solvent. If the problem possesses radial

symmetry, we can write

$$\varepsilon_m \frac{\partial^2 G}{\partial r^2} + \left(\frac{2\varepsilon_m}{r} + \frac{\partial \varepsilon_m}{\partial p} \frac{\partial p}{\partial r} \right) \frac{\partial G}{\partial r} = \delta(\underset{\sim}{r} - \underset{\sim}{r}') \ . \qquad (3.5)$$

When the solution is near the θ point $p(r) \sim 1/r$ so using this value of $p(r)$ we get

$$\varepsilon_m \frac{\partial^2 G}{\partial r^2} + \frac{2\varepsilon_m}{r} \left(1 - \frac{p}{2\varepsilon_m} \frac{\partial \varepsilon_m}{\partial p} \right) \frac{\partial G}{\partial r} = \delta(\underset{\sim}{r} - \underset{\sim}{r}') \ . \qquad (3.6)$$

But since $\varepsilon_s >> p(\partial \varepsilon_m / \partial p)$ we can to leading order neglect spatial variations in ε_m when evaluating the self-energy.

Returning now to equation (3.2), we note that since only molecules in the neighbourhood of the polymer bead in question contribute significantly to its self-energy, so for a dilute solution we can account for the distribution of other polymer segments by allowing ε_m in equation (3.2) for the self-energy G_p, to depend on the density $p(r)$ of other segments. For the one-body potential, we write

$$\phi(r) = \frac{4\pi}{b^2 \pi^{3/2}} kT \sum_{n=0}^{\infty}{}' \left\{ \frac{\alpha_p(i\xi_n)}{\varepsilon_m(i\xi_n)} - \frac{\alpha_p(i\xi)}{\varepsilon_s(i\xi)} \right\} , \qquad (3.7)$$

where the second term describes the bead-solvent interaction in the absence of all other polymer beads. Thus it follows that the constant of integration in equation (2.9) is zero because far away from the polymer $\varepsilon_m = \varepsilon_s$ since $p(\infty) = 0$.

To obtain an expression for the dielectric susceptibility of the polymer solution ε_m in terms of the bead density $p(r)$ we assume that the polarizabilities of the polymer beads and the segment molecules are additive[27] and are related to ε_m by the Claussius-Mossotti relation.[28] Such assumptions are reasonable for non-polar media. We write

$$\frac{\varepsilon_m - 1}{\varepsilon_m + 2} = \frac{4\pi}{3} [p(r)\alpha_p + (n_s - p(r))\alpha_s] \ , \qquad (3.8)$$

where n_s is the density of solvent molecules in a pure solvent and is taken to be constant. In other words we "remove" a solvent molecule and "replace" it by a monomer unit. The density of molecules in the solution remains the same as that in the pure solvent. Equation (3.8) may be rearranged to give

$$\varepsilon_m = \frac{\varepsilon_s + \frac{8\pi}{3} p(r)(\alpha_p - \alpha_s)/(1-\Delta_s)}{1 - \frac{4\pi}{3} p(r)(\alpha_p - \alpha_s)/(1-\Delta_s)} \tag{3.9}$$

$$\simeq \varepsilon_s + p(r) \frac{4\pi(\alpha_p - \alpha_s)}{(1-\Delta_s)^2} + p^2(r) \frac{(4\pi)^2(\alpha_p - \alpha_s)^2}{3(1-\Delta_s)^3} + O(p^3(r)) \ldots , \tag{3.10}$$

where

$$\Delta_s \equiv \frac{\varepsilon_s - 1}{\varepsilon_s + 2} = \frac{4\pi}{3} n_s \alpha_s . \tag{3.11}$$

We now seek a solution of equation (2.9) for which p(r) is radially symmetric. Combining equations (2.9), (2.10) and (3.10) we get, to leading order in p(r)

$$\frac{(4\pi)^2 kT}{b^3 \pi^{3/2}} \left\{ \sum_{n=0}^{\infty}{}' \frac{\alpha_p(\alpha_s - \alpha_p)}{\varepsilon_s^2 (1-\Delta_s)^2} p^3(r) + \frac{8\pi}{3} \sum_{n=0}^{\infty}{}' \frac{\alpha_p \alpha_p (\alpha_s - \alpha_p)^2}{\varepsilon_s^3 (1-\Delta_s)^3} p^4(r) \right\}$$

$$+ O(p^5(r)) = \frac{3kT}{2a^2} \frac{1}{(4\pi r^2)^2} . \tag{3.12}$$

In general, the $p^3(r)$ term always dominates the left hand side and we have

$$p(r) \sim r^{-4/3} ; \quad \langle r^2 \rangle \sim N^{6/5} . \tag{3.13}$$

This is the familiar situation where excluded volume effects are significant. On the other hand, when the coefficient of $p^3(r)$ becomes identically zero, then

$$p(r) \sim r^{-1} ; \quad \langle r^2 \rangle \sim N \tag{3.14}$$

and the mean square radius is like that of a random flight chain. The singular situation when the coefficient of $p^3(r)$ vanishes corresponds to

the θ point. The physical significance of the coefficients of p(r) in equation (3.12) can be seen as follows. The coefficient of $p^3(r)$ is

$$A_3 = \frac{(4\pi)^2 kT}{b^3 \pi^{3/2}} \sum_{n=0}^{\infty}{}' \frac{(\alpha_p \alpha_s - \alpha_p \alpha_p)}{\varepsilon_s^2 (1-\Delta_s)^2} \tag{3.15}$$

and that of $p^4(r)$ is

$$A_4 = \frac{2(4\pi)^3}{3b^3 \pi^{3/2}} kT \sum_{n=0}^{\infty}{}' \frac{(\alpha_p \alpha_p \alpha_p + \alpha_p \alpha_s \alpha_s - 2\alpha_p \alpha_p \alpha_s)}{\varepsilon_s^3 (1-\Delta_s)^3} . \tag{3.16}$$

We see that to leading order in α, A_3 describes the competition between two-body solvent-polymer and polymer-polymer interactions, and A_4 describes the competition among the three-body polymer-polymer-polymer, polymer-solvent-solvent and polymer-polymer-solvent interactions.[36-38] Under normal conditions the two-body interactions are dominant and they give rise to the $\langle r^2 \rangle \sim N^{6/5}$ behaviour. However, under special circumstances when the two-body interactions cancel exactly, the three-body term then give the $\langle r^2 \rangle \sim N$, random flight configuration. The sign of any particular term in the sum A_3, corresponding to some frequency ξ_j, may be $\gtrless 0$ depending on whether $(\alpha_p \alpha_s - \alpha_p \alpha_p) \gtrless 0$ at ξ_j. If $(\alpha_p \alpha_s - \alpha_p \alpha_p) > 0$ polymer-solvent interactions are favoured over polymer-polymer interactions and if $(\alpha_p \alpha_s - \alpha_p \alpha_p) < 0$, the converse is true. It is quite possible that for a given polymer/solvent pair $(\alpha_p \alpha_s - \alpha_p \alpha_p)$ may change sign during the course of the frequency summation. If the net result is that $A_3 > 0$, then on the whole polymer-solvent interactions are preferred over polymer-polymer interactions and the polymer exhibit a positive excluded volume effect. In other words, the solvent "expands" the polymer. If $A_3 < 0$ the present theory predicts a collapse of the polymer ($\langle r^2 \rangle < 0$!); however in this regime short-range effects need to be taken into account. The condition under which the two-body terms cancel (θ-point) depends on a delicate balance of the absorption spectra

of the materials and the complicated summation over imaginary frequencies ($i\xi_n = i2\pi nkT/\hbar$). Therefore the existence of the θ point for a given polymer/solvent system depends critically on the dielectric properties of both the solvent and the polymer as well as on the temperature, mainly through variations in the dielectric constant. This point will be taken further in the next section.

4. APPLICATION TO REAL POLYMER-SOLVENT SYSTEMS

Before applying our formulae to real systems it is worth while to recapitulate the assumptions made so far.

(i) We have assumed the polymer can be modelled as a string of beads held at a fixed distance a apart, and each bead has an isotropic polarizability.

(ii) The solvent is assumed to be isotropic and structureless and is only characterized by its dielectric susceptibility ε_s.

(iii) Only long-range dipole-dipole dispersion interactions are examined. Short-range effects such as fixed bond angles hindered rotation and hard core volume effects are not considered. However, these are unimportant provided we remain in the random flight or positive excluded volume regimes. Evidently these assumptions are fairly extreme. Nonetheless we have an order of magnitude agreement with observed trends even at this level of sophistication.

To investigate the magnitude of the coefficient A_3 near the θ point, we need a representation of the frequency dependent polarizabilities and dielectric susceptibilities along the imaginary frequency axis. It has been found in work connected with the calculation of dispersion forces between macroscopic bodies[29-33] that it is

sufficient to write

$$\varepsilon(i\xi) = 1 + \sum_j \frac{c_j}{1 + (\xi/\omega_j)^2 + \gamma_j \, \xi/\omega_j} + \sum_r \frac{D_r}{1 + \xi/\Omega_r} \, .$$

The terms in c_j describe Lorentzian relaxations of strength c_j at frequency ω_j, and that in D_r, simple Debye rotational relaxations. For non-polar organic materials, where there are no Debye relaxations and the band width γ_j is always small compared with ω_j, the required dielectric properties can be represented by the simple form

$$\varepsilon(i\xi) = 1 + \frac{R^2 - 1}{1 + \xi^2/\omega_{uv}^2} \, . \tag{4.1}$$

Here we have summarized the absorption spectra by one principal absorption frequency ω_{uv} in the ultraviolet. The static dielectric constant $\varepsilon(0)$ is related to the refractive index R by

$$\varepsilon(0) = R^2 \, . \tag{4.2}$$

The polarizability is connected to the dielectric susceptibility via the Claussius-Mossotti relation[28]

$$\Delta_i \equiv \frac{\varepsilon_i - 1}{\varepsilon_i + 2} = \frac{4\pi}{3} n_i \alpha_i \, , \quad i = s,p \text{ for solvent or polymer} \, . \tag{4.3}$$

The value of n_i, the density of molecules that contribute to dielectric dispersion in a pure substance i, is uncertain. But since most organic solvents and monomers have similar molecular weights and densities, it seems reasonable to assume that the values for the solvent and the polymer do not differ significantly. Henceforth we set $n_p \simeq n_0 \simeq n_s$. For $\varepsilon(i\xi)$ of the general form given in equation (4.1) it can be easily shown that $\alpha(i\xi)$

$$\alpha_i(i\xi) = \frac{\alpha_i(0)}{1 + (\xi/\omega_0^i)^2} \, , \tag{4.4}$$

where

$$\alpha_i(0) = \frac{3}{4\pi n_i}\left(\frac{\varepsilon_i(0)-1}{\varepsilon_i(0)+2}\right) \equiv \frac{3}{4\pi n_0}\Delta_i^0 , \quad i = s,p . \tag{4.5}$$

The absorption frequency ω_0^i is different from ω_{uv} for the bulk material. Since α_i is the polarizability of a monomer or solvent molecule and because of the lack of detailed spectroscopic data, $\hbar\omega_0$ can be approximated by the *gaseous* first ionization potential of the appropriate molecule. The form of $\alpha(i\xi)$, according to equations (4.4) and (4.5), is represented schematically in Fig. 4.1.

Returning now to equation (3.15) we see that at the θ point A_3 must vanish. This implies that $(\alpha_s - \alpha_p)$ must change sign as ξ varies from 0 to ∞. From equations (4.4) and (4.5) we see that

$$(\alpha_s - \alpha_p) \propto \left(\frac{\Delta_s^0}{1+(\xi/\omega_0^s)^2} - \frac{\Delta_p^0}{1+(\xi/\omega_0^p)^2}\right) . \tag{4.6}$$

Hence for $(\alpha_s - \alpha_p)$ to change sign, the curves $\alpha_p(i\xi)$ and $\alpha_s(i\xi)$ must intersect in the manner similar to that shown in Fig. 4.1. Therefore, a necessary condition for a polymer/solvent pair to exhibit a θ point within a temperature range is that, within this range, if

$$(\Delta_s^0 - \Delta_p^0) \gtrless 0 \quad \text{then} \quad \left(\frac{\Delta_p^0}{\omega_0^{s^2}} - \frac{\Delta_s^0}{\omega_0^{p^2}}\right) \gtrless 0 , \tag{4.7}$$

and vice versa. The summation over frequencies in equation (3.15) samples the difference between the two curves in Fig. 4.1 at intervals $\Delta\xi = 2\pi kT/\hbar$. Geometrically, this summation is roughly the same as the difference between the two shaded areas labelled 1 and 2. So for a θ-point to exist, a delicate balance of the absorption spectra of the polymer and solvent is needed. In other words, for a polymer/solvent pair that exhibits a θ point, we conclude, under the present model, that condition (4.7) should hold between the *gaseous* first ionization potentials, I, and the static dielectric constants, $\varepsilon(0)$, of the polymer

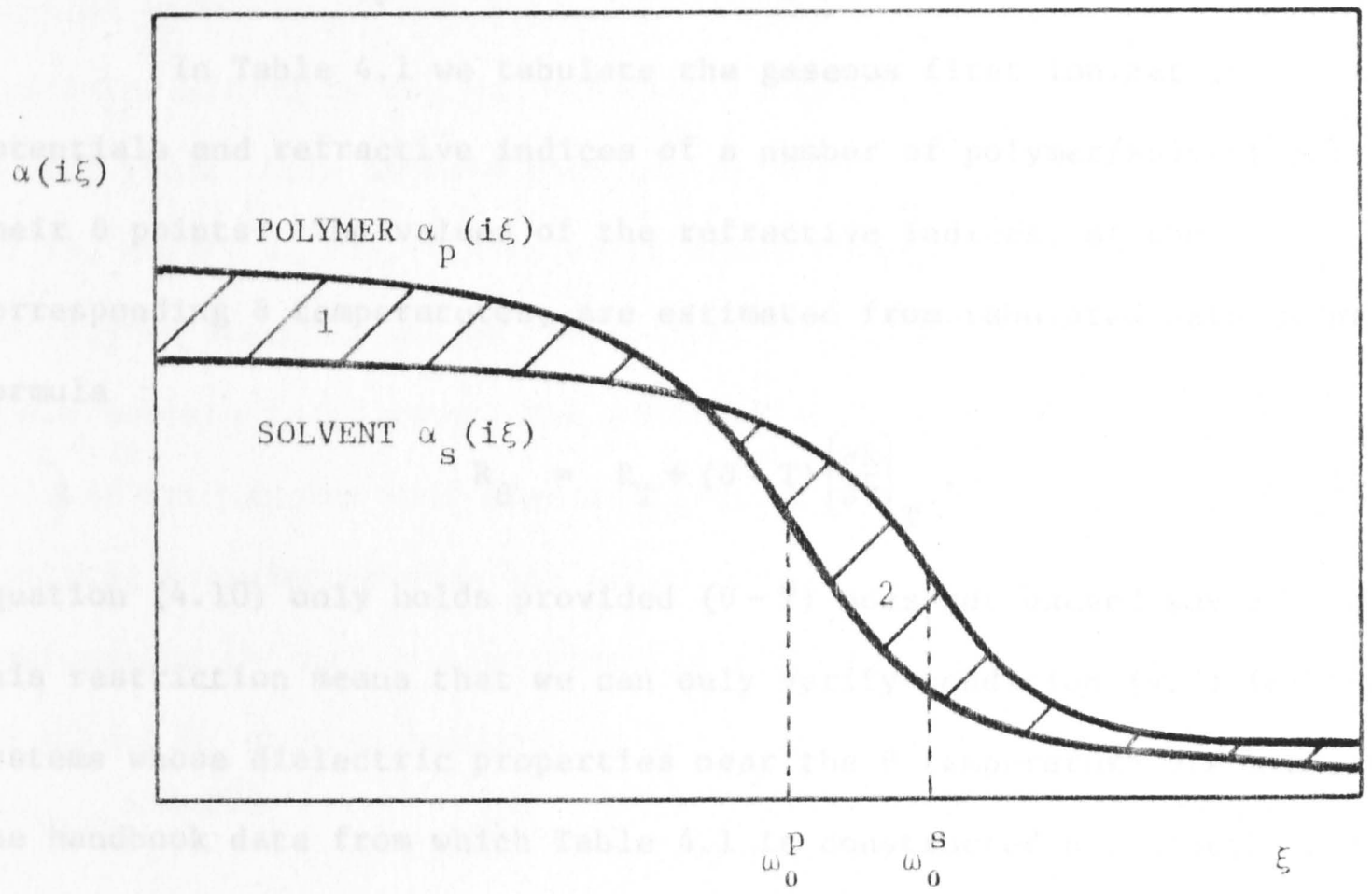

Figure 4.1: Schematic representation of the polarizabilities of the polymer and solvent $\alpha_p(i\xi)$, $\alpha_s(i\xi)$ along the imaginary frequency axis.

and the solvent. We define

$$I_p = \hbar\omega_0^p \quad ; \quad I_s = \hbar\omega_0^s \tag{4.8}$$

and

$$\frac{\varepsilon_p(0) - 1}{\varepsilon_p(0) + 2} = \Delta_p^0 \; ; \quad \frac{\varepsilon_s(0) - 1}{\varepsilon_s(0) + 2} = \Delta_s^0 \; . \tag{4.9}$$

In Table 4.1 we tabulate the gaseous first ionization potentials and refractive indices of a number of polymer/solvent pairs at their θ points. The values of the refractive indices, at the corresponding θ temperatures, are estimated from tabulated data using the formula

$$R_\theta = R_T + (\theta - T)\left(\frac{\partial R}{\partial T}\right)_T \; . \tag{4.10}$$

Equation (4.10) only holds provided $(\theta - T)$ does not exceed say ± 30 °K. This restriction means that we can only verify condition (4.7) for those systems whose dielectric properties near the θ temperature are available. The handbook data from which Table 4.1 is constructed are listed in the Appendix at the end of this chapter. Indeed, for all the systems listed, condition (4.7) does appear to be satisfied.

System	Measured θ Temperature (°K)	Gaseous First Ionization Potential (eV)	Refractive Index at θ
Polyisobutene in toluene	261	9.23 8.82	1.516 1.574
Polyisobutene in ethyl benzene	251	9.23 8.76	1.523 1.577
Polystyrene in cyclohexane	307	8.47 9.80	1.555 1.422
Polystyrene in decalin	304	8.47 9.61	1.554 1.481

Table 4.1: Data for polymers and solvents (see Appendix).

The criterion for a θ point stated above is expected to be satisfied by non-polar polymers in non-polar solvents. When the static dielectric constants of the polymer and solvent are more nearly equal, such as that for polystyrene in benzene, $\theta = 24\ ^{\circ}C$ (see Appendix), a more detailed knowledge of the higher ionization potentials and corresponding oscillator strengths may be necessary to determine the θ point. In general where there is more than one relaxation frequency, it is possible for the curves in Fig. 4.1 to cross several times. As for cases where the polymer segments and/or the solvent molecules possess permanent dipole moments (e.g. water) the position and degree of Debye relaxations at lower frequencies will also influence the θ point. If systems involving polyelectrolytes are under study, the analysis must be supplemented to include electrostatic contributions to the potential ϕ. The effect of charged segments in ionic solution is to expand the polymer.[34,35]

5. A COMPARISON BETWEEN THEORY AND EXPERIMENT

Using available data at or near the θ temperature, we would like to check if this theory does predict a θ point, that is, whether or not the coefficient of $p^3(r)$ in equation (3.12) is "vanishingly small". To facilitate a comparison, we rewrite equation (3.12), with the aid of the following results

$$\Delta_i \equiv \left(\frac{\varepsilon_i - 1}{\varepsilon_i + 2}\right) = \frac{4\pi}{3} n_i \alpha_i , \qquad i = s,p \tag{5.1}$$

$$n_i \simeq n_0 , \qquad i = s,p \tag{5.2}$$

to give

$$\frac{9kT}{b^3 \pi^{3/2}} \left\{ s_3 + s_4 \left(\frac{p(r)}{n_0}\right) \right\} \left(\frac{p(r)}{n_0}\right)^3 + O\ p^5(r) = \frac{3kT}{2a^2} \frac{1}{(4\pi r^2)^2} \tag{5.3}$$

where

$$s_3 = \sum_{n=0}^{\infty}{}' \frac{\Delta_p(\Delta_s - \Delta_p)}{\varepsilon_s^2(1-\Delta_s)^2} \tag{5.4}$$

$$s_4 = 2\sum_{n=0}^{\infty}{}' \frac{\Delta_p(\Delta_s - \Delta_p)^2}{\varepsilon_s^3(1-\Delta_s)^3} \ . \tag{5.5}$$

The θ point is then taken to be where the ratio of the two dimensionless coefficients $|s_3/s_4|$ vanishes.

Since we are identifying α to be the polarizability of a monomer or solvent molecule, we take $\hbar\omega_0$ in equation (4.4)

$$\alpha(i\xi) = \frac{\alpha(0)}{1+\xi^2/\omega_0^2} \tag{4.4}$$

to be the *gaseous* first ionization potential. Using equation (5.1) we find[39] (cf. equation (4.1))

$$\varepsilon(i\xi) = 1 + \frac{\varepsilon(0)-1}{1+\xi^2/\omega_{uv}^2} \ , \tag{5.6}$$

where

$$\omega_{uv} = \omega_0\left[1-\left(\frac{\varepsilon(0)-1}{\varepsilon(0)+2}\right)\right]^{\frac{1}{2}} \tag{5.7}$$

$$\varepsilon(0) = R^2 \ . \tag{5.8}$$

In other words, the ionization potentials of molecules is lowered in passing from the vapour phase to the liquid or solid phase — a phenomenon that has been known for some time.[40,41] Although equation (5.7) predicts reductions in the ionization potential that are comparable to those observed experimentally,[42] (for non-polar dielectric at least) it would be much more satisfactory if optical and spectroscopic data of the bulk material were available so that we can construct $\varepsilon(i\xi)$ directly.

We calculated the sums s_3 and s_4 (equations (5.4) and (5.5)) at the θ temperature by assuming that ω_0 is given by the gaseous first ionization potential for the various polymer/solvent pairs listed in

Table 4.1, and found that the ratio $|s_3/s_4|$ does not vanish ($|s_3| \sim 1$, $|s_4| \sim 10^{-3}$). But we know that the first ionization potential is only an approximation to the absorption frequency ω_0. To see what deviations from the tabulated ionization potential are needed to make $|s_3/s_4|$ vanish we use the tabulated ionization potential of the polymer (solvent) and find the "new" ionization potential of the solvent (polymer) for which $|s_3/s_4|$ vanishes. These "new" values are given in brackets in Table 5.1 for the various polymer/solvent systems, together with the tabulated values.

System	I_p	I_s
Polyisobutene in toluene	9.23	8.82
	(10.10)	8.82
	9.23	(8.07)
Polyisobutene in ethyl benzene	9.23	8.76
	(9.91)	8.76
	9.23	(8.15)
Polystyrene in cyclohexane	8.47	9.80
	(6.30)	9.80
	8.47	(13.20)
Polystyrene in decalin	8.47	9.61
	(7.83)	9.61
	8.47	(10.40)

Table 5.1: "New" values of the ionization potential (in brackets) for which $|s_3/s_4|$ vanishes at θ.

From the results of Table 5.1 we see that a larger difference in the ionization potential is needed to produce a θ point. With the exception of polystyrene/cyclohexane, a deviation of less than 10% from the gaseous values is sufficient. This indicates that the existence of a θ point ($|s_3/s_4| \leqslant 10^{-5}$) is very sensitive to dielectric and spectroscopic data. The apparently large deviation needed for polystyrene/cyclohexane

is due to the fact that the first ionization potential of cyclohexane is a poor estimate of ω_0. In fact, it has been found that in a plot of molar polarizability against frequency, the usual technique of extrapolation to zero frequency indicates that cyclohexane has a strong absorption peak at 866 Å or about 13.6 eV.[43]

Evidently we can see from the results that data available at present cannot predict the θ point correctly. This is because dielectric data at the θ temperature is not available and only a single frequency representation for the absorption spectrum is used (and even then we are uncertain of the exact value of this frequency). However, at this unsophisticated level of approach, we cannot expect more than general trends to emerge. It seems reasonable that a variation of less than 10% in the gaseous first ionization potential is sufficient to produce a θ point. We have also been able to obtain a criterion (4.7) for selecting θ solvents for non-polar solvents and polymers in terms of the relative values of the static dielectric constants and principal absorption peaks.

This theory also provides a physical basis for the phase transition $\langle r^2 \rangle \sim N^{6/5}$ to $\langle r^2 \rangle \sim N$ at the θ point and gives some insight into how the interplay between dielectric properties of the polymer and solvent, and changes in temperature can bring about a θ point. Until more refined spectroscopic data come to hand,† not a great deal can be gained by allowing for the possibility of an anisotropic polarizability for the polymer segments or by the "correct" handling of the spatial distribution of polymer segments in calculation of the effective one-body potential.

---

† However, we do not expect contributions from the far ultraviolet to be important. This is because the solvents and monomers have similar molecular weights and densities; therefore their far ultraviolet spectra should be similar.[30,31]

APPENDIX

DIELECTRIC DATA FOR SOME POLYMERS AND SOLVENTS

The following is a list of dielectric and spectroscopic data for polymers and θ solvents obtained from data handbooks.[44-46] The temperatures at which the values were measured, in °C, are given in brackets next to the substance. The first ionization potentials (in electron volts) of the polymers, taken to be the gaseous first ionization potential of the constituent monomer units, are assumed to be temperature independent. When values of the change of refractive index with temperature dR/dT are not available, they are assumed to be close to that of a structurally similar compound. For these non-polar substances, the static dielectric constant can be taken as the square of the refractive index.

Substance	Gaseous First Ionization Potential (eV)	Refractive Index	$-(dR/dT) \times 10^4$ ($°C^{-1}$)
Polystyrene (20)	8.47	1.550†	1.42
Polyisobutene (25)	9.23	1.493	6
Benzene (25)	9.23	1.50	~ 2*
Toluene (-15) (Methyl benzene)	8.82	1.574	~ 2*
Ethyl benzene (20)	8.76	1.552	~ 2*
Cyclohexane (25)	9.8	1.426	~ 5ǂ
Decalin (30)	9.61	1.48	~ 5ǂ

† Styrene monomer.

* Estimated from that of polystyrene.

ǂ Estimated from that of methyl cyclohexane.

REFERENCES

(1) C. Domb, *Polymer* 15, 259 (1974).

(2) P.J. Flory, *Principles of Polymer Chemistry*, Cornell University Press (1953), Ch. XII.

(3) *Ibid.*, Ch. X.

(4) For a review on the application of the theory of random walks to polymer conformation problems see M.N. Barber and B.W. Ninham, *Random and Restricted Walks*, Gordon and Breach, N.Y. (1970).

(5) S.F. Edwards, *Proc. Phys. Soc.* 85, 613 (1965).

(6) H. Fujita, K. Okita and T. Norisuye, *J. Chem. Phys.* 47, 2723 (1967).

(7) G.C. Berry, *J. Chem. Phys.* 44, 4550 (1966); see also Ch. XIV of reference (2).

(8) J.M. Hammersley and D.C. Handscomb, *Monte Carlo Methods*, Methuen and Co., London (1964).

(9) F.T. Wall, S. Windwer and P.J. Gans, *J. Chem. Phys.* 38, 2220 (1963).

(10) F.T. Wall, S. Windwer and P.J. Gans, *J. Chem. Phys.* 38, 2228 (1963).

(11) S. Windwer, *J. Chem. Phys.* 43, 115 (1965).

(12) J. Mazur, *J. Res. Nat. Bur. Std.* A69, 355 (1965).

(13) J. Mazur, *J. Chem. Phys.* 43, 4354 (1965).

(14) S. Bluestone and M.J. Vold, *J. Polymer Sci.* A2, 289 (1964).

(15) C. Domb, J. Gillis and G. Wilmers, *Proc. Roy. Soc.* 85, 625 (1965).

(16) C. Domb, A.J. Barrett and M. Lax, *J. Phys. A* 6, L82 (1973).

(17) A. Bellemans, *Physica* 68, 209 (1973).

(18) P.J. Flory, *J. Chem. Phys.* 17, 303 (1949).

(19) P.J. Flory and W.R. Krigbaum, *J. Chem. Phys.* 18, 1086 (1950).

(20) P.J. Flory and S. Fisk, *J. Chem. Phys.* 44, 2243 (1966).

(21) See also reference (2), Ch. XIV.

(22) P.G. deGennes, *Rep. Progr. Phys.* 32, 187 (1969).

(23) J. Mahanty and B.W. Ninham, *J. Chem. Phys.* 59, 6157 (1973).

(24) See for example G.W. Castellan, *Physical Chemistry*, Addison-Wesley, Reading, Mass. (1972), Ch. 28.

(25) Reference (2), Ch. XIV.

(26) I.E. Dzyaloshinskii, E.M. Lifshitz and L.P. Pitaevskii, *Adv. Phys.* 10, 165 (1961).

(27) R.C. Weast (ed.), *Handbook of Chemistry and Physics*, Chemical Rubber Publishing Co., Cleveland, Ohio (1971-2).

(28) See for example J.H. Van Vleck, *The Theory of Electric and Magnetic Susceptibilities*, Oxford U.P. (1965).

(29) V.A. Parsegian and B.W. Ninham, *Biophys. J.* 10, 664 (1970).

(30) V.A. Parsegian and B.W. Ninham, *J. Chem. Phys.* 52, 4578 (1970).

(31) B.W. Ninham and V.A. Parsegian, *J. Chem. Phys.* 53, 3398 (1970).

(32) P. Richmond, B.W. Ninham and R.H. Ottewill, *J. Colloid Interface Sci.* 45, 69 (1973).

(33) See also references cited in B.W. Ninham and P. Richmond, *J. Chem. Soc., Faraday II* 69, 658 (1973), and J. Mahanty and B.W. Ninham, *Dispersion Forces*, Academic Press, London (1975).

(34) Reference (2), Ch. XIV.

(35) P. Richmond, *J. Phys. A* 6, L109 (1973).

(36) A.D. McLachlan, *Proc. Roy. Soc.* A271 387 (1963); *ibid.*, A274, 80 (1963); *Mol. Phys.* 6, 423 (1963); *ibid.*, 7, 381 (1964); *Disc. Farad. Soc.* 40, 239 (1965).

(37) D.J. Mitchell, B.W. Ninham and P. Richmond, *Aust. J. Phys.* 25, 33 (1972).

(38) J.N. Israelachvili, *Proc. Roy. Soc.* A331, 39 (1972).

(39) L.R. White, Private communication.

(40) L.E. Lyons and J.C. Mackie, *Proc. Chem. Soc.* 71, (1962).

(41) L.E. Lyons and J.C. Mackie, *Nature (London)* 197, 589 (1963).

(42) R. Evans and D.H. Napper, *J. Colloid Interface Sci.* 45, 138 (1973).

(43) W. Kauzmann, *Quantum Chemistry*, Academic Press, N.Y. (1957).

(44) J. Brandrup and E.H. Immergut (eds.), *Polymer Handbook*, Interscience, N.Y. (1966).

(45) J. Timmermans, *Physico-Chemical Constants of Pure Organic Compounds*, Elsevier, Amsterdam, Vol. I (1960), Vol. II (1965).

(46) See also reference (27).

CHAPTER 2

THE CONFORMATION OF AN ADSORBED POLYMER

1. INTRODUCTION

As outlined in the introduction of the previous chapter, we shall consider some distinguished features of a polymer in the adsorbed state.

The conformational characteristics of an adsorbed polymer is of interest and of fundamental importance to the understanding of phenomena such as the influence of macromolecules on the stability of colloidal dispersions,[1-3] polymer bridging,[4] and the growth of polymer lamellar crystals.[5] A fair amount of experimental data[6,7] has been accumulated on the conformation of adsorbed macromolecules which require theoretical interpretation.

Historically,[8] the first serious theoretical attempt at the problem of polymer adsorption was by Frisch *et al.*[9-11] who used a random walk model where the substrate was represented by a reflecting barrier. This model was later modified to include interactions between the polymer and the surface.[12-13] However, the general use of reflecting barriers fails to assign adsorbed monomer units the correct statistical weight.[14]

The most successful *lattice walk* model was that due to DiMarzio and McCrackin,[15] and to Rubin.[16,17] Their work and subsequent extensions[18,19]† gave physically reasonable results for characteristics such as the fraction of polymer adsorbed as a function of

---

† An error in this work[18] was noted in reference (20); the correction is in reference (21).

the adsorption energy. Unfortunately, quantities such as the degree of spreading on the surface, the density distribution, and the position of the centre-of-mass of the polymer are not readily accessible by this method.

Another approach to the problem of polymer adsorption is through a statistical mechanical formulation. Here, the adsorbed state of a polymer is analysed in terms of distribution functions for loops (segments of polymer with both ends adsorbed) and trains (segments of polymer with all units adsorbed) obtained from random walk statistics.[22-26] The contribution from tails (segments with only one end adsorbed) was later included when their importance in determining the conformations of weakly adsorbed polymers was recognized.[27-29] Results obtained by this method support those of Rubin.

A third method, which circumvents the use of lattice or random walk models, is the diffusion equation approximation.[14,30,31] In this quasi-continuum approach, the integral equation for the partition function of a polymer is approximated by a diffusion equation. The error involved in this replacement, in the absence of boundaries, is negligible over distances that are large compared with the bond length and provided the polymer is long (that is the number of monomers >> 1). However in the vicinity of boundaries, the appropriate initial and boundary conditions for the diffusion equation are uncertain. Further there is also the question of the validity of replacing the integral equation by a diffusion equation in the neighbourhood of boundaries because of the piece-wise nature of the solution. These points will be taken up again later on in this chapter (Section 6).

From the above brief introduction, we see that considerable effort has been devoted to construct a realistic theory of polymer

adsorption. Although these treatments bring out most of the qualitative features of the conformation of adsorbed polymers, this is by no means the complete story. To quote Edwards:[32] "... until the continuum models of polymers have been fully understood one will not obtain mastery over the problem of real polymers".

In this chapter, we study the conformation of an adsorbed polymer by considering the statistical mechanics of a polymer confined in a half space by an impenetrable flat surface with which the polymer may interact. The polymer is modelled by a string of non-interacting beads (monomers) joined by freely rotating bonds whose length are governed by a given probability density function. (It may be a fair conceit, but perhaps appropriate, to draw an analogy between this model in the theory of polymer adsorption and that of the ideal gas model in kinetic theory.) We include only configurations where at least one bead is adsorbed. The configurational partition function (CPF) for the polymer can be analysed in terms of generating functions (GF) for the CPF for loops and tails. We derive general expressions for important conformational characteristics of an adsorbed polymer, namely, the average number of beads adsorbed on the wall $\langle n \rangle$, the mean square end-to-end separation of adsorbed beads on the wall $\langle \rho^2 \rangle$, the centre-of-mass of the polymer $\langle x \rangle$, and the density of beads off the wall $n(x)$, in terms of the CPF for loops and tails. A modified Wiener-Hopf method is used to obtain appropriate asymptotic solutions of the integral equation for the GF of the CPF for loops and tails. The conformational characteristics of the polymer, obtained for various regimes of the adsorption energy parameter W, are found to have a phase transition at some critical value W_c. An explicit expression for W is given assuming only dispersion interactions between the polymer and the wall. From this expression, numerical values of W

are obtained, using available dielectric and spectroscopic data, for several real polymer/solvent/wall systems. It is found that this adsorption/desorption phase transition can be induced by temperature variations or by varying the dielectric properties of the solvent through changing the composition of mixed solvents.

2. THE FORMULATION

We consider a "non-interacting" polymer consisting of N freely rotating links (N+1 beads) confined in the half-space $x > 0$ by an unpenetrable flat surface. By "non-interacting" we mean that the potential energy of the polymer is the sum of one-particle potentials $V(\underset{\sim}{r}_i)$, $\underset{\sim}{r}_i$ being the position vector of the i^{th} bead (monomer unit). That is, bead-bead interactions and excluded volume effects are ignored. In real systems, there is an ill-defined though narrow interfacial region within which a bead interacts strongly with the wall and may be considered to be adsorbed. Thus $V(\underset{\sim}{r}_i)$ may be replaced by the sum of an adsorption potential $\psi(x_i)$ and an external potential $\phi(\underset{\sim}{r}_i)$.

Since the adsorption potential is short-range, we shall replace the Boltzmann factor by a pseudo-potential

$$e^{-\beta V(\underset{\sim}{r}_i)} = e^{-\beta \phi(\underset{\sim}{r}_i)}\, e^{-\beta \psi(x_i)} \tag{2.1}$$

$$\approx e^{-\beta \phi(\underset{\sim}{r}_i)}\, [\theta(x_i) + W\, \delta(x_i)] \,, \tag{2.2}$$

where $\beta = 1/kT$ and the adsorption energy parameter

$$W = \int_0^\infty (e^{-\beta \psi(x)} - 1)\, dx \tag{2.3}$$

is reminiscent of the "second virial coefficient". The unit step function $\theta(x)$ is defined as

$$\theta(x) = 1 , \quad x > 0$$
$$= 0 , \quad x < 0 \tag{2.4}$$

and $\delta(x)$ is the Dirac delta function. The replacement (2.2) is a convenient mathematical method of handling the interfacial region. It assigns the adsorption region with the correct weight while avoiding the necessity of treating such a region with finite thickness.

The length of each of the freely rotating links, $|\underset{\sim}{r}_{i,i-1}| = |\underset{\sim}{r}_i - \underset{\sim}{r}_{i-1}|$, which join neighbouring beads, is determined by a normalized probability density function $\bar{f}(|\underset{\sim}{r}_{i,i-1}|)$. The configurational partition function (CPF) for the polymer is then

$$Q_N = \int \cdots \int d^3\underset{\sim}{r}_0 \cdots d^3\underset{\sim}{r}_N \prod_{i=1}^{N} \bar{f}(|\underset{\sim}{r}_{i,i-1}|)\, e^{-\beta \sum_{j=0}^{N} V(\underset{\sim}{r}_j)} , \tag{2.5}$$

where

$$e^{-\beta \sum_{j=0}^{N} V(\underset{\sim}{r}_j)} = e^{-\beta \sum_{j=0}^{N} \phi(\underset{\sim}{r}_i)} \prod_{i=0}^{N} [\theta(x_i) + W\,\delta(x_i)] . \tag{2.6}$$

Expanding the product of Boltzmann factors and performing the x integration wherever a δ-function occurs, we obtain

$$Q_N = \sum_{n=1}^{N} W^n \sum_{\{M_i\}} \int \cdots \int d^2\underset{\sim}{\rho}_1 \cdots d^2\underset{\sim}{\rho}_n\, \bar{G}^f_{M_1}(\underset{\sim}{\rho}_1) \prod_{i=2}^{n} G_{M_i}(\underset{\sim}{\rho}_{i-1}, \underset{\sim}{\rho}_i)\, \bar{G}^f_{M_{n+1}}(\underset{\sim}{\rho}_n) \times e^{-\beta\phi(\rho_n)} . \tag{2.7}$$

$\underset{\sim}{\rho}_i$ is the transverse component of the position vector $\underset{\sim}{r}_i$ and we use the convention

$$\prod_{i=2}^{n} f_i = 1 \quad \text{for} \quad n < 2 . \tag{2.8}$$

The quantity $\bar{G}^f_M(\underset{\sim}{\rho})$ is the CPF of a (free) tail of M links (M+1 beads) with the zeroth bead on the wall and all others in the half-space $x > 0$. That is

$$\bar{G}_0^f(\underset{\sim}{\rho}) = 1 \tag{2.9}$$

$$\bar{G}_M^f(\underset{\sim}{\rho}) = \int_{(x_i>0)} \cdots \int d^3\underset{\sim}{r}_1 \cdots d^3\underset{\sim}{r}_M \prod_{i=1}^{M} \bar{f}(|\underset{\sim}{r}_{i,i-1}|)\, e^{-\beta \sum_{j=1}^{M} \phi(\underset{\sim}{r}_j)} ,$$

$$(M > 1,\ \underset{\sim}{r}_0 = \underset{\sim}{\rho}) . \tag{2.10}$$

The quantity $\bar{G}_M(\underset{\sim}{\rho},\underset{\sim}{\rho}')$ is the CPF of a loop of M links (M+1 beads) with the zeroth bead on the wall (x = 0) at $\underset{\sim}{\rho}$ and the M^{th} bead on the wall at $\underset{\sim}{\rho}'$ and all others in the half-space x > 0. That is

$$\bar{G}_0(\underset{\sim}{\rho},\underset{\sim}{\rho}') = 0 \tag{2.11}$$

$$\bar{G}_1(\underset{\sim}{\rho},\underset{\sim}{\rho}') = \bar{f}(|\underset{\sim}{\rho} - \underset{\sim}{\rho}'|)\, e^{-\beta\phi(\underset{\sim}{\rho})} \tag{2.12}$$

$$\bar{G}_M(\underset{\sim}{\rho},\underset{\sim}{\rho}') = \int_{(x_i>0)} \cdots \int d^3\underset{\sim}{r}_1 \cdots d^3\underset{\sim}{r}_{M-1} \prod_{i=1}^{M} \bar{f}(|\underset{\sim}{r}_{i,i-1}|)\, e^{-\beta \sum_{j=0}^{M-1} \phi(\underset{\sim}{r}_i)} ,$$

$$(M > 2,\ \underset{\sim}{r}_0 = \underset{\sim}{\rho},\ r_M = \underset{\sim}{\rho}') . \tag{2.13}$$

Thus equation (2.7) for Q_N represents the sum of all diagrams shown in Figure 2.1. Although not specifically shown, "train"-type diagrams are merely a succession of loops of one link ($\bar{G}_1$). The index n counts the number of beads adsorbed on the wall. The symbol $\sum_{\{M_i\}}$ for a given n indicates that what follows is to be summed over all possible sets of numbers $\{M_i\} = (M_1, M_2, \ldots, M_{n+1})$ with the restrictions $0 < M_i \leq N$ and, since M_i represents the number of links in a loop or tail,

$$\sum_{i=1}^{n+1} M_i = N . \tag{2.14}$$

As we are only interested in adsorbed polymers, the term corresponding to n = 0 in equation (2.5) has been omitted in equation (2.7). This is equivalent to requiring there be at least one contact with the wall, and the polymer is not free to move arbitrarily far from the wall.

Let us consider the properties of the normalized probability density function $\bar{f}(|\underset{\sim}{r}|)$ which determines the distance between successive beads. Since the polymer links are, by assumption, free to rotate

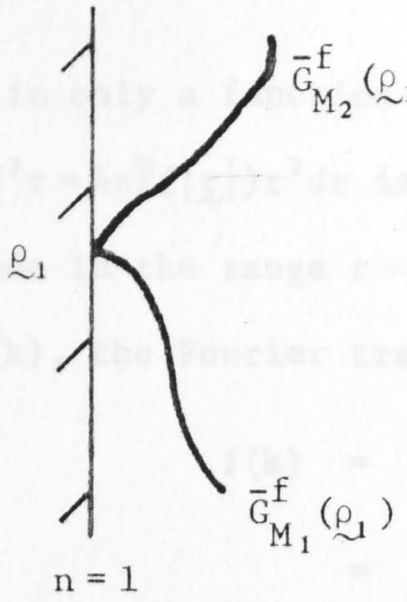

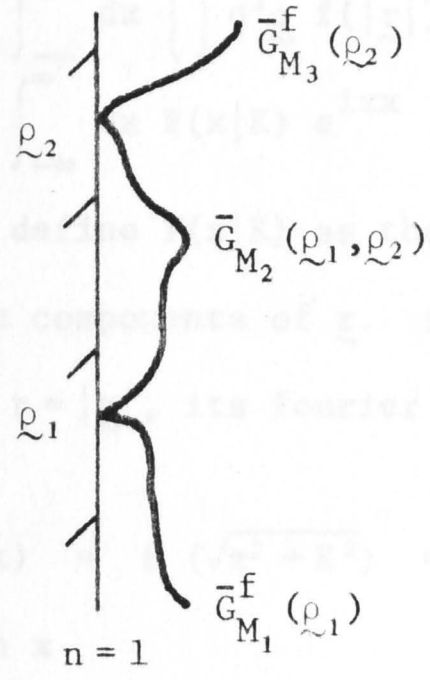

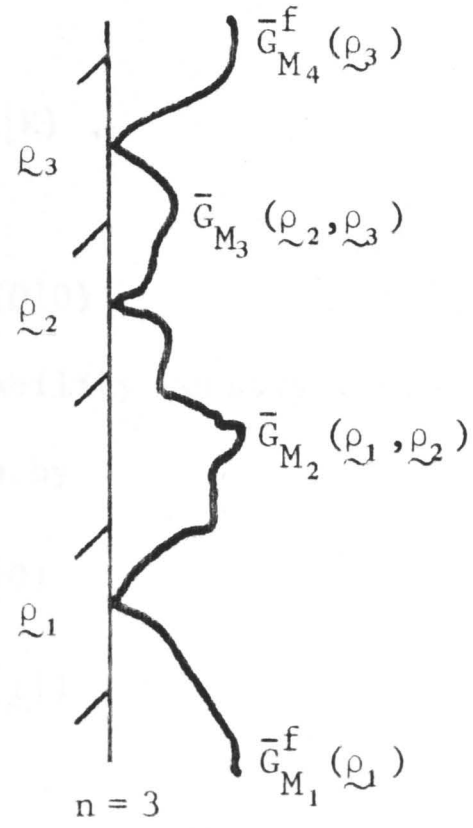

Figure 2.1: The first few diagrams in the partition function Q_N corresponding to one, two and three adsorbed beads showing the contributions of loop partition functions $\bar{G}_M(\underset{\sim}{\rho},\underset{\sim}{\rho}')$ and free tail partition functions $\bar{G}^f_M(\underset{\sim}{\rho})$.

$\bar{f}(|\underset{\sim}{r}|)$ is only a function of the magnitude $r = |\underset{\sim}{r}|$. Hence $\bar{f}(|\underset{\sim}{r}|)d^3r = 4\pi\bar{f}(|\underset{\sim}{r}|)r^2dr$ is the *a priori* probability of a link having a magnitude in the range $r \to r+dr$ (in any direction). We further require that $f(k)$, the Fourier transform of $\bar{f}(|\underset{\sim}{r}|)$, exists, that is

$$f(k) = \int d^3r\, \bar{f}(|\underset{\sim}{r}|)\, e^{i\underset{\sim}{k}\cdot\underset{\sim}{r}} \tag{2.15}$$

$$= \int_{-\infty}^{\infty} dx \left(\int d^2\underset{\sim}{\rho}\, \bar{f}(|\underset{\sim}{r}|)\, e^{i\underset{\sim}{K}\cdot\underset{\sim}{\rho}} \right) e^{izx} \tag{2.16}$$

$$\equiv \int_{-\infty}^{\infty} dx\, F(x|K)\, e^{izx} \equiv f(z|K)\ . \tag{2.17}$$

Equation (2.17) serves to define $F(x|K)$ as the Fourier transform of $f(|\underset{\sim}{r}|)$ over the transverse components of $\underset{\sim}{r}$. Since $\bar{f}(|\underset{\sim}{r}|)$ is only a function of the magnitude $r = |\underset{\sim}{r}|$, its Fourier transform is a function of $k = |\underset{\sim}{k}|$ only, that is

$$f(k) = f(\sqrt{z^2+K^2}) = f(z|K) \tag{2.18}$$

and that $F(x|K)$ is even in x

$$F(x|K) = F(-x|K)\ . \tag{2.19}$$

Further, normalization requires that

$$f(0) = 1 = f(0|0) \tag{2.20}$$

so that $F(x|0)$ has the properties of a probability density function in one dimension. We can define its variance σ by

$$\sigma^2 \equiv \int_{-\infty}^{\infty} dx\, x^2\, F(x|0) \tag{2.21}$$

$$= \frac{1}{3}\int d^3\underset{\sim}{r}\, r^2\, f(|\underset{\sim}{r}|)\ . \tag{2.22}$$

From (2.16) and (2.17) we find

$$f(|\underset{\sim}{r}_i - \underset{\sim}{r}_{i-1}|) = \frac{1}{(2\pi)^2}\int d^2\underset{\sim}{K}\, F(x_i - x_{i-1}|K)\, e^{-i\underset{\sim}{K}\cdot(\underset{\sim}{\rho}_i - \underset{\sim}{\rho}_{i-1})}\ . \tag{2.23}$$

Further simplification of the quantities $\bar{G}^f_M(\underset{\sim}{\rho})$, $\bar{G}_M(\underset{\sim}{\rho},\underset{\sim}{\rho}')$ and Q_N is not possible unless we assume the external potential $\phi(\underset{\sim}{r})$ is a function of x only. We shall be mainly concerned in this chapter with the case $\phi(x) = 0$.

Using this simplification and the result (2.23) we may carry out the transverse integrations in equations (2.10) and (2.13) to yield

$$\bar{G}_M^f(\underset{\sim}{\rho}) = G_M^f(0) , \tag{2.24}$$

where

$$G_0^f(0) = 1 \tag{2.25}$$

$$G_M^f(0) = \int_0^\infty \cdots \int_0^\infty dx_1 \cdots dx_M \; F(x_1|0)\; F(x_2 - x_1|0) \cdots F(x_M - x_{M-1}|0) \times e^{-\beta \sum_{i=1}^{M} \phi(x_i)} , \quad (M > 0) . \tag{2.26}$$

The argument in $G_M^f(0)$ indicates that the zeroth bead of the tail is at the wall $x = 0$. Also

$$\bar{G}_M(\underset{\sim}{\rho},\underset{\sim}{\rho}') = \frac{1}{(2\pi)^2} \int d^2\underset{\sim}{K}\; G_M(0|K)\; e^{-i\underset{\sim}{K}\cdot(\underset{\sim}{\rho}-\underset{\sim}{\rho}')} , \tag{2.27}$$

where

$$G_0(0|K) = 0$$

$$G_1(0|K) = F(0|K)\; e^{-\beta\phi(0)} \tag{2.29}$$

$$G_M(0|K) = \int_0^\infty \cdots \int_0^\infty dx_1 \cdots dx_{M-1} \; F(x_1|K)\; F(x_2 - x_1|K) \cdots F(x_{M-1} - x_{M-2}|K) \times F(x_{M-1}|K)\; e^{-\beta \sum_{i=0}^{M-1} \phi(x_i)} , \quad (M > 1,\; x_0 = 0) . \tag{2.30}$$

The argument 0 in $G_M(0|M)$ indicates that the zeroth bead of the loop starts at $x = 0$.

Substituting equations (2.24) and (2.27) into the partition function, equation (2.7), we obtain

$$Q_N = \frac{e^{-\beta\phi(0)}}{(2\pi)^2} \int d^2\underset{\sim}{K} \iint d^2\underset{\sim}{\rho}_1\; d^2\underset{\sim}{\rho}_n\; e^{-i\underset{\sim}{K}\cdot(\underset{\sim}{\rho}_n - \underset{\sim}{\rho}_1)}\; q_N(K) , \tag{2.31}$$

where

$$q_N(K) = \sum_{n=1}^{N} W^n \sum_{\{M_i\}} G_{M_1}^f(0) \prod_{i=2}^{n} G_{M_i}(0|K)\; G_{M_{n+1}}^f(0) . \tag{2.32}$$

The quantity $|\underset{\sim}{\rho}|$ defined by

$$\underset{\sim}{\rho} = \underset{\sim}{\rho}_N - \underset{\sim}{\rho}_1 \tag{2.33}$$

is the distance between the first and last beads on the wall. Its expectation value is a measure of the spread of the polymer on the wall. After a change of variables (2.33), the partition function becomes

$$Q_N = A' e^{-\beta\phi(0)} \int d^2\underset{\sim}{\rho} \left(\frac{\int d^2\underset{\sim}{K}}{(2\pi)^2} e^{-i\underset{\sim}{K}\cdot\underset{\sim}{\rho}} q_N(K) \right) \tag{2.34}$$

$$\equiv A' e^{-\beta\phi(0)} \int d^2\underset{\sim}{\rho}\, \bar{q}_N(\rho) \ , \tag{2.35}$$

where A' is the area on the wall to which the polymer is confined. The quantity $\bar{q}_N(\rho)$ is defined by equation (2.35). For convenience, we write $A = A' e^{-\beta\phi(0)}$, and perform the integrals in equation (2.34) to yield

$$\begin{aligned} Q_N &= A\, q_N(0) \\ &= A \sum_{n=1}^{N} W^n \sum_{\{M_i\}} G^f_{M_1}(0) \prod_{i=2}^{n} G_{M_i}(0|0)\, G^f_{M_{n+1}}(0) \ . \end{aligned} \tag{2.36}$$

This expression can be simplified by forming the generating function (GF)

$$Q(s) = \sum_{N=1}^{\infty} s^N (Q_N/A) \ . \tag{2.37}$$

Then (Q_N/A) is just the coefficient of s^N in the Taylor expansion of $Q(s)$ (about $s = 0$) which we shall denote by

$$Q_N = A[Q(s)]_N \ . \tag{2.38}$$

Multiplying both sides of equation (2.36) by s^N we obtain

$$Q(s) = \frac{W[G^f(s,0)]^2}{1 - W\, G(s,0|0)} \ , \tag{2.39}$$

where

$$G^f(s,0) = \sum_{M=0}^{\infty} s^M G^f_M(0) \tag{2.40}$$

$$G(s,0|K) = \sum_{M=0}^{\infty} s^M G_M(0|K) \tag{2.41}$$

are respectively the GF of the CPF for tails and loops. Therefore

$$Q_N = A\left[\frac{W\, G^f(s,0)^2}{1 - W\, G(s,0|0)}\right]_N \tag{2.42}$$

and similarly

$$q_N(K) = \left[\frac{W\, G^f(s,0)^2}{1 - W\, G(s,0|K)}\right]_N . \tag{2.43}$$

3. THE EXPECTATION VALUES OF CONFORMATION CHARACTERISTICS

We shall derive general expressions for four characteristics which describe the polymer configuration near an interacting wall. These are:

(a) $\langle n \rangle$, the average number of beads adsorbed on the wall,

(b) $\langle \rho^2 \rangle$, the mean square end-to-end distance ("spread") of beads on the wall,

(c) $n(x)$, the density of beads off the wall,

(d) $\bar{x}$, the distance of the centre-of-mass of the polymer from the wall.

Two fundamental relations between these quantities are:

$$\bar{x} = \frac{1}{N+1}\int_0^\infty x\, n(x)\, dx \tag{3.1}$$

$$N+1 = \int_0^\infty n(x)\, dx + \langle n \rangle . \tag{3.2}$$

Relation (3.2) serves as a self-consistent check on the results derived for $n(x)$ and $\langle n \rangle$.

3a. Number of beads adsorbed $\langle n \rangle$

Since the index n in equation (2.36) for Q_N counts the number of beads on the wall, it follows that

$$\langle n \rangle = \frac{A}{Q_N} \sum_{n=1}^{N} n\, W^n \sum_{\{M_i\}} G^f_{M_1}(0) \prod_{i=2}^{n} G_{M_i}(0|0)\, G^f_{M_{n+1}}(0)$$

$$\langle n \rangle = W \frac{\partial}{\partial W} (\ln Q_N) \,. \tag{3.3}$$

3b. The spread of the polymer on the wall $\langle \rho^2 \rangle$

From equation (2.35), it is clear that

$$\langle \rho^2 \rangle = \frac{A}{Q_N} \int d^2\underset{\sim}{\rho}\, \rho^2\, \bar{q}_N(\rho) \,. \tag{3.4}$$

But it follows from the definition of $\bar{q}_N(\rho)$, (2.34), that

$$\int d^2\underset{\sim}{\rho}\, \rho^2\, \bar{q}_N(\rho) = - \nabla_K^2\, q_N(K)\Big|_{K=0} \,, \tag{3.5}$$

where ∇_K^2 is the two-dimensional Laplacian. Therefore we have

$$\langle \rho^2 \rangle = \frac{A}{Q_N} \left[- \nabla_K^2\, q_N(K) \right]_{K=0} \tag{3.6}$$

$$= \frac{A}{Q_N} \left[W\, G^f(s,0)^2 \left[- \nabla_K^2 \frac{1}{1 - W\, G(s,0|K)} \right]_{K=0} \right]_N \,, \tag{3.7}$$

where the second equality follows from equation (2.43).

In the next section, equation (4.87), it will be shown quite generally that

$$\frac{d}{dK} G(s,0|K)\Big|_{K=0} = 0 \,. \tag{3.8}$$

Since $G(s,0|K)$ depends on $K = |\underset{\sim}{K}|$ only ($F(x|K)$ depends on $|\underset{\sim}{K}|$ only) we obtain

$$- \nabla_K^2 \frac{1}{1 - W\, G(s,0|K)}\Big|_{K=0} = - \frac{W[\nabla_K^2\, G(s,0|K)]_{K=0}}{[1 - W\, G(s,0|0)]^2} \,. \tag{3.9}$$

Substituting this into equation (3.7) we have

$$\langle \rho^2 \rangle = \frac{A}{Q_N} \left[\left[\frac{W\, G^f(s,0)}{1 - W\, G(s,0|0)} \right]^2 \left[- \nabla_K^2\, G(s,0|K) \right]_{K=0} \right]_N \,. \tag{3.10}$$

3c. The density of beads off the wall

We derive formulae for the density of beads off the wall for three cases of interest:

(i) a tail of N links (Figure 3.1a), $n_N^f(x)$,

(ii) a loop of N links (Figure 3.1b), $n_N^{\ell}(x)$,

(iii) the general problem of an N-link polymer whose zeroth and N^{th} bead may be anywhere in $n \geq 0$ (Figure 3.1 c-e), $n(x)$.

Before we can proceed it is necessary to introduce generalizations of the quantities $G_M^f(0)$ and $G_M(0|0)$, namely $G_M^f(x)$ and $G_M(x|0)$ defined by

$$G_0^f(x) = 1 \tag{3.11}$$

$$G_M^f(x) = \int_0^\infty \cdots \int_0^\infty dx_1 \cdots dx_M \; F(x - x_1|0) \; F(x_2 - x_1|0) \cdots F(x_M - x_{M-1}|0) \times e^{-\beta \sum_{i=1}^{M} \phi(x_i)}, \quad (M > 0) \tag{3.12}$$

and

$$G_0(x|0) = 1 \tag{3.13}$$

$$G_1(x|0) = F(x|0) \; e^{-\beta\phi(x)} \tag{3.14}$$

$$G_M(x|0) = \int_0^\infty \cdots \int_0^\infty dx_1 \cdots dx_{M-1} \; F(x - x_1|0) \; F(x_2 - x_1|0) \cdots \times F(x_{M-1} - x_{M-2}|0) \; F(x_{M-1}|0) \; e^{-\beta \sum_{i=0}^{M-1} \phi(x_i)}, \quad (M > 1, \; x_0 = x) . \tag{3.15}$$

They are interpreted physically as follows:

$G_M^f(x)$ is the CPF of an M-link segment whose zeroth bead is at x (≥ 0) and all others are in the half-space $x > 0$;

$G_M(x|0)$ is the CPF of an M-link segment whose zeroth bead is at x (≥ 0), the M^{th} bead is on the wall ($x = 0$), and all others are in the half-space $x > 0$.

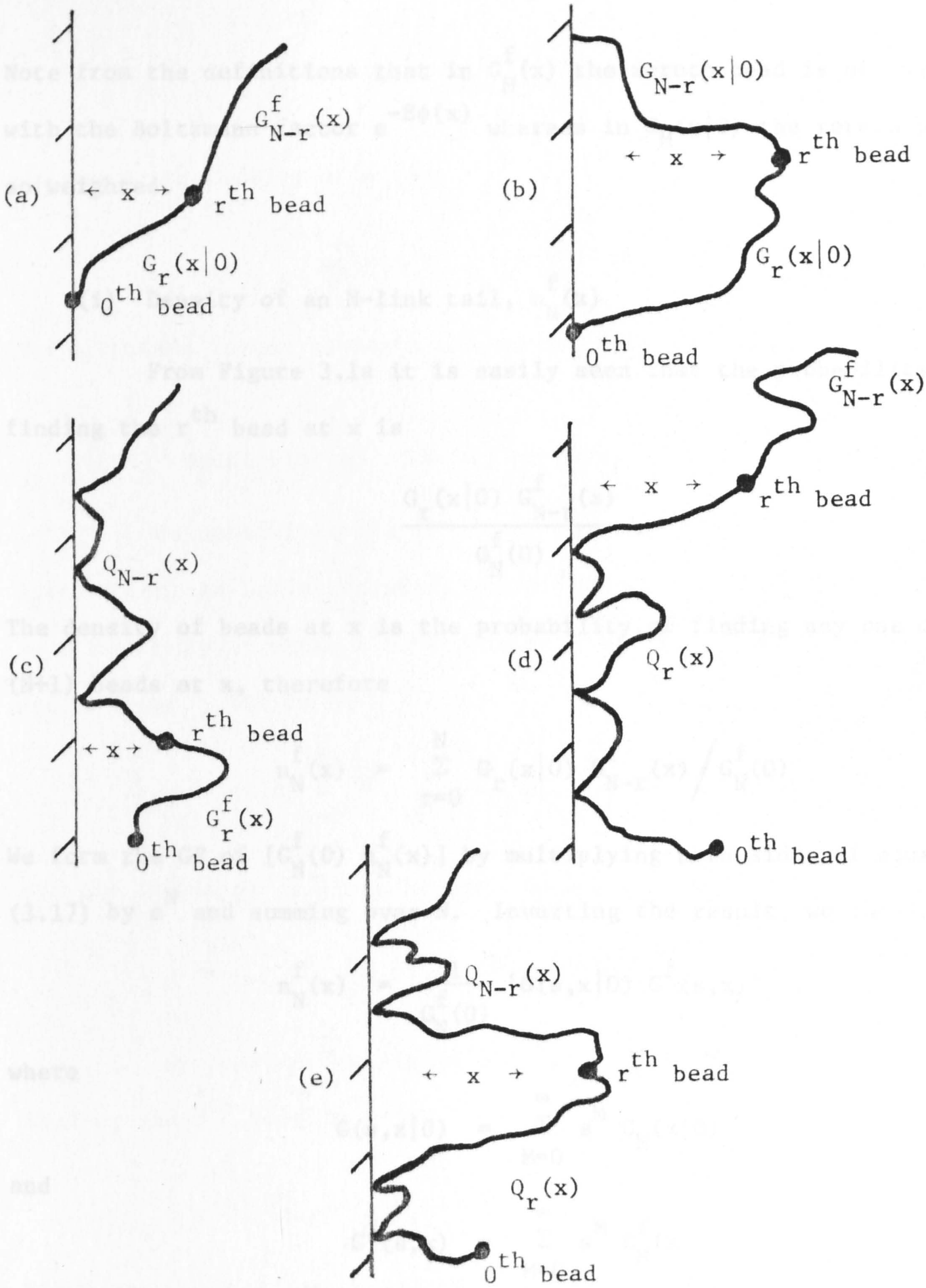

Figure 3.1: Diagrams used to derive expressions for the density of beads off the wall for the cases:

(a) a tail with one end on an impenetrable wall,

(b) a loop with both ends on an impenetrable wall,

(c), (d) and (e) an adsorbed polymer with many possible contacts. In this case the r^{th} bead can be in any one of the positions shown.

Note from the definitions that in $G_M^f(x)$ the zeroth bead is not weighted with the Boltzmann factor $e^{-\beta\phi(x)}$ whereas in $G_M(x|0)$ the zeroth bead is so weighted.

(i) Density of an N-link tail, $n_N^f(x)$

From Figure 3.1a it is easily seen that the probability of finding the r^{th} bead at x is

$$\frac{G_r(x|0)\ G_{N-r}^f(x)}{G_N^f(0)} . \tag{3.16}$$

The density of beads at x is the probability of finding any one of the (N+1) beads at x, therefore

$$n_N^f(x) = \sum_{r=0}^{N} G_r(x|0)\ G_{N-r}^f(x) \Big/ G_N^f(0) . \tag{3.17}$$

We form the GF of $[G_N^f(0)\ n_N^f(x)]$ by multiplying both sides of equation (3.17) by s^N and summing over N. Inverting the result, we obtain

$$n_N^f(x) = \frac{1}{G_N^f(0)} [G(s,x|0)\ G^f(s,x)]_N , \tag{3.18}$$

where

$$G(s,x|0) = \sum_{M=0}^{\infty} s^M\ G_M(x|0) \tag{3.19}$$

and

$$G^f(s,x) = \sum_{M=0}^{\infty} s^M\ G_M^f(x) \tag{3.20}$$

are generalizations of the GF $G(s,0|0)$ and $G^f(s,0)$ given in equations (2.40) and (2.41).

(ii) Density of an N-link loop, $n_N^{\ell}(x)$

Following the line of reasoning given for the case of a tail, we obtain the probability of finding the r^{th} bead at x,

$$e^{\beta\phi(x)} \frac{G_r(x|0)\ G_{N-r}(x|0)}{G_N(0|0)} , \tag{3.21}$$

and hence the density of a loop

$$n_N^{\ell}(x) = \frac{e^{\beta\phi(x)}}{G_N(0|0)} [G(s,x|0)^2]_N . \tag{3.22}$$

The Boltzmann factor corrects the overweighting of the r^{th} bead.

(iii) Density of an adsorbed polymer, $n(x)$

We generalize the CPF Q_N of equation (2.36) to the function $Q_N(x)$ which can be interpreted, apart from the constant A, as the CPF for an N link polymer whose N^{th} bead is at x and has at least one bead on the wall. From (2.36) we have

$$Q_N(x) = A \sum_{n=1}^{N} W^n \sum_{\{M_i\}} G^f_{M_1}(0) \prod_{i=2}^{n} G_{M_i}(0|0)\ G_{M_{n+1}}(x|0) \tag{3.23}$$

and its GF $Q(s,x)$ is given by (cf. equation (2.39))

$$Q(s,x) = \frac{W\ G^f(s,0)\ G(s,x|0)}{1 - W\ G(s,0|0)} . \tag{3.25}$$

By considering Figure 3.1 c,d,e we see that the probability of finding the r^{th} bead at x is

$$\frac{1}{Q_N} \left[G^f_r(x)\ Q_{N-r}(x) + Q_r(x)\ G^f_{N-r}(x) + \frac{e^{\beta\phi(x)}}{A} Q_r(x)\ Q_{N-r}(x) \right] . \tag{3.26}$$

The first, second, and third term represent contributions from diagrams in Figure 3.1 c, d and e respectively. A summation over all beads yields the density

$$n(x) = \frac{1}{Q_N} \sum_{r=0}^{N} \left\{ G^f_r(x)\ Q_{N-r}(x) + Q_r(x)\ G^f_{N-r}(x) + \frac{e^{\beta\phi(x)}}{A} Q_r(x)\ Q_{N-r}(x) \right\} . \tag{3.27}$$

In terms of the GF and equation (3.25) this becomes

$$n(x) = \frac{A}{Q_N}\left[e^{\beta\phi(x)}\ Q^2(s,x) + 2Q(s,x)\ G^f(s,x)\right]_N \tag{3.28}$$

$$n(x) = \frac{A}{Q_N}\left[e^{\beta\phi(x)}\ \left\{\frac{W\ G^f(s,0)\ G(s,x|0)}{1 - W\ G(s,0|0)}\right\}^2 + \frac{2\,W G^f(s,0)\ G^f(s,x)\ G(s,x|0)}{1 - W\ G(s,0|0)}\right]_N . \tag{3.29}$$

In summary, the conformational properties of an adsorbed polymer are determined by the quantities $G(s,0|K)$, $G(s,x|0)$ and $G^f(s,x)$ as follows:

$$\langle n \rangle = W \frac{\partial(\ln Q_N)}{\partial W} \tag{3.3}$$

$$\langle \rho^2 \rangle = \frac{A}{Q_N}\left[\left[\frac{W\ G^f(s,0)}{1 - W\ G(s,0|0)}\right]^2 \left[-\nabla_K\ G(s,0|K)\right]_{K=0}\right]_N \tag{3.10}$$

$$n(x) = \frac{A}{Q_N}\left[e^{\beta\phi(x)}\ \left\{\frac{W\ G^f(s,0)\ G(s,x|0)}{1 - W\ G(s,0|0)}\right\}^2 + \frac{2\,W G^f(s,0)\ G^f(s,x)\ G(s,x|0)}{1 - W\ G(s,0|0)}\right]_N \tag{3.29}$$

$$\bar{x} = \frac{1}{(N+1)} \int_0^\infty x\, n(x)\, dx\ . \tag{3.1}$$

4. THE GENERATING FUNCTIONS $G(s,x|K)$ AND $G^f(s,x)$

In this section, we shall evaluate the functions $G(s,x|K)$ and $G^f(s,x)$ for the case where the external potential is zero, i.e. $\phi(x) = 0$.

From the definitions (3.12) and (3.15) we can write down the following recurrence relations

$$G_M^f(0) = \int_0^\infty G_M(x|0)\, dx \quad , \quad (M > 1) \tag{4.1}$$

$$G_{M+1}(x|K) = \int_0^\infty F(x - x')\, G_M(x'|K)\, dx' \quad , \quad (M \geq 1) \; . \tag{4.2}$$

Multiplying (4.2) by s^{M+1} and summing from $M = 1$ to infinity we obtain the integral equation for the GF

$$G(s,x|K) = sF(x|K) + s \int_0^\infty F(x - x'|K)\, G(s,x'|K)\, dx' \; , \tag{4.3}$$

where we have used equation (3.14) for $G_1(x|K)$. A similar operation on equation (4.1) yields

$$G^f(s,0) = 1 + \int_0^\infty G(s,x|0)\, dx \; . \tag{4.4}$$

Owing to the nature of the physical problem we are faced with integral equations involving half-range convolutions, whose solution require some amount of mathematical manipulations. For ease of later reference, we shall first summarize the results and then present their derivations.

It turns out that if we wish to study the conformation of the polymer as a function of the adsorption energy parameter W, only the results for s near zero ($s \sim 0$) and s close to but less than one ($s \lesssim 1$) are needed. The quantities necessary to evaluate polymer conformational characteristics are given in Table 4.1. These results are asymptotic unless stated otherwise. During the course of the derivation, we find it convenient to define the "one-dimensional" variance of the probability density function $\bar{f}(|\underset{\sim}{r}|)$ by (cf. equations (2.21) and (2.22))

$$\sigma^2 = \int \bar{f}(|\underset{\sim}{r}|)\, x^2\, d^3r = \int_{-\infty}^{\infty} F(x|0)\, x^2\, dx = -\left.\frac{d^2 f(z)}{dz^2}\right|_{z=0} ;$$

and the "two-dimensional" variance of the probability density function $\bar{f}(|\underset{\sim}{r}|)$ when $\underset{\sim}{r}$ is confined to the plane $x = 0$, by

Table 4.1: Summary of results for the generating functions for s near 0 and s near 1. Numbers in brackets refer to the corresponding equations in the text.

	$s \sim 0$		$s \leq 1$	
$G(s,x\|0)$	$sF(x\|0) + s^2 \int_0^\infty F(x-x'\|0)\, F(x'\|0)\, dx' + \ldots$	(4.49)	$\underline{x = 0}$ $G(1,0\|0) - 2^{\frac{1}{2}}(1-s)^{\frac{1}{2}}/\sigma$ $\left(G(1,0\|0) = -\frac{1}{2\pi}\int_{-\infty}^{\infty} ln\left(1-f(z)\right)dz\right)$	(4.64)
			$\underline{2^{\frac{1}{2}}(1-s)^{\frac{1}{2}}x/\sigma >> 1}$ $\frac{2^{\frac{1}{2}}}{\sigma} e^{-2^{\frac{1}{2}}(1-s)^{\frac{1}{2}}x/\sigma}$	(4.61)
$\frac{\partial G(s,0\|0)}{\partial s}$	$F(0\|0)$	(4.66)	$\frac{1}{2^{\frac{1}{2}}(1-s)^{\frac{1}{2}}\sigma}$	(4.67)
$G^f(s,x)$	$\underline{x = 0}$ $(1-s)^{-\frac{1}{2}}$ exact	(4.68)	$\underline{x = 0}$ $(1-s)^{-\frac{1}{2}}$ exact	(4.68)
	$\underline{x > 0}$ $1 + s\int_0^\infty F(x-x'\|0)\, dx' + \ldots$	(4.84a)	$\underline{2^{\frac{1}{2}}(1-s)^{\frac{1}{2}}s/\sigma >> 1}$ $\frac{1 - e^{-2^{\frac{1}{2}}(1-s)^{\frac{1}{2}}x/\sigma}}{1-s}$	(4.84)
$\nabla_K^2\, G(s,0\|K)$ at $K = 0$	$-s\lambda^2 F(0\|0)$	(4.99)	$-\frac{2^{\frac{1}{2}}\sigma}{(1-s)^{\frac{1}{2}}}$	(4.92)

$$\lambda^2 = \frac{\int \bar{f}(|\underset{\sim}{\rho}|)\, \rho^2\, d^2\underset{\sim}{\rho}}{\int \bar{f}(|\underset{\sim}{\rho}|)\, d^2\underset{\sim}{\rho}} = \frac{\int \bar{f}(|\underset{\sim}{\rho}|)\, \rho^2\, d^2\underset{\sim}{\rho}}{F(0|0)} . \qquad (4.98)$$

We also adopt the convention that when $K = 0$, the K argument in all functions are suppressed, that is

$$G(s,x|0) \equiv G(s,x)$$

$$F(x|0) \equiv F(x) .$$

The remainder of this section is devoted to deriving the results given in Table 4.1 and may be omitted by the reader without loss of continuity.

4a. The Function G(s,x)

We first study the integral equation (4.3) for $K = 0$, namely

$$G(s,x) = sF(x) + s \int_0^\infty F(x - x')\, G(s,x')\, dx' . \qquad (4.5)$$

In general the solution of this equation, if one exists, may or may not be unique. However, the only admissible solution in this problem is the unique solution that is analytic in the neighbourhood of $s = 0$ because the Taylor expansion of $G(s,x)$ about $s = 0$ is equivalent to the recurrence relation (4.2). The integral equation (4.5) may be solved using a variation of the Wiener-Hopf method[33,34] to yield a Fourier transformable solution analytic at $s = 0$.

Before solving this equation, we examine the solution $P(s,x)$ of the full range equation,

$$P(s,x) = sF(x) + s \int_{-\infty}^\infty F(x - x')\, P(s,x')\, dx' . \qquad (4.6)$$

Physically,

$$P(s,x) \equiv \sum_{N=1}^{\infty} s^N P_N(x)$$

is the GF of the CPF, $P_N(x)$, for an N-link polymer in full space

$(-\infty < x < \infty)$ whose zeroth bead is at $x = 0$ and the N^{th} bead at x. Equation (4.6) can be solved in the usual manner by taking a Fourier transform, defined by

$$p(s,z) = \int_{-\infty}^{\infty} P(s,x)\, e^{izx}\, dx \,, \tag{4.7}$$

to yield

$$p(s,z) = sf(z) + sf(z)\, p(s,z) \,. \tag{4.8}$$

Therefore

$$p(s,z) = \frac{sf(z)}{1 - sf(z)} \tag{4.9}$$

and by the inversion formula

$$P(s,x) = \frac{1}{2\pi} \int_{-\infty}^{\infty} \frac{sf(z)}{1 - sf(z)}\, e^{-izx}\, dz \,. \tag{4.10}$$

We define the functions

$$G^{+}(s,x) = \theta(x)\, G(s,x) \tag{4.11}$$

$$G^{-}(s,x) = \theta(-x)\, G(s,x) \,, \tag{4.12}$$

where $\theta(x)$ is the step function. The Fourier transform of these functions,

$$g^{+}(s,z) = \int_{0}^{\infty} G^{+}(s,x)\, e^{izx}\, dx \tag{4.13}$$

and

$$g^{-}(s,z) = \int_{-\infty}^{0} G^{-}(s,x)\, e^{izx}\, dx \,, \tag{4.14}$$

are analytic in the upper half plane (UHP) and the lower half plane (LHP) respectively. We assume that G(s,x) has a continuous Fourier transform in the conventional sense (for z real). It then follows that

$$g^{\pm}(s,z) \to 0 \tag{4.15}$$

as $|z| \to \infty$ in their respective analytic HPs and that $g^{\pm}(s,z)$ is continuous on the real axis. Following the standard Wiener-Hopf method, we take the Fourier transform of equation (4.5) and obtain

$$g^{+}(s,z) + g^{-}(s,z) = sf(z) + sf(z)\, g^{+}(s,z) \tag{4.16}$$

or

$$g^{+}(s,z)\left(1-sf(z)\right) \;=\; sf(z)-g^{-}(s,z)\;. \tag{4.17}$$

We then seek a factorization of $\left(1-sf(z)\right)$ in the form

$$1-sf(z) \;=\; \frac{\gamma^{+}(s,z)}{\gamma^{-}(s,z)} \tag{4.18}$$

such that $\gamma^{+}(s,z)$ and $\gamma^{-}(s,z)$ are analytic and free of zeros in the UHP and LHP respectively and are continuous on the real z axis. Further, we shall require

$$\gamma^{\pm}(s,z) \;\to\; 1 \tag{4.19}$$

as $|z|\to\infty$ in their respective analytic HPs. Provided such a factorization can be found, equation (4.17) may be rearranged to yield

$$\gamma^{+}(s,z)\left(1+g^{+}(s,z)\right) \;=\; \gamma^{-}\left(1-g^{-}(s,z)\right)\;. \tag{4.20}$$

The LHS represents a function analytic in the UHP and the RHS, a function analytic in the LHP and the two functions are continuous and equal on the real axis. This is sufficient[34] to ensure that the RH function represents the analytic continuation of the LH function into the LHP. Therefore the function E(z) defined by

$$E(z) \;=\; \gamma^{+}(s,z)\left(1+g^{+}(s,z)\right) \;=\; \gamma^{-}(s,z)\left(1-g^{-}(s,z)\right) \tag{4.21}$$

is an entire function. Further we deduce from equations (4.15) and (4.19) that

$$E(z) \;\to\; 1 \tag{4.22}$$

as $|z|\to\infty$. Thus E(z) is a bounded entire function and, by Liouville's theorem, is a constant, namely

$$E(z) \;=\; 1\;. \tag{4.23}$$

Therefore we have

$$g^{+}(s,z) = \frac{1}{\gamma^{+}(s,z)} - 1 \tag{4.24}$$

$$g^{-}(s,z) = 1 - \frac{1}{\gamma^{-}(s,z)} . \tag{4.25}$$

It remains then to determine the appropriate factorization of $1 - sf(z)$ that has the properties invoked above. The factorization of $1 - sf(z)$ is equivalent to splitting

$$ln\left(1 - sf(z)\right) = ln\ \gamma^{+}(s,z) - ln\ \gamma^{-}(s,z) . \tag{4.26}$$

The function

$$h(s,z) \equiv - ln\left(1 - sf(z)\right) \tag{4.27}$$

can be written as the sum

$$h(s,z) = h^{+}(s,z) + h^{-}(s,z) \tag{4.28}$$

by the formulae[34]

$$h^{+}(s,z) = \frac{1}{2\pi i}\int_{-\infty}^{\infty} \frac{h(s,t)}{t-z}\, dt , \qquad (Im\ z > 0) \tag{4.29}$$

$$h^{-}(s,z) = -\frac{1}{2\pi i}\int_{-\infty}^{\infty} \frac{h(s,t)}{t-z}\, dt , \qquad (Im\ z < 0) \tag{4.30}$$

such that h^{+} and h^{-} are continuous on the real axis and are analytic and vanishing as $|z| \to \infty$ in the UHP and LHP respectively. With these properties, we can obtain from $h^{\pm}$, using equations (4.26) and (4.28),

$$\gamma^{+}(s,z) = e^{-h^{+}(s,z)} \tag{4.31}$$

$$\gamma^{-}(s,z) = e^{h^{-}(s,z)} . \tag{4.32}$$

Now γ^{+} and γ^{-} have the required analytic properties. Therefore, from (4.25) and (4.26)

$$g^{+}(s,z) = e^{h^{+}(s,z)} - 1 \tag{4.33}$$

$$g^{-}(s,z) = 1 - e^{-h^{-}(s,z)} . \tag{4.34}$$

From equations (4.9) and (4.27) we see that

$$h(s,z) = \int_0^s \frac{p(s,z)}{s}\, ds \tag{4.35}$$

$$= \int_0^s \frac{f(z)}{1 - sf(z)}\, ds \ . \tag{4.36}$$

Thus the function

$$H(s,x) = \frac{1}{2\pi} \int_{-\infty}^{\infty} h(s,z)\ e^{-izx}\ dz \tag{4.37}$$

is given by

$$H(s,z) = \int_0^s \frac{P(s,x)}{s}\, ds \tag{4.38}$$

and, $h^+(s,z)$ and $h^-(s,z)$ are Fourier transforms of

$$H^+(s,x) = \theta(x)\ H(s,x) \tag{4.39}$$

and

$$H^-(s,z) = \theta(-x)\ H(s,x) \tag{4.40}$$

respectively.

Useful results now emerge from the above analysis. Inversion of the expression for $g^+(s,z)$ in equation (4.33) yields, for $x > 0$,

$$G(s,x) = H^+(s,x) + \frac{1}{2!} \int_{-\infty}^{\infty} H^+(s,x-x')\ H^+(s,x')\ dx'$$

$$+ \frac{1}{3!} \int_{-\infty}^{\infty} \int_{-\infty}^{\infty} H^+(s,x-x')\ H^+(s,x'-x'')\ H^+(s,x'')\ dx'\ dx''$$

$$+ \ \ldots \ . \tag{4.41}$$

But since $H^+(s,x) = 0$ for $x < 0$, it follows that

$$\lim_{x \to 0_+} G(s,x) = G(s,0) = H^+(s,0) \tag{4.42}$$

$$= \int_0^s \frac{P(s,0)}{s}\, ds \ . \tag{4.43}$$

From equation (4.10) we deduce the result, for $s < 1$,

$$P(s,0) = \frac{1}{2\pi} \int_{-\infty}^{\infty} \frac{sf(z)}{1 - sf(z)}\, dz$$

$$= \frac{1}{2\pi} \sum_{N=1}^{\infty} s^N \int_{-\infty}^{\infty} [f(z)]^N\, dz \equiv \sum_{N=1}^{\infty} s^N\, P_N(0) \tag{4.44}$$

since for z real $f(z) \leq 1$ (cf. equations (2.17) and (2.20)). Consequently,

$$G(s,0) = \frac{1}{2\pi} \sum_{N=1}^{\infty} \frac{s^N}{N} \int_{-\infty}^{\infty} [f(z)]^N \, dz \equiv \sum_{N=1}^{\infty} s^N \, G_N(0) \, . \qquad (4.45)$$

A comparison of equations (4.44) and (4.45) reveals an interesting side result

$$G_N(0) = \frac{1}{N} P_N(0) \, . \qquad (4.46)$$

In other words, for any given N-link polymer, whose bond distribution function $\bar{f}(|\underset{\sim}{r}|)$ satisfies the above requirements, the number of configurations starting and ending at the plane $x = 0$ that can be taken up by such a polymer in full space is exactly N times that for the corresponding situation in a half-space ($x > 0$, say).

Since F(x) is a real even function, f(z) and therefore h(s,z) is even in z. Therefore

$$h^+(s,0) = h^-(s,0) = \tfrac{1}{2} h(s,0) \qquad (4.47)$$

and from the definition of h(s,z), (4.27), we have

$$h^+(s,0) = -\tfrac{1}{2} \ln(1-s) = h^-(s,0) \, . \qquad (4.48)$$

For a given bond distribution function $\bar{f}(|\underset{\sim}{r}|)$, or f(z), equations (4.33) and (4.34) constitute an exact solution of the integral equation (4.5). However, to obtain physically interesting results, we only need solutions in the neighbourhood of $s = 0$ and $s = 1$. In these regimes, the problem becomes amenable to further formal asymptotic analysis.

Around $s = 0$, the solution can be obtained by iteration

$$G(s,x) = sF(x) + s^2 \int_0^{\infty} F(x-x') \, F(x') \, dx' + \ldots \, . \qquad (4.49)$$

In the neighbourhood of $s = 1$, the function G(s,x) is more complicated. Since f(z) is even, then if z_0 is a (in general, complex)

zero of $1 - f(z)$, so is $-z_0$. For s less than but close to one ($s \lesssim 1$), there are two zero $\pm z_0$ in the neighbourhood of $z = 0$, and as $s \to 1$ from below, the two zeros converge to the origin. Consider the integral taken along the real axis (cf. equations (4.9) and (4.29))

$$p^+(s,z) = \frac{1}{2\pi i} \int_{-\infty}^{\infty} \frac{sf(t)}{1 - sf(t)} \frac{dt}{t - z}, \quad (Im\ z > 0) \qquad (4.50)$$

which diverges at $s = 1$ on account of the pole in the integrand at $t = z_0 = 0$. Due to the coalescence at the origin of the two poles from above and below the real axis, $p^+(s,z)$ will have a branch point at $s = 1$. For $s \lesssim 1$, the main contribution to the integral in (4.50) will come from t near zero so that we can replace f(t) by its Taylor expansion about $t = 0$. From the properties of the bond distribution function we have (see Section 2)

$$f(0) = 1$$

$$f'(0) = i \int_{-\infty}^{\infty} x\, F(x)\, dx = 0$$

$$f''(0) = -\int_{-\infty}^{\infty} x^2\, F(x)\, dx \equiv -\sigma^2,$$

therefore we can write

$$f(z) = 1 - \tfrac{1}{2}\sigma^2 z^2 + \ldots \qquad (4.51)$$

for z near zero.

Thus in the regime $s \lesssim 1$, we have

$$p^+(s,z) \simeq \frac{s}{2\pi i} \int_{-\infty}^{\infty} \frac{1}{(1-s) + \frac{1}{2}\sigma^2 t^2} \frac{dt}{t - z}, \quad (Im\ z > 0) \qquad (4.52)$$

$$\simeq \frac{i/(2^{\frac{1}{2}}(1-s)^{\frac{1}{2}}\sigma)}{z + i2^{\frac{1}{2}}(1-s)^{\frac{1}{2}}/\sigma} \qquad (4.53)$$

and from equation (4.35)

$$h^+(s,z) = -\ln\left(z + i2^{\frac{1}{2}}(1-s)^{\frac{1}{2}}/\sigma\right), \quad (s \lesssim 1). \qquad (4.54)$$

From this we see that for $s \lesssim 1$ and z near $z_0 = -i2^{\frac{1}{2}}(1-s)^{\frac{1}{2}}/\sigma$, $g^+(s,z)$ has

the form

$$g^+(s,z) = e^{h^+(s,z)} - 1$$

$$\simeq \frac{A}{z - z_0} . \qquad (4.55)$$

But we have

$$g^+(s,0) = e^{h^+(s,0)} - 1 \qquad (4.56)$$

$$\simeq \frac{A}{-z_0} , \qquad (s \lesssim 1) , \qquad (4.57)$$

therefore it follows from equation (4.48) that

$$A = \frac{i2^{\frac{1}{2}}(1-s)^{\frac{1}{2}}}{\sigma} (e^{h^+(s,0)} - 1)$$

$$= i2^{\frac{1}{2}}/\sigma . \qquad (4.58)$$

Thus we have the asymptotic solution

$$g^+(s,z) = \frac{i2^{\frac{1}{2}}/\sigma}{z + i2^{\frac{1}{2}}(1-s)^{\frac{1}{2}}/\sigma} + \ldots , \qquad (s \lesssim 1) \qquad (4.59)$$

where smaller contributions from poles further away from the real axis have been omitted. We obtain $G^+(s,x)$ by the inverse Fourier transform

$$G^+(s,x) = \frac{1}{2\pi} \int_{-\infty}^{\infty} g^+(s,z)\, e^{-izx}\, dz \qquad (4.60)$$

which may be evaluated using Cauchy's Theorem by completing the contour in the LHP. However, when x is sufficiently large, only the pole of $g^+(s,z)$ with the smallest imaginary part will contribute significantly. Contributions from other poles will be exponentially small. Substituting equation (4.59) into (4.60) we obtain, for $s \lesssim 1$, and x large (i.e. $2^{\frac{1}{2}}(1-s)^{\frac{1}{2}}x/\sigma >> 1$),

$$G^+(s,x) \simeq \frac{2^{\frac{1}{2}}}{\sigma} e^{-2^{\frac{1}{2}}(1-s)^{\frac{1}{2}}x/\sigma} + \ldots . \qquad (4.61)$$

To obtain an expression for $G^+(s,0)$ for $s \lesssim 1$, we consider the expression for $P(s,0)$, namely

$$P(s,0) = \frac{1}{2\pi}\int_{-\infty}^{\infty} \frac{sf(z)}{1-sf(z)}\,dz\ . \tag{4.62}$$

As before for $s \lesssim 1$ we expand $f(z)$ about $z = 0$ to obtain

$$P(s,0) \doteq \frac{1}{2\pi}\int_{-\infty}^{\infty} \frac{1}{(1-s)+\frac{1}{2}\sigma^2 z^2}\,dz$$

$$= \frac{1}{2^{\frac{1}{2}}(1-s)^{\frac{1}{2}}\sigma}\ . \tag{4.63}$$

Since

$$G^{+}(s,0) = \lim_{x\to 0_{+}} G(s,x)$$

we have from equations (4.43) and (4.63)

$$G(s,0) \simeq G(1,0) - 2^{\frac{1}{2}}(1-s)^{\frac{1}{2}}/\sigma\ , \qquad s \lesssim 1\ , \tag{4.64}$$

where the numerical constant $G(1,0)$ is given by

$$G(1,0) = -\frac{1}{2\pi}\int_{-\infty}^{\infty} ln\big(1-f(z)\big)\,dz\ . \tag{4.65}$$

We also note that

$$\frac{d}{ds}G(s,0) = \frac{1}{s}P(s,0)$$

$$\simeq F(0) \qquad \text{for} \quad s\sim 0 \tag{4.66}$$

and

$$\simeq \frac{1}{2^{\frac{1}{2}}(1-s)^{\frac{1}{2}}\sigma} \qquad \text{for} \quad s \lesssim 1\ . \tag{4.67}$$

4b. The Function $G^{f}(s,x)$

The expression for $G^{f}(s,0)$ follows from equations (4.4), (4.13) and (4.33)

$$G^{f}(s,0) = 1 + \int_{0}^{\infty} G^{+}(s,x)\,dx$$

$$= 1 + g^{+}(s,0)$$

$$= e^{h^{+}(s,0)}\ .$$

But since

$$h^{+}(s,0) = -\tfrac{1}{2}\ln(1-s) \qquad (4.48)$$

we obtain the exact result for all $0 \leq s < 1$

$$G^{f}(s,0) = (1-s)^{-\frac{1}{2}} . \qquad (4.68)$$

For $x > 0$, we introduce the function $G(s,x,x')$ which is the generating function for a chain which starts at x and ends at x' (> 0). Then the GF for a chain starting at x, $G^{f}(s,x)$, is given by

$$G^{f}(s,x) = 1 + \int_{0}^{\infty} G(s,x,x')\, dx' . \qquad (4.69)$$

It is easily seen that $G(s,x,x')$ satisfies the integral equation

$$G(s,x,x') = sF(x-x') + s\int_{0}^{\infty} F(x'-t)\, G(s,x,t)\, dt . \qquad (4.70)$$

As before, we take the Fourier transform wrt x' to yield

$$g^{+}(s,x,z) + g^{-}(s,x,z) = se^{ixz} f(z) + sf(z)\, g^{+}(s,x,z) . \qquad (4.71)$$

Using the splitting

$$1 - sf(z) = \frac{\gamma^{+}(s,z)}{\gamma^{-}(s,z)} , \qquad (4.18)$$

where $\gamma^{\pm}$ have their usual properties, we obtain

$$\gamma^{+}(s,z)\, g^{+}(s,x,z) + \gamma^{-}(s,z)\, g^{-}(s,x,z) = e^{ixz}\left(\gamma^{-}(s,z) - \gamma^{+}(s,z)\right)$$

$$\equiv q(s,x,z) . \qquad (4.72)$$

Applying the formulae (4.29) and (4.30) we split $q(s,x,z)$ into a sum of $q^{+}(s,x,z)$ and $q^{-}(s,x,z)$ which are analytic in the UHP and LHP respectively and vanishing as $|z| \to \infty$ in their respective analytic HPs. Equation (4.72) can then be rearranged to yield

$$\gamma^{+}(s,z)\, g^{+}(s,x,z) - q^{+}(s,x,z) = q^{-}(s,x,z) - \gamma^{-}(s,z)\, g^{-}(s,x,z)$$

$$\equiv E(z) \qquad (4.73)$$

which defines an entire function $E(z)$ because the RHS (analytic in the

LHP) is now the analytic continuation of the LHS (analytic in the UHP) into the LHP. The asymptotic behaviour ($|z| \to \infty$) of $\gamma^{\pm}$, $g^{\pm}$ and $q^{\pm}$ give $E(z) \to 0$ as $|z| \to \infty$ which implies $E(z) = 0$. Therefore

$$g^{+}(s,x,z) = \frac{q^{+}(s,x,z)}{\gamma^{+}(s,x)} \tag{4.74}$$

and it follows from (4.69) that

$$G^{f}(s,x) = 1 + g^{+}(s,x,0) \; . \tag{4.75}$$

From equations (4.31) and (4.48) we know that

$$\gamma^{\pm}(s,0) = (1-s)^{\pm\frac{1}{2}} \tag{4.76}$$

so to calculate $g^{+}(s,x,0)$ we need only $q^{+}(s,x,0)$.

From equations (4.29) and (4.72) we have

$$q^{+}(s,x,0) = \frac{1}{2\pi i} \int_{-\infty - i\delta}^{\infty - i\delta} e^{ixt} \left[\gamma^{-}(s,t) - \gamma^{+}(s,t)\right] \frac{dt}{t} \; , \tag{4.77}$$

where the contour has been displaced just below the real axis. The poles of the integrand above the contour are the poles of $\gamma^{-}(s,t)$ in the UHP and the pole at $t = 0$. For $s \lesssim 1$, we can derive an expression for $h^{-}(s,z)$ in a similar manner to the derivation of equation (4.54) for $h^{+}(s,z)$. (Alternatively, we can deduce this by considering equations (4.27), (4.28) and (4.54) for $z \sim 0$ and $s \lesssim 1$.) We get

$$h^{-}(s,z) = - \ln\left(z - i2^{\frac{1}{2}}(1-s)^{\frac{1}{2}}/\sigma\right) + \ldots \tag{4.78}$$

which according to equation (4.32) shows that for $s \lesssim 1$, $\gamma^{-}(s,z)$ has a pole at

$$z_0 = i2^{\frac{1}{2}}(1-s)^{\frac{1}{2}}/\sigma \; . \tag{4.79}$$

As before, we write for $s \lesssim 1$, $z \sim z_0 \sim 0$

$$\gamma^{-}(s,z) \doteq \frac{B}{z - z_0} \tag{4.80}$$

so that

$$\gamma^-(s,0) \simeq \frac{B}{-z_0} = 1 - e^{-h^-(s,0)} \quad . \tag{4.81}$$

Now for x large, we displace the contour in equation (4.77) over the poles at $t = 0$ and $t = z_0$ up to z_1, the next pole or singularity of $\gamma^-(s,z)$. The original integral is then the sum of the residues at $t = 0$ and z_0 plus the integral along the line $Im\, t = Im\, z_1 - \delta$, which is exponentially small if x is large. Thus $q^+(s,x,0)$ can be approximated by only contributions from the first two poles,

$$q^+(s,x,0) \simeq \left(\gamma^-(s,0) - \gamma^+(s,0)\right) + \frac{Be^{iz_0 x}}{z_0} \tag{4.82}$$

which from equation (4.81) may be rewritten as

$$q^+(s,x,0) \simeq \gamma^-(s,0)\left(1 - e^{iz_0 x}\right) - \gamma^+(s,0) \quad . \tag{4.83}$$

And finally from equations (4.74) - (4.76) and (4.79) we obtain

$$G^f(s,x) \simeq \frac{1 - e^{-2^{\frac{1}{2}}(1-s)^{\frac{1}{2}}x/\sigma}}{1-s} , \quad (s \lesssim 1,\ 2^{\frac{1}{2}}(1-s)^{\frac{1}{2}}x/\sigma >> 1) \ . \tag{4.84}$$

For $s \sim 0$, successive iterations of equation (4.70) yield

$$G(s,x,x') = sF(x-x') + s^2 \int_0^\infty F(x'-t)\ F(x-t)\ dt$$

whence from (4.69) gives

$$G^f(s,x) \simeq 1 + s\int_0^\infty F(x-x')\ dx' + \ldots \ , \quad (s \sim 0) \ . \tag{4.84a}$$

4c. The Function $\nabla_K^2\ G(s,0|K)$ at $K = 0$

Since $G(s,0|K)$ is a function of $K = |\underset{\sim}{K}|$ only, we may write the two-dimensional ∂_K^2 operator as

$$\nabla_K^2 = \frac{\partial^2}{\partial K^2} + \frac{1}{K}\frac{\partial}{\partial K} \ . \tag{4.85}$$

In a similar manner to the derivation of equation (4.41) for $G^+(s,0) \equiv G(s,0|0)$ we derive

$$G(s,0|K) = -\frac{1}{2\pi}\int_{-\infty}^{\infty} ln\left(1 - sf(\sqrt{z^2+K^2})\right) dz \,. \tag{4.86}$$

Therefore a differentiation with respect to K yields

$$\frac{\partial G(s,0|K)}{\partial K} = \frac{1}{2\pi}\int_{-\infty}^{\infty} \frac{sf'(\sqrt{z^2+K^2})}{1 - sf(\sqrt{z^2+K^2})} \frac{K}{\sqrt{z^2+K^2}} dz \tag{4.87}$$

which gives the result quoted in (3.8), namely

$$\left.\frac{\partial G(s,0|K)}{\partial K}\right|_{K=0} = 0 \,, \tag{4.88}$$

and the relation

$$\left[\frac{1}{K}\frac{\partial G(s,0|K)}{\partial K}\right]_{K=0} = \frac{1}{2\pi}\int_{-\infty}^{\infty} \frac{sf'(z)}{1-sf(z)}\frac{dz}{z} \,. \tag{4.89}$$

A second differentiation of equation (4.87) gives

$$\left.\frac{\partial^2 G(s,0|K)}{\partial K^2}\right|_{K=0} = \frac{1}{2\pi}\int_{-\infty}^{\infty} \frac{sf'(z)}{1-sf(z)}\frac{dz}{z} \,. \tag{4.90}$$

Therefore from equations (4.85), (4.87) and (4.90) we have

$$\nabla_K^2 \, G(s,0|K)\Big|_{K=0} = \frac{1}{\pi}\int_{-\infty}^{\infty} \frac{sf'(z)}{1-sf(z)}\frac{dz}{z} \,. \tag{4.91}$$

Since $\lim_{z=0} f'(z)/z = f''(0) = -\sigma^2$ is finite, so for $s \lesssim 1$, we can again expand the denominator $\left(1 - sf(z)\right)$ as before and obtain the approximate expression

$$\nabla_K^2 \, G(s,0|K)\Big|_{K=0} \simeq -\frac{2^{\frac{1}{2}}\sigma}{(1-s)^{\frac{1}{2}}} \,, \quad (s \lesssim 1) \,. \tag{4.92}$$

Finally we also require this quantity for $s \sim 0$. From the integral equation (4.3) we have by successive iteration

$$G(s,0|K) = sF(0|K) + \ldots \,. \tag{4.93}$$

Therefore

$$-\nabla_K^2 G(s,0|K)\Big|_{K=0} = -s\,\nabla_K^2 \, F(0|K)\Big|_{K=0} + \ldots \,. \tag{4.94}$$

Now from equation (2.17)

$$F(0|K) = \int \bar{f}(|\underset{\sim}{\rho}|)\, e^{i\underset{\sim}{K}\cdot\underset{\sim}{\rho}}\, d^2\underset{\sim}{\rho} \tag{4.95}$$

so

$$-\nabla_K^2 F(0|K)\Big|_{K=0} = \int \bar{f}(|\underset{\sim}{\rho}|)\,\rho^2\,d^2\underset{\sim}{\rho} \tag{4.96}$$

$$= \lambda^2\ F(0)\ , \tag{4.97}$$

where

$$\lambda^2 = \frac{\int \bar{f}(|\underset{\sim}{\rho}|)\,\rho^2\,d^2\underset{\sim}{\rho}}{\int \bar{f}(|\underset{\sim}{\rho}|)\,d^2\underset{\sim}{\rho}} \tag{4.98}$$

is the "two-dimensional" variance of the link distribution function $\bar{f}(|\underset{\sim}{r}|)$ where $\underset{\sim}{r}$ is confined to the plane $x = 0$. Therefore for s near zero

$$-\nabla_K^2 G(s,0|K)\Big|_{K=0} \simeq s\,\lambda^2\,F(0)\ , \quad (s\sim 0) \tag{4.99}$$

We have now derived all the results tabulated at the beginning of this section.

5. POLYMER CONFORMATION AS A FUNCTION OF W

We recall from section 2, the partition function

$$Q_N = A\left[\frac{WG^f(s,0)^2}{1-WG(s,0|0)}\right]_N\ , \tag{2.42}$$

where $[...]_N$ denotes the coefficient of s^N of the Taylor expansion of the function inside the brackets. From the results of the previous section, we see that the quantity

$$Q(s) = \frac{WG^f(s,0)^2}{1-WG(s,0|0)} \tag{5.1}$$

has two singularities: a branch point or square root singularity at $s = 1$ and a pole at $s = s_0$, where

$$1 - WG(s_0,0|0) = 0\ . \tag{5.2}$$

The zero s_0 nearest the origin of $1 - WG(s_0,0|0)$ is always on the positive real s axis. This follows from the fact that the CPFs $G_m(0|0)$, from which the GF $G(s,0|0)$ is formed, are all strictly positive. For very large W corresponding to the case of a very attractive wall, the

pole s_0 is near the origin since $G(s_0, 0|0)$ must tend to zero as $W \to \infty$. As W decreases, s_0 moves away from the origin along the positive real axis. At a critical value of $W = W_c$, the pole s_0 coincides with the branch point at $s = 1$. We can see from equations (5.2) and Table 4.1 that

$$W_c = \frac{1}{G(1,0|0)} = \frac{1}{G(1,0)} . \tag{5.3}$$

When W is just bigger than W_c, $s_0 \lesssim 1$. For $0 < W < W_c$, there is no pole s_0 for $|s| < 1$.

According to Darboux's Theorem[35] the N^{th} coefficient in a Taylor expansion of a function f(s) is given asymptotically by the coefficient of s^N in the dominant term of f(s) about its singularity nearest the origin. Hence as W changes from $W > W_c$ to $W < W_c$, the singularity of the function, (5.1), nearest the origin changes from the pole $s = s_0$ to the branch point at $s = 1$. The positions of the singularities in the s-plane are illustrated in Figure 5.1 for four regimes of interest. We now discuss the conformational characteristics of the polymer in each regime.

5a. $W >> W_c$

We first derive an expression for the pole $s = s_0$ which is the singularity of Q(s) nearest the origin. For W very large, we expect $s = s_0 \sim 0$. From Table 4.1 we have ($s \sim 0$)

$$G(s,0|0) = sF(0) + s^2 \int_0^\infty F(t)^2 \, dt + \ldots \tag{5.4}$$

which from equation (5.2) gives

$$1 - W\left[s_0 F(0) + s^2 \int_0^\infty F(t)^2 \, dt\right] = 0 \tag{5.5}$$

or

$$s_0 \simeq \frac{1}{WF(0)} \left\{1 - \frac{1}{W} \int_0^\infty \left[\frac{F(t)}{F(0)}\right]^2 dt\right\} \tag{5.6}$$

to second order in 1/W. Therefore for $s \sim s_0$ we have

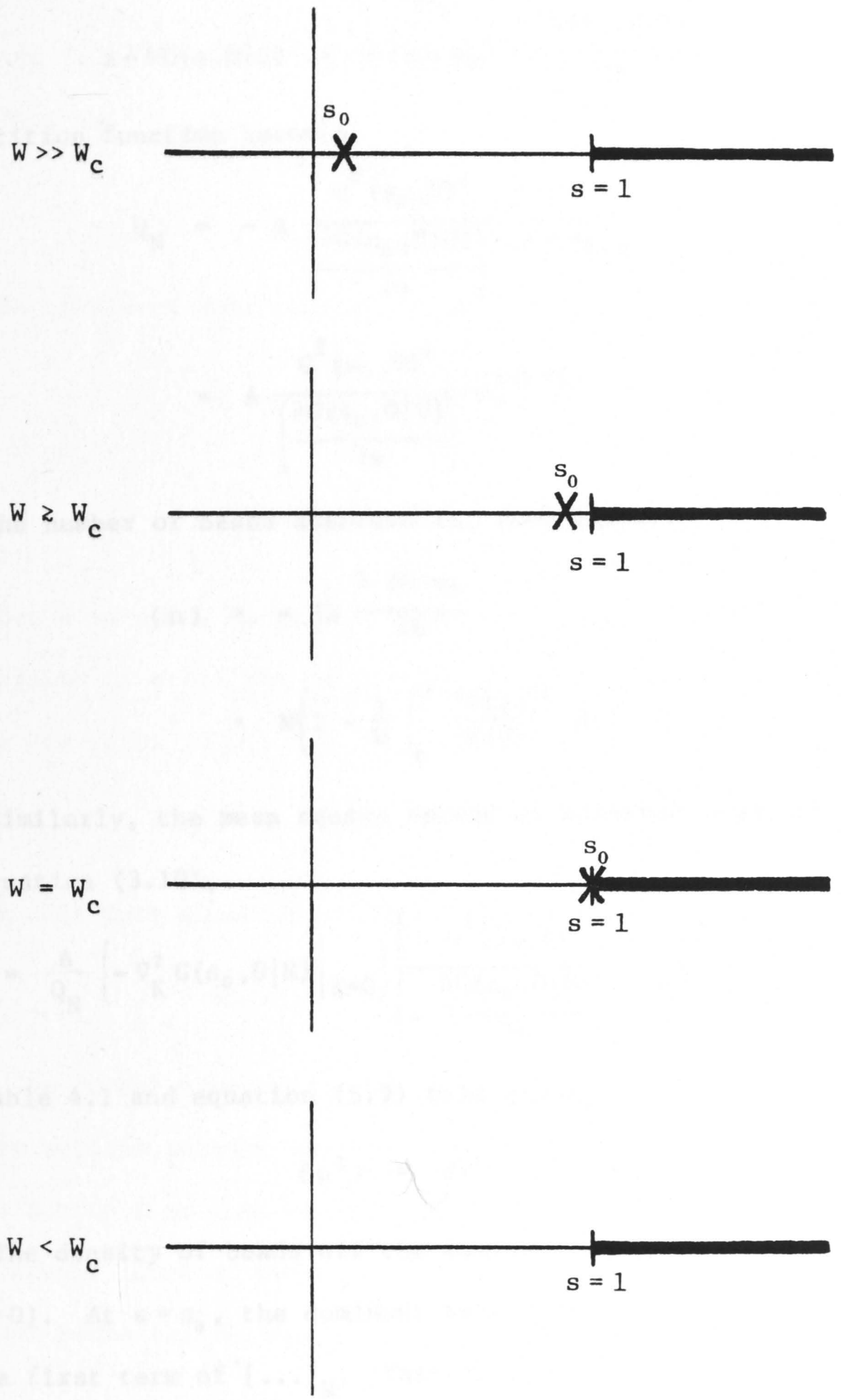

Figure 5.1: The positions of the singularities of the generating function for the partition function that are nearest the origin of the s-plane in the various regimes of W.

$$1 - WG(s,0|0) \simeq -(s - s_0)\, W \frac{\partial G(s_0,0|0)}{\partial s} \tag{5.7}$$

and the partition function becomes

$$Q_N = -A \frac{G^f(s_0,0)^2}{\left(\frac{\partial G(s_0,0|0)}{\partial s}\right)} \left[\frac{1}{s - s_0}\right]_N \tag{5.8}$$

$$= A \frac{G^f(s_0,0)^2}{\left(\frac{\partial G(s_0,0|0)}{\partial s}\right)} s_0^{-(N+1)} . \tag{5.9}$$

The number of beads adsorbed is, from equation (3.3)

$$\langle n \rangle \simeq -NW \frac{\partial \ln s_0}{\partial W} \tag{5.10}$$

$$\simeq N\left\{1 - \frac{1}{W}\int_0^\infty \left(\frac{F(t)}{F(0)}\right)^2 dt\right\} . \tag{5.11}$$

Similarly, the mean square spread of adsorbed beads on the wall is, from equation (3.10),

$$\langle \rho^2 \rangle = \frac{A}{Q_N}\left(-\nabla_K^2 G(s_0,0|K)\Big|_{K=0}\right)\left(\frac{G^f(s_0,0)}{-\frac{\partial G(s_0,0|0)}{\partial s}}\right)^2 \left[\frac{1}{(s - s_0)^2}\right]_N \tag{5.12}$$

and from Table 4.1 and equation (5.9) this gives

$$\langle \rho^2 \rangle = N\lambda^2 . \tag{5.13}$$

The density of beads off the wall is obtained from equations (3.29) ($\phi = 0$). At $s = s_0$, the dominant term comes from the second order pole in the first term of $[\ldots]_N$. Therefore

$$n(x) \doteq \frac{A}{Q_N}\left\{\frac{G^f(s_0,0)\; G(s_0,x|0)}{-\frac{\partial G(s_0,0|0)}{\partial s}}\right\}^2 \left[\frac{1}{(s - s_0)^2}\right]_N \tag{5.14}$$

$$= \frac{N}{s_0} \frac{G(s_0,x|0)^2}{\left(\frac{\partial G(s_0,0|0)}{\partial s}\right)}$$

$$\simeq \frac{N}{W}\left(\frac{F(x)}{F(0)}\right)^2 \tag{5.15}$$

to first order in 1/W. Note that to this order in 1/W, equation (3.2) is satisfied, that is,

$$N = \int_0^\infty n(x)\, dx + \langle n \rangle .$$

The centre-of-mass of the polymer, given by equation (3.1), is

$$\bar{x} = \frac{1}{W} \int_0^\infty x \left(\frac{F(x)}{F(0)} \right)^2 dx . \qquad (5.16)$$

5b. $W \gtrsim W_c$

When W is close to but still greater than $W_c = 1/G(1,0)$ the dominant singular is still the pole at $s = s_0$; but now $s_0 \lesssim 1$. From Table 4.1 we can write ($s \lesssim 1$)

$$G(s,0\ 0) \simeq \frac{1}{W_c} - 2^{\frac{1}{2}}(1-s)^{\frac{1}{2}}/\sigma . \qquad (5.17)$$

Substituting this into equation (5.2), we can solve for s_0

$$s_0 \simeq 1 - \frac{\sigma^2}{2} \left(\frac{1}{W_c} - \frac{1}{W} \right)^2 \qquad (5.18)$$

for $W \gtrsim W_c$. The formal expressions derived for the case $W >> W_c$ still holds for the various polymer characteristics $\langle n \rangle$, $\langle \rho^2 \rangle$, etc. provided s_0 is not too close to 1 so that contributions from the branch point is still unimportant. However we must bear in mind that generating functions from Table 4.1 for the limit $s \lesssim 1$ and equation (5.17) should now be used.

The number of adsorbed beads is now

$$\langle n \rangle = - NW \frac{\partial \ln s_0}{\partial W} \qquad (5.10)$$

$$= \frac{N\sigma^2}{W} \left(\frac{1}{W_c} - \frac{1}{W} \right) \qquad (5.19)$$

and the spread of these beads on the wall is

$$\langle \rho^2 \rangle = \frac{N(-\nabla_K^2 G(s_0,0|K)\big|_{K=0})}{s_0\left(\frac{\partial G(s_0,0|0)}{\partial s}\right)} \tag{5.12}$$

$$= 2N\sigma^2 \ . \tag{5.20}$$

The density of beads off the wall is as before

$$n(x) \simeq \frac{N}{s_0}\frac{\partial G(s_0,x|0)^2}{\left(\frac{\partial G(s_0,0|0)}{\partial s}\right)} \tag{5.14}$$

Since we know $G(s_0,x|0)$ only for $x=0$ and x large we derive, using Table 4.1

$$n(0) = \frac{N\sigma^2}{W_c^2}\left(\frac{1}{W_c} - \frac{1}{W}\right) \tag{5.21}$$

and

$$n(x) = 2N\left(\frac{1}{W_c} - \frac{1}{W}\right) e^{-2x\left(\frac{1}{W_c} - \frac{1}{W}\right)} \tag{5.22}$$

for x large. Using the expression for $n(x)$ for large x (equation (5.22)) we obtain

$$\int_0^\infty n(x)\,dx = N \ .$$

This is consistent with the result (5.19) which shows that although $\langle n \rangle$ is of the order N, it vanishes as W approaches W_c. That is, to leading order in $\left(\frac{1}{W_c} - \frac{1}{W}\right)$ the results satisfy the relation

$$\int_0^\infty n(x)\,dx + \langle n \rangle = N \ .$$

The centre-of-mass of this density distribution is

$$\bar{x} = \frac{1}{2\left(\frac{1}{W_c} - \frac{1}{W}\right)} \tag{5.23}$$

which tends to infinity as W tends to W_c from above.

5c. $W = W_c$

At $W = W_c$ the pole s_0 is coincident with the branch point at $s = 1 = s_0$. The analytic structure of $Q(s)$ in equation (5.1) needs to be investigated. From Table 4.1 we have ($s \lesssim 1$)

$$1 - W_c\, G(s,0|0) = \frac{2^{\frac{1}{2}} W_c}{\sigma} (1-s)^{\frac{1}{2}} \tag{5.24}$$

and

$$G^f(s,0) = (1-s)^{-\frac{1}{2}} . \tag{5.25}$$

Thus the partition is given by

$$Q_N = \frac{A\sigma}{2^{\frac{1}{2}}} \left[\frac{1}{(1-s)^{3/2}}\right]_N . \tag{5.26}$$

From the identity[36]

$$(1-s)^{-M} = \sum_{N=0}^{\infty} \frac{\Gamma(M+N)}{N!\ \Gamma(M)} s^N , \tag{5.27}$$

where $\Gamma(x)$ is the gamma function, for N large and $M \ll N$ we deduce that

$$\left[(1-s)^{-M}\right]_N \simeq \frac{N^{M-1}}{\Gamma(M)} . \tag{5.28}$$

Therefore we have $\left(\Gamma(3/2) = \tfrac{1}{2}\sqrt{\pi}\right)$

$$Q_N = \frac{\sqrt{2}\ A\sigma N^{\frac{1}{2}}}{\pi^{\frac{1}{2}}} . \tag{5.29}$$

which is independent of W at $W = W_c$.

To evaluate the expectation value $\langle n \rangle$, we must differentiate the more general expression for Q_N given by equation (5.1). From equation (3.3) we have

$$\langle n \rangle = \frac{WA}{Q_N} \left[\frac{WG^f(s,0)^2\ G(s,0|0)}{(1 - WG(s,0|0))^2} + \frac{G^f(s,0)^2}{1 - WG(s,0|0)}\right]_N . \tag{5.30}$$

At $W = W_c$ the contribution from the second term to the coefficient of s^N can be neglected to leading order in N. Therefore from equations (5.24), (5.25) and (5.29) we have

$$\langle n \rangle = \frac{(2\pi)^{\frac{1}{2}}\sigma}{4 W_c N^{\frac{1}{2}}} \left[\frac{1}{(1-s)^2}\right]_N \tag{5.3}$$

$$= \frac{(2\pi)^{\frac{1}{2}}\sigma}{4 W_c} N^{\frac{1}{2}} . \tag{5.32}$$

Similarly, the spread of adsorbed beads on the wall can be obtained from Table 4.1 and equations (3.10), (5.24) and (5.29)

$$\langle \rho^2 \rangle = \frac{\sqrt{\pi}\ \sigma^2}{2N^{\frac{1}{2}}} \left[(1-s)^{-5/2}\right]_N \tag{5.33}$$

$$= \frac{2\sigma^2}{3} N . \tag{5.34}$$

The density of beads off from equation (3.29) is ($\phi = 0$)

$$n(x) = \frac{A}{Q_N}\left[\left(\frac{WG^f(s,0)\ G(s,x|0)}{1 - WG(s,0|0)}\right)^2 + \frac{2WG^f(s,0)\ G^f(s,x)\ G(s,x|0)}{1 - WG(s,x|0)}\right]_N . \tag{5.35}$$

For $W = W_c$ and x non-zero, both terms contribute. From the results of Table 4.1, we have

$$n(x) = \frac{(2\pi)^{\frac{1}{2}}}{2\sigma N^{\frac{1}{2}}} \left[\frac{2\ e^{-2^{\frac{1}{2}}(1-s)^{\frac{1}{2}}x/\sigma} - e^{-2^{3/2}(1-s)^{\frac{1}{2}}x/\sigma}}{(1-s)^2}\right]_N . \tag{5.36}$$

The coefficient of s^N of a function of the form $(1-s)^{-\alpha}\ e^{-y(1-s)^{\frac{1}{2}}}$ is given in Appendix A. In this case, we use the result

$$I_2(y) = \left[\frac{e^{-y(1-s)^{\frac{1}{2}}}}{(1-s)^2}\right]_N$$

$$= 2N\left[(t^2 + \tfrac{1}{2})\ \mathrm{erfc}\ t - \frac{t}{\sqrt{\pi}}\ e^{-t^2}\right] , \tag{A.15}$$

where $t = \frac{1}{2} y N^{-\frac{1}{2}}$. Therefore we have

$$n(x) = \frac{(2\pi)^{\frac{1}{2}} N^{\frac{1}{2}}}{\sigma}\left[(2u^2 + 1)\ \mathrm{erfc}\ u - (4u^2 + \tfrac{1}{2})\ \mathrm{erfc}\ 2u - \frac{2u}{\sqrt{\pi}}\ (e^{-u^2} - e^{-4u^2})\right] , \tag{5.37}$$

where

$$u = \frac{1}{(2N)^{\frac{1}{2}}}\frac{x}{\sigma} . \tag{5.38}$$

As discussed in Appendix A, this result holds for (x/σ) of the order of $N^{\frac{1}{2}}$.

We note that using the result for large x (equation (5.37)) the result

$$\int_0^\infty n(x)\,dx \;=\; N$$

is consistent with the fact that

$$\langle n \rangle \;=\; O(N^{\frac{1}{2}}) \;<<\; N$$

for N large, and the relation

$$\int_0^\infty n(x)\,dx + \langle n \rangle \;=\; N$$

is again satisfied.

For the density at $x = 0$, we find that the first term in equation (5.35) is the dominant term and from Table 4.1

$$n(0) \;\simeq\; \frac{(2\pi)^{\frac{1}{2}}\sigma}{4\,W_c^2\,N^{\frac{1}{2}}}\,[(1-s)^{-2}]_N \qquad (5.39)$$

$$= \frac{(2\pi)^{\frac{1}{2}}}{4W_c^2}\,\sigma N^{\frac{1}{2}}\,. \qquad (5.40)$$

The centre-of-mass of the polymer is

$$\bar{x} \;=\; \int_0^\infty x\,n(x)\,dx \qquad (3.1)$$

$$= \frac{7(2\pi)^{\frac{1}{2}}}{32}\,\sigma N^{\frac{1}{2}}\,. \qquad (5.41)$$

The "reduced" density

$$n(x)/\left((2N\pi)^{\frac{1}{2}}/\sigma\right)$$

is plotted in Figure 5.2.

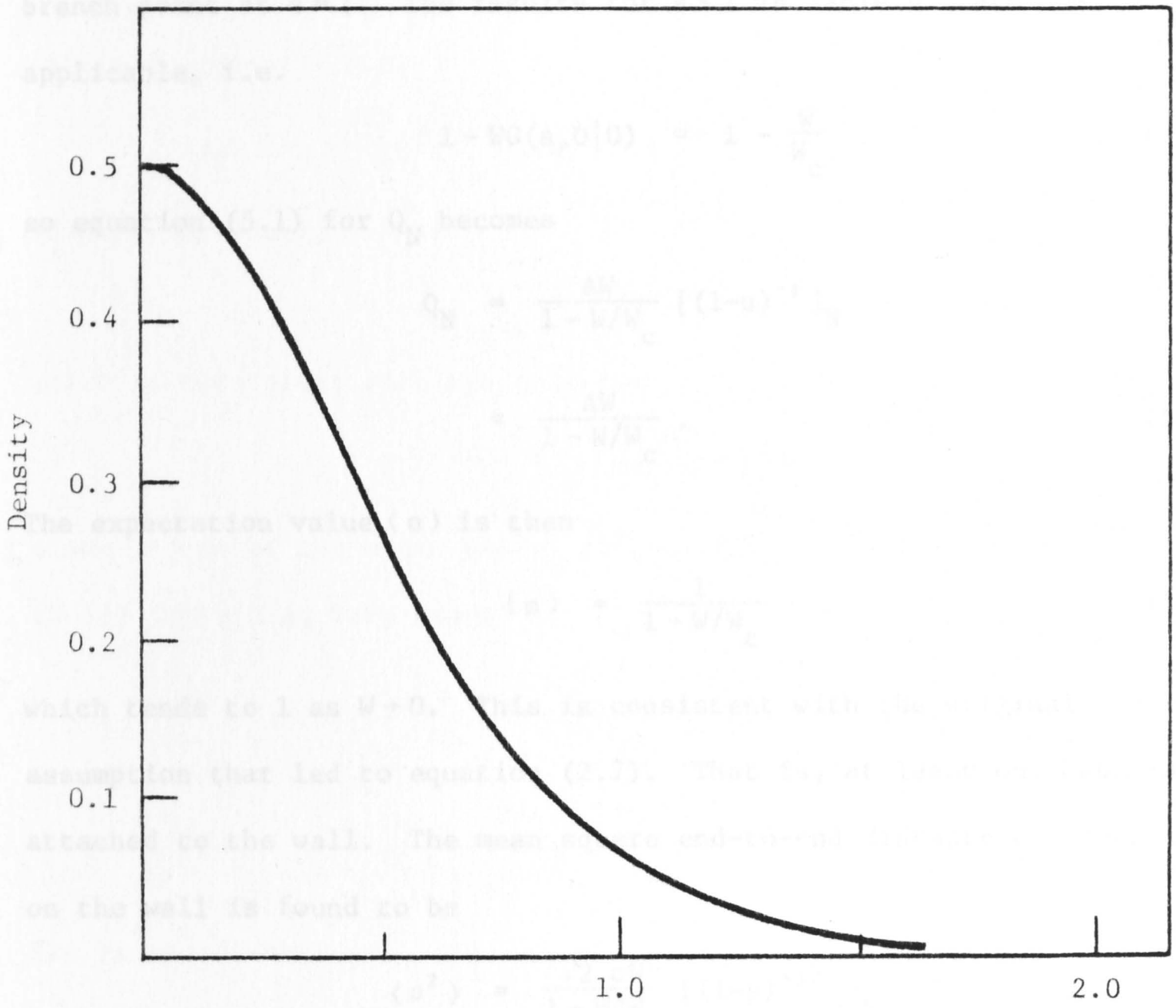

Figure 5.2: The density of beads off the wall at $W = W_c$ as a function of the distance from the wall. The density is in reduced units $n(x)/(\sqrt{2\pi N}/\sigma)$. The distance is scaled to $x/(\sqrt{2}\,\sigma N^{\frac{1}{2}})$.

5d. $W < W_c$

For $W < W_c$, the singularity of Q(s) nearest the origin is the branch point at $s = 1$. The results for $s \lesssim 1$ in Table 4.1 are now applicable, i.e.

$$1 - WG(s,0|0) \simeq 1 - \frac{W}{W_c} \tag{5.42}$$

so equation (5.1) for Q_N becomes

$$Q_N = \frac{AW}{1 - W/W_c} [(1-s)^{-1}]_N$$

$$\simeq \frac{AW}{1 - W/W_c} . \tag{5.51}$$

The expectation value $\langle n \rangle$ is then

$$\langle n \rangle = \frac{1}{1 - W/W_c} \tag{5.52}$$

which tends to 1 as $W \to 0$. This is consistent with the original assumption that led to equation (2.7). That is, at least one bead is attached to the wall. The mean square end-to-end distance of contacts on the wall is found to be

$$\langle \rho^2 \rangle = \frac{\sqrt{2}\ \sigma W}{1 - W/W_c} [(1-s)^{-3/2}]_N$$

$$\simeq \frac{2^{3/2}\ \sigma N^{\frac{1}{2}}}{\sqrt{\pi}} \frac{W}{1 - W/W_c} . \tag{5.53}$$

Since $\langle n \rangle \to 0$ as $W \to 0$, $\langle \rho^2 \rangle$ also vanishes in this limit as expected.

When the branch point ($s = 1$) is the dominant singularity the first term in the general expression for the bead density n(x), equation (5.35), may be neglected. This leads to

$$n(x) = \frac{2^{3/2}}{\sigma} \left[\frac{e^{-2^{\frac{1}{2}}(1-s)^{\frac{1}{2}}x/\sigma} (1 - e^{-2^{\frac{1}{2}}(1-s)^{\frac{1}{2}}x/\sigma})}{(1-s)^{3/2}} \right]_N . \tag{5.54}$$

Using the result from Appendix A ($t = \frac{1}{2} y N^{-\frac{1}{2}}$)

$$I_{3/2}(y) = [e^{-y(1-s)^{\frac{1}{2}}}(1-s)^{-3/2}]_N$$

$$= 2N\left[\frac{1}{\sqrt{\pi}}e^{-t^2} - t\,\mathrm{erfc}\,t\right] \qquad (A.14)$$

we obtain $(u = x/(\sqrt{2N}\,\sigma)$

$$n(x) = \frac{2^{5/2}N^{\frac{1}{2}}}{\sigma}\left[\frac{1}{\sqrt{\pi}}(e^{-u^2} - e^{-4u^2}) - u(\mathrm{erfc}\,u - 2\mathrm{erfc}\,2u)\right] . \qquad (5.55)$$

We note, as usual,

$$\int_0^\infty n(x)\,dx = N$$

which is consistent with the relation

$$\int_0^\infty n(x)\,dx + \langle n\rangle = N$$

since $\langle n\rangle$ is of the order unity. The density at $x = 0$ is from equation (5.35) (retaining both terms)

$$n(0) = \frac{A}{Q_N}\left\{\left(\frac{W/W_c}{1 - W/W_c}\right)^2 + \frac{2(W/W_c)}{1 - W/W_c}\right\}[(1-s)^{-1}]_N$$

$$= \frac{1}{W_c}\left(\frac{2 - W/W_c}{1 - W/W_c}\right). \qquad (5.56)$$

The centre-of-mass is

$$\bar{x} = \frac{2^{5/2}}{\sqrt{\pi}}\sigma N^{\frac{1}{2}} . \qquad (5.57)$$

The reduced density $n(x)/\left((2\pi N)^{\frac{1}{2}}/\sigma\right)$ is plotted in Figure 5.3.

6. DISCUSSION

We have calculated four quantities which characterize the conformation of a long polymer adsorbed at an impenetrable flat surface as a function of the adsorption energy W: the average number of beads adsorbed $\langle n\rangle$; the mean square end-to-end distance of *adsorbed* beads $\langle \rho^2\rangle$; the position of the centre-of-mass of the polymer $\bar{x}$; and the density of beads off the wall n(x). The expressions for these quantities

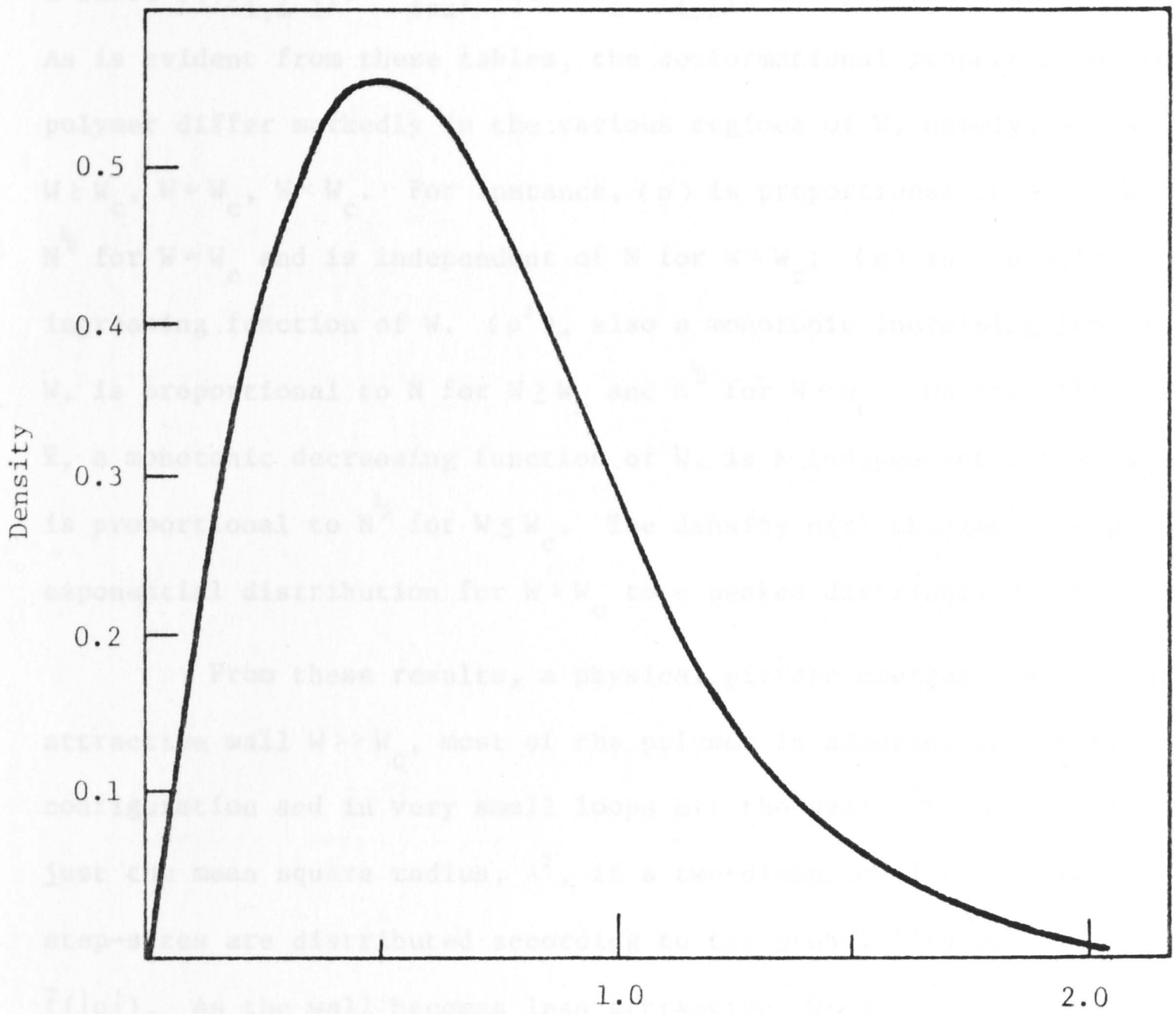

Figure 5.3: The density of beads off the wall in regime $W < W_c$ as a function of the distance from the wall. The density is in reduced units $n(x)/\left(\sqrt{2\pi N}/\sigma\right)$. The distance is scaled to $x/\left(\sqrt{2}\ \sigma N^{1/2}\right)$.

are shown in Table 6.1 for an arbitrary link probability density function $\bar{f}(|\underset{\sim}{r}|)$. The corresponding results for a polymer with a fixed bond length a where $\bar{f}(|\underset{\sim}{r}_{i,i-1}|) = \frac{1}{4\pi a^2}\,\delta(a - |\underset{\sim}{r}_i - \underset{\sim}{r}_{i-1}|)$ are presented in Table 6.2. As is evident from these tables, the conformational properties of the polymer differ markedly in the various regimes of W, namely, $W >> W_c$, $W \gtrsim W_c$, $W = W_c$, $W < W_c$. For instance, $\langle n \rangle$ is proportional to N for $W > W_c$, $N^{\frac{1}{2}}$ for $W = W_c$ and is independent of N for $W < W_c$; $\langle n \rangle$ is a monotonic increasing function of W. $\langle \rho^2 \rangle$, also a monotonic increasing function of W, is proportional to N for $W \geq W_c$ and $N^{\frac{1}{2}}$ for $W < W_c$. On the other hand, $\bar{x}$, a monotonic decreasing function of W, is N independent for $W > W_c$ and is proportional to $N^{\frac{1}{2}}$ for $W \leq W_c$. The density n(x) changes from an exponential distribution for $W > W_c$ to a peaked distribution for $W < W_c$.

From these results, a physical picture emerges. For a very attractive wall $W >> W_c$, most of the polymer is adsorbed in the train configuration and in very small loops off the wall. We note that $\langle \rho^2 \rangle$ is just the mean square radius, λ^2, if a two-dimensional random walk whose step-sizes are distributed according to the probability density function $\bar{f}(|\underset{\sim}{\rho}|)$. As the wall becomes less attractive, $W \to W_c$, the number of contacts with the wall decreases; the centre-of-mass of the polymer moves away from the wall; and the spread of the polymer on the wall tends to that of the two-dimensional projection to that of the unrestricted polymer in free space.

As W passes through W_c, the number of adsorbed beads decreases sharply to become independent of N and the bulk of the polymer moves away from the wall, $\bar{x} \sim \sigma N^{\frac{1}{2}}$. These results are illustrated schematically in Figure 6.1.

The phase transition at $W = W_c$ is due to the classical competition between energy gained on adsorption and the consequent loss

Table 6.1: Expectation values of polymer characteristics in the various regimes of W (see text) for a general link probability density function $\bar{f}(|\underset{\sim}{r}_{i,i-1}|)$.

	$W >> W_c$	$W \gtrsim W_c$	$W = W_c$	$W < W_c$
$\langle n \rangle$	$N\left(1 - \frac{1}{W}\int_0^\infty \left(\frac{F(x)}{F(0)}\right)^2 dx\right)$	$\frac{N\sigma^2}{W}\left(\frac{1}{W_c} - \frac{1}{W}\right)$	$\frac{\sqrt{2\pi}\ \sigma}{4W_c} N^{\frac{1}{2}}$	$\left(1 - \frac{W}{W_c}\right)^{-1}$
$\langle \rho^2 \rangle$	$N\lambda^2$	$2N\sigma^2$	$\frac{2}{3} N\sigma^2$	$\left(\frac{2N}{\pi}\right)^{\frac{1}{2}} \left(\frac{2\sigma W}{1 - \frac{W}{W_c}}\right)$
$\bar{x}$	$\frac{1}{W}\int_0^\infty x\left(\frac{F(x)}{F(0)}\right)^2 dx$	$\frac{1}{2}\left(\frac{1}{W_c} - \frac{1}{W}\right)^{-1}$	$\frac{7\sqrt{2\pi}}{32} N^{\frac{1}{2}}\sigma$	$\left(\frac{2N}{\pi}\right)^{\frac{1}{2}} (4\sigma)$
$n(x)$	$\frac{N}{W}\left(\frac{F(x)}{F(0)}\right)^2$	$\frac{N\sigma^2}{W_c^2}\left(\frac{1}{W_c} - \frac{1}{W}\right)$ $\cdot$ $(x = 0)$ $2N\left(\frac{1}{W_c} - \frac{1}{W}\right) e^{-2x\left(\frac{1}{W_c} - \frac{1}{W}\right)}$ $(x >> 0)$	$\frac{\sqrt{2\pi}}{4W_c^2} N^{\frac{1}{2}}\sigma$ $(x = 0)$ $\frac{(2\pi N)^{\frac{1}{2}}}{\sigma}\left\{(2t^2 + 1)\ \mathrm{erfc}\ t - (4t^2 + \frac{1}{2})\ \mathrm{erfc}\ 2t - \frac{2t}{\sqrt{\pi}}(e^{-t^2} - e^{-4t^2})\right\}$ $(x >> 0)$ $t = x/(\sigma\sqrt{2N})$	$\frac{1}{W_c}\left(\frac{2 - \frac{W}{W_c}}{1 - \frac{W}{W_c}}\right)$ $(x = 0)$ $\frac{4(2N)^{\frac{1}{2}}}{\sigma}\left\{\frac{1}{\sqrt{\pi}}(e^{-t^2} - e^{-4t^2}) - t(\mathrm{erfc}\ t - 2\mathrm{erfc}\ 2t)\right\}$ $(x >> 0)$ $t = x/(\sigma\sqrt{2N})$

$$G(1,0|0) = \frac{1}{W_c} = -\frac{1}{2\pi}\int_{-\infty}^{\infty} ln(1 - f(z))\, dz$$

Table 6.2: Expectation values of polymer characteristics in various regimes of W (see text) for the fixed-length bond law $\bar{f}(|\underset{\sim}{r}_{i,i-1}|) = \frac{1}{4\pi a^2}\,\delta(a - |\underset{\sim}{r}_i - \underset{\sim}{r}_{i-1}|)$.

	$W >> W_c$	$W \gtrsim W_c$	$W = W_c$	$W < W_c$
$\langle n \rangle$	$N\left(1 - \frac{a}{W}\right)$	$\frac{Na^2}{3W}\left(\frac{1}{W_c} - \frac{1}{W}\right)$	$\left(\frac{2\pi}{3}\right)^{1/2} \frac{a}{4W_c} N^{1/2}$	$\left(1 - \frac{W}{W_c}\right)^{-1}$
$\langle \rho^2 \rangle$	Na^2	$\frac{2}{3} Na^2$	$\frac{2}{9} Na^2$	$\left(\frac{2N}{3\pi}\right)^{1/2} \left(\frac{2aW}{1 - \frac{W}{W_c}}\right)$
$\bar{x}$	$\frac{a^2}{2W}$	$\frac{1}{2}\left(\frac{1}{W_c} - \frac{1}{W}\right)^{-1}$	$\left(\frac{2\pi}{3}\right)^{1/2} \frac{7a}{32} N^{1/2}$	$\left(\frac{2N}{3\pi}\right)^{1/2}$ (4a)
$n(x)$	$\frac{N}{W}\,\theta(a - x)$	$\frac{3Na^2}{W_c^2}\left(\frac{1}{W_c} - \frac{1}{W}\right)$ $(x = 0)$ $2N\left(\frac{1}{W_c} - \frac{1}{W}\right) e^{-2x\left(\frac{1}{W_c} - \frac{1}{W}\right)}$ $(x >> 0)$	$\left(\frac{2\pi}{3}\right)^{1/2} \frac{\sigma}{4W_c^2} N^{1/2}$ $(x = 0)$ $\frac{(6\pi N)^{1/2}}{a}\Big[(2t^2 + 1)\,\mathrm{erfc}\,t - (4t^2 + \frac{1}{2})\,\mathrm{erfc}\,2t - \frac{2t}{\sqrt{\pi}}(e^{-t^2} - e^{-4t^2})\Big]$ $(x >> 0)$	$\frac{1}{W_c}\left(\frac{2 - \frac{W}{W_c}}{1 - \frac{W}{W_c}}\right)$ $(x = 0)$ $(6N)^{1/2} \frac{4}{a}\left[\frac{1}{\sqrt{\pi}}(e^{-t^2} - e^{-4t^2}) - t(\mathrm{erfc}\,t - 2\mathrm{erfc}\,2t)\right\}$ $(x >> 0)$
		$t = \sqrt{3}\,x/(a\sqrt{2N})$	$t = \sqrt{3}\,x/(a\sqrt{2N})$	$t = \sqrt{3}\,x/(a\sqrt{2N})$

$$\bar{f}(|\underset{\sim}{r}_{i,i-1}|) = \frac{1}{4\pi a^2}\,\delta(a - |\underset{\sim}{r}_i - \underset{\sim}{r}_{i-1}|)\,; \qquad W_c = 0.62439a\,; \qquad \sigma^2 = a^2/3$$

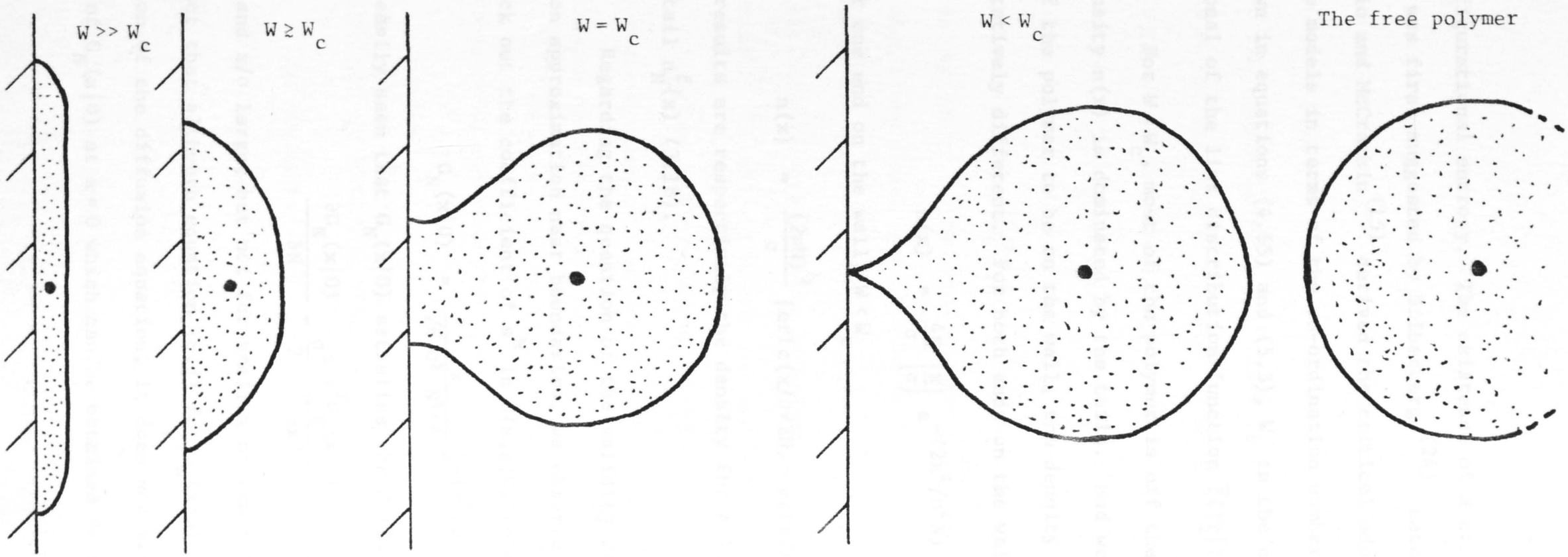

Figure 6.1: Schematic representation of the state of the adsorbed polymer as a function of W.

of configurational entropy. The existence of a critical adsorption energy was first suggested by Silberberg.[24] Later Rubin[16,17] and DiMarzio and McCrackin[15] derived the critical adsorption energy for lattice models in terms of the co-ordination number of the lattice type. As shown in equations (4.65) and (5.3), W_c in the continuum model is a functional of the link distribution function $\bar{f}(|\underset{\sim}{r}|)$.

For $W < W_c$, most of the polymer is off the wall. As expected, the density n(x) is dominated by the tails. Had we required one or both ends of the polymer to be on the wall, the density distribution would be quantitatively different. For both ends on the wall and $W < W_c$

$$n(x) = \frac{4\pi}{\sigma}\left(\frac{x}{\sigma}\right) e^{-(2x^2/\sigma^2 N)} \tag{6.1}$$

and for one end on the wall, $W < W_c$

$$n(x) = \frac{(2\pi N)^{\frac{1}{2}}}{\sigma}\left[\operatorname{erfc}(x/\sigma\sqrt{2N}) - \operatorname{erfc}(\sqrt{2}\ x/\sigma\sqrt{N})\right] . \tag{6.2}$$

These results are respectively the density for a loop $n_N^{\ell}(x)$ (3.22) and for a tail $n_N^{f}(x)$ (3.18).

Regarding the question of the validity of the diffusion equation approximation near boundaries, we observe that for N large, we may pick out the coefficient of s^N in $G(s,x|0)$ to obtain (x large)

$$G_N(x|0) = \frac{x}{\sqrt{\pi}\ \sigma^2\ N^{3/2}} e^{-(x^2/2N\sigma^2)} . \tag{6.3}$$

It is easily seen that $G_N(x|0)$ satisfies the diffusion equation

$$\frac{\partial G_N(x|0)}{\partial N} - \frac{\sigma^2}{2}\frac{\partial^2 G_N(x|0)}{\partial x^2} = 0 \tag{6.4}$$

for N and x/σ large, but *not* for small x or small N. This follows from the fact that although equation (6.3) for $G_N(x|0)$ *is* is the appropriate solution of the diffusion equation, it does *not* agree with the exact value of $G_N(x|0)$ at $x = 0$ which can be obtained from G(s,0) (Table 4.1).

To completely determine $G_N(x|0)$ from (6.4) one would need initial or boundary conditions. However, we cannot use initial conditions at $x = 0$ and $N = 0$ even if they are known because the diffusion equation breaks down in these regions.

We have considered the conformation of an adsorbed polymer which does not interact with itself. The next logical step is to examine the effect of intramolecular interactions in the various conformational characteristics. Since an *ab initio* calculation would soon become intractable, perhaps a solution may be obtained by perturbing about the non-interacting polymer using a method similar to that developed by Flory[37] for studying the excluded volume effect. Dispersion force theory can then be used to estimate the magnitude of the excluded volume parameter and its influence on the phase transition. There are already some attempts at this problem using computer simulation[38,39] and correlated lattice walk models.[17,19]

Another important extension of ideas developed here is to consider the problem of a polymer confined between two adsorbing surfaces. Some aspects of this problem have already been considered by a number of authors,[40-42] especially with reference to the influence of polymers on the stability of colloidal systems.[7,43-45]

7. NUMERICAL VALUES OF W FOR SOME SYSTEMS OF POLYMER/SOLVENT/SUBSTRATE

Before making numerical estimates of the adsorption energy parameter W, it is worthwhile to recall the assumptions made in deriving W. We have assumed that the potential energy of the whole polymer is just the sum of one-body potentials for the beads (monomers). Each bead interacts independently with the substrate via a one-dimensional

potential $\psi(x)$. The adsorption energy parameter W is defined as

$$W = \int_0^\infty (e^{-\psi(x)/kT} - 1)\, dx \,. \tag{2.3}$$

For situations where dispersion interactions are dominant one can calculate the value of $\psi(x)$. The dispersion interaction energy between a molecule of frequency dependent polarizability $\alpha_M(\omega)$ in a solvent and a half-space is (equation (B.9), Appendix B)

$$V(d) = -kT \sum_{n=0}^{\infty}{}' \sum_{P=1}^{\infty} \left(\frac{2^P + 2}{P}\right) \left[\frac{\alpha_M(i\xi_n)\ \Delta_{ws}(i\xi_n)}{8\varepsilon_s(i\xi_n)d^3}\right]^P \,. \tag{7.1}$$

Here

$$\Delta_{ws}(i\xi_n) = \frac{\varepsilon_w(i\xi_n) - \varepsilon_s(i\xi_n)}{\varepsilon_w(i\xi_n) + \varepsilon_s(i\xi_n)} \tag{7.2}$$

and, ε_w and ε_s are respectively the frequency dependent relative permittivity or dielectric constant of the substrate (wall) and the solvent evaluated at imaginary frequencies $i\xi_n \equiv i2\pi nkT/\hbar$ with $(2\pi\hbar)$ the Planck's constant. The prime on the n-sum denotes half-weight for the $n = 0$ term.

For the purpose of calculating W for organic polymers in organic solvents, the first term in α_M $(P = 1)$ of equation (7.1) is an adequate representation for V(d). The reasoning for this is as follows. Along the imaginary frequency axis, the dielectric constant decreases monotonically from its static value to unity.[46] Therefore we have the relation $|\Delta_{ws}| < 1$. However with non-polar organic materials, $\varepsilon \sim 2\text{-}3$ and a more realistic limit is $|\Delta_{ws}| \leq 0.2$. Further since the static polarizability $\alpha_M(0)$ is of the order of the volume of the molecule (bead), the first term $(P = 1)$ will indeed be a good approximation for V(d) provided d is larger than the molecular size.

On the other hand, the dispersion energy given in equation (7.1) treats the monomer as a polarizable dipole. At small distances, this approximation is inaccurate as higher multi-pole interactions and electron overlap effects become important. Since the substrate is, by assumption, impenetrable, we shall account for the short range interactions by assuming that there is some distance of closest approach to the wall b (> 0) for the monomers, and that the dipole approximation is valid for $d \geq b$. Typically this cut-off distance is of the order of $\alpha_m(0)^{1/3}$.

In view of the above comments, it is clear that the phase space of the monomer $x \geq 0$ corresponds to the region $d \geq b$. Therefore, the interaction energy $\psi(x)$ of the monomer can be taken to be the dispersion energy $V(x+b)$. Thus W becomes

$$W = \int_b^\infty \exp[(A/kTx^3) - 1]\, dx \,, \tag{7.3}$$

where

$$A = kT \sum_{n=0}^{\infty}{}' \frac{\alpha_m(i\xi_n)\, \Delta_{ws}(i\xi_n)}{2\varepsilon_s(i\xi_n)} \,. \tag{7.4}$$

The integral can be taken to give

$$W = b \sum_{j=1}^{\infty} \frac{1}{j!(3j-1)} \left(\frac{A}{kTb^3}\right)^j \,. \tag{7.5}$$

Therefore the calculation of W requires a knowledge of the dielectric constants at imaginary frequencies. It has been found in work connected with the calculation of dispersion forces between macroscopic bodies[47] that the representation

$$\varepsilon(i\xi) = 1 + \frac{R^2 - 1}{1 + (\xi/\omega_0)^2} \tag{7.6}$$

is adequate for non-polar organic materials. Here R is taken to be the refractive index. In principle, ω_0 should be the Lorentzian relaxation frequency in the ultra-violet for the *bulk* medium. However in the

absence of detailed spectroscopic data, this is approximated by the first ionization potential. The polarizability of the monomer is estimated from the dielectric constants of the polymer ε_p using the Claussius-Mossotti relation

$$\alpha_M(i\xi) = \frac{3}{4\pi\rho}\left(\frac{\varepsilon_p(i\xi) - 1}{\varepsilon_p(i\xi) + 2}\right), \qquad (7.7)$$

where ρ is the number density of monomer units.

Using the dielectric and spectroscopic data listed in Appendix C we calculate the quantity (W/W_c) for a number of polymer/solvent pairs against a glass substrate at 300 °K; we use $W_c = 0.62439a$ as tabulated in Table 6.2. We have assumed that the relative permittivity of glass has the simple representation given by equation (7.6). Clearly there is some laxitude in the choice of the bond length a and the cut-off distance b. Following earlier work on the dispersion contribution to surface energies of organic liquids,[49] we choose b ~ 2 Å. The value a is estimated from the linear dimensions of the monomer units.[51] For polystyrene, we take a to be 4 Å and for polyisobutene, a = 3 Å (see Appendix C).

Table 7.1: Values of W/W_c for various polymer/solvent pairs against a glass substrate at 300 °K.

Solvent \ Polymer	Polystyrene	Polyisobutene
Cyclohexane	1.49	1.06
Methyl cyclohexane	1.58	1.12
Decalin	0.63	0.50
Benzene	0.42	0.35
Toluene	0.04	0.04
Ethyl benzene	0.19	0.17
Diphenyl ether	0.04	0.04

With reference to the results in Table 7.1, the consistently higher values of W/W_c for polystyrene is attributed to the larger polarizability of the phenyl group of the styrene monomer unit. We note also that for a given polymer and substrate, W/W_c decreases (thus favouring the desorbed state) as the refractive index of the solvent increases (cf. Table C1, Appendix C). This is because it is energetically more favourable for a molecule to be in a region of higher dielectric permittivity.

Calculations for a metal substrate yield values of $W/W_c \sim 10^3$. Here we used the representation

$$\varepsilon(i\xi) = 1 + \omega_p^2/\xi^2 \qquad (7.8)$$

for the permittivity of a metal. The plasma frequency ω_p is typically of the order of 2×10^{16} rad/sec.[48] The corresponding large values of W/W_c obtained for a metal substrate is due, of course, to the very large dielectric constant at low frequencies. Although we have neglected spatially dispersive effects which are important for metallic substrates at short distances, none the less the large values of W/W_c obtained should be a general characteristic for metallic walls.

On the other hand, for a teflon substrate the values of W/W_c are negative for all polymer solvent pairs, thus strongly favouring the desorbed state. This can be accounted for by the unusually low value of the refractive index of teflon as compared with those of the solvents.

The uncertainties in a,b and in the ultra-violet relaxation frequencies ω_0 mean that the values of W/W_c in Table 7.1 must be treated as approximate only. However dispersion theory does predict values of W/W_c for a glass substrate that are distributed about unity where the phase transition occurs. This suggests that it might be possible to

induce adsorption-desorption phase transitions by varying external conditions.

7a. Temperature Induced Phase Transitions

In Table 7.2 we list W/W_c as a function of temperature for polyisobutene in cyclohexane and in methyl cyclohexane against a glass substrate. We see that reasonable changes in temperature can bring W/W_c through unity. The temperature dependence of W is due mainly to the 1/T term in the Boltzmann factor in equation (7.3). Temperature variations in the dielectric properties of the polymer, solvent or substrate and the temperature dependence in the frequency summation (equation (7.4)) are all second order effects. To see this, we replace the sum in equation (7.4) by an integral

$$kT \sum_{n=0}^{\infty}{}' \rightarrow \frac{\hbar}{2\pi} \int_0^{\infty} d\xi$$

and the constant A becomes temperature "independent". This procedure is justified when ω_0 is in the ultra-violet.[50]

Table 7.2: Values of W/W_c as a function of temperature for polyisobutene in cyclohexane and in methyl cyclohexane against a glass substrate.

Temperature °K	Cyclohexane	Methyl Cyclohexane
280	1.21	1.28
300	1.10	1.17
320	1.01	1.06
340	0.93	0.98

7b. Mixed Solvent Effects

From Table 7.1 we see that for polystyrene in methyl cyclohexane $W/W_c = 1.58$, while in decalin $W/W_c = 0.63$. This immediately suggests that by changing the composition of an appropriate mixed solvent we can take the polymer/solvent/substrate system through the adsorption-desorption transition point at $W/W_c = 1$. In Figure 7.1 W/W_c is given as a function of the volume fraction v of that component of the mixed solvent which favours adsorption, for three systems. We assume, as a first approximation, that the excess volume of mixing is negligible and that the Claussius-Mossotti relation holds. Under these approximations, the dielectric constant of the mixed solvent ε_{ms} is then

$$\left(\frac{\varepsilon_{ms} - 1}{\varepsilon_{ms} + 2}\right) = \left(\frac{\varepsilon_1 - 1}{\varepsilon_1 + 2}\right) v + \left(\frac{\varepsilon_2 - 1}{\varepsilon_2 + 2}\right) (1-v) \ , \qquad (7.9)$$

where v is the volume fraction of solvent component 1, and ε_1 and ε_2 are the permittivities of the two pure components. The existence of a critical volume fraction v_c $(W = W_c)$ indicates that solvent induced adsorption-desorption phase transitions should be experimentally observable.

In the above calculations, we have used the "fixed-bond" probability density function $\bar{f}(|\underset{\sim}{r}_{i,i-1}|) = \frac{1}{4\pi a^2} \delta(a - |\underset{\sim}{r}_{i,i-1}|)$ which gives $W_c = 0.62439a$ (Table 6.2). Clearly had we used another probability density function, the values of the phase transition temperature and critical volume fraction which give $W/W_c = 1$ would be different. However, as mentioned earlier the values of W/W_c are only approximate, therefore our particular choice of value for W_c should not invalidate the main conclusions regarding temperature and mixed solvent induced phase transitions.

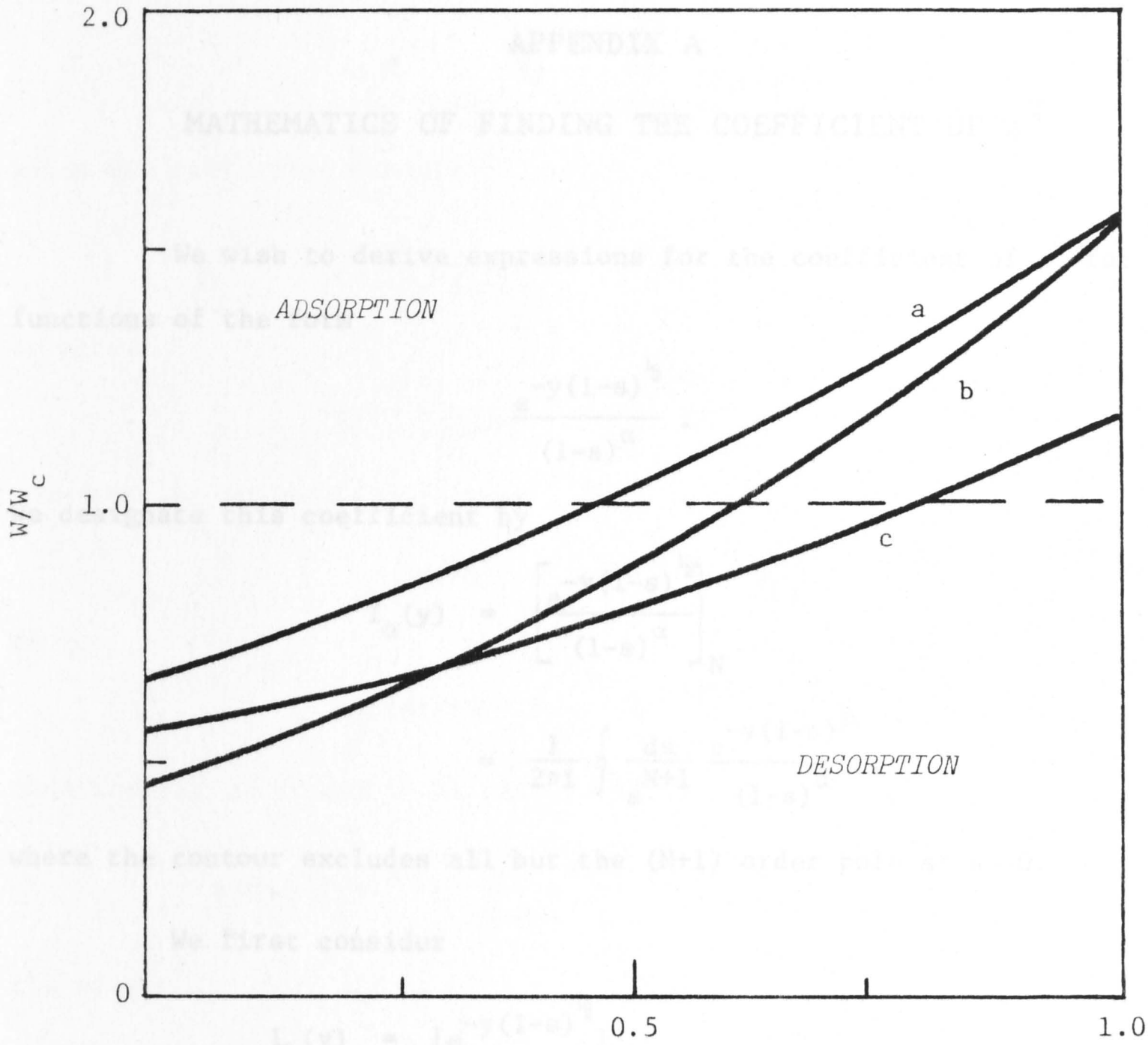

Figure 7.1: W/W_c as a function of the volume fraction v of methyl cyclohexane for the following mixed solvent systems:

(a) Polystyrene in methyl cyclohexane + decalin;

(b) Polystyrene in methyl cyclohexane + benzene;

(c) Polyisobutene in mehtyl cyclyhexane + decalin

against a glass substrate at 300 °K.

APPENDIX A

MATHEMATICS OF FINDING THE COEFFICIENT OF s^N

We wish to derive expressions for the coefficient of s^N for functions of the form

$$\frac{e^{-y(1-s)^{\frac{1}{2}}}}{(1-s)^{\alpha}} .$$

We designate this coefficient by

$$I_{\alpha}(y) = \left[\frac{e^{-y(1-s)^{\frac{1}{2}}}}{(1-s)^{\alpha}}\right]_N$$

$$= \frac{1}{2\pi i}\oint \frac{ds}{s^{N+1}} \frac{e^{-y(1-s)^{\frac{1}{2}}}}{(1-s)^{\alpha}} ,$$

where the contour excludes all but the (N+1) order pole at $s = 0$.

We first consider

$$I_0(y) = [e^{-y(1-s)^{\frac{1}{2}}}]_N$$

$$= [\cosh y(1-s)^{\frac{1}{2}}]_N - [\sinh y(1-s)^{\frac{1}{2}}]_N . \qquad (A.1)$$

Since

$$\cosh y(1-s)^{\frac{1}{2}} = \sum_{m=0}^{\infty} \frac{1}{(2m)!} y^{2m}(1-s)^m$$

the terms for which $m < N$ do not contribute to the coefficient of s^N. For y sufficiently small, contributions from the remaining terms ($m \geq N$) will also be negligible and a sufficient condition for this is $y \sim N^{\frac{1}{2}}$. Now we can expand the sinh term as

$$\sinh y(1-s)^{\frac{1}{2}} = \sum_{m=0}^{\infty} \frac{y^{2m+1}}{\Gamma(2m+2)} (1-s)^{m+\frac{1}{2}} \tag{A.2}$$

$$= \sum_{m=0}^{\infty} \frac{y^{2m+1}}{\Gamma(2m+2)} \sum_{N=0}^{\infty} \frac{(-)^N \Gamma(m+3/2)}{\Gamma(N+1)\Gamma(m-N+3/2)} s^N \ . \tag{A.3}$$

Using the reflection formula[36]

$$\frac{1}{\Gamma(1-z)} = \frac{\sin \pi z}{\pi} \Gamma(z)$$

we obtain

$$\frac{1}{\Gamma(1-(N-m-\frac{1}{2}))} = \frac{(-)^{N-m-1}}{\pi} \Gamma(N-m-\tfrac{1}{2}) \tag{A.4}$$

and from the duplication formula[36]

$$\Gamma(z+\tfrac{1}{2}) = \pi^{\frac{1}{2}} 2^{-2z+1} \frac{\Gamma(2z)}{\Gamma(z)}$$

we get

$$\Gamma(m+1+\tfrac{1}{2}) = \pi^{\frac{1}{2}} 2^{-(2m+1)} \frac{\Gamma(2(2m+1)}{\Gamma(m+1)} \ . \tag{A.5}$$

Substituting (A.4) and (A.5) into (A.3) we get

$$-\sinh y(1-s)^{\frac{1}{2}} = \sum_{N=0}^{\infty} s^N \sum_{m=0}^{\infty} \frac{(-)^m (y/2)^{2m+1} \Gamma(N-m-\frac{1}{2})}{\sqrt{\pi}\ \Gamma(N+1)\ \Gamma(m+1)} \ ; \tag{A.6}$$

therefore

$$-[\sinh y(1-s)^{\frac{1}{2}}]_N = \frac{y}{2} \sum_{m=0}^{\infty} \frac{(y^2/4)^m}{\Gamma(m+1)} \frac{\Gamma(N-m-\frac{1}{2})}{\Gamma(N+1)} \ . \tag{A.7}$$

Now for z large[36]

$$\Gamma(z) \simeq e^{-z} z^{z-\frac{1}{2}} (2\pi)^{\frac{1}{2}} \left(1 + O(1/z) + \ldots\right)$$

hence for $N >> 1$

$$\frac{\Gamma(N+\beta)}{\Gamma(N+1)} \simeq N^{\beta-1} \ , \quad N >> \beta \ . \tag{A.8}$$

Therefore, if y is sufficiently small, then

$$-[\sinh y(1-s)^{\frac{1}{2}}]_N \simeq \frac{y}{2\sqrt{\pi}\ N^{3/2}} \sum_{m=0}^{\infty} \frac{(y^2/2N)^m}{\Gamma(m+1)}$$

$$= \frac{y}{2\sqrt{\pi}\ N^{3/2}} e^{-y^2/4N} \ . \tag{A.9}$$

Equation (A.9) holds provided we can replace $\Gamma(N-m-\frac{1}{2})/\Gamma(N+1)$ by $N^{-(m+3/2)}$ for all m. However this replacement is valid only when $m \ll N$. But if when $m \gtrsim N$, the term $(y^2/4)^m/\Gamma(m+1)$ becomes sufficiently small so that the remaining part of the m-series is negligible anyway then the approximation invoked in deriving equation (A.9) will be valid. That is we require

$$\frac{(y^2/4)^m}{\Gamma(m+1)} \lesssim 1 \quad \text{when} \quad m \sim N$$

which implies $y \sim N^{\frac{1}{2}}$. Therefore the contribution from the term $\cosh y(1-s)^{\frac{1}{2}}$ is indeed negligible.

Returning to equation (A.1), we have

$$I_0(y) = \frac{y^2}{2\sqrt{\pi}\, N^{3/2}} e^{-y^2/4N} \tag{A.10}$$

$$I_{\frac{1}{2}}(y) = \int_y^\infty I_0(y')\, dy' \tag{A.11}$$

$$= \frac{1}{\sqrt{\pi}\, N^{\frac{1}{2}}} e^{-y^2/4N} \tag{A.12}$$

and

$$I_1(y) = \int_y^\infty I_{\frac{1}{2}}(y')\, dy'$$

$$= \operatorname{erfc}(y/2N^{\frac{1}{2}}) , \tag{A.13}$$

where erfc(x) is the complementary error function.[36] Integrating again, we have

$$I_{3/2}(y) = \int_y^\infty I_1(y')\, dy'$$

$$= \frac{2N^{\frac{1}{2}}}{\sqrt{\pi}} e^{-y^2/4N} - y \operatorname{erfc}(y/2N^{\frac{1}{2}}) \tag{A.14}$$

and

$$I_2(y) = \int_y^\infty I_{3/2}(y')\, dy'$$

$$= 2N\left[\left(\frac{y^2}{4N} + \tfrac{1}{2}\right) \operatorname{erfc}(y/2N^{\frac{1}{2}}) - \frac{y}{2\sqrt{\pi}\, N^{\frac{1}{2}}} e^{-y^2/4N}\right] . \tag{A.15}$$

APPENDIX B

DISPERSION INTERACTION BETWEEN AN ISOTROPIC POINT DIPOLE AND A FLAT SURFACE

We consider the non-retarded dispersion interaction energy between an isotropic point dipole of polarizability $\alpha(\omega)$, immersed in a solvent of dielectric constant $\varepsilon_s(\omega)$, and a wall of dielectric constant $\varepsilon_w(\omega)$ at a distance d away.

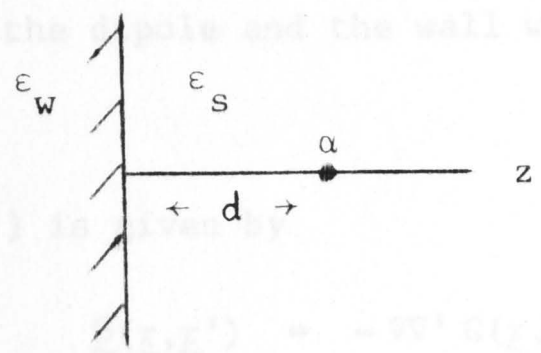

A similar problem has previously been considered,[53-56] by a number of authors. The effect of a finite size dipole has also been studied[57] but the algebra involved in obtaining the next correction term is extremely cumbersome.

We shall adopt the van Kampen normal mode formalism where the interaction energy is given by[58-60]

$$V(d) = kT \sum_{n=0}^{\infty}{}' \log D(i\xi_n;d) , \qquad (B.1)$$

where $D(i\xi_n;d)$ is the secular determinant for allowed modes evaluated at imaginary frequencies $i\xi_n = in(2\pi kT/\hbar)$, where k is the Boltzmann constant, T the absolute temperature and $(2\pi\hbar)$ the Planck's constant. The prime on the summation sign means that the $n = 0$ term must be multiplied by $\frac{1}{2}$. $D(i\xi_n;d)$ is derived as follows.

The dipole moment for the dipole at $\underset{\sim}{r}$ due to an electric field $E(\underset{\sim}{r})$ is

$$\underset{\sim}{p}(\underset{\sim}{r}) = \alpha \underset{\sim}{E}(\underset{\sim}{r}) \tag{B.2}$$

while the field at $\underset{\sim}{r}'$ due to a dipole at $\underset{\sim}{r}$ is

$$\underset{\sim}{E}(\underset{\sim}{r}') = \underset{\approx}{G}(\underset{\sim}{r}',\underset{\sim}{r})\ \underset{\sim}{p}(\underset{\sim}{r}) \ . \tag{B.3}$$

Combining (B.2) and (B.3) we get the secular determinant

$$D(i\xi_n;\underset{\sim}{r}) = \lim_{r\to r'} \left| \underset{\approx}{I} - \underset{\approx}{G}(\underset{\sim}{r}',\underset{\sim}{r}) \right| \ . \tag{B.4}$$

We note that the Green function $\underset{\approx}{G}$ contains a term for the self-interaction of the dipole. Since we are only interested in the interaction between the dipole and the wall we shall not include this term in (B.4).

Now $\underset{\approx}{G}(\underset{\sim}{r},\underset{\sim}{r}')$ is given by

$$\underset{\approx}{G}(\underset{\sim}{r},\underset{\sim}{r}') = -\nabla\nabla' G(\underset{\sim}{r},\underset{\sim}{r}') \ , \tag{B.5}$$

where $G(\underset{\sim}{r},\underset{\sim}{r}')$ is the solution of

$$\nabla^2 G(r,r') = -\frac{4\pi}{\varepsilon_s}\,\delta(r-r') \tag{B.6}$$

subject to the usual boundary conditions, namely, G, $\varepsilon \frac{\partial G}{\partial n}$ continuous across a dielectric discontinuity. The solution of equation (B.6) for this problem is

$$G(\underset{\sim}{r},\underset{\sim}{r}') = -\Delta_{ws}\left[(x-x')^2 + (y-y')^2 + (z+z')^2\right]^{-\frac{1}{2}} + \frac{1}{|\underset{\sim}{r}-\underset{\sim}{r}'|} \ .$$

After some straightforward algebra we obtain (neglecting the self-energy term)

$$\underset{\approx}{G}(\underset{\sim}{r},\underset{\sim}{r}) = \frac{\Delta_{ws}}{8\varepsilon_s d^3} \begin{pmatrix} 1 & 0 & 0 \\ 0 & 1 & 0 \\ 0 & 0 & 2 \end{pmatrix} \ , \quad \underset{\sim}{r} = (0,0,d) \ , \tag{B.7}$$

where $\Delta_{ws} = (\varepsilon_w - \varepsilon_s)/(\varepsilon_w + \varepsilon_s)$. Inserting equation (B.7) into (B.1) and

(B.4) we get

$$V(d) = kT \sum_{n=0}^{\infty}{}' \ln\left\{\left(1 - \frac{\alpha\Delta_{ws}}{8\varepsilon_s d^3}\right)^2 \left(1 - \frac{\alpha\Delta_{ws}}{4\varepsilon_s d^3}\right)\right\} \tag{B.8}$$

$$= - kT \sum_{n=0}^{\infty}{}' \sum_{m=1}^{\infty} \frac{1}{m} (2^m + 2) \left(\frac{\alpha\Delta_{ws}}{8\varepsilon_s d^3}\right)^m \tag{B.9}$$

$$= - kT \sum_{n=0}^{\infty} \left\{\frac{\alpha\Delta_{ws}}{2\varepsilon_s d^3} + \frac{3}{64} \Delta_{ws}^2 \frac{\alpha^2}{d^6} + \ldots\right\} . \tag{B.10}$$

APPENDIX C

DATA FOR CALCULATING THE ABSORPTION ENERGY PARAMETER W

The dielectric and spectroscopic data for the polymer, solvents and substrates are listed below in Table C1. The absorption frequency ω_0 is taken to be the gaseous first ionization potential of molecules of the solvent or monomer units of polymers.

The density of monomer unit ρ (see equation (7.10)) and the bond length a for each polymer is obtained as follows:

Polyisobutene

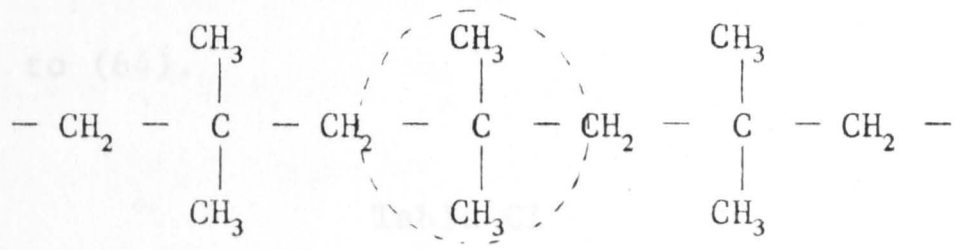

The repeating unit is taken to be C_4H_8 which has molecular weight 56. The C - C bond distance is 1.54 Å and the density of polyisobutene is 0.79 gm/cc. Therefore we taken the "bond" length a to be 3 Å and the density of monomer units to be

$$\rho = (6.023 \times 10^{23}) \times (0.79) \times \left(\frac{1}{56}\right)$$

$$= 8.51 \times 10^{21} \text{ cc}^{-1} .$$

Polystyrene

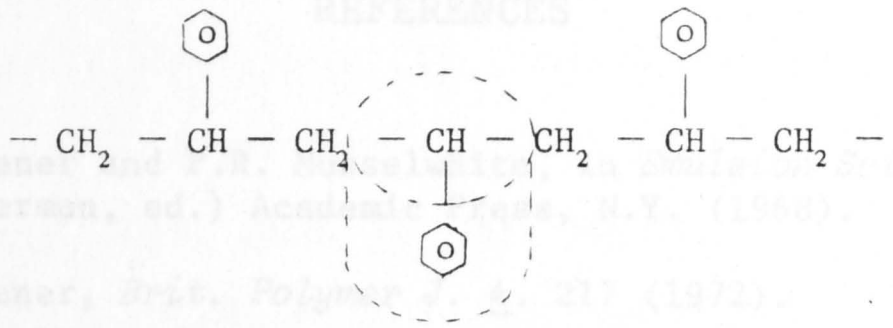

The repeat unit is C_8H_8 of molecular weight 104. It is approximated by a cylinder of diameter 3 Å and length 5 Å. This has the same volume as a sphere of diameter 4 Å. We shall take this as a "bond" length a. The density of polystyrene is 1.07 gm/cc. This means that the density of monomer units is

$$\rho = (6.023 \times 10^{23}) \times (1.07) \times \left(\frac{1}{104}\right)$$

$$= 6.08 \times 10^{21} \text{ cc}^{-1} .$$

The data contained in this Appendix are obtained from references (61) to (64).

Table C1

Material	Refractive Indices	Absorption Frequency in eV
Cyclohexane	1.43	9.80
Methyl Cyclohexane	1.42	9.85
Decalin	1.48	9.61
Benzene	1.51	9.24
Toluene	1.57	8.82
Ethyl Benzene	1.55	8.76
Diphenyl Ether	1.57	8.82
Polystyrene	1.55	8.47
Polyisobutene	1.49	9.23
Glass	1.54	9.90
Teflon	1.30	12.00

REFERENCES

1. J.A. Kitchener and P.R. Musselwhite, in *Emulsion Science* (P. Sherman, ed.) Academic Press, N.Y. (1968).

2. J.A. Kitchener, *Brit. Polymer J.* 4. 217 (1972).

3. J. Lyklema, *Adv. Coll. Interface Sci.* 2, 65 (1968).

4. A.S.G. Curtis, *Prog. in Biophys. and Molec. Biol.* 27, 317 (1973).

5. H.D. Keith, F.J. Padden, Jr. and R.G. Vadimsky, *Science* 150, 1026 (1965).

6. A. Silberberg, *J. Phys. Chem.* 66, 1884 (1962).

7. D.H. Everett (ed.), *Specialist Periodical Report: Colloid Science, Vol. 1*, The Chemical Society, London (1973).

8. See, for example, M.N. Barber and B.W. Ninham, *Random and Restricted Walks*, Gordon & Breach, N.Y. (1970).

9. H.L. Frisch, R. Simha and F.R. Eirich, *J. Chem. Phys.* 21, 365 (1953).

10. H.L. Frisch, R. Simha and F.R. Eirich, *J. Phys. Chem.* 57, 584 (1953).

11. H.L. Frisch and R. Simha, *J. Phys. Chem.* 58, 507 (1954).

12. H.L. Frisch, *J. Phys. Chem.* 59, 633 (1955).

13. W.I. Higuchi, *J. Phys. Chem.* 65, 487 (1961).

14. E.A. DiMarzio, *J. Chem. Phys.* 42, 2101 (1965).

15. E.A. DiMarzio and F.L. McCrackin, *J. Chem. Phys.* 43, 539 (1965).

16. R.J. Rubin, *J. Chem. Phys.* 43, 2392 (1965).

17. R.J. Rubin, *J. Res. Natl. Bur. Std* B69, 301 (1965); *J. Res. Natl. Bur. Std* B70, 237 (1966).

18. K. Motomura and R. Matuura, *Mem. Fac. Sci. Kyushu Univ.* 6, 97 (1968); *J. Chem. Phys.* 50, 1281 (1969).

19. K. Motomura, K. Sekita and R. Matuura, *Bull. Chem. Soc. Japan* 44, 1243 (1971).
    K. Motomura, Y. Moroi and R. Matuura, *Bull. Chem. Sci. Japan* 44, 1248 (1971).

20. R.J. Rubin, *J. Chem. Phys.* 51, 4681 (1969).

21. K. Motomura, *J. Chem. Phys.* 51, 4681 (1969).

22. C.A.J. Hoeve, E.A. DiMarzio and P. Peyser, *J. Chem. Phys.* 42, 2558 (1965).

23. C.A.J. Hoeve, *J. Chem. Phys.* 43, 3007 (1965).

24. A. Silberberg, *J. Phys. Chem.* 66, 1872 (1966).

25. D.J. Meier, *J. Phys. Chem.* 71, 1861 (1967).

26. F.Th. Hesselink, *J. Phys. Chem.* 73, 3488 (1969).

27. R.-J. Roe, *Proc. Natl. Acad. Sci.* 53, 50 (1965).

28. R.-J. Roe, *J. Chem. Phys.* 43, 1591 (1965).

29. R.-J. Roe, *J. Chem. Phys.* 44, 4264 (1966).

30. S.F. Edwards, *J. Phys. A* 2, 145 (1969).

31. P.-G. deGennes, *Rep. Prog. Phys.* 32, 187 (1969).

32. S.F. Edwards, *Disc. Farad. Soc.* 49, 43 (1970).

33. P.M. Morse and H. Feshbach, *Methods of Theoretical Physics*, Vol. I, McGraw-Hill, N.Y. (1953).

34. G.F. Carrier, M. Krook and C.E. Pearson, *Functions of a Complex Variable*, McGraw-Hill, N.Y. (1966).

35. M.G. Darboux, *J. Math.* 3, 377 (1878).

36. M. Abramowitz and I.A. Stegun (eds.), *Handbook of Mathematical Functions*, Dover, N.Y. (1965).

37. P.J. Flory, *Principles of Polymer Chemistry*, Cornell U.P., Ithaca (1952).

38. F.L. McCrackin, *J. Chem. Phys.* 47, 1980 (1967).

39. M. Lax, *J. Chem. Phys.* 60, 2245 (1974).

40. S.F. Edwards and K.F. Freed, *J. Phys. A (Gen. Phys.)* 2, 145 (1969); see also R. Collins and A. Wragg, *J. Phys. A (Gen. Phys.)* 2, 151 (1969).

41. E.A. DiMarzio and R.J. Rubin, *J. Chem. Phys.* 55, 4318 (1971).

42. P. Richmond and M. Lal, *Chem. Phys. Lett.* 24, 594 (1974).

43. F. Hesselink, *J. Phys. Chem.* 75, 65 (1971).

44. F. Hesselink, A. Vrij and J.Th.G. Overbeek, *J. Phys. Chem.* 75, 2094 (1971).

45. A.K. Dolan and S.F. Edwards, *Proc. Roy. Soc. London* A337, 509 (1974).

46. L.D. Landau and E.M. Lifshitz, *Electrodynamics of Continuous Media*, Pergamon (1960).

47. See, for example, references (29) - (33) in the previous chapter.

48. J.D. Jackson, *Classical Electrodynamics*, Wiley, N.Y. (1962).

49. J.N. Israelachvili, *J. Chem. Soc., Faraday II* 69, 1729 (1973).

50. I.E. Dzyaloshinskii, E.M. Lifshitz and L.P. Pitaevskii, *Adv. Phys.* 10, 165 (1961).

51. *Tables of Interatomic Distances and Configurations in Molecules and Ions*, J. Chem. Soc. Spec. Publ. No. 11 (1958); No. 18 (1965).

52. R.I. Schoen, *J. Chem. Phys.* 37, 2032 (1962).

53. A.D. McLachlan, *Proc. Roy. Soc., London* A271, 387 (1963).

54. M.J. Renne, *Physica* 56, 125 (1971).

55. J.N. Israelachvili, *Proc. Roy. Soc., London* A331, 39 (1972).

56. P. Richmond and K.W. Sarkies, *J. Phys. C: Solid St. Phys.* 6, 401 (1973).

57. J. Mahanty and B.W. Ninham, *J. Chem. Phys.* 59, 6157 (1973).

58. N.G. van Kampen, B.R.A. Nijboer and K. Schram, *Phys. Lett.* 26A, 307 (1968).

59. B.W. Ninham, V.A. Parsegian and G.H. Weiss, *J. Stat. Phys.* 2, 323 (1970).

60. P. Richmond and B.W. Ninham, *J. Phys. C: Solid St. Phys.* 4, 1988 (1971).

61. J. Brandrup and E.H. Immergut (eds.), *Polymer Handbook*, Interscience, N.Y. (1966).

62. J. Timmermans, *Physico-Chemical Constants of Pure Organic Compounds*, Elsevier, Amsterdam, Vol. I (1950): Vol. II (1965).

63. R.C. Weast (ed.), *Handbook of Chemistry and Physics*, Chemical Rubber Publ. Co., Cleveland, Ohio, 52nd ed. (1971-2).

PART III

VAN DER WAALS AND DYNAMICAL INTERACTIONS

CHAPTER 1

TWO- AND THREE-BODY INTERACTIONS BETWEEN OPTICALLY ACTIVE MOLECULES — A SEMI-CLASSICAL APPROACH

1. INTRODUCTION

The phenomenon of optical activity has been observed as early as 1811 when Arago[1] discovered that quartz rotates the polarization of linearly polarized light that is directed along its optic axis. A similar effect was also noted by Biot[2] in certain liquids.

The optical activity of a medium refers to the phenomenon of optical rotation and circular dichroism associated with light propagation through the medium.[3] Both effects arise from differences in the response of a medium to light of different polarization states. In optical rotation, the plane of polarization of linearly polarized light is rotated because the left and right circularly polarized components have different refractive indices and hence different phase velocities. Positive rotation and the direction of propagation is related by the left hand screw. In circular dichroism, the absorption coefficients of left and right circularly polarized light are different so that linearly polarized light become elliptically polarized.†

In crystals such as quartz, the spatial arrangement of atoms or molecules account for optical rotation. However, in media without special symmetry or long-range ordering, such as liquids (e.g. in sugar solutions the rotation amounts to tens of degrees per decimetre), the optical activity must be due to intrinsic properties of the constituent molecules.[4-11]

---

† Linearly polarized light can always be considered as a superposition of a right circularly polarized wave with a phase $e^{i\delta}$ and a left circularly polarized wave with phase $e^{-i\delta}$. See reference (54) for a detailed discussion.

The fact that molecular properties can be responsible for a medium becoming optically active leads one to ask the interesting question: can the interaction between such molecules differ from optically inactive ones? It has been observed that the interaction between optically active chemical species possessing optical isomers — the laevo (ℓ) and dextro (d) form — is discriminative; the interaction of a dextro molecule of species A with a dextro molecule of species B is not the same as with a laevo B.[12-18] From the difference in solubility between the ℓ and d isomers of a compound in the presence of another optically active species, Dwyer and co-workers[12-14] concluded that the thermodynamic activity coefficients of ℓA and dA isomers are different in the presence of another optically active species ℓB say. In other words, the interaction energies dA with dB and ℓA with ℓB are different. This difference is exploited in the Pasteur Method of separating optical isomers in a racemic mixture [equimolar mixture of ℓ and d forms of the same chemical species]. This "configurational activity" as termed by Dwyer also manifests itself in differences in redox potentials, rates of mixing and diffusion between d and ℓ species in the presence of d and ℓ species of another type.[15] Thus, it is important to have an understanding of the interaction between optically active molecules and between optically active and inactive molecules. This may enable us to have a better understanding of phenomena such as the Pfeiffer effect[16-18] [the change in optical rotation of a solution of an optically active solution upon the addition of racemic mixtures of certain other optically active compounds] and induced optical activity.[19] Many molecules of biological importance are optically active or contain optically active groups[20] and a knowledge of how such molecules interact will give us a better insight into specificity in biological processes.

The two-body interaction (dispersive and inductive) energy between optically active molecules in the dipole approximation has been treated by a number of authors.[21-23] They approached the problem using quantum mechanical perturbative[22,23] and field theoretic techniques[21] and found that the interaction between isomers is discriminative. That is, the interaction of a dextro molecule of species A with a dextro B is different from that with a laevo B. The results have been applied to investigate the dispersive contribution to the cohesive energy of optically active crystals.[24]

Here we employ a semi-classical method[25] to calculate the dispersion interaction between non-polar optically active molecules represented as dipoles. This simple non-perturbative approach gives the energy exactly for all distances of separation between the molecules and reduces to the London[26] or Casimir-Polder[27] limit respectively at small or large separations. The basis of this theory is Maxwell's equations and Planck's hypothesis. The interaction energy is taken as the change of the zero-point energy of the allowed modes of electromagnetic oscillations as determined by Maxwell's equations and the linear response function of the molecules. This method has been exploited extensively in evaluating the dispersion interaction energy between molecules,[28-31] macroscopic bodies[32-50] and the dispersion contribution to surface energies.[51]

2. THE RESPONSE FUNCTION OF OPTICALLY ACTIVE MOLECULES

The interaction of an optically active molecule with an external electromagnetic field was first treated by Rosenfeld.[52] Since then similar problems have been considered by a number of workers.[53-57]

Here we recapitulate their results and rederive the complete response function for optically active molecules. (In previous work, the molecules are assumed to be non-magnetic, that is, the term $\underset{\approx}{\eta}$ given by equation (2.21) is assumed to be zero.)

In the semi-classical treatment of radiation, the Hamiltonian of a molecule in an external electromagnetic field specified by vector and scalar potentials $\underset{\sim}{A}$ and ϕ is[58]

$$H = \frac{1}{2m}\sum_i \left(p_i - \frac{e}{c}\underset{\sim}{A}(\underset{\sim}{r}_i,t)\right)^2 + \sum_i e\,\phi(\underset{\sim}{r}_i,t) - \frac{e}{mc}\sum_i \underset{\sim}{s}_i\cdot\nabla\times\underset{\sim}{A}(\underset{\sim}{r}_i,t) + V^{int} \quad . \tag{2.1}$$

In the Coulomb gauge ($\nabla\cdot\underset{\sim}{A} = 0 = \phi$) the Hamiltonian can be linearized to give

$$H = H_0 + V(t) \quad , \tag{2.2}$$

where

$$H_0 = \frac{1}{2m}\sum_i p_i^2 + V^{int} \tag{2.3}$$

$$V(t) = -\frac{e}{mc}\sum_i \underset{\sim}{A}(\underset{\sim}{r}_i,t)\cdot\underset{\sim}{p}_i + \underset{\sim}{s}_i\cdot(\nabla\times\underset{\sim}{A}(\underset{\sim}{r}_i,t)) \quad . \tag{2.4}$$

The summation is taken over all electrons which have charge e, mass m and spin magnetic moment $\frac{e}{mc}\underset{\sim}{s}_i$. V^{int} denotes a sum over all electron-electron, electron-nuclei and nuclei-nuclei interactions in the molecule. The interaction between the external field and the nuclei can be neglected since the nuclei are more massive than the electrons. The wave function corresponding to H in equation (2.2) can be expanded in terms of the eigenstates of the unperturbed Hamiltonian H_0 (equation (2.3)),

$$\psi = |0\rangle\, e^{-i\omega_0 t} + \sum_n c_n(t)|n\rangle\, e^{-i\omega_n t} \quad , \tag{2.5}$$

where

$$H_0|n\rangle = E_n|n\rangle = \hbar\omega_n|n\rangle \quad . \tag{2.6}$$

The coefficients $c_n(t)$ are given by first order perturbation theory[58] as

$$i\hbar \frac{\partial}{\partial t} c_n(t) = \langle n|V(t)|0\rangle e^{i\omega_{n0}t} \tag{2.7}$$

when the system is initially in state $|0\rangle$ with $\omega_{n0} = \omega_n - \omega_0$.

For an incident plane wave we have

$$\underset{\sim}{A}(\underset{\sim}{r},t) = \tfrac{1}{2}\left\{\underset{\sim}{a}\, e^{i(\underset{\sim}{k}\cdot\underset{\sim}{r}-\omega t)} + \underset{\sim}{a}^* e^{-i(\underset{\sim}{k}\cdot\underset{\sim}{r}-\omega t)}\right\} \tag{2.8}$$

hence

$$\langle n|V(t)|0\rangle = \tfrac{1}{2}\langle n|V_-|0\rangle e^{-i\omega t} + \tfrac{1}{2}\langle n|V_+|0\rangle e^{i\omega t}\ , \tag{2.9}$$

where

$$\langle n|V_-|0\rangle = -\frac{e}{mc}\langle n|\sum_i e^{i\underset{\sim}{k}\cdot\underset{\sim}{r}_i}\,\underset{\sim}{a}\cdot\underset{\sim}{p}_i|0\rangle - \frac{e}{mc}\langle n|\sum_i \underset{\sim}{s}_i\cdot\left(i\underset{\sim}{k}\times\underset{\sim}{a}\, e^{i\underset{\sim}{k}\cdot\underset{\sim}{r}_i}\right)|0\rangle \tag{2.10}$$

$$\simeq -\frac{e}{mc}\langle n|\sum_i \underset{\sim}{a}\cdot\underset{\sim}{p}_i|0\rangle - \frac{e}{mc}\langle n|\sum_i (i\underset{\sim}{k}\cdot\underset{\sim}{r}_i)(\underset{\sim}{a}\cdot\underset{\sim}{p}_i)|0\rangle$$

$$- \frac{e}{mc}\langle n|\sum_i \underset{\sim}{s}_i\cdot(i\underset{\sim}{k}\times\underset{\sim}{a})|0\rangle\ . \tag{2.11}$$

The approximation $e^{i\underset{\sim}{k}\cdot\underset{\sim}{r}} \simeq 1 + i\underset{\sim}{k}\cdot\underset{\sim}{r}$ made in the first term of equation (2.10) is equivalent to assuming that the wavelength λ of the external field is large compared with the molecular size d, and only first order correction terms in (d/λ) are taken into account. The electric dipole moment of the molecule is

$$\underset{\sim}{p} = \sum_i e\underset{\sim}{r}_i \tag{2.12}$$

and the magnetic dipole moment of the molecule is

$$\underset{\sim}{m} = \frac{1}{2mc}\left(\sum_i \underset{\sim}{r}_i\times\underset{\sim}{p}_i + 2\underset{\sim}{s}_i\right)\ . \tag{2.13}$$

Substituting these expressions into equation (2.11) we obtain[59]

$$\langle n|V_-|0\rangle = -\underset{\sim}{a}\cdot\frac{i\omega_{n0}}{c}\langle n|\underset{\sim}{p}|0\rangle - \langle n|\underset{\sim}{m}|0\rangle\cdot(i\underset{\sim}{k}\times\underset{\sim}{a})\ . \tag{2.14}$$

Here the small correction term corresponding to the quadrupole moment $\underset{\approx}{Q} = \sum_i e\,\underset{\sim}{r}_i\,\underset{\sim}{r}_i$ has been omitted since it does not contribute to any new effects.[54] Similarly, we have

$$\langle n|V_+|0\rangle = -\underset{\sim}{a}^*\cdot\frac{i\omega_{n0}}{c}\langle n|\underset{\sim}{p}|0\rangle + \langle n|\underset{\sim}{m}|0\rangle\cdot(i\underset{\sim}{k}\times\underset{\sim}{a}^*) \quad . \tag{2.15}$$

Hence equation (2.7) may be integrated to give (taking $V(t) = 0$ at $t = -\infty$)

$$c_n(t) = -\frac{1}{\hbar}\left\{\frac{\langle n|V_-|0\rangle}{\omega_{n0}-\omega}\,e^{i(\omega_{n0}-\omega)t} + \frac{\langle n|V_+|0\rangle}{\omega_{n0}+\omega}\,e^{i(\omega_{n0}+\omega)t}\right\}. \tag{2.16}$$

Now the change in the expectation value of an observable O due to interactions with the external field is, to first order in V, given by

$$\begin{aligned}\Delta\langle O\rangle &= \langle\psi|O|\psi\rangle - \langle 0|O|0\rangle \\ &= -2R\left\{\sum_n \frac{\langle 0|O|n\rangle\langle n|V_-|0\rangle}{\hbar(\omega_{n0}-\omega)}\,e^{-i\omega t}\right. \\ &\qquad \left. + \sum_n \frac{\langle 0|O|n\rangle\langle n|V_+|0\rangle}{\hbar(\omega_{n0}+\omega)}\,e^{i\omega t}\right\},\end{aligned} \tag{2.17}$$

where $R\{...\}$ denotes the real part of the expression in braces. In particular, the resultant electric and magnetic moments induced in a molecule by the electric field $\underset{\sim}{E}$ ($= -1/c\ \partial\underset{\sim}{A}/\partial t$) and magnetic field $\underset{\sim}{B}$ ($= \nabla\times\underset{\sim}{A}$) are

$$\underset{\sim}{p} = \underset{\approx}{\alpha}\cdot\underset{\sim}{E} - \underset{\approx}{\beta}\cdot\frac{\partial\underset{\sim}{B}}{\partial t} + \underset{\approx}{\gamma}\cdot\underset{\sim}{B} \tag{2.18}$$

$$\underset{\sim}{m} = \underset{\approx}{\beta}\cdot\frac{\partial\underset{\sim}{E}}{\partial t} + \underset{\approx}{\eta}\cdot\underset{\sim}{B} + \underset{\approx}{\chi}\cdot\underset{\sim}{E}\ , \tag{2.19}$$

where

$$\underset{\approx}{\alpha} = \frac{2}{\hbar}\sum_n \frac{\omega_{n0}\ R\{\langle 0|\underset{\sim}{p}|n\rangle\langle n|\underset{\sim}{p}|0\rangle\}}{(\omega_{n0}^2-\omega^2)} \tag{2.20}$$

$$\underset{\approx}{\eta} = \frac{2}{\hbar}\sum_n \frac{\omega_{n0}\ R\{\langle 0|\underset{\sim}{m}|n\rangle\langle n|\underset{\sim}{m}|0\rangle\}}{(\omega_{n0}^2-\omega^2)} \tag{2.21}$$

$$\underset{\approx}{\beta} = \frac{2}{\hbar}\sum_n \frac{I\{\langle 0|\underset{\sim}{p}|n\rangle\langle n|\underset{\sim}{m}|0\rangle\}}{(\omega_{n0}^2-\omega^2)} \tag{2.22}$$

and

$$\underset{\approx}{\gamma} = \frac{2}{\hbar}\sum_n \frac{\omega_{n0}\ R\{\langle 0|\underset{\sim}{p}|n\rangle\langle n|\underset{\sim}{m}|0\rangle\}}{(\omega_{n0}^2-\omega^2)} \tag{2.23}$$

(where $I\{...\}$ denotes the imaginary part), $\underset{\approx}{\alpha}$ and $\underset{\approx}{\eta}$ are respectively the

electric and magnetic polarizability tensors, $\underset{\approx}{\beta}$ and $\underset{\approx}{\gamma}$ are responsible for optical rotation when the various matrix elements are non-zero. The term $\underset{\approx}{\gamma}$ only has a second order effect[54] and will henceforth be omitted in the following discussion.

3. PROPERTIES OF THE OPTICAL ROTATORY PSEUDO TENSOR $\underset{\approx}{\beta}$

We now consider some of the properties of the optical rotatory pseudo tensor. From equation (2.22) we have

$$\underset{\approx}{\beta} = \frac{2}{\hbar} \sum_n \frac{\underset{\approx}{R}_{n0}}{\omega_{n0}^2 - \omega^2} , \tag{3.1}$$

where we define the rotating strength $\underset{\approx}{R}_{n0}$ for the transition $0 \to n$ by

$$\underset{\approx}{R}_{n0} = I\{\langle 0|\underset{\sim}{p}|n\rangle\langle n|\underset{\sim}{m}|0\rangle\} . \tag{3.2}$$

It is clear that the relation

$$\underset{\approx}{R}_{n0} = - \underset{\approx}{R}_{0n} \tag{3.3}$$

holds, since interchanging 0 and n replaces the matrix elements by its complex conjugate which reverses the sign of the imaginary part. The Kuhn sum rule[60] then follows immediately, i.e.,

$$\sum_n \underset{\approx}{R}_{n0} = \sum_n I\{\langle 0|\underset{\sim}{p}|n\rangle\langle n|\underset{\sim}{m}|0\rangle\} = I\{\langle 0|\underset{\sim}{p}\,\underset{\sim}{m}|0\rangle\} = 0 . \tag{3.4}$$

We observe that $\underset{\approx}{\beta}$ is frequency dependent, and therefore should give rise to an additional dispersion interaction between optically active molecules, provided the rotatory strengths are non-zero. For there to be optical rotation (non-zero $\underset{\approx}{R}_{n0}$) the states $|0\rangle$ and $|n\rangle$ must be connected by both electric and magnetic dipole transitions; or taking a more mechanistic viewpoint, a displacement of charges (associated with a $0 \to n$ transition) must be accompanied by a circulation of charged and vice

versa. This coupling of electric and magnetic effects arises because we have taken into account, to first order, the spatial variation of the fields over the molecule[61] (cf. equation (2.11)) and because the molecule possesses an intrinsic left or right handedness in its structure so as to react preferentially to light of different polarization states.[7] From the response equations (2.18) and (2.19) (neglecting the terms in $\underset{\approx}{\gamma}$) a time varying magnetic field gives rise to an electric dipole moment. But according to Maxwell's equations, time variations in the magnetic field are associated with spatial inhomogeneities in the electric field, so we can say that spatial variations in the electric field also contribute to the electric dipole moment of optically active molecules.[61] (Corrections to the dipole term due to quadrupole effects are small. Also these effects do not produce any new type of light propagation nor contribute to the discriminative energy.) Similar remarks also apply to that part of the magnetic moment due to time varying electric fields or inhomogeneous magnetic fields. Further, it also follows from this discussion that optical activity vanishes in the static limit as well as in the high frequency limit (cf. equation (2.18)).

From equation (3.2) we see that the rotatory strength $\underset{\approx}{R}_{no}$ is a diadic made up of a polar vector $\underset{\sim}{p}$ and an axial vector $\underset{\sim}{m}$. This means that $\underset{\approx}{\beta}$ is a pseudo tensor, that is, it changes sign on passing from a right-handed to a left-handed co-ordinate system. In other words, two molecules that are mirror images of each other (optical isomers) will have equal and opposite rotatory strengths.

4. RETARDED AND NON-RETARDED TWO-BODY INTERACTIONS

Consider two optically active molecules with one of them at the origin of a cartesian co-ordinate system and the other at a distance r away along the z axis. The mutually induced electric and magnetic dipole moments interact to give the two-body interaction energy.

Suppose that the instantaneous electric and magnetic dipole moments of a molecule are, respectively, $\underset{\sim}{p}(t) = \underset{\sim}{p}\, e^{-i\omega t}$ and $\underset{\sim}{m}(t) = \underset{\sim}{m}\, e^{-i\omega t}$. The electric and magnetic fields generated at a distance r (>> molecular dimensions) are[62]

$$\underset{\sim p}{E}(\underset{\sim}{r},t) = \underset{\sim p}{E}\, e^{-i\omega t} = \underset{\approx}{F}\cdot\underset{\sim}{p}\, e^{-i\omega t} \tag{4.1}$$

$$\underset{\sim m}{E}(\underset{\sim}{r},t) = \underset{\sim m}{E}\, e^{-i\omega t} = -\underset{\approx}{G}\cdot\underset{\sim}{m}\, e^{-i\omega t} \tag{4.2}$$

$$\underset{\sim p}{B}(\underset{\sim}{r},t) = \underset{\sim p}{B}\, e^{-i\omega t} = \underset{\approx}{G}\cdot\underset{\sim}{p}\, e^{-i\omega t} \tag{4.3}$$

$$\underset{\sim m}{B}(\underset{\sim}{r},t) = \underset{\sim m}{B}\, e^{-i\omega t} = \underset{\approx}{F}\cdot\underset{\sim}{m}\, e^{-i\omega t}\,, \tag{4.4}$$

where

$$\underset{\approx}{F} = \begin{pmatrix} f(r) & 0 & 0 \\ 0 & f(r) & 0 \\ 0 & 0 & g(r) \end{pmatrix} \tag{4.5}$$

$$\underset{\approx}{G} = \begin{pmatrix} 0 & -k(r) & 0 \\ k(r) & 0 & 0 \\ 0 & 0 & 0 \end{pmatrix} \tag{4.6}$$

$$f(r) = \left[\left(\frac{\omega r}{c}\right)^2 + \left(\frac{i\omega r}{c}\right) - 1\right] \frac{e^{i\omega r/c}}{r^3} \tag{4.7}$$

$$g(r) = 2\left[1 - \frac{i\omega r}{c}\right] \frac{e^{i\omega r/c}}{r^3} \tag{4.8}$$

$$k(r) = \left[\left(\frac{\omega r}{c}\right)^2 + \left(\frac{i\omega r}{c}\right)\right] \frac{e^{i\omega r/c}}{r^3} \tag{4.9}$$

and c is the velocity of light in vacuo.

We specify the response of a molecule according to the constitutive equations derived in Section 2 (equations (2.18) and (2.19) without the terms in $\underset{\approx}{\gamma}$). Thus for molecule "a" we have

$$\underset{\sim}{p}(a) = \underset{\approx}{\alpha}(a)\cdot\underset{\sim}{E}(a) + i\omega\underset{\approx}{\beta}(a)\cdot\underset{\sim}{B}(a) \tag{4.10}$$

$$\underset{\sim}{m}(a) = - i\omega\underset{\approx}{\beta}(a)\cdot\underset{\sim}{E}(a) + \underset{\approx}{\eta}(a)\cdot\underset{\sim}{B}(a) \ , \tag{4.11}$$

where $\underset{\sim}{E}(a)$ and $\underset{\sim}{B}(a)$ are the electric and magnetic fields produced by the electric *and* magnetic moments of molecule "b" at molecule "a" and $\underset{\approx}{\alpha}$, $\underset{\approx}{\eta}$ and $\underset{\approx}{\beta}$ are the electric polarizability, magnetic polarizability and optical rotatory pseudo tensor given by equations (2.20) to (2.22). From equations (4.1) to (4.4), (4.10) and (4.11) we obtain

$$\begin{pmatrix} \underset{\sim}{p}(a) \\ \underset{\sim}{m}(a) \end{pmatrix} = \begin{pmatrix} \underset{\approx}{\alpha}(a)\underset{\approx}{F} & + i\omega\underset{\approx}{\beta}(a)\underset{\approx}{G} & -\underset{\approx}{\alpha}(a)\underset{\approx}{G} & + i\omega\underset{\approx}{\beta}(a)\underset{\approx}{F} \\ -i\omega\underset{\approx}{\beta}(a)\underset{\approx}{F} + \underset{\approx}{\eta}(a)\underset{\approx}{G} & & i\omega\underset{\approx}{\beta}(a)\underset{\approx}{G} + \underset{\approx}{\eta}(a)\underset{\approx}{F} & \end{pmatrix} \begin{pmatrix} \underset{\sim}{p}(b) \\ \underset{\sim}{m}(b) \end{pmatrix}$$

$$\equiv \underset{\approx}{\Omega}(a) \begin{pmatrix} \underset{\sim}{p}(b) \\ \underset{\sim}{m}(b) \end{pmatrix} . \tag{4.12}$$

Molecule "b" responds similarly to the fields from molecule "a". The dispersion relation for allowed modes is the condition for non-trivial solutions for the electric and magnetic dipole moments:

$$\mathrm{Det}[\underset{\approx}{I} - \underset{\approx}{\Omega}(a)\ \underset{\approx}{\Omega}(b)] = 0 . \tag{4.13}$$

Strictly this calculation should be done by enclosing the dipoles in a large box of volume v and letting $v \to \infty$ after obtaining equation (4.15). Otherwise (4.13) has no zeros in the retarded case.

The interaction energy at zero temperature is related to the secular determinant by[48,49,51]

$$V(r) = \frac{1}{2\pi i}\oint d\omega(\tfrac{1}{2}\hbar\omega)\ \frac{d}{d\omega}\ ln\ \mathrm{Det}[\underset{\approx}{I} - \underset{\approx}{\Omega}(a)\ \underset{\approx}{\Omega}(b)] \tag{4.14}$$

$$= \frac{\hbar}{2\pi}\int_0^\infty d\xi\ ln\ \mathrm{Det}[\underset{\approx}{I} - \underset{\approx}{\Omega}(a)\ \underset{\approx}{\Omega}(b)] \ , \tag{4.15}$$

where in the first integral, which essentially assigns as zero point energy of ($\frac{1}{2}\hbar\omega$) to each allowed mode, the contour encloses the positive real axis. It is then mapped into the integral along the imaginary frequency axis $\omega = i\xi$ in the second integral. For large separations r (i.e. α/r^3, $\omega\beta/r^3$, $\eta/r^3 < 1$) we can expand the logarithm to leading order in 1/r to give

$$V(r) \simeq \frac{\hbar}{2\pi}\int_0^\infty d\xi \ \text{Trace}[-\underset{\approx}{\Omega}(a)\ \underset{\approx}{\Omega}(b)]$$

$$= \frac{\hbar}{2\pi}\int_0^\infty d\xi [D_1 + D_2 + D_3 + D_4 + D_5] \ . \qquad (4.16)$$

The five terms in brackets are as follows:

(i) $$V_1 = -\frac{\hbar}{2\pi}\int_0^\infty d\xi \ \text{Trace}[\underset{\approx}{\alpha}(a)\underset{\approx}{F}\ \underset{\approx}{\alpha}(b)\underset{\approx}{F}] \ . \qquad (4.17)$$

This yields the dispersion energy due to electric dipole fluctuations. A detailed discussion for a general polarizability tensor $\underset{\approx}{\alpha}$ has been given elsewhere.[28,63] However for identical isotropic polarizabilities, namely $\underset{\approx}{\alpha}(a) = \underset{\approx}{\alpha}(b) = \alpha\underset{\approx}{I}$ we obtain in the non-retarded London limit ($\omega_0 r/c << 1$)

$$V_1 = -\frac{3\hbar\omega_0\ \alpha_0^2}{4r^6} \qquad (4.18)$$

or in the retarded Casimir-Polder limit ($\omega_0 r/c >> 1$)

$$V_1 = -\frac{23\hbar c\ \alpha_0^2}{4\pi\ r^7} \ , \qquad (4.19)$$

where ω_0 is the characteristic absorption (angular) frequency of the dipoles and α_0 the static polarizability.

(ii) $$V_2 = -\frac{\hbar}{2\pi}\int_0^\infty d\xi \ \text{Trace}[\underset{\approx}{\eta}(a)\underset{\approx}{F}\ \underset{\approx}{\eta}(b)\underset{\approx}{F}] \ . \qquad (4.20)$$

This is the magnetic analogue of the previous term where the electric polarizabilities are replaced by magnetic polarizabilities.[64] In general, this term is small because the magnetic polarizabilities are small.

$$\text{(iii)} \quad V_3 = \frac{\hbar}{2\pi}\int_0^\infty d\xi\ \text{Trace}[\underset{\approx}{\alpha}(a)\underset{\approx}{G}\ \underset{\approx}{\eta}(b)\underset{\approx}{G} + \underset{\approx}{\eta}(a)\underset{\approx}{G}\ \underset{\approx}{\alpha}(b)\underset{\approx}{G}] \ . \qquad (4.21)$$

This term is only non-zero when retardation effects are taken into account. The electric (magnetic) dipole moment of one molecule produces a magnetic (electric) field which then induces a magnetic (electric) dipole moment on the other molecule and vice versa. In the special case of isotropic polarizabilities we obtain

$$V_3 = \frac{7\hbar c}{4\pi r^7}\left[\alpha_0(a)\ \eta_0(b) + \alpha_0(b)\ \eta_0(a)\right] , \qquad (4.22)$$

where α_0 and η_0 are the static polarizabilities. This result has been obtained earlier by field theoretic techniques.[64] It is interesting to note that the contributions to the interaction energy from V_1 and V_2 are always attractive while that from V_3 is always repulsive.

We are primarily interested in the discrimination energy. These are given in terms (iv) and (v):

$$\begin{aligned}\text{(iv)} \quad V_4 = \frac{\hbar}{2\pi}\int_0^\infty d\xi\ \xi\ \text{Trace}[&\underset{\approx}{\alpha}(a)\underset{\approx}{F}\ \underset{\approx}{\beta}(b)\underset{\approx}{G} + \underset{\approx}{\beta}(a)\underset{\approx}{G}\ \underset{\approx}{\alpha}(b)\underset{\approx}{F} \\ &+ \underset{\approx}{\alpha}(a)\underset{\approx}{G}\ \underset{\approx}{\beta}(b)\underset{\approx}{F} + \underset{\approx}{\beta}(a)\underset{\approx}{F}\ \underset{\approx}{\alpha}(b)\underset{\approx}{G} \\ &+ \underset{\approx}{\eta}(a)\underset{\approx}{F}\ \underset{\approx}{\beta}(b)\underset{\approx}{G} + \underset{\approx}{\beta}(a)\underset{\approx}{G}\ \underset{\approx}{\eta}(b)\underset{\approx}{F} \\ &+ \underset{\approx}{\eta}(a)\underset{\approx}{G}\ \underset{\approx}{\beta}(b)\underset{\approx}{F} + \underset{\approx}{\beta}(a)\underset{\approx}{F}\ \underset{\approx}{\eta}(b)\underset{\approx}{G}] \qquad (4.23)\end{aligned}$$

$$\text{(v)} \quad V_5 = \frac{\hbar}{2\pi}\int_0^\infty d\xi\ 2\xi^2\ \text{Trace}[\underset{\approx}{\beta}(a)\underset{\approx}{F}\ \underset{\approx}{\beta}(b)\underset{\approx}{F} - \underset{\approx}{\beta}(a)\underset{\approx}{G}\ \underset{\approx}{\beta}(b)\underset{\approx}{G}] \ . \qquad (4.24)$$

Using equations (4.5) and (4.6) we can expand equation (4.23) to give

$$\begin{aligned}V_4 = \frac{\hbar}{2\pi}\int_0^\infty d\xi\ \xi\ \Big[\Big\{\Big(&[\alpha_{xx}(a)\ \beta_{xy}(b) + \alpha_{xy}(a)\ \beta_{yy}(b) \\ &- \alpha_{yx}(a)\ \beta_{xx}(b) - \alpha_{yy}(a)\ \beta_{yx}(b)] + [a \rightleftharpoons b]\Big) f(r)k(r) \\ &+ \left(\alpha_{ij}(a) \rightleftharpoons \beta_{ij}(a)\ ;\ \alpha_{ij}(b) \rightleftharpoons \beta_{ij}(b)\right) f(r)k(r) \\ &+ \Big([\alpha_{xz}(a)\ \beta_{zy}(b) - \alpha_{zy}(a)\ \beta_{zx}(b)] + [a \rightleftharpoons b]\Big) g(r)k(r)\Big\} \\ &+ \{\alpha_{ij} \to \eta_{ij}\}\Big] , \qquad (4.25)\end{aligned}$$

where α_{ij}, β_{ij} and η_{ij} are elements of the polarizability tensors in the laboratory or space frame of reference. In the freely rotating limit ($\alpha_{ij} = 0 = \beta_{ij} = \eta_{ij}$ for $i \neq j$) or in the non-retarded limit [$k(r) = 0$] this term vanishes identically. In the retarded regime ($\omega_0 r/c >> 1$)

$$V_0 \simeq \frac{\hbar}{2\pi} A_0 \int_0^\infty d\xi\, \xi\, f(r)k(r) + \frac{\hbar}{2\pi} B_0 \int_0^\infty d\xi\, \xi\, g(r)k(r) , \qquad (4.26)$$

where A_0 and B_0 are the coefficients of $f(r)k(r)$ and $g(r)k(r)$ in equation (4.25) evaluated at $\xi = 0$. Using the definitions of $f(r)$, $g(r)$ and $k(r)$ in equations (4.7) - (4.9) we get

$$V_4 = \frac{\hbar c^2}{4\pi r^8} \left(\frac{35}{4} A_0 - 7B_0 \right) \qquad (4.27)$$

which can be an attractive or repulsive contribution to the interaction energy depending on the relative static values of α_{ij}, η_{ij} and β_{ij} in A_0 and B_0.

The other contribution to the discrimination energy (V_5) remains finite in both the retarded and non-retarded limits. To proceed further, we choose the rotatory tensor $\underset{\approx}{\beta}'$ in the *body* frame such that $\beta'_{ij} = \beta$ for $i = j = z'$ and zero otherwise. $\underset{\approx}{\beta}'$ is related to its counterpart in the space frame $\underset{\approx}{\beta}$ by[65]

$$\underset{\approx}{\beta} = \underset{\approx}{R}^T \underset{\approx}{\beta}' \underset{\approx}{R} , \qquad (4.28)$$

where the unitary transformation matrix in terms of the Euler angles (θ,ϕ,ψ) between the space and body axes is

$$\underset{\approx}{R} = \begin{pmatrix} \cos\phi\cos\psi - \cos\theta\sin\phi\sin\psi & \sin\phi\sin\psi + \cos\theta\cos\phi\sin\psi & \sin\theta\sin\psi \\ -\cos\theta\sin\phi\cos\psi - \cos\phi\sin\psi & \cos\theta\cos\phi\cos\psi - \sin\phi\sin\psi & \sin\theta\cos\psi \\ \sin\theta\sin\phi & -\sin\theta\cos\phi & \cos\theta \end{pmatrix} \qquad (4.29)$$

and $\underset{\approx}{R}^T$ is its transpose. From equation (3.1) we take β to be of the form

$$\beta = \frac{2}{\hbar} \sum_{n} \frac{R_{no}}{(\omega_{no}^2 - \omega^2)} , \qquad (4.30)$$

where $R_{no} = I\{\langle 0|\underset{\sim}{p}|n\rangle \cdot \langle n|\underset{\sim}{m}|0\rangle\}$ is the rotational strength for the absorption at frequency ω_{no}.

Case (a): $\dfrac{\omega_0 r}{c} << 1 \quad (\omega_0 = \max\{\omega_{no}\} \text{ say})$.

This is the non-retarded limit and we can replace f(r) by $-\frac{1}{r^3}$, g(r) by $\frac{2}{r^3}$ and k(r) by zero in equation (4.24). This together with equations (4.28) - (4.30) gives

$$V_5 = \frac{2(\cos\gamma - 3\cos\theta_a \cos\theta_b)}{r^6} \sum_{m,n} \frac{R_{mo}(a)\, R_{no}(b)}{\hbar[\omega_{mo}(a) + \omega_{no}(b)]} , \qquad (4.31)$$

where the molecules are allowed to rotate freely about the z' body axis. Here γ is the angle between the z' axes of the molecules and θ_a, θ_b are the angles between the z' body axes of molecules "a" and "b" and the line joining the centres of the molecules (the z axis in the space frame). Further averaging over the remaining angles yields the non-retarded two-body discrimination energy in the freely rotating limit

$$V_5 = \frac{4}{3r^6} \sum_{m,n} \frac{R_{mo}(a)\, R_{no}(b)}{\hbar[\omega_{mo}(a) + \omega_{no}(b)]} . \qquad (4.32)$$

The results in (4.31) and (4.32) have been obtained previously using quantum mechanical methods.[22,23]

Case (b): $\dfrac{\omega_0 r}{c} >> 1 \quad (\omega_0 = \min\{\omega_{no}\} \text{ say})$.

Here we must use the forms of f(r), g(r) and k(r) given by equations (4.7) - (4.9) (with the replacement $\omega \to i\xi$) in equation (4.24) for V_5, but the β's can be replaced by their static values. The resultant expression for the discrimination energy, in the freely rotating limit, becomes[21]

$$V_S = \frac{\hbar c^3}{9\pi r^9} [\beta(a)\ \beta(b)]_{\xi=0} \int_0^\infty dx\, x^2$$

$$\times e^{-2x}[2(x^2+x+1)^2 + 2(x^2+x)^2 + 4(x+1)^2]$$

$$= \frac{70}{3} \frac{c^3}{\pi\hbar r^9} \sum_{m,n} \frac{R_{mo}(a)\ R_{no}(b)}{\omega_{mo}^2(a)\ \omega_{no}^2(b)} \cdot \qquad (4.33)$$

From the above calculation we conclude that the rotatory power of optically active molecules gives rise to additional terms in the dispersion interaction between molecules. This contribution is a function of the rotatory strength R_{no} which has different signs for laevo and dextro isomers. In particular, the term V_S is positive for the interaction between similar optical species and negative for dissimilar species. Hence like species repel and unlike attract. This extra contribution to the dispersion energy is relatively short-ranged — it passes from a r^{-6} dependence at small separations to a r^{-8}, r^{-9} dependence at large separations. Thus it seems that when the non-polar optically active molecules are far apart (retarded) the dominant interaction is the Casimir-Polder potential, and they are unable to differentiate between different isomers. However at close separations (non-retarded) the r^{-6} discriminating term becomes operative and like/unlike species will be able to "recognize" each other. The distance at which the transition from the retarded to the non-retarded behaviour takes place is of the order of c/ω_0 where ω_0 is the principle absorption frequency (typically $\sim 10^{16}$ rad/sec).

Before going on to make a comparison between the relative strengths of the discrimination energy and the ordinary dispersion energy, let us first consider the problem of three interacting optically active molecules.

5. NON-RETARDED THREE-BODY INTERACTIONS

Consider three optically active molecules that are located at the vertices of a triangle as shown in Figure 5.1. Let $\underset{\sim}{p}(i,t) = \underset{\sim}{p}(i)\, e^{-i\omega t}$ and $\underset{\sim}{m}(i,t) = \underset{\sim}{m}(i)\, e^{-i\omega t}$ be the instantaneous electric and magnetic dipole moments of molecule $i = A,B,C$. To avoid cumbersome algebra, we shall only consider the problem in the non-retarded regime. The electric and magnetic fields $\underset{\sim}{E}$ and $\underset{\sim}{B}$ at a distance r_{ij} from dipole i are respectively $\underset{\approx}{T}_{ij}\, \underset{\sim}{p}(i)$ and $\underset{\approx}{T}_{ij}\, \underset{\sim}{m}(i)$, where $\underset{\approx}{T}_{ij} = r_{ij}^{-3}(3\hat{\underset{\sim}{r}}_{ij}\hat{\underset{\sim}{r}}_{ij} - 1)$. Proceeding as before, we let each dipole respond to the field of the other two dipoles according to constitutive equations used in the previous section. We obtain

$$\underset{\sim}{p}(A) = \underset{\approx}{\alpha}(A)[\underset{\approx}{T}_{BA}\, \underset{\sim}{p}(B) + \underset{\approx}{T}_{CA}\, \underset{\sim}{p}(C)] + i\omega\underset{\approx}{\beta}(A)[\underset{\approx}{T}_{BA}\, \underset{\sim}{m}(B) + \underset{\approx}{T}_{CA}\, \underset{\sim}{m}(C)] \qquad (5.1)$$

$$\underset{\sim}{m}(A) = -i\omega\underset{\approx}{\beta}(A)[\underset{\approx}{T}_{BA}\, \underset{\sim}{p}(B) + \underset{\approx}{T}_{CA}\, \underset{\sim}{p}(C)] + \underset{\approx}{\eta}(A)[\underset{\approx}{T}_{BA}\, \underset{\sim}{m}(B) + \underset{\approx}{T}_{CA}\, \underset{\sim}{m}(C)] \qquad (5.2)$$

along with similar equations for dipoles B and C.

To carry out the algebraic manipulations, it is convenient to define the matrix (see Figure 5.1)

$$\underset{\approx}{T}_i = \frac{1}{r_i^3}\begin{pmatrix} 2 & 0 & 0 \\ 0 & -1 & 0 \\ 0 & 0 & -1 \end{pmatrix}, \quad i = 1,2,3\ . \qquad (5.3)$$

Therefore

$$\left.\begin{aligned} \underset{\approx}{T}_{AB} &= \underset{\approx}{T}_{BA} = \underset{\approx}{T}_3 \\ \underset{\approx}{T}_{CA} &= \underset{\approx}{T}_{AC} = \underset{\approx}{R}_A\, \underset{\approx}{T}_1\, \underset{\approx}{R}_A^T \\ \underset{\approx}{T}_{CB} &= \underset{\approx}{T}_{BC} = \underset{\approx}{R}_B\, \underset{\approx}{T}_2\, \underset{\approx}{R}_B^T \end{aligned}\right\}, \qquad (5.4)$$

where

$$\underset{\approx}{R}_j = \begin{pmatrix} \cos\theta_j & -\sin\theta_j & 0 \\ \sin\theta_j & \cos\theta_j & 0 \\ 0 & 0 & 0 \end{pmatrix}, \quad j = A,B \qquad (5.5)$$

and the superscript T denotes the transpose matrix.

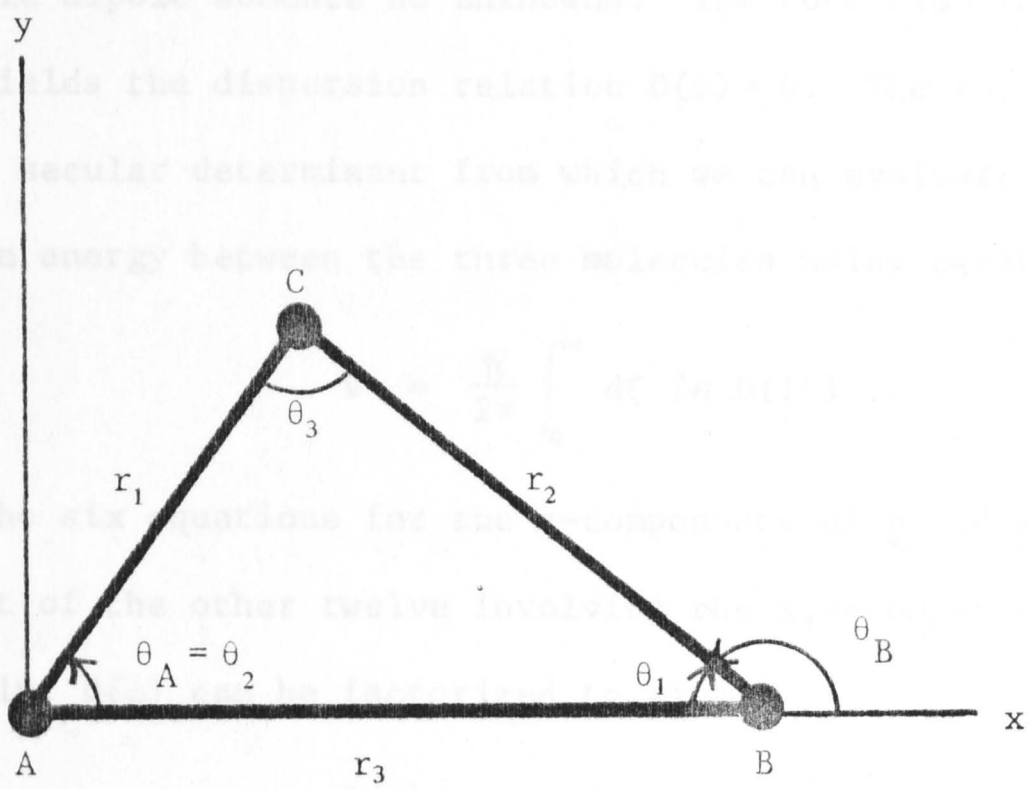

Figure 5.1: Diagram showing the relative positions of the dipoles for the three-body problem. All three molecules lie in the x-y plane.

We shall assume that in the body frame $\underset{\approx}{\beta}'$ has only one non-zero element, namely $\beta'_{zz} = \beta$. In the freely rotating limit, which we shall assume for this problem, $\underset{\approx}{\beta}$ reduces to a scalar: $\beta/3$ and $\underset{\approx}{\alpha}$ and $\underset{\approx}{\eta}$ become isotropic.

Substituting equations (5.3) - (5.5) in to (5.1) and (5.2) and the corresponding equations for molecules B and C, we obtain 18 homogeneous linear equations with the spatial components of the electric and magnetic dipole moments as unknowns. The condition for non-trivial solution yields the dispersion relation $D(\omega) = 0$. The function $D(\omega)$ is the 18×18 secular determinant from which we can evaluate the interaction energy between the three molecules using equation (4.15)

$$V = \frac{\hbar}{2\pi} \int_0^\infty d\xi \; ln \; D(i\xi) \; . \tag{5.6}$$

However, the six equations for the z-components of $\underset{\sim}{p}$ and $\underset{\sim}{m}$ are independent of the other twelve involving the x,y-components.

Consequently, $D(\omega)$ can be factorized to give

$$D(\omega) = D_z(\omega) \; D_{xy}(\omega) \; ,$$

where $D_z(\omega)$ is the determinant of the 6×6 matrix in the following equation

$$\begin{pmatrix}
1 & \frac{\alpha(A)}{r_3^3} & \frac{\alpha(A)}{r_1^3} & 0 & \frac{i\omega\beta(A)}{3r_3^3} & \frac{i\omega\beta(A)}{3r_1^3} \\
\frac{\alpha(B)}{r_3^3} & 1 & \frac{\alpha(B)}{r_2^3} & \frac{i\omega\beta(B)}{3r_3^3} & 0 & \frac{i\omega\beta(B)}{3r_1^3} \\
\frac{\alpha(C)}{r_1^3} & \frac{\alpha(C)}{r_2^3} & 1 & \frac{i\omega\beta(C)}{3r_1^3} & \frac{i\omega\beta(C)}{3r_2^3} & 0 \\
0 & -\frac{i\omega\beta(A)}{3r_3^3} & -\frac{i\omega\beta(A)}{3r_1^3} & 1 & \frac{\eta(A)}{r_3^3} & \frac{\eta(A)}{r_1^3} \\
-\frac{i\omega\beta(B)}{3r_3^3} & 0 & -\frac{i\omega\beta(B)}{3r_2^3} & \frac{\eta(B)}{r_3^3} & 1 & \frac{\eta(B)}{r_2^3} \\
-\frac{i\omega\beta(C)}{3r_1^3} & -\frac{i\omega\beta(C)}{3r_2^3} & 0 & \frac{\eta(C)}{r_1^3} & \frac{\eta(C)}{r_2^3} & 1
\end{pmatrix}
\begin{pmatrix}
p_z(A) \\ p_z(B) \\ p_z(C) \\ m_z(A) \\ m_z(B) \\ m_z(C)
\end{pmatrix}
= 0 \tag{5.7}$$

and D_{xy} is the determinant in the 12×12 matrix in

$$\begin{pmatrix} \underset{\approx}{M}_{11} & \underset{\approx}{M}_{12} \\ \underset{\approx}{M}_{21} & \underset{\approx}{M}_{22} \end{pmatrix} \begin{pmatrix} p_x(A) \\ p_y(A) \\ p_x(B) \\ \cdot \\ \cdot \\ \cdot \\ m_x(A) \\ \cdot \\ \cdot \\ \cdot \\ m_y(C) \end{pmatrix} = 0 \qquad (5.8)$$

with

$$\underset{\approx}{M}_{11} = \begin{pmatrix} 1 & 0 & -2\alpha(A)f_3 & 0 & -\alpha(A)f_1 V_A & -\alpha(A)f_1 S_A \\ 0 & 1 & 0 & \alpha(A)f_3 & -\alpha(A)f_1 S_A & -\alpha(A)f_1 W_A \\ -2\alpha(B)f_3 & 0 & 1 & 0 & -\alpha(B)f_2 V_B & -\alpha(B)f_2 S_B \\ 0 & \alpha(B)f_3 & 0 & 1 & -\alpha(B)f_2 S_B & -\alpha(B)f_2 W_B \\ -\alpha(C)f_1 V_A & -\alpha(C)f_1 S_A & -\alpha(C)f_2 V_B & -\alpha(C)f_2 S_B & 1 & 0 \\ -\alpha(C)f_1 S_A & -\alpha(C)f_1 W_A & -\alpha(C)f_2 S_B & -\alpha(C)f_2 W_B & 0 & 1 \end{pmatrix}$$

$$\underset{\approx}{M}_{12} = \begin{pmatrix} 0 & 0 & -2\gamma(A)f_3 & 0 & -\gamma(A)f_1 V_A & -\gamma(A)f_1 S_A \\ 0 & 0 & 0 & \gamma(A)f_3 & -\gamma(A)f_1 S_A & -\gamma(A)f_1 W_A \\ -2\gamma(B)f_3 & 0 & 0 & 0 & -\gamma(B)f_2 V_B & -\gamma(B)f_2 S_B \\ 0 & \gamma(B)f_3 & 0 & 0 & -\gamma(B)f_2 S_B & -\gamma(B)f_2 W_B \\ -\gamma(C)f_1 V_A & -\gamma(C)f_1 S_A & -\gamma(C)f_2 V_B & -\gamma(C)f_2 S_B & 0 & 0 \\ -\gamma(C)f_1 S_A & -\gamma(C)f_1 W_A & -\gamma(C)f_2 S_B & -\gamma(C)f_2 W_B & 0 & 0 \end{pmatrix}$$

$$\underset{\approx}{M}_{21} = \begin{pmatrix} 0 & 0 & 2\gamma(A)f_3 & 0 & \gamma(A)f_1 V_A & \gamma(A)f_1 S_A \\ 0 & 0 & 0 & -\gamma(A)f_3 & \gamma(A)f_1 S_A & \gamma(A)f_1 W_A \\ 2\gamma(B)f_3 & 0 & 0 & 0 & \gamma(B)f_2 V_B & \gamma(B)f_2 S_B \\ 0 & -\gamma(B)f_3 & 0 & 0 & \gamma(B)f_2 S_B & \gamma(B)f_2 W_B \\ \gamma(C)f_1 V_A & \gamma(C)f_1 S_A & \gamma(C)f_2 V_B & \gamma(C)f_2 S_B & 0 & 0 \\ \gamma(C)f_1 S_A & \gamma(C)f_1 W_A & \gamma(C)f_2 S_B & \gamma(C)f_2 W_B & 0 & 0 \end{pmatrix}$$

$$\underset{\approx}{M}_{22} = \begin{pmatrix} 1 & 0 & -2\eta(A)f_3 & 0 & -\eta(A)f_1 V_A & -\eta(A)f_1 S_A \\ 0 & 1 & 0 & \eta(A)f_3 & -\eta(A)f_1 S_A & -\eta(A)f_1 W_A \\ -2\eta(B)f_3 & 0 & 1 & 0 & -\eta(B)f_2 V_B & -\eta(B)f_2 S_B \\ 0 & \eta(B)f_3 & 0 & 1 & -\eta(B)f_2 S_B & -\eta(B)f_2 W_B \\ -\eta(C)f_1 V_A & -\eta(C)f_1 S_A & -\eta(C)f_2 V_B & -\eta(C)f_2 S_B & 1 & 0 \\ -\eta(C)f_1 S_A & -\eta(C)f_1 W_A & -\eta(C)f_2 S_B & -\eta(C)f_2 W_B & 0 & 1 \end{pmatrix}$$

where

$$f_i = r_i^{-3}, \qquad i = 1,2,3$$

$$S_j = 3\cos\theta_j \sin\theta_j$$

$$W_j = (3\sin^2\theta_j - 1)$$

$$V_j = (3\cos^2\theta_j - 1), \quad j = A,B$$

$$\gamma = i\omega\beta/3 .$$

We now expand the logarithm in equation (5.6) and neglect terms of order r^{-12} and higher. This procedure yields the two- and three-body terms

$$V = \frac{\hbar}{2\pi}\int_0^\infty d\xi\Bigg\{-6\left(\frac{\alpha(A)\alpha(C)}{r_1^6}+\frac{\alpha(B)\alpha(C)}{r_2^6}+\frac{\alpha(A)\alpha(B)}{r_3^6}\right)$$

$$+6[1+3\cos\theta_1\cos\theta_2\cos\theta_3]\frac{\alpha(A)\alpha(B)\alpha(C)}{(r_1r_2r_3)^3}$$

$$-6\left(\frac{\eta(A)\eta(C)}{r_1^6}+\frac{\eta(B)\eta(C)}{r_2^6}+\frac{\eta(A)\eta(B)}{r_3^6}\right)$$

$$+6[1+3\cos\theta_1\cos\theta_2\cos\theta_3]\frac{\eta(A)\eta(B)\eta(C)}{(r_1r_2r_3)^6}$$

$$+\frac{12}{9}\xi^2\left(\frac{\beta(A)\beta(C)}{r_1^6}+\frac{\beta(B)\beta(C)}{r_2^6}+\frac{\beta(A)\beta(B)}{r_3^6}\right)$$

$$-\frac{6}{9}\xi^2[\beta(A)\beta(B)\alpha(C)+\beta(A)\alpha(B)\beta(C)+\alpha(A)\beta(B)\beta(C)$$

$$+\beta(A)\beta(B)\eta(C)+\beta(A)\eta(B)\beta(C)+\eta(A)\beta(B)\beta(C)]$$

$$\times\frac{[1+3\cos\theta_1\cos\theta_2\cos\theta_3]}{(r_1r_2r_3)^3}+O\left(\frac{1}{r^{12}}\right)\Bigg\}, \qquad (5.9)$$

where

$$\theta_1 = \pi - \theta_B$$

$$\theta_2 = \theta_A$$

$$\theta_3 = \theta_B - \theta_A$$

(see Figure 5.1). The first two terms gives the familiar two-[21,26,28,63] and three-body[28,66-69] contributions to the dispersion energy. The next two are corresponding magnetic analogues. We shall not consider these further. The fifth term is the two-body non-retarded discrimination energy (see equation (4.32)). The last term in equation (5.9) is the three-body discrimination energy. This term can enhance or reduce the discrimination effect of the two-body term depending on the sign of the angular factor.

Let us consider a special case where the magnetic polarizabilities are small ($\eta \sim 0$) and only two molecules A and B say are optically active ($\beta(C) = 0$). Take for simplicity

$$\alpha = \frac{\alpha_0}{1 + (\xi/\omega_0)^2} \tag{5.10}$$

$$\beta = \frac{\beta_0}{1 + (\xi/\omega_0)^2} \tag{5.11}$$

then the two-body discrimination term is

$$V(2) = \frac{\hbar\omega_0}{6r_3^6}\, \beta_0(A)\beta_0(B) \tag{5.12}$$

and the three-body term is

$$V(3) = -\frac{\hbar\omega_0^3}{48(r_1 r_2 r_3)^3}\, \beta_0(A)\beta_0(B)\alpha_0(C)\ [1 + 3\cos\theta_1\ \cos\theta_2\ \cos\theta_3]. \tag{5.13}$$

Comparing the relative magnitudes of V(2) and V(3), it is clear that the three-body term can only be important when the optically inactive molecule (C) is close to the other two. In particular, the strongest effect is obtained when molecule C lies midway between molecules A and B. Then $r_1 = r_2 = r_3/2$ and $[1 + 3\cos\theta_1\ \cos\theta_2\ \cos\theta_3] = -2$, and we obtain

$$\frac{V(3)}{V(2)} = \frac{16\ \alpha_0(C)}{r_3^3}\ .$$

Choosing some typical values $r^3 \sim 8 - 10$ Å, $\alpha_0(C) \sim 5$ Å, we obtain $V(3)/V(2) \sim 8 - 16\%$ which is a significant contribution.

It is believed that many-body effects are important for a thorough understanding of the structure of molecular crystals.[70,71] If the crystals are composed of both optically active and inactive molecules, the terms derived here may likewise be important for a complete understanding of the properties of the system.

6. SOME NUMERICAL ESTIMATES

It is instructive to compare the relative magnitudes of the two-body dispersion (V_{disp}) and discrimination (V_{disc}) energy in the non-retarded limit. For the case of identical molecules, we find from equations (2.20), (3.2), (4.18) and (4.32) that

$$\left|\frac{V_{disc}}{V_{disp}}\right| = \frac{2}{9}\left(\frac{I\{\langle 0|p|n\rangle\langle n|m|0\rangle\}}{R\{\langle 0|p|n\rangle\langle n|p|0\rangle\}}\right)^2 . \qquad (6.1)$$

Now the electric dipole matrix element $\langle 0|p|n\rangle$ may for simple molecules be expected to be of the order of the electron charge times the first Bohr radius a_0 and the magnetic dipole matrix element $\langle n|m|0\rangle$ may likewise be of the order of the Bohr magneton $eh/2mc$. We therefore obtain

$$\left|\frac{V_{disc}}{V_{disp}}\right| \sim \frac{2}{9}\left(\frac{(ea_0)(eh/2mc)}{(ea_0)\ (ea_0)}\right)^2$$

$$\sim \frac{2}{9}\left(\frac{0.927\times 10^{-20}}{2.54\times 10^{-18}}\right)^2$$

$$\sim 3\times 10^{-6} .$$

However for more complex molecules such as those occurring in biological systems the magnetic dipole transition moments may be considerably larger and it is for these types of molecules where we expect the discriminating effect to play a significant role.

REFERENCES

(1) F.A. Jenkins and H.E. White, *Fundamentals of Optics*, McGraw-Hill (1950), Ch. 27.

(2) Biot, *Bull. Soc. philomath.* 190 (1815).

(3) P. Crabbé, *Optical Rotatory Dispersion and Circular Dichroism in Organic Chemistry*, Holden Day (1965).
D.J. Caldwell and H. Eyring, *Theory of Optical Activity*, Interscience Monograph on Physical Chemistry, Wiley, N.Y. (1971).

(4) P. Drude, *The Theory of Optics*, Dover, N.Y. (1959), p.402 ff.

(5) W. Kuhn, *Zeit. Physik. Chem.* B20, 325 (1933).

(6) T.M. Lowry, *Optical Rotatory Power*, Dover, N.Y. (1964), p.372 ff.

(7) G.E. Desobry and P.K. Kabir, *Am. J. Phys.* 41, 1350 (1973).

(8) M.R. Philpott, *J. Chem. Phys.* 56, 683 (1972).

(9) W. Moffit, *J. Chem. Phys.* 25, 467 (1956); *Proc. Natl. Acad. Sci.* 43, 723 (1956).

(10) Ando, *Prog. Theoret. Phys.* 40, 470 (1968).

(11) E.U. Condon, W. Alter and H. Eyring, *J. Chem. Phys.* 5, 753 (1937).

(12) F.P. Dwyer, M.F. O'Dwyer and E.C. Gyarfas, *Nature* 167, 1036 (1951).

(13) F.P. Dwyer and E.C. Gyarfas, *Nature* 168, 29 (1951).

(14) See also J.D. Roberts and M.C. Caseria, *Basic Principles of Organic Chemistry*, Benjamin, N.Y. (1965).

(15) D.P. Mellor, *Proc. Roy. Aust. Chem. Inst.* 37, 199 (1970).

(16) P. Pfeiffer and K. Quehl, *Ber.* 64, 2267 (1931).

(17) P. Pfeiffer and K. Quehl, *Ber.* 65, 560 (1932).

(18) S. Kirshner and K. Magnell in Werner Centennial, *Advances in Chemistry Series* No. 62 (G. Kauffman, ed.), Washington, D.C.: *Am. Chem. Soc.* (1967).

(19) P.E. Schipper, Ph.D Thesis, Aust. Natl. Univ. (1972).

(20) M.V. Volkershtein, *Molecules and Life*, Plenum Press, N.Y. (1970).

(21) C. Mavroyannis and M.J. Stephens, *Mol. Phys.* 5, 629 (1962).

(22) D.P. Craig, E.A. Power and T. Thirumanachandran, *Chem. Phys. Lett.* 6, 211 (1970).

(23) D.P. Craig, E.A. Power and T. Thirumanachandran, *Proc. Roy. Soc. London* A322, 165 (1971).

(24) E.A. Power and T. Thirumanachandran, *Phys. Rev.* B3, 3546 (1971).

(25) J.O. Hirschfelder, C.F. Curtiss and R.B. Byde, *Molecular Theory of Gases and Liquids*, Wiley, N.Y. (1964).

(26) F. London, *J. Phys. Chem.* 46, 305 (1952).

(27) H.B.G. Casimir and D. Polder, *Phys. Rev.* 73, 360 (1948).

(28) D.J. Mitchell, B.W. Ninham and P. Richmond, *J. Phys. B* 4, L81 (1971); *Aust. J. Phys.* 25, 33 (1972).

(29) J. Mahanty and B.W. Ninham, *J. Phys. A: Gen. Phys.* 5, 1447 (1972).

(30) P. Richmond and K.W. Sarkies, *J. Phys. C: Solid State Phys.* 6, 401 (1973).

(31) J. Mahanty and B.W. Ninham, *J. Phys. A: Math. Nucl. Gen.* 6, 1140 (1973).

(32) N.G. van Kampen, B.R.A. Nijboer and K. Schram, *Phys. Lett.* 26A, 307 (1968).

(33) D.J. Mitchell and B.W. Ninham, *J. Chem. Phys.* 56, 1117 (1972).

(34) V.A. Parsegian and B.W. Ninham, *J. Theor. Biol.* 38, 101 (1973).

(35) B.W. Ninham and V.A. Parsegian, *J. Chem. Phys.* 53, 3398 (1970).

(36) V.A. Parsegian and G.H. Weiss, *J. Adhesion* 3, 259 (1972).

(37) B. Davies and B.W. Ninham, *J. Chem. Phys.* 56, 5797 (1972).

(38) M.J. Renne, *Physica* 56, 125 (1971).

(39) M.J. Renne, *Physica* 53, 193 (1971).

(40) K. Schram, *Phys. Lett.* 43A, 282 (1973).

(41) B.W. Ninham and V.A. Parsegian, *J. Chem. Phys.* 52, 4578 (1970).

(42) V.A. Parsegian, *J. Chem. Phys.* 56, 4393 (1972).

(43) D.J. Mitchell, B.W. Ninham and P. Richmond, *Biophys. J.* 13, 359 (1973).

(44) D.J. Mitchell, B.W. Ninham and P. Richmond, *Biophys. J.* 13, 370 (1973).

(45) D.J. Mitchell and B.W. Ninham, *J. Chem. Phys.* 59, 1246 (1973).

(46) D.J. Mitchell, B.W. Ninham and P. Richmond, *J. Theor. Biol.* 37, 251 (1972).

(47) B. Davies, B.W. Ninham and P. Richmond, *J. Chem. Phys.* 58, 744 (1973).

(48) B.W. Ninham, V.A. Parsegian and G.H. Weiss, *J. Stat. Phys.* 2, 323 (1970).

(49) P. Richmond and B.W. Ninham, *J. Phys. C: Solid State Phys.* 4, 1988 (1971).

(50) D. Langbein, *J. Adhesion* 1, 237 (1969); *J. Phys. Chem. Solid* 32, 133 (1971); *J. Phys. Chem. Solid* 32, 1657 (1971); *J. Phys. A: Gen. Phys.* 4, 471 (1971) *J. Adhesion* 3, 213 (1972); *Phys. Rev.* B2, 3371 (1970); *J. Phys. A: Math. Nucl. Gen.* 6, 1149 (1973).

(51) J. Mahanty and B.W. Ninham, *J. Chem. Phys.* 59, 6157 (1973).
D.J. Mitchell and P. Richmond, *Chem. Phys. Lett.* 21, 113 (1973); *J. Coll. Interface Sci.* 46, 118 (1974).
R.A. Craig, *Phys. Rev.* B6, 1134 (1972)

(52) L. Rosenfeld, *Z. Physik* 52, 161 (1928).

(53) M. Born and P. Jordan, *Elementare Quanten-mechanik*, Berlin (1930).

(54) E.U. Condon, *Rev. Mod. Phys.* 9, 432 (1937).

(55) M.J. Stephens, *Proc. Camb. Phil. Soc.* 54, 81 (1958).

(56) E.A. Power and R. Shail, *Proc. Camb. Phil. Soc.* 55, 87 (1959).

(57) H. Nakano and H. Kimura, *J. Phys. Soc. Japan* 27, 519 (1969).

(58) L.I. Schiff, *Quantum Mechanics*, McGraw-Hill, N.Y. (1968).

(59) L.R.B. Elton, *Introductory Nuclear Theory*, Pitman, London (1959).

(60) W. Kuhn, *Z. Physik Chem.* B4, 14 (1929).

(61) L.D. Landau and E.M. Lifshitz, *Electrodynamics of Continuous Media*. Pergamon Press, N.Y. (1960).

(62) J.D. Jackson, *Classical Electrodynamics*, Wiley, N.Y. (1962).

(63) D.P. Craig and E.A. Power, *Int. J. Quantum Chem.* 3, 903 (1969).

(64) G. Feinberg and J. Sucher, *Phys. Rev.* A2, 2395 (1970).

(65) H. Goldstein, *Classical Mechanics*, Addison-Wesley, Cambridge, Mass. (1950).

(66) B.M. Axilrod and E. Teller, *J. Chem. Phys.* 11, 299 (1943).

(67) B.M. Axilrod, *J. Chem. Phys.* 19, 719 (1954).

(68) R.J. Bell, *J. Phys.* B3, 751 (1970).

(69) A.D. McLachlan, *Mol. Phys.* 6, 423 (1963).

(70) L. Jansen, *Phys. Rev.* 135, A1292 (1964).

(71) A. Huller, *Z. Physik* 245, 324 (1971).

CHAPTER 2

CLASSICAL THEORY OF DYNAMICAL IMAGE INTERACTION

1. INTRODUCTION

Of the various types of experimental techniques used in the investigation of bulk and surface properties of solids, perhaps the most important involves the use of charged particles as probes.[1] It is essential then to know the interaction potential of the charged particle with the solid surface in order, for example, to deduce from fast electron spectroscopy the collective excitations[2-4] and the heights of surface barrier from lower energy electron diffraction (LEED).[5] In principle, a complete quantum mechanical calculation should yield all we need to know about the system. However, owing to our rudimentary knowledge of the dynamical properties of solids, such a calculation involves considerable difficulties.

It has been recognized for some time that classical electrodynamics can be used to obtain surface plasmon[7-11] and magneto plasmon[12-14] dispersion relations for single surfaces and films as well as for the energy loss of fast charged particles due to bulk and surface plasmon excitations.[15-19] The results are identical to those obtained using more elaborate quantum mechanical methods.[20-23] However, the interaction potential of moving charged particles with surfaces has generally been treated using quantum mechanical methods[24-26] although classical treatments of the similar problems have appeared recently.[27]

Calculations have shown that asymptotically, moving charges do behave like a classical particle in a "modified" image potential.[6] Here we derive the dynamical image potential using classical electrodynamics. The result agrees with that obtained previously by

quantum mechanical methods that included multiple plasmon excitations. When classical methods are applicable, they are generally much simpler to use than quantum mechanical procedures and as shown by many recent calculations of van der Waals forces, where retardation effects, non-planar surfaces and inhomogeneous interfaces can be readily handled.[28] To avoid obscuring the main points, we suppose the surface is planar and ignore retardation effects. For "fast" particles which are reflected at the surface, we can assume that the velocity $\underset{\sim}{v}$ remains constant. The definition of a "fast" particle will depend on the type of excitations in the solid. Here, "fast" particles means those whose recoil associated with the process of emission or absorption of collective excitations may be neglected. In the case where the particles are electrons, the typical energy range is $10 - 10^5$ eV.

2. THE IMAGE POTENTIAL

Consider a particle with charge q in the half space (vacuum) $z > 0$ impinging upon a planar solid surface, of dielectric susceptibility $\varepsilon(\omega)$, at $z = 0$. We assume that the particle has some *constant* velocity $\underset{\sim}{v}$ and is reflected elastically off the surface at time $t = 0$. We can always chose a co-ordinate system such that the position vector of the particle is $\underset{\sim}{r}' = (0,\ v_{\|}\, t,\ v_{\perp}\,|t|)$, where $\underset{\sim}{v} = (0,\ v_{\|}, v_{\perp})$, so that the charge density is $\rho = q\delta(x)\delta(y - v_{\|}\, t)\delta(z - v_{\perp}\,|t|)$.

If we ignore retardation effects due to the finite velocity of light, the electric scalar potential can be determined from Poisson's equation

$$\nabla^2 \Phi \;=\; -\,4\pi q\ \delta(x)\ \delta(y - v_{\|}\, t)\ \delta(z - v_{\perp}\,|t|) \qquad (2.1)$$

together with the usual boundary conditions. Using the Fourier expansion

$$\Phi(x,y,z;t) = \frac{1}{(2\pi)^3}\int_{-\infty}^{\infty} dk_x \int_{-\infty}^{\infty} dk_y \int_{-\infty}^{\infty} d\omega\, e^{i(k_x x + k_y y)}\, e^{-i\omega t}\, \phi(k_x,k_y;\omega|z) \tag{2.2}$$

we can obtain the solution of equation (2.1) for $z < 0$, where there are no free charges, $(k^2 = k_x^2 + k_y^2)$

$$\Phi = \frac{1}{(2\pi)^3}\int d^2\underset{\sim}{k}\int_{-\infty}^{\infty} d\omega\, e^{i(k_x x + k_y y)}\, e^{-i\omega t}\, e^{kz}\, B(k_x,k_y;\omega) \tag{2.3}$$

and for $z > 0$,

$$\Phi = \frac{1}{(2\pi)^3}\int d^2\underset{\sim}{k}\int_{-\infty}^{\infty} d\omega\, e^{i(k_x x + k_y y)}\, e^{-i\omega t}\, e^{-kz}\, A(k_x,k_y;\omega)$$

$$+ \frac{q}{[x^2 + (y - v_{\|}\, t)^2 + (z - v_{\perp}|t|)^2]^{\frac{1}{2}}} . \tag{2.4}$$

Both equations (2.3) and (2.4) follows from the condition that $\Phi \to 0$ as $z \to \pm\infty$. The first term in equation (2.4) is the induced potential due to the presence of the interface at $z = 0$. The second term is the "direct" potential of the moving charge which can be rewritten as

$$\frac{1}{(2\pi)^3}\int d^2\underset{\sim}{k}\int_{-\infty}^{\infty} d\omega \frac{4\pi q v_{\perp}\{2\cos[(\omega - k_y v_{\|})z/v_{\perp}] - e^{-kz}\}e^{i(k_x x + k_y y)}\, e^{-i\omega t}}{(\omega - k_y v_{\|})^2 + k^2 v_{\perp}^2} . \tag{2.5}$$

From the continuity of the potential and the normal component of the displacement vector at the boundary $(z = 0)$ we can solve for the Fourier coefficients, giving

$$A = -\left(\frac{\varepsilon - 1}{\varepsilon + 1}\right)\frac{4\pi q v_{\perp}}{(\omega - k_y v_{\|})^2 + k^2 v_{\perp}^2} \tag{2.6}$$

$$B = \frac{2}{(\varepsilon + 1)}\frac{4\pi q v_{\perp}}{(\omega - k_y v_{\|})^2 + k^2 v_{\perp}^2} . \tag{2.7}$$

Therefore the induced potential is

$$\Phi^{ind} = -\frac{1}{(2\pi)^3}\int_{-\infty}^{\infty} dk_x \int_{-\infty}^{\infty} dk_y \int_{-\infty}^{\infty} d\omega\, e^{i(k_x x + k_y y)}\, e^{-i\omega t}$$

$$\times \left(\frac{\varepsilon(\omega)-1}{\varepsilon(\omega)+1}\right) \frac{4\pi q v_\perp\, e^{-kz}}{(\omega - k_y v_{||})^2 + (kv_\perp)^2} \,. \qquad (2.8)$$

The image (free) energy is given by[29,30]

$$V = \tfrac{1}{2}\int \rho\, \Phi^{ind}\, d^3\underset{\sim}{r} \qquad (2.9)$$

$$= -\frac{q^2 v_\perp}{(2\pi)^2}\int d^2\underset{\sim}{k} \int_{-\infty}^{\infty} d\omega\, e^{-i(\omega - k_y v_{||})t}$$

$$\times \left(\frac{\varepsilon(\omega)-1}{\varepsilon(\omega)+1}\right) \frac{e^{-kz}}{(\omega - k_y v_{||})^2 + (kv_\perp)^2} \,, \qquad (2.10)$$

where in equation (2.10) $z = v_\perp |t|$. For a particle approaching the surface, $t < 0$, $z = -v_\perp t$, we can do the ω-integral by completing the contour in the upper half complex ω plane to give

$$V = -\frac{q^2}{4\pi}\int d^2\underset{\sim}{k}\, \frac{e^{-2kz}}{k} \left(\frac{\varepsilon(\omega)-1}{\varepsilon(\omega)+1}\right)_{\omega = k_y v_{||} + ikv_\perp} \,. \qquad (2.11)$$

This is a general result for the image potential ($z > 0$) since causality guarantees that $\varepsilon(\omega)$ is analytic and well behaved in the upper half of the complex frequency ω-plane.[16]

3. SPECIAL RESULTS AND DISCUSSION

For a *metallic* medium with a dielectric susceptibility $\varepsilon(\omega) = 1 - \omega_p^2/\omega^2$,[16] we get from equation (2.11)

$$V^{metal} = -\frac{q^2}{4\pi}\int \frac{d^2\underset{\sim}{k}}{k}\, \frac{e^{-2kz}}{1 - 2(k_y v_{||} + ikv_\perp)^2/\omega_p^2} \,. \qquad (3.1)$$

If the particle is travelling *parallel* to the surface, i.e. $v_\perp = 0$, and if $\alpha_{||} \equiv \sqrt{2}\,\omega_p z/v_{||} >> 1$, this reduces to

$$V_{\|}^{metal} = -\frac{q^2}{4z}\left(1+\alpha_{\|}^{-2}+O(\alpha_{\|}^{-4})\right), \quad \alpha_{\|} >> 1 \tag{3.2}$$

which yields a force in the *normal* direction

$$F_{\| z} = -\frac{\partial V_{\|}^{metal}}{\partial z}$$

$$= -\frac{q^2}{4z^2}\left(1+3\alpha_{\|}^{-2}+O(\alpha_{\|}^{-4})\right). \tag{3.3}$$

The last result has been obtained earlier by Takimoto.[17]

On the other hand, for normal incidence, $v_{\|} = 0$, we get, from equation (3.1), ($\alpha_{\perp} = \sqrt{2}\,\omega_p z/v_{\perp}$)

$$V_{\perp}^{metal} = -\frac{q^2}{4z}\,\alpha_{\perp}\,f(\alpha_{\perp}), \tag{3.4}$$

where

$$f(\alpha) = \int_0^{\infty} dx\,\frac{e^{-\alpha x}}{1+x^2}, \tag{3.5a}$$

This result is identical to that obtained by Ray and Mahan[26] using the quantum mechanical model Hamiltonian of Sunjic and Lucas[23] which included multiple plasmon excitations. Complete asymptotic expansions can be obtained by doing the Laplace transform to obtain[31]

$$f(\alpha) = [\tfrac{1}{2}\pi - Si(\alpha)]\cos\alpha + Ci(\alpha)\sin\alpha \tag{3.5b}$$

(see Figure 3.1) and

$$V_{\perp}^{metal} = -\frac{q^2\alpha_{\perp}}{4z}\left\{\frac{\pi}{2} - \alpha_{\perp}\left[(1-\gamma) - ln\,\alpha_{\perp} + \frac{\pi}{4}\,\alpha_{\perp}\right] + O(\alpha_{\perp}^3)\right\}, \tag{3.6}$$

$$\alpha_{\perp} << 1,$$

where $\gamma = 0.5772\ldots$ is Euler's constant.[31] For $\alpha_{\perp} >> 1$, we get

$$V_{\perp}^{metal} = -\frac{q^2}{4z}\left\{1 - 2\alpha_{\perp}^{-2} + O(\alpha_{\perp}^{-4})\right\}, \quad \alpha_{\perp} >> 1. \tag{3.7}$$

For the case of normal incidence ($v_{\|} = 0$) upon a dielectric, whose dielectric susceptibility along the imaginary frequency ($\omega = ikv_{\perp}$) axis can be written as[32]

$$\varepsilon(i\xi) = 1 + \frac{\varepsilon_0 - 1}{1 + (\xi/\omega_0)^2}, \tag{3.8}$$

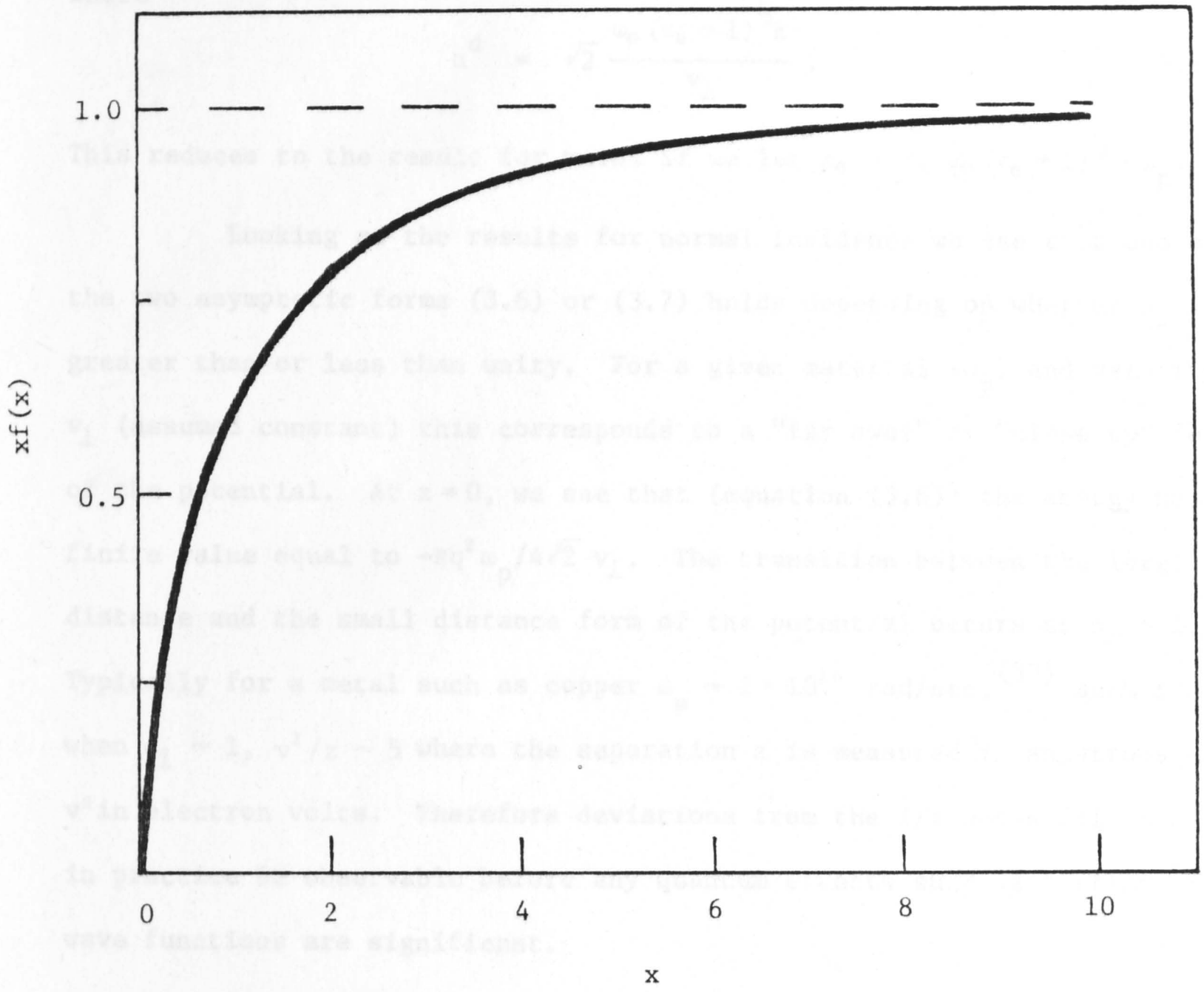

Figure 3.1: A plot of the function xf(x) (equation (3.5b))

$$xf(x) = x\left\{\left(\frac{\pi}{2} - Si(x)\right)\cos x + Ci(x)\ \sin x\right\} .$$

Special values:

x	xf(x)
~ 0	$\frac{\pi}{2}\,x$
$\to \infty$	$\to 1$
1.0	0.62
0.6	0.5

we get

$$V_{\perp}^{diel} = -\frac{q}{4z}\left(\frac{\varepsilon_0 - 1}{\varepsilon_0 + 1}\right)\alpha^d f(\alpha^d) \ , \tag{3.9}$$

where

$$\alpha^d = \sqrt{2}\,\frac{\omega_0\,(\varepsilon_0 + 1)^{\frac{1}{2}} z}{v_{\perp}} \ . \tag{3.10}$$

This reduces to the result for metal if we let $\varepsilon_0 \to \infty$, $\omega_0\,(\varepsilon_0 + 1)^{\frac{1}{2}} \to \omega_p$.

Looking at the results for normal incidence we see that one of the two asymptotic forms (3.6) or (3.7) holds depending on whether $\alpha_{\perp}$ is greater than or less than unity. For a given material (ω_p) and velocity $v_{\perp}$ (assumed constant) this corresponds to a "far away" or "close up" form of the potential. At $z = 0$, we see that (equation (3.6)) the energy has a finite value equal to $-\pi q^2 \omega_p / 4\sqrt{2}\ v_{\perp}$. The transition between the large distance and the small distance form of the potential occurs at $\alpha_{\perp} \sim 1$. Typically for a metal such as copper $\omega_p \sim 2 \times 10^{16}$ rad/sec,[33] such that when $\alpha_{\perp} \sim 1$, $v^2/z \sim 5$ where the separation z is measured in angstroms and v^2 in electron volts. Therefore deviations from the 1/z potential should in practice be observable before any quantum effects such as overlap of wave functions are significant.

We have demonstrated how a very simple method based on classical electrodynamics can be used to account for modifications of the static image potential due to plasmon excitations. The generalization of this method to more complicated geometries including thin films and surface layers or spatially dispersive media is relatively straightforward.[34] There are, also, other refinements such as diffuseness of the surface,[35,36] retardation and quantum effects which a more rigorous theory should include. It can be argued that the assumption regarding a *constant* velocity of approach may be invalid at low velocities or energies. A more satisfactory approach would be to assume some general

particle trajectory (as a function of position and time), and calculate the potential and hence the force acting on the particle. The trajectory function can then be determined self-consistently using the equation of motion.[27]

REFERENCES

(1) For a review, see for example, A.A. Lucas and M. Sunjic, *Prog. in Surface Sci.* 2, 75 (1972).

(2) D. Pines, *Elementary Excitations in Solids*, Benjamin, N.Y. (1964).

(3) H. Raether, *Springer Tracts in Mod. Phys.* 38, 84 (1965).

(4) G. Ruthermann, *Ann. Phys.* 6, 113 (1948).

(5) P.J. Jennings, *Surface Sci.* 25, 513 (1971).

(6) P.J. Feibelman, C.B. Duke and A. Bagchi, *Phys. Rev.* B5, 2436 (1972).

(7) R.A. Fewell, *Phys. Rev.* 111, 1214 (1958).

(8) R. Stern and R.A. Farrell, *Phys. Rev.* 120, 130 (1960).

(9) R.A. Ritchie and Eldridge, *Phys. Rev.* 126, 1935 (1962).

(10) E.N. Economou, *Phys. Rev.* 182, 539 (1969).

(11) A.A. Lucas, *Phys. Rev.* B7, 3527 (1973).

(12) K.W. Chiu and J.J. Quinn, *Phys. Rev.* B5, 4707 (1972).

(13) I.L. Tyler, B. Fischer and R.J. Bell, *Optic Comm.* 8, 145 (1973)

(14) R.F. Wallis, J.J. Brion, E. Burstein and A. Hartstein, *Phys. Rev.* B9, 3424 (1974); and references cited therein.

(15) R.H. Ritchie, *Phys. Rev.* 106, 874 (1957).

(16) L.D. Landau and E.M. Lifshitz, *Electrodynamics of Continuous Media*, Pergamon, Oxford (1960).

(17) N. Takimoto, *Phys. Rev.* 146, 366 (1966).

(18) A.A. Lucas and E. Kartheuser, *Phys. Rev.* B1, 3588 (1972).

(19) J.G. deVooght, *Annals of Phys.* 75, 249 (1973).

(20) A. Griffin and J. Harris, *Phys. Rev.* A5, 2190 (1970).

(21) J. Harris and A. Griffin, *Phys. Rev.* B3, 749 (1971); *Phys. Lett.* 37A, 387 (1971); *Can. J. Phys.* 48, 2592 (1970).

(22) A.A. Lucas, E. Kartheuser and R.G. Badro, *Phys. Rev.* B2, 2488 (1970).

(23) M. Sunjic and A.A. Lucas, *Phys. Rev.* B3, 719 (1971).

(24) J. Sak, *Phys. Rev.* B6, 3981 (1972).

(25) R.H. Ritchie, *Phys. Lett.* 38A, 189 (1972).

(26) R. Ray and G.D. Mahan, *Phys. Lett.* 21A, 301 (1972).

(27) J. Harris and R.O. Jones, *J. Phys. C: Solid St. Phys.* 6, 3585 (1973);
J. Heinrichs, *Phys. Rev.* B8, 1346 (1973).

(28) See references (32) to (50) in the preceding chapter.

(29) D.J. Mitchell and P. Richmond, *J. Coll. Interface Sci.* 46, 118 (1974).

(30) P. Richmond, *J. Chem. Soc., Faraday II* 70, 1066 (1974).

(31) M. Abramowitz and I.A. Stegun, *Handbook of Mathematical Functions*, NBS, Washington (1964).

(32) B.W. Ninham and V.A. Parsegian, *J. Chem. Phys.* 53, 3398 (1970).

(33) J.D. Jackson, *Classical Electrodynamics*, Wiley, N.Y. (1962).

(34) D. Chan, unpublished work.

(35) A.J. Bennett, *Phys. Rev.* B1, 203 (1970).

(36) N.D. Lang and W. Kohn, *Phys. Rev.* B1, 4555 (1970); *Phys. Rev.* B7, 3541 (1973).